The Molecular Localisation of *Staphylococcus aureus* Surface Protein A

By

Thomas Leigh Hamer, BSc. MSc.

(University of South Wales, University of Birmingham)

A thesis submitted for the degree of Doctor of Philosophy

April 2023

School of Biosciences, University of Sheffield, Firth Couth, Western Bank,

Sheffield, S10 2TN

Summary

Staphylococcus aureus presents an important and significant burden on global healthcare systems. The ability to of *S. aureus* to colonise the human population and cause a wide range of diseases is heavily dependent on the display of various proteins on its cell surface. These proteins serve multiple functions, including adhesion to host molecules, chelation of host iron, and the evasion of both innate and adaptive mammalian immune systems. Therefore, the development of new and novel strategies to combat *S. aureus* infection dynamics and disease progression is dependent on an advanced understanding of how these key virulence determinants are displayed and develop over time.

The aim of this project was to construct reporter fusions for four surface displayed virulence determinants fused to SNAP-tag, an O^6-benzylguanine-DNA-benzyltransferase, to then localise them on the cell surface of *S. aureus*. The proteins were iron-regulated surface determinant A (IsdA), iron-regulated surface determinant B (IsdB), clumping factor A (ClfA), and surface protein A (SpA). Due to a lack of sensitivity of the SNAP reporter fusion, an alternative approach of immunofluorescence microscopy was also used, with which the localisation of SpA and its development over time was elucidated.

Immunolabelling for SpA localisation in this study has shown that SpA is displayed only on a subset of the bacterial population of *S. aureus* SH1000, a well characterised and model laboratory strain. Within this subpopulation, SpA localises over the whole of single cells. *S. aureus* cells actively dividing present SpA at their respective peripheries but not the newly exposed septum, displaying a horseshoe-like pattern of SpA fluorescence. In conjunction with atomic force microscopy data of the cell wall architecture of live *S. aureus* cells, the horseshoe pattern was believed to be the result of the surface exposure of dense, nascent cell wall material at the division septum that acts as an additional layer of peptidoglycan without Spa bound to this layer. Further investigations into the role of genes involved in cell wall associated processes identified several targets that appear vital for SpA display. Finally, the impact of high methicillin resistance *S. aureus* (MRSA) and antibiotic challenge on SpA localisation was determined. My project has further elucidated those mechanisms which control the display of the important virulence determinant SpA on the surface of *S. aureus*.

Acknowledgments

I would like to thank Professor Simon Foster, the University of Sheffield, and the White Rose Consortium for the opportunity to carry out my PhD.

Thanks to past and present members of the Foster lab for both their scientific help and their support. I would also like to thank Mariana Tinajero-Trejo, Lucia Lafage, and Joshua Sutton for their patience and guidance in the writing of this thesis.

I extend my special thanks and gratitude to Jessica Davis and Robert Brench for their constant empowerment, insight, and friendship. Their stalwart companionship has enriched this experience far more than I could have hoped for. I would also like to thank James Plunkett and Laura Gee for being a constant source of comfort and encouragement, Naznin Choudhury for her invaluable support and humour, and Hannah Fisher for both helping me prepare for, and distract me from, my viva.

Finally, I would like to express my special thanks and endless gratitude to Maria Saunders, who has supported me throughout my PhD in countless ways. This work, and so much more, would not have been possible without her generous love, relentless empowerment, and boundless optimism.

These amazing people have left an indelible impression on me and have changed my life entirely for the better. Their collective kindness and love have made this experience better than I could have ever anticipated. I will be forever grateful.

Abbreviation List

%	Percentage
~	Approximately
°	Degree
°C	Degree Celsius
µF	Microfarad
µg	Microgram
µl	Microlitre
µm	Micrometre
µM	Micromolar
Φ	Phage
Ω	Ohm
AF	Alexafluor
AFM	Atomic force microscopy
Amp	Ampicillin
ATP	Adenosine triphosphate
bp	Base pair
BSA	Bovine serum albumin
D-ala	D-alanine
dH_2O	Distilled water
DMSO	Dimethyl sulfoxide
DNA	Deoxyribonucleic acid
EDTA	Ethylenediaminetetraacetic acid
Erm	Erythromycin
g	Grams
Glc*N*Ac	*N*-acetylglucosamine
Kan	Kanamycin
Kb	Kilobase pair
kDa	Kilodalton
kV	Kilovolt
L	Litre
LB	Lysogeny broth
Lin	Lincomycin
LK	Lysogeny broth with potassium
LTA	Lipoteichoic acid
M	Molar
Meth	Methicillin
mg	Milligram
MIC	Minimum inhibitory concentration
min	Minutes
mL	Millilitres
mM	Millimolar
MRSA	Methicillin resistant *Staphylococcus aureus*
ms	Milliseconds
MSSA	Methicillin susceptible *Staphylococcus aureus*
Mur*N*Ac	*N*-acetylmuramic acid

NaCit	Sodium citrate
OD_{600}	Optical density measured at 600 nanometres
PBP	Penicillin binding protein
PCR	Polymerase chain reaction
PCR	Polymerase chain reaction
rcf	Relative centrifugal force
RNA	Ribonucleic acid
rpm	Revolutions per minute
s	Seconds
SDS	Sodium dodecyl sulphate
SDS-PAGE	Sodium dodecyl sulphate – polyacrylamide gel electrophoresis
SIM	Structured illumination microscopy
STORM	Stochastic optical reconstruction microscopy
TAE	Tris acetate EDTA
Tet	Tetracycline
TSB	Tryptic soy broth
v/v	Volume per volume
w/w	Weight per weight
WTA	Wall teichoic acid
x	Times

Table of Contents

Table of Figures

List of Tables

Chapter 1

Introduction

1.1. *Staphylococcus aureus* Epidemiology

Staphylococcus aureus is a Gram-positive, spheroid Firmicute within the Family Staphylococcaceae, which ranges in size between 0.5 – 1.5 µm (Masalha *et al*, 2001). It is a facultatively anaerobic, commensal bacterium commonly found on the skin, anterior nares, and lower respiratory tract of humans and other mammals (Tong *et al*, 2015). *S. aureus* is distinguished macroscopically by its formation of smooth, slightly raised golden colonies on solid media, the coloration of which is due to the production of the carotenoid staphyloxanthin (Holt *et al*, 2011). *S. aureus* is also an opportunistic pathogen, capable of causing several nosocomial and community acquired diseases. *S. aureus* is the causative agent of many skin, nasal, and respiratory tract infections, such as abscesses, impetigo, cellulitis, folliculitis, and sinusitis. Additionally, *S. aureus* can cause severe and life-threatening illnesses, such as pneumonia, meningitis, osteomyelitis, toxic shock syndrome, and bacteraemia. *S. aureus*' ability to cause disease is largely attributed to the secretion and surface display of virulence proteins (Archer, 1998; Lowy, 1998; Von Eiff *et al*, 2001; Fowler *et al*, 2003).

The implantation of medical devices confers a particular risk of *S. aureus* related infections, due to their coating in human serum and potential contact with patient's skin. *S. aureus* can adhere to fibrinogen and other molecules found in the extracellular matrices of mammalian sera and aggregate – forming biofilms on medical apparatus following implantation. These infections are notoriously difficult to treat due to the increased resistance to antibiotics that biofilms provide (Stewart & Costerton, 2001). Additionally, the increasing prevalence of penicillin and methicillin resistant *Staphylococcus aureus* (MRSA) makes treatment of these diseases more complicated. Methicillin typically binds to the bacterial penicillin binding proteins (PBPs) which are responsible for the transglycosylation and transpeptidation of the peptidoglycan cell wall and are therefore vital to the growth and division of the cell (Section 1.2.) (Hackbarth *et al*, 1995). These enzymes were named after their affinity for binding to penicillin, which in turn inhibit their cell wall synthesis activity (Waxman *et al*, 1983). *S. aureus*' ability to resist these antibiotics, as well as others, is a cause of great concern for global healthcare systems.

1.2. *S. aureus* Cell Division

Cell division by binary fission in *S. aureus* is a highly conserved, heavily regulated, and complex process which allows the exponential proliferation of bacterial cells (Tzagoloff & Novick, 1977). The division process of *S. aureus* can occur in three orthogonal planes (Turner *et al*, 2010) and completes every 20 – 30 minutes under optimum conditions. This includes both the synthesis and hydrolysis of peptidoglycan for cells to expand in size and septate into daughter cells (Egan *et al*, 2020), as well as the replication and segregation of DNA. This process is thought to be initiated by formation of a ring structure of the mammalian tubulin homologue FtsZ (Matsui *et al*, 2012). FtsZ is an essential GTPase which, once activated by GTP binding, forms a ring through the *S. aureus* mid cell. While required for the activation of FtsZ, GTP is thought to primarily facilitate FtsZ subunit recycling by polymer destabilisation (Mateos-Gil *et al*, 2012). FtsZ also recruits a variety of other proteins which are vital to cell division. One such example is FtsA, which has been shown to be an essential division protein in *S. aureus* that is thought to anchor FtsZ to the membrane, thereby facilitating the localisation of FtsZ at the membrane where cell division is initiated following the recruitment of a multi-protein divisome complex (Pinho & Errington, 2003; Maggi *et al*, 2008). Components of this divisome complex include, but are not limited to: DivIBC, FtsL, and EzrA (figure 1.1.) (Steele *et al*, 2011; Tinajero-Trejo *et al*, 2022).

EzrA is a division protein which is important for cell growth, as its loss results in delocalised cell division machinery and an inhibition of PBP mediated peptidoglycan synthesis (Steele *et al*, 2011). FtsL is a bitopic membrane bound protein which interacts with a host of division proteins in the Gram-positive bacteria *Bacillus subtilis* and *S. aureus*, including EzrA, DivIB, DivIC, and FtsW (Daniel *et al*, 2006). In fact, some of these interactions have been shown to be essential to maintain FtsL in *B. subtilis*, as the protein is naturally unstable (Robson *et al*, 2006). For example, FtsL is stabilised by DivIC, which prevents the zinc metalloprotease RasP from degrading FtsL as a substrate (Wadenpohl & Bramkamp, 2010). DivIB, like FtsL, is a membrane spanning protein with a hydrophobic N-terminal domains that are essential for localisation at the membrane and subsequent recruitment to the septum of *B. subtilis* (Wadsworth *et al*, 2008). Meanwhile, DivIC interacts with both DivIB and FtsL via a C-terminal trimeric complex at the membrane (Glas *et al*, 2015). DivIC also facilitates the arrangement

of peptidoglycan at the developing septum and binds to wall teichoic acids within the cell wall of *S. aureus* (Tinajero-Trejo *et al*, 2022).

The localisation of *S. aureus* membrane bound PBPs is also associated with the formation of the division complex. The PBPs are required to synthesise peptidoglycan at the mid-cell for cell division, as well as at the periphery of *S. aureus* cells (Wacnik *et al*, 2022). PBPs are essential for the final stages of peptidoglycan synthesis (Pinho *et al*, 2013), of which *S. aureus* has four. The synthesis of peptidoglycan by these PBPs can be observed as nascent cell wall material in dividing cells using fluorescent amino acid derivatives of D-alanine – a crucial and terminal amino acid in the peptide side chain of peptidoglycan (Chapters 3, 4, and 5). A septal plate of peptidoglycan is formed during division which bisects the cell, initiated by the FtsZ ring and the complex of multiple divisome components (Figure 1.1). Hydrolysis by autolysins, such as Atl and Sle1, at the outer edge of the septal plate initiate the septation of daughter cells from one another (Yamada *et al*, 1996; Kajimura *et al*, 2005). However, *S. aureus* cells do not always separate fully following septation and will often continue to grow while still attached to one another, giving rise to their characteristic clumping morphology (Pereira *et al*, 2007; Myrbråten *et al*, 2022; Takahashi *et al*, 2002; Touhami *et al*, 2004).

The synthesis of septal peptidoglycan is not only recognised as the initiation of cell septation and division but is also the primary site at which many surface proteins are incorporated into the cell wall. It is thought that, due to this being the predominant site of peptidoglycan synthesis in the cell, this is where surface proteins are anchored to the cell wall, which are then subsequently displayed on the surface following cell division when newly synthesised cell wall material is exposed (Zhang *et al* 2021). The hydrolysis of cell wall material as a natural part of bacterial growth and division is achieved by a range of peptidoglycan hydrolases, or autolysins (Wheeler *et al*, 205).

A

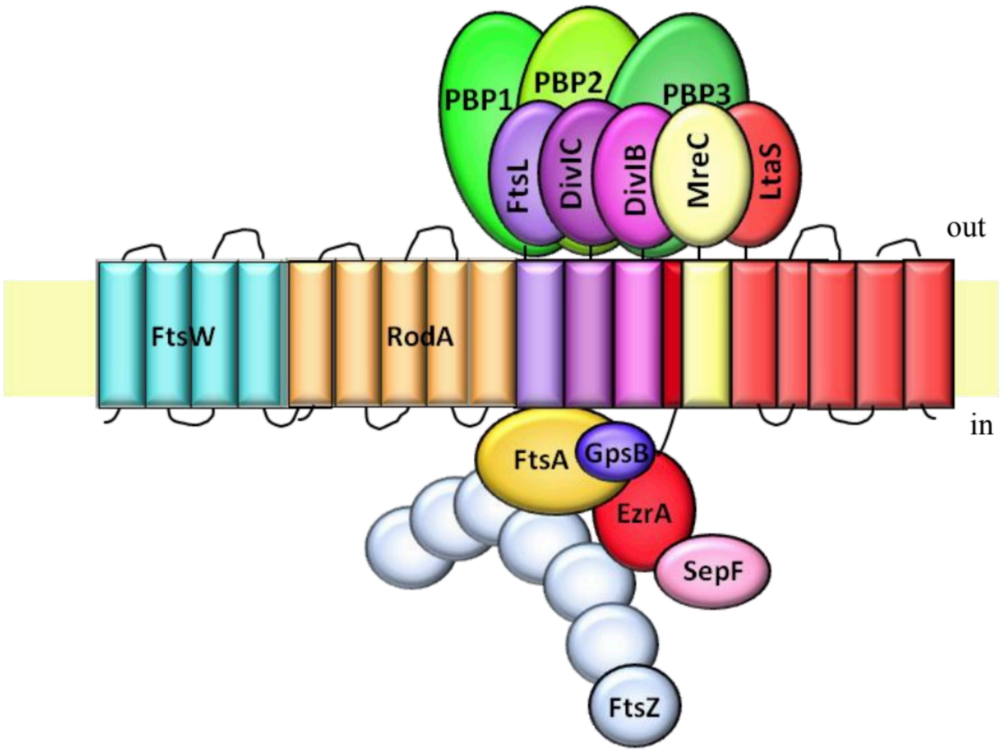

B

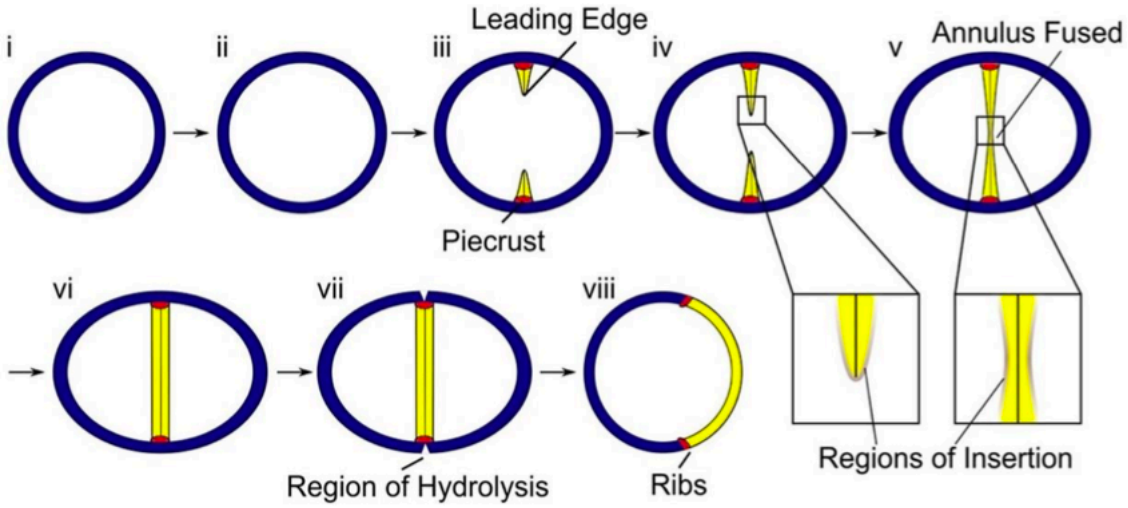

Figure 1.1. Septation and division in *S. aureus*

(A) Schematic representation of cell division components in *S. aureus*. CM refers to the cytoplasmic membrane of the cell. Taken from Bottomley, 2011. **(B)** Schematic model of *S. aureus* division and septal plate formation. Septal peptidoglycan (yellow) is synthesised at the leading edge of the septum, which meet to form the septal plate (iii – vi). The cell wall at the lagging edge of the septal plate is hydrolysed to initate seperation of daughter cells (vii – viii). Taken from Lund *et al*, 2018.

1.3. The Cell Wall of *S. aureus*

The cell wall is the outermost structure of Gram-positive bacteria and is primarily composed of peptidoglycan (Figure 1.2.). This structure provides essential integrity to the cell to maintain internal turgor pressure, osmolarity, and cell morphology. The peptidoglycan macromolecule is comprised of an *N*-acetylglucosamine (Glc-*N*Ac) – *N*-acetylmuramic acid (Mur-*N*Ac) sugar backbone, linked by β 1-4 bonds, with a peptide stem branching off the lactoyl group of Mur-*N*Ac's third carbon (Vollmer *et al*, 2008). The synthesis of peptidoglycan is a multi-step process involving several proteins and enzymatic reactions. Firstly, cytoplasmic fructose-6-phosphate and glutamine are converted to the peptidoglycan precursor uridine diphosphate-*N*-acetylglucosamine (UDP-Glc*N*Ac). UDP-Glc*N*Ac is then converted into UDP-Mur*N*Ac by the MurAB ligases. The synthesis of the pentapeptide stem to UDP-Mur*N*Ac and its subsequent attachment to undecaprenyl phosphate to form Lipid I is facilitated by MurCDEF and MraY (Patin *et al*, 2010). UDP-Glc*N*Ac is then linked to Lipid I to form Lipid II. Then, the FemXAB proteins build the pentaglycine bridge from the peptide stem's L-Lysine, while MurT and GatD facilitate the addition of a free amine group onto D-Glutamine (Giannouli *et al*, 2010; Münch *et al*, 2012). The cell wall precursor is then translocated across the phospholipid bilayer membrane by the flippase FtsW, before being cross-linked to pre-existing cell wall peptidoglycan (Taguchi *et al*, 2019). The transglycosylation of the sugar backbone and the transpeptidation of peptidoglycan is performed by membrane-bound penicillin binding proteins 1 and 3 (PBP1, 3) which form cognate pairs with FtsW and RodA (Meeske *et al*, 2016).

The peptide stem consists of L-Alanine, D-Glutamine, L-Lysine, which also includes a penta-glycine bridge with a free an amine group (NH_2) in *S. aureus,* followed by two terminal D-Alanine. The peptide stem is cross-linked to other peptide stems of the cell wall by the pentaglycine bridge, providing rigidity and structure to the cell wall (Gautam *et al*, 2015). This process is facilitated by the transpeptidase activity of certain PBPs. The synthesis and subsequent remodelling of the peptidoglycan layer is essential for the division of bacteria and is mediated by a complex co-ordination of enzymes collectively called the divisome (de Kruijff *et al*, 2008). For their critical and essential role in bacterial cell wall synthesis and cell division, many of the constituents of cell wall synthesis are targeted for antibiotic inhibition (Silver,

2003; Figure 1.2.).The inhibition of cell wall synthesis, achieved initially by β-lactam inhibition of PBPs, causes a bactericidal effect whereby bacterial cells are unable to grow and divide due to the lack of peptidoglycan transglycosylation and transpeptidation (Martin *et al*, 2022). Because of the essential nature of many of the elements of cell wall synthesis, antibiotics have been developed to target a range of cell wall synthesis and assembly pathways (Figure 1.4.). Of the four penicillin binding proteins in *S. aureus*, only PBP1 and PBP2 are essential. PBP1 facilitates transpeptidation activity, while PBP2 is bifunctional – capable of both transpeptidation and transglycosylation (Wacnik *et al*, 2022).

The biosynthesis of the bacterial cell wall peptidoglycan is a highly regulated and conserved pathway across all bacterial species, with similarities being shared in associated pathways – like mycolic acid synthesis in *Mycobacterium tuberculosis* (Peregrín-Alvarez *et al*, 2009; Lovering *et al*, 2012). Bacteria also produce a wide range of hydrolases, which cleave covalent bonds of the peptidoglycan cell wall (Vollmer *et al*, 2008). This suite of enzymes, sometimes referred to as autolysins, allows bacteria to remodel their cell wall – accommodating growth while also serving to turnover older cell wall material and release it into the extracellular milieu (Lee & Huang *et al*, 2013). Some of the most well-known autolysins of *S. aureus* that facilitate growth in *S. aureus* include SagB and LytH, responsible for cleaving long glycan chains to make the cell wall more flexible, and to break down uncrosslinked peptide stems, respectively (Sutton *et al*, 2021; Do *et al*, 2020). Hydrolases are vital, not only for bacterial growth, but also for the division of bacterial cells. For example, *S. aureus* produces the Atl autolysin, which cleaves at the leading edge of diplococcal cells to facilitate their division (Nega *et al*, 2020), while Sle1 cleaves the *N*-acetylmuramyl-L-Ala bond of peptidoglycan to facilitate cell separation (Kajimura *et al*, 2005). Some hydrolases are used in molecular microbiological research such as the endopeptidase lysostaphin, produced by *S. simulans* biovar *staphylolyticus*, to weaken the cell wall by peptide stem cleavage, such that cells can be lysed and their contents analysed (Kumar, 2008). While other peptidoglycan hydrolases play a role in both immune evasion and host-pathogen interactions through the remodelling of the cell wall (Dziarski & Gupta, 2010). Various autolysins also overlap in function, creating a redundancy among families of hydrolase enzymes, emphasising their essentiality toward bacterial growth (Heidrich *et al*, 2002). Peptidoglycan hydrolases are even utilised by some bacteriophage as a method to enter and exit bacterial cells (Vollmer *et al*, 2008).

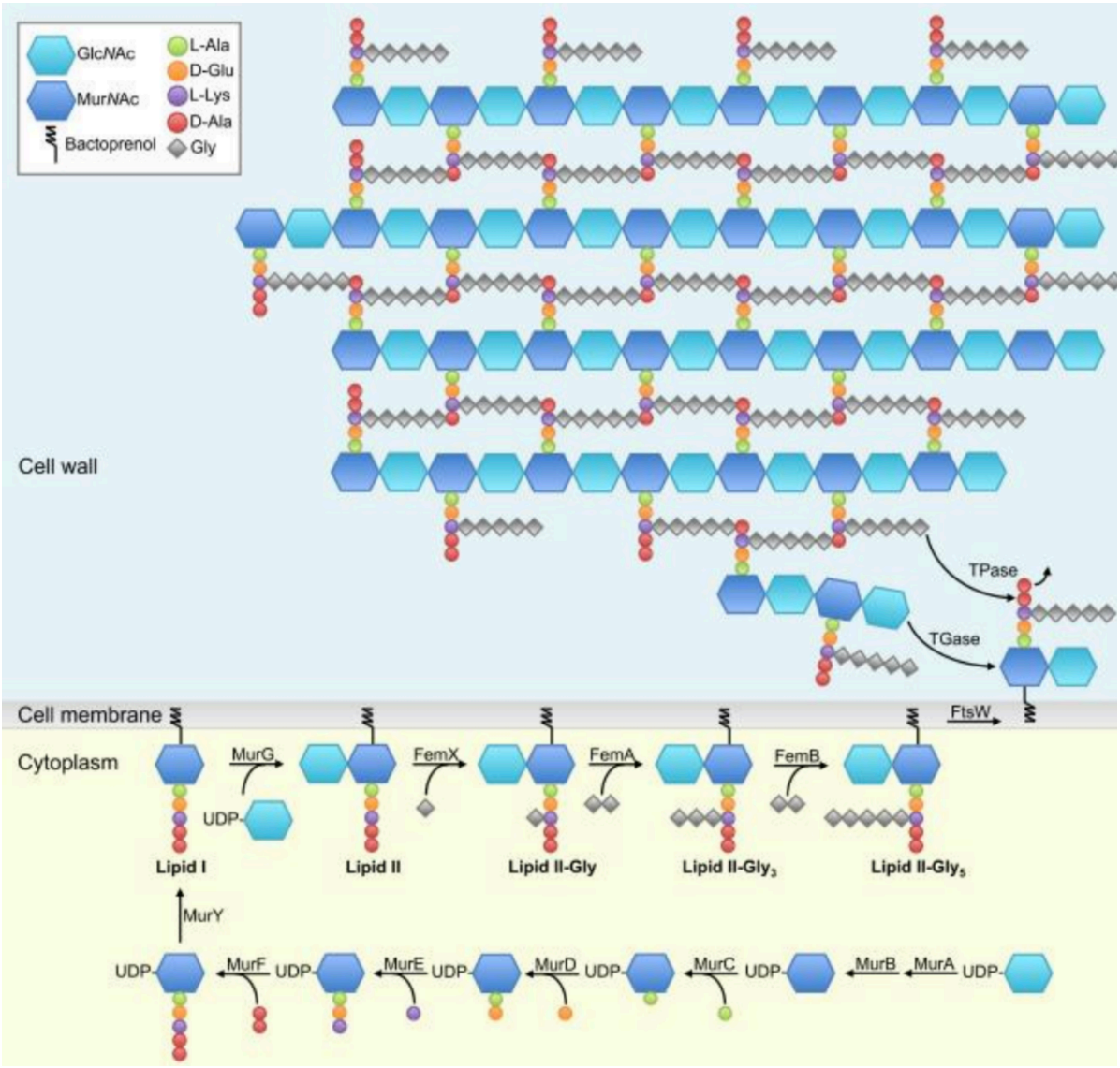

Figure 1.2. Schematic representation of peptidoglycan synthesis in *S. aureus*

Precursor molecules of peptidoglycan are synthesised in the cytoplasm of *S. aureus* before Lipid II is translocated across the phospholipid bilayer membrane. Transglycosylation and transpeptidation of Lipid II into the pre-existing peptidoglycan architecture is mediated by penicillin binding proteins MurJ has seen been shown to be the flippase in *S. aureus* which flips the Lipid II- Gly_5 across the membrane, in place of FtsW (Barbuti *et al*, 2023). Adapted from Typas *et al*, 2012.

Given the numerous applications and the essential nature of peptidoglycan hydrolases, a delicate balance of hydrolase regulation and peptidoglycan synthesis is required for the proper proliferation and growth of *S. aureus* cells, as an abundance of peptidoglycan synthesis without cell wall hydrolysis leads to the cessation of growth (Salamaga *et al*, 2021).

While the chemical composition of the peptidoglycan cell wall of bacteria is well understood, little is known about the architecture of this complex, interconnected macromolecule. Various models have been proposed based on what is understood about the chemical composition of the bacterial peptidoglycan cell wall (Dmitriev *et al*, 2005). However, recent work using Atomic Force Microscopy (AFM) has uncovered the distinct and detailed architecture of the cell wall of live *S. aureus* cells (Figure 1.3.; Pasquina-Lemonche *et al*, 2020). AFM is a high-resolution scanning probe microscopy technique that enables the elucidation of surface structures to a nanometre scale. This technique can be used to generate topographical maps of material surfaces, including the cell wall of *S. aureus*.

Figure 1.3. shows that the cell wall of *S. aureus* is far from homogeneous. *S. aureus* appears to possess two distinct cell wall architectures on the surface: a porous, mesh-like structure of older cell wall material, and a tight, concentric ring-like structure of nascent peptidoglycan. This work by Pasquina-Lemonche *et al* (2020) notes that the internal sacculus is a dense mesh throughout, even at the division septa where, on the external cell wall, they observed the ring organisation of peptidoglycan. The ring structure is degraded over time, following cell division, to reveal the mesh structure observed beneath. This is likely achieved by hydrolysis of *S. aureus* peptidoglycan via various autolysins (Chapter 6). When topographical AFM is used, intricate details of the cell wall are observed, with the ability to visualise individual glycan strands. However, other constituents of the cell wall, besides the architecture of peptidoglycan, cannot be observed by topographical AFM alone. The localisation of cell wall associated surface proteins, for example, requires alternative and specific methods of investigation.

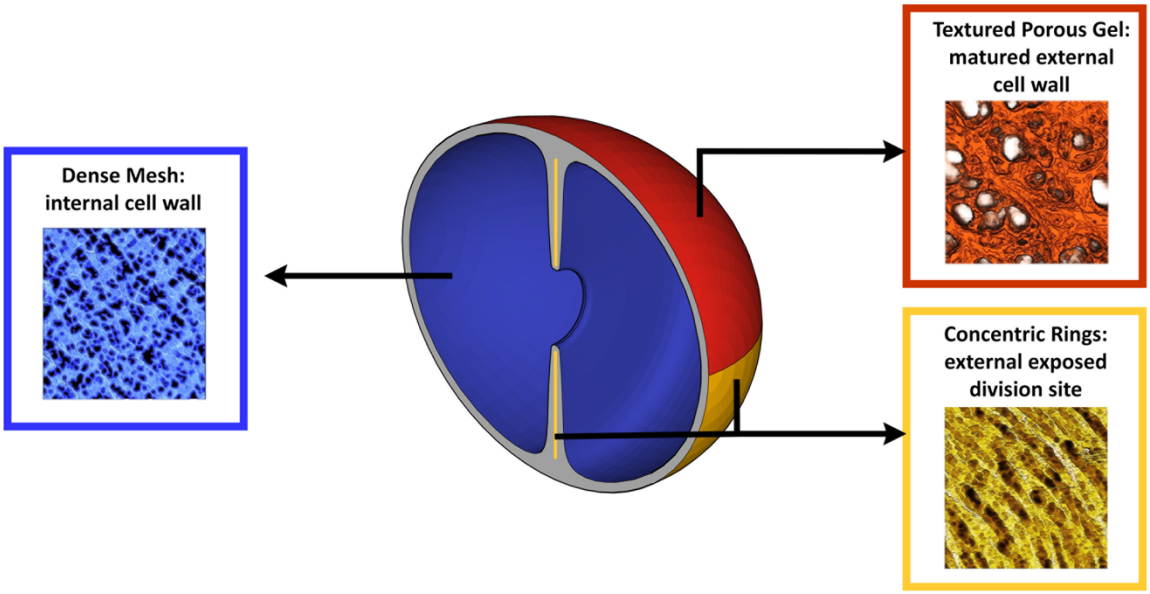

Figure 1.3. *S. aureus* cell wall architecture model as defined by AFM

Schematic representation of *S. aureus* cell wall architecture determined by atomic force microscopy. Blue represents the mesh structure observed throughout the internal sacculus. Yellow shows concentric ring architecture within the septal plate that becomes observable on the cell surface at the division site. Red demonstrates the porous mesh structure of the mature, external cell wall. Taken from Pasquina-Lemonche *et al*, 2020.

1.4. Antibiotic Resistance in *S. aureus*

The first recorded instance of penicillin resistant *S. aureus* occurred just two years after its implementation as an antibiotic in 1940. The mechanism for this resistance was later attributed to the acquisition of the *blaZ* gene, which encodes the penicillinase enzyme. This enzyme cleaves penicillin's β-lactam ring, thereby neutralising its effect as a D-ala-D-ala mimicking molecule to irreversibly bind and inhibit PBPs (Sabath, 1982). To counter the first emergence of antibiotic resistance, another β-lactam antibiotic was developed that was not affected by penicillinase, called methicillin (Lowy, 2003). However, methicillin resistant *S. aureus* (MRSA) isolates were cultured from a patient suffering from septic arthritis in 1960 (Jevons *et al*, 1963). The subsequent proliferation of patients with both methicillin susceptible *S. aureus* (MSSA) and MRSA infections have contributed significantly to *S. aureus*' status as both a community acquired disease, and a nosocomial pathogen (Cosgrove *et al*, 2003). Additionally, cases of livestock infections with MRSA have also increased with the prevalence of antibiotic use in agricultural feed (Butaye *et al*, 2016). As a result of these consequences, such as implicated side effects like interstitial nephritis, and its impact on global healthcare systems, methicillin is no longer available for clinical use in many countries (Sanchez-Alamo *et al*, 2023). However, MRSA is still used to describe *S. aureus* infections that are generally resistant to β-lactam antibiotics as well as extensively resistant *S. aureus* infections that include antibiotics besides β-lactams (Enright *et al*, 2002). The acquisition of the *mecA* gene which encodes penicillin binding protein 2a (PBP2a) allows *S. aureus* to grow in the presence of β-lactam antibiotics, including methicillin (Llarrull *et al*, 2009). This is thought to be the result of PBP2a having a functional site of a different physical structure to that of β-lactam susceptible PBPs (Lim *et al*, 2002), while still being able to synthesise peptidoglycan. As such, other antibiotics are being more heavily relied upon to treat staphylococcal infections, such as vancomycin, a cell wall synthesis inhibitor, trimethoprim, a nucleic acid synthesis inhibitor, and linezolid, a protein synthesis inhibitor (Moor *et al*, 2023; Quinlivan *et al*, 2000; Livermore, 2003; Figure 1.4.). However, resistance to these last-resort antibiotics has also been reported in extensively resistant *S. aureus* which require over 256 μg mL^{-1} methicillin to achieve the minimum inhibitory effect (MIC) (Assadullah *et al*, 2003). As such, alternative treatments, and an enhanced understanding of the mechanisms of antibiotic resistance in *S. aureus* are of critical importance to combat antibiotic resistant infections.

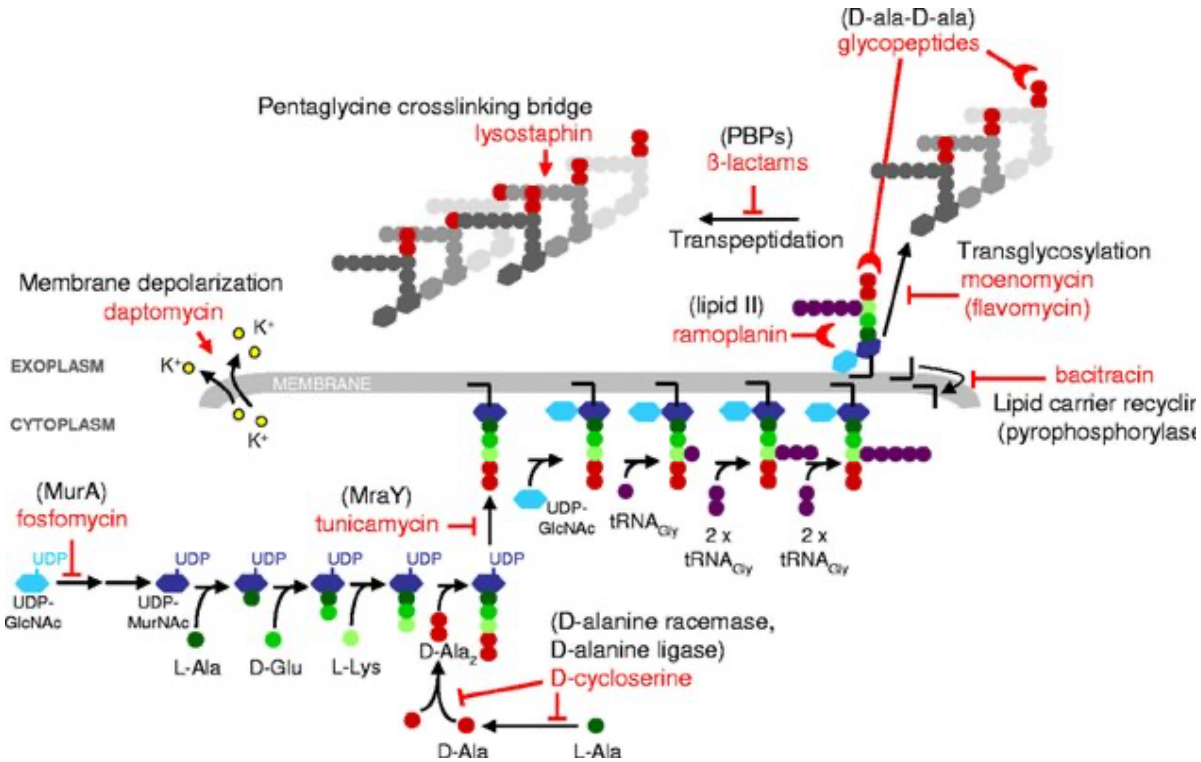

Figure 1.4. Schematic representation of peptidoglycan cell wall synthesis, including antibiotic targets

Red text indicates antibiotics that target their associated bacterial processes. Pointed arrows indicate antibiotics that inhibit peptide stem cleavage and disruption of the membrane associated ion exchange, such as lysostaphin and daptomycin, respectively. Flat arrows signify antibiotics that inhibit enzymatic reactions, such as tunicamycin and bacitracin. Crescent arrows indicate antibiotics that affect cell wall synthesis, such as glycopeptides and ramoplanin. Taken from McCallum *et al*, 2011.

1.5. Teichoic Acids

The thick peptidoglycan layer of the Gram-positive cell wall not only provides structural integrity and protection against osmotic shock to the cell but is also used as an anchor point for many polypeptides and other molecules (van Dalen *et al*, 2020). These allow *S. aureus* to interact with its environment via the adhesion of surface proteins and teichoic acids to various molecules in the extracellular matrices of hosts (Chavakis *et al*, 2005). Teichoic acids are an important component of the Gram-positive cell wall. Both wall teichoic acids and lipoteichoic acids, anchored within the peptidoglycan cell wall and phospholipid bilayer membrane respectively, are known to play a role in the virulence of Gram-positive bacteria and are essential for colonising multiple niches (Weidenmaier *et al*, 2004; Holland *et al*, 2011). It has also been shown that teichoic acids play a role in the regulation of PBP4 activity cross-linking peptidoglycan, particularly at the division septa of *S. aureus* (Atilano *et al*, 2010). Additionally, teichoic acids are thought to play a crucial role in the regulation of surface protein display (Atilano *et al*, 2010). However, studies have also shown that teichoic acids are not essential for viability in many Gram-positives, including *Bacillus subtilis* and *S. aureus* (D'Elia *et al*, 2006).

1.6. Covalently Bound Surface Proteins

S. aureus is known to express several surface proteins associated with the peptidoglycan cell wall (Foster, 2019). Many of these are covalently bound to the cell wall, while other are ionically bound to the surface of the cell. Surface proteins are mediators of infection – facilitating adhesion to various molecules and surfaces within the human body, which allow the bacteria to subsequently cause disease (Foster, 2019). It is therefore imperative to not only understand their individual function, but also their molecular localisation on the surface of *S. aureus*. Many surface proteins contain motifs at their N and C termini which are thought to contribute to translocation dynamics and cell wall binding, respectively. These include the N-terminal YSIRK motif, and the C-terminal LPXTG motif in *S. aureus*, both of which are highly conserved, with slight variations of the Isoleucine and Arginine of the YSIRK sequence (Bae & Schneewind, 2003). Table 1 contains the most well studied and prominent genes encoding surface proteins in *S. aureus* and has been listed in ascending order of molecular mass.

Table 1.1. Staphylococcal surface proteins

Gene name	Product / function	Binding to cell wall	Sorting signal	Signal peptide	Molecular mass (kDa)	Reference
SasX	Colonisation / pathogenesis in MRSA	Covalent	LPXTG	-	15	Chen *et al*, 2012
SasG	Adhesion / biofilm formation	Covalent	LPKTG	-	21	Corrigan *et al*, 2007
SasD	Adhesion	Covalent	LPXTG	-	22	Mäder *et al*, 2016
SasK	Cell structure / peptidase	Covalent	LPXTG	-	23	Trad *et al*, 2004
IsdC	Iron acquisition	Covalent	NPQTN	-	25	Reniere & Skaar, 2008
IsdA	Iron acquisition	Covalent	LPXTG	-	39	Clarke *et al*, 2004
LytN	Cell wall hydrolase	Ionic	-	YSIRK-GXXS	42	Frankel *et al*, 2011
SpA	IgG binding	Covalent	LPXTG	YSIRK-GXXS	56	Foster & Höök, 1998
SasF	Adhesion	Covalent	LPXTG	-	71	King *et al*, 2012

IsdB	Iron acquisition	Covalent	LPXTG	YSIRK-GXXS	72	Gaudin *et al*, 2011
GehB	Lipase	Ionic	-	YSIRK-GXXS	76	Cadieux *et al*, 2014
GehA	Hydrolase / lipase	Ionic	-	YSIRK-GXXS	77	Cadieux *et al*, 2014
AdsA	Adenosine synthase	Covalent	LPXTG	-	83	Thammavongsa *et al*, 2009
ClfB	Fibrinogen adhesion	Covalent	LPXTG	YSIRK-GXXS	94	Foster & Hoök, 1998
ClfA	Fibrinogen adhesion	Covalent	LPXTG	YSIRK-GXXS	96	Foster & Hoök, 1998
IsdH	Iron acquisition	Covalent	LPXTG	YSIRK-GXXS	101	Sæderup *et al*, 2016
FnbB	Adhesion / Fibronectin binding	Covalent	LPXTG	YSIRK-GXXS	101	Speziale & Pietrocola, 2020
SdrC	Biofilm formation	Covalent	LPXTG	YSIRK-GXXS	103	Barbu *et al*, 2014
FnbA	Adhesion / Fibronectin binding	Covalent	LPXTG	YSIRK-GXXS	109	Speziale & Pietrocola, 2020

SdrE	Calcium binding / adhesion	Covalent	LPXTG	YSIRK-GXXS	124	Sharp *et al*, 2012
Cna	Collagen binding	Covalent	LPXTG	-	133	Zong *et al*, 2005
SdrD	Calcium binding / adhesion	Covalent	LPXTG	YSIRK-GXXS	146	Josefsson *et al*, 1998
SasL	Unknown	Covalent	LPXTG	YSIRK-GXXS	180	Foster *et al*, 2014
SraP	Platelet binding	Covalent	LPXTG	KxYKxGKxW	228	Siboo *et al*, 2005
pls	Biofilm formation	Covalent	LPXTG	YSIRK-GXXS	230	Savolainen *et al*, 2001
SasC	Peptidase	Covalent	LPXTG	YSIRK-GXXS	238	Schroeder *et al*, 2009
bap	Biofilm formation	Covalent	LPXTG	YSIRK-GXXS	240	Cucarella *et al*, 2001
FmtB	Cell wall biosynthesis / methicillin resistance	Covalent	LPXTG	YSIRK-GXXS	263	Komatsuzawa *et al*, 2000
Ebh	Unknown	Ionic	-	YSIRK-GXXS	1030	Clarke *et al*, 2002

1.7. Sortase A

The translocation and surface display of many of *S. aureus*' surface proteins are required for the colonisation and subsequent infection of host organisms. This is facilitated for many virulence factors by Sortase A (SrtA). SrtA is a membrane-bound transpeptidase that cleaves the bond between threonine and glycine in the LPXTG sorting signal motif (Leucine, Proline, any amino acid, Threonine, Glycine) found at the C-terminus of many of *S. aureus*' surface proteins (Zong *et al*, 2004). This forms an acyl-enzyme intermediate between Sortase and the carboxyl group of threonine within a protein's LPXTG motif. SrtA then catalyses the transpeptidation of the surface protein to the peptidoglycan precursor Lipid II (undecaprenyl-pyrophosphate-MurNac(-L-Ala-D-iGln-L-Lys(NH_2-Gly_5)-D-Ala-D-Ala)-β1-4-GlcNac), via the free amine group of the pentaglycine bridge (figure 1.5.) (Ruzin *et al*, 2002; Suree *et al*, 2009). Then, via transglycosylation, the surface protein-peptidoglycan Lipid II precursor is incorporated into the cell wall (Maňásková *et al*, 2016). As Lipid II precursors are incorporated into the cell wall architecture, the protein attached to it is displayed on the cell surface, where it can interact with the environment when fully exposed on the bacterial cell surface. Surface protein A (SpA) display has previously been used to suggest the localisation of SrtA at the developing septum of *S. aureus* cells (Zhang *et al*, 2021).

There are three forms of Sortase – A, B, and C (SrtABC) – that are present in Gram-positive bacteria, such as Bacilli, Listeria, Streptococcus, and Clostridium species (Bierne *et al*, 2004; Marraffini *et al*, 2007). Each Sortase form recognises a distinct pentapeptide sequence like LPXTG and serves various functions. SrtA recognises the LPXTG motif and is used to incorporate a wide range of proteins into the cell surface (Figure 1.5.). SrtB recognises the NPQTN pentapeptide and is associated with the iron deprivation response in *S. aureus* and Listeria. While SrtC binds to the QVPTG sequence and is associated with the polymerisation of pilin (Clancy *et al*, 200). It has been shown previously, using a murine infection model, that SrtA is required for the development of severe arthritis, while SrtB is thought to play a role in the pathogenesis of *S. aureus* (Jonsson *et al*, 2003).

It is thought that the inhibition of Sortases may result in the reduced virulence capacity of *S. aureus*, due to its role in surface protein display (Suree *et al*, 2009). However, many bacterial proteins also contain the Lysine Motif (LysM domain), which can ionically bind proteins to the cell envelope, including the N-acetylmuramyl-L-alanine amidase (Sle1), elastin-binding protein (EbpS), and surface protein A (SpA) (Buist *et al*, 2008; Figure 1.8.). These ionic bonds are much weaker than their covalent counterparts, such as those facilitated by Sortase activity, and are therefore prone to detachment or denaturation from the cell wall in unfavourable environmental conditions, such as adverse temperatures and changes in pH (McGettrick & Worrall, 2004).

Sortases can also be used to analyse proteins possessed of an LPXTG motif, both native and recombinant, by immobilising them to a variety of surfaces or bacterial species. Additionally, sortases have been used for the purification of proteins functionally similar to tags such as hexahistidine and biotin (Popp & Ploegh, 2011). Using Sortase enzymes to isolate, immobilise, and purify proteins affords several advantages from a biotechnological perspective. For example, the acyl-enzyme intermediate bond between Sortase and a peptide containing the LPXTG sequence is consistent in its orientation, relative to the sorting motif. Additionally, the nature of Sortase interactions with the LPXTG motif means that a range of recombinant proteins can be studied under the same conditions, removing the need to optimise for ligation under different experimental conditions, as well as being usable to bind proteins to the surface of bacteria.

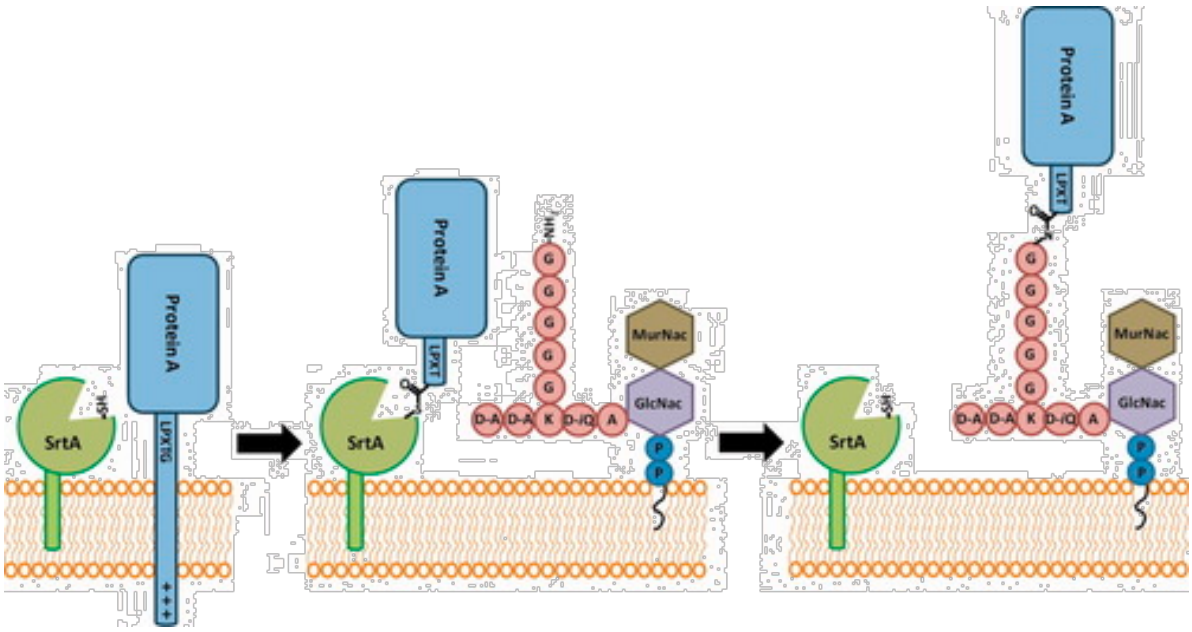

Figure 1.5. Schematic representation of LPXTG-containing surface protein translocation and Sortase activity

Surface proteins of *S. aureus* are translocated across the phospholipid bilayer membrane. Proteins containing an LPXTG motif at their C-terminus form an acyl-enzyme intermediate with Sortase A, which is then relieved by and covalently bound to the free amine group of the peptide stem's pentaglycine bridge of the LipidII linked muropeptide. Taken from Clancy *et al*, 2010.

1.8. Iron-Regulated Surface Determinants

A range of iron-regulated surface determinant (Isd) proteins are expressed by *S. aureus*, which contain the NEAr-iron Transporter (NEAT) domain. It was originally believed that these domains were involved in siderophore binding (Honsa & Maresso, 2011; Grigg *et al*, 2010; Mazmanian *et al*, 2003; Andrade *et al*, 2002). However, it has since been shown that NEAT domains allow Gram-positive bacteria to acquire heme-iron from both its mammalian host's haemoglobin and the haptoglobin-hemoglobin complexes (Honsa *et al*, 2014). Proteins with the NEAT motif are typically covalently bound to the peptidoglycan cell wall in *S. aureus* and deliver heme-iron through to the bacterial cytosol (Bates *et al*, 2003; Skaar & Schneewind, 2004; Figure 1.6.). NEAT domains are characterised by 8 β-strands and a 3_{10} alpha helix that acts as a hydrophobic heme-binding pocket (Sharp *et al*, 2007). This work will focus on IsdA and IsdB. IsdA is a broad-spectrum adhesin that binds to elements of the extracellular matrix (ECM), such as fibrinogen and fibronectin, as well as acting as a transferrin receptor of heme-iron (Mazmanian *et al*, 2003; Clarke *et al*, 2004). IsdA has also been shown to confer resistance against the antimicrobial properties of fatty acids found on human skin (Clarke *et al*, 2007). IsdB binds haem, haemoglobin, and 3β integrins. It is also thought to be involved in the invasion of non-phagocytic cells (Zapotoczna *et al*, 2013). IsdB uses host haemoproteins, haemoglobin, and myoglobin to acquire iron, but does not bind hemopexin, haptoglobin or the haemoglobin-haptoglobin complex (which is instead achieved by IsdH). IsdB possesses a C-terminal LPXTG motif, which is recognised by Sortase A (SrtA) and is therefore covalently bound to the cell wall peptidoglycan. IsdA possesses one NEAT domain, while IsdB possesses two – both at their N-terminus (Sæderup *et al*, 2016).

1.7.1. Iron-Regulated Surface Determinant Regulation and Translocation

The proteins IsdABCH are thought to be regulated by the ferric uptake regulator protein (Fur), which is in turn regulated by PerR – a self-regulating Fur homologue – though the precise mechanisms of regulation are unknown (Wiltshire *et al*, 2001; Torres *et al*, 2010). IsdA possesses the LPXTG sorting signal motif and is anchored into the cell wall by SrtA activity. IsdB possesses a YSIRK signal peptide motif, which is generally associated with the SecYEG translocation machinery, and an LPXTG sorting signal motif associated with SrtA (Bae & Schneewind, 2003).

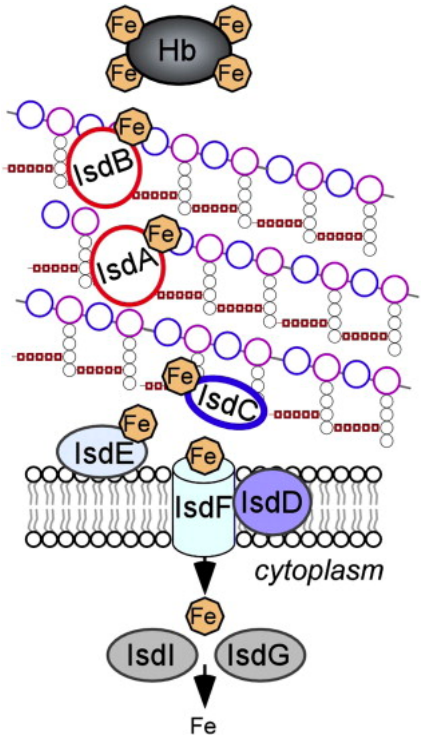

Figure 1.6. Schematic of iron-regulated surface determinant transfer of host iron

The Iron-regulated surface determinant cascade binds to heme iron in the host and transports it through the Gram-positive cell wall of *S. aureus* and across the phospholipid bilayer membrane into the cyoplasm for metabolism. IsdA and IsdB are anchored to the cell wall by Sortase A, acting a receptors for heme iron. The transport of iron through the cell wall is facilitated by IsdC, which is anchored to the cell wall by Sortase B. Heme iron is then transported across the membrane by the IsDEF complex, and is subsequently degraded by IsdG and IsdI. Taken from Schneewind & Missiakas, 2014.

1.9. Clumping Factor A

Clumping factor A (ClfA) is a covalently bound surface protein responsible for bacterial adhesion to the gamma chain of the human glycoprotein fibrinogen (Figure 1.7.). It also promotes the clumping of bacterial cells, which is known to allow *S. aureus* to evade phagocytosis due to the size of aggregated bacteria (McDevitt, *et al*, 1997). ClfA has also been shown to degrade C3b, a vital component of the mammalian innate immune system's complement cascade, which thereby prevents opsonisation and subsequent phagocytosis of the bacteria (Ghasemian *et al*, 2015).

ClfA is one of several Microbial Surface Components Recognising Adhesive Matrix Molecules (MSCRAMMs), which are collectively responsible for mediating the initial attachment of the bacteria to its host – along with other secreted factors and teichoic acids (Patti *et al*, 1994). Many MSCRAMMs facilitate the formation of biofilms, such as ClfA, collagen-binding protein (Cna), and fibronectin-binding protein (FnbP). FnbP is a major MSCRAMM of *S. aureus* known to facilitate the colonisation of mammalian hosts via adhesion to fibrinogen and fibronectin and is also known to confer resistance to antibiotic treatments (Herman-Bausier *et al*, 2016). MSCRAMMs typically have a structural domain organisation consisting of a signal sequence (S) followed by a ligand binding domain (A), a β-repeat region (B), a Serine-aspartic acid repeat region (R), a wall-spanning region (W), an LPXTG motif which is recognised by SrtA for the covalent binding of proteins to the cell wall, a transmembrane region (M), and a cytoplasmic domain (C) (Jonsson *et al*, 2003).

1.9.1. Clumping Factor A Regulation and Translocation

ClfA is thought to be negatively regulated by MgrA and is predominantly produced during stationary growth phase. This repression is alleviated by the ArlRS two component system though an unknown signal. This cascade also represses the expression of Ebh, SraP, and SasG, which act as umbrella proteins – obfuscating ClfA-mediated fibrinogen binding. The repression of these umbrella proteins allows ClfA to bind to fibrinogen in its host's extracellular matrices by making it a prominent and ubiquitously expressed surface protein (Jenul & Horswill, 2019). ClfA is translocated across the bacterial membrane via the SecYEG complex, and covalently bound to the cell wall by SrtA (Tsompanidou *et al*, 2012).

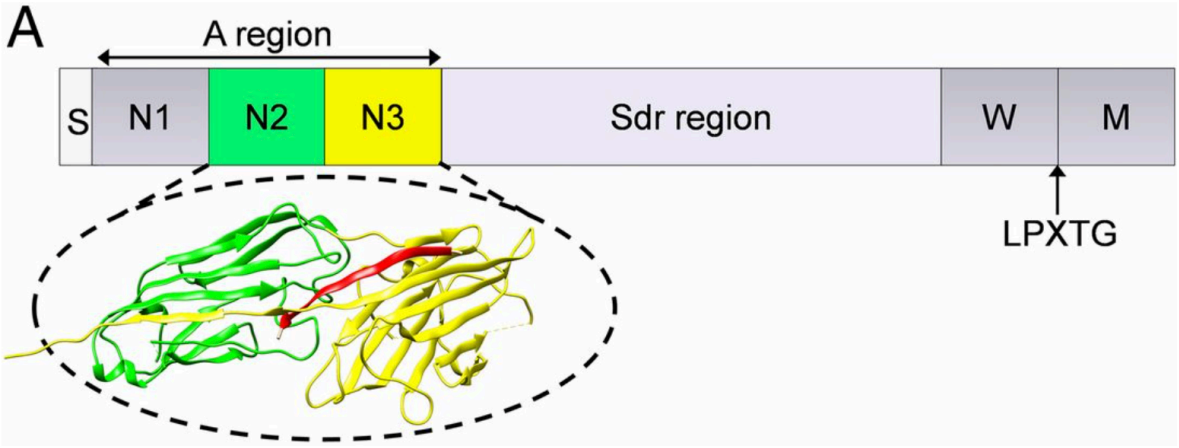

Figure 1.7. Schematic and crystal structure of ClfA

Schematic representation of ClfA domain organisation. The signal sequence (S) is located at the N-terminus, followed by the A region, which is comprised of the N1, N2, and N3 domains, a serine-aspartate repeat region (Sdr), a cell wall spanning region (W), the sorting signal LPXTG, and the cytoplasmic tail (M) at the C-terminus. Ligand binding regions N2 and N3 are highlighted in green and yellow, respectively. The red sheet located within the binding trench of N2 and N3 is representative of the carboxy terminus of the γ-chain of fibrinogen. Adapted from Herman-Bausier *et al*, 2018.

1.10. Surface Protein A

Another MSCRAMM of *S. aureus* is Protein A (SpA). While it does not bind fibronectin – a trait shared by the majority of MSCRAMMS – this highly immunogenic protein binds the constant (Fc) domain of IgG and IgM, as well as the Fab domain of antibodies (Foster & Höök, 1998). The binding of immunoglobulins by SpA is achieved via five homologous binding domains: E, D, A, B, and C (Graille *et al*, 2000; Figure 1.8.). This enables evasion of the innate and adaptive immune systems by impairing phagocytosis and preventing opsonisation (Muthukrishnan *et al*, 2011). SpA is also capable of binding the V_H3^+ Fab fragments displayed on the surface of B lymphocytes, promoting the clonal expansion of B lymphocytes and their subsequent cell death (Sasso *et al*, 1991). As a result, the host B cell response and antibody secretion against *S. aureus* infection is prevented, thereby prolonging the infection. Additionally, both covalently surface-bound protein A and secreted protein A have been shown to play a part in biofilm formation, disease progression, and immune evasion contributing significantly to the increase of antibiotic resistant infections and disease prevalence (Merino *et al*, 2009; Becker *et al*, 2014). SpA is also known to interact with von Willebrand factor, as well as tumour necrosis factor receptor 1 (Hartleib *et al*, 2000; Gómez *et al*, 2004). Mutant strains of *S. aureus* lacking SpA have been shown to possess greatly reduced virulence capacities. Mice infection models have been shown to promote *S. aureus* specific antibodies in the absence of SpA display, such that reduced pathogenesis is observed upon subsequent infection with *S. aureus* strains displaying SpA (Johnson *et al*, 1985; Cheng *et al*, 2009). Similarly, it has been shown that the release of SpA into the extracellular milieu contains the intact sorting signal motif LPXTG, implicating a lack of SrtA processing (O'Halloran *et al*, 2015).

SpA is considered a ubiquitous protein of *S. aureus* and as such has been widely studied (Gao *et al*, 2004). So much so that SpA is used to characterise *S. aureus* isolates globally in a range of healthcare settings as an assessment of virulence. These characterisations of *S. aureus* isolates are used to inform potential treatment strategies. This approach is known as SpA typing (Asadollahi *et al*, 2018; Strommenger *et al*, 2008). SpA has also been used as the target for the development of vaccines against *S. aureus*, with successful results displayed in mice (Kobayashi & DeLeo, 2013).

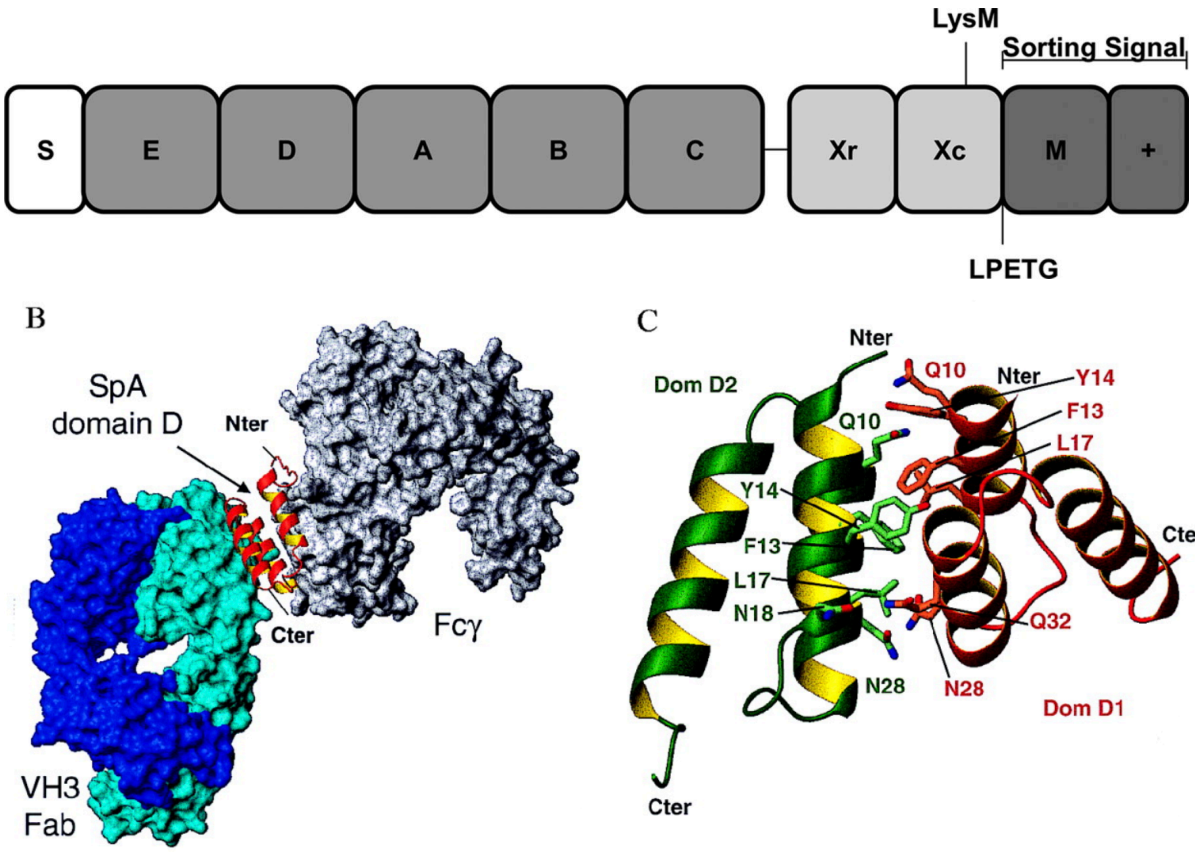

Figure 1.8. Crystal structure of SpA complexed with both the constant domain and Fab domain of immunoglobulins

(A) Schematic representation of SpA domains, including the signal sequence (S) Ig binding domains E, D, A, B, and C, the antigenic variable region (Xr), a cell wall spanning region (Xc) which contains the LysM domain. The sorting signal contains the LPXTG sorting signal motif, a hydrophobic membrane region (M), and a positively charged tail region (+). Taken from O'Halloran *et al*, 2015. **(B)** Cross linking of the V_H3 Fab domain (cyan) and an Fc domain of mammalian immunoglobulins by SpA domain D. **(C)** Purification of IgG binding domain D of surface protein A is composed of three α-helices (red; Dom D1), shown dimerised to a second purified D domain (green; Dom D2) as an asymmetric unit. Taken from Graille *et al*, 2000.

1.10.1. Surface Protein A Regulation and Translocation

The regulation and translocation of SpA to the cell surface of *S. aureus* is well understood. The expression of *spa* is negatively regulated by the global virulence regulator Agr (accessory gene regulator) which is a quorum sensing system that contains a response regulator (AgrA) and a sensor histidine kinase (AgrC) (Paulander *et al*, 2018). *S. aureus*, like many bacteria, secrete various autoinducing peptides which signal cell density within and across species (Sturme *et al*, 2002). In response to the reception of AgrD autoinducing peptides (AIPs) during stationary growth phase, the Agr system is upregulated. AgrC binds AgrD AIP at critical concentrations, resulting in an autophosphorylation event of AgrC. A phosphate group is transferred from AgrC to AgrA, which then induces the expression of RNAIII – binding the *spa* transcript and preventing translation – thereby negatively regulating SpA production (Figure 1.9.). As such, SpA is only produced, and therefore incorporated into the cell wall, during exponential growth phase, when AgrD AIP are at lower concentrations (Cheung, *et al*, 2008; Canovas *et al*, 2016). This transition also marks a shift in *S. aureus* whereby the production of secreted toxins is repressed, and the production of surface proteins is upregulated by the AgrA-induced transcription of RNAIII (Thompson & Brown, 2021). In addition, the SarA family of proteins is known to play a role in the regulation of Agr during this growth phase transition. The *sarA* locus is repressed by SarA and SarR, while the stress-induced transcription factor SigB promotes the expression of SarA. This in turn regulates the activation of Agr, and therefore the repression of SpA (Oriol *et al*, 2021). Additional contributing factors to *spa* expression include the Rot virulence regulator protein, MgrA repression, temperature, and pH levels (Zhu *et al*, 2019; Ingavale *et al*, 2005; Huang *et al*, 2012).

The structure and function of SpA has been well studied, but the localisation of this surface exposed virulence factor is poorly understood. One structural element of surface protein A includes the presence of the LPXTG motif at its C-terminus. This motif is recognised by the membrane bound SrtA, which facilitates the covalent binding of SpA into the cell wall architecture. A second, N-terminal motif known as YSIRK directs SpA to the cross wall of dividing cells for cell wall incorporation and subsequent display on the cell surface (Roche *et al*, 2003; DeDent *et al*, 2008). Translocation of SpA and many other surface proteins is facilitated by the SecYEG secretion system (Sibbald *et al*, 2010).

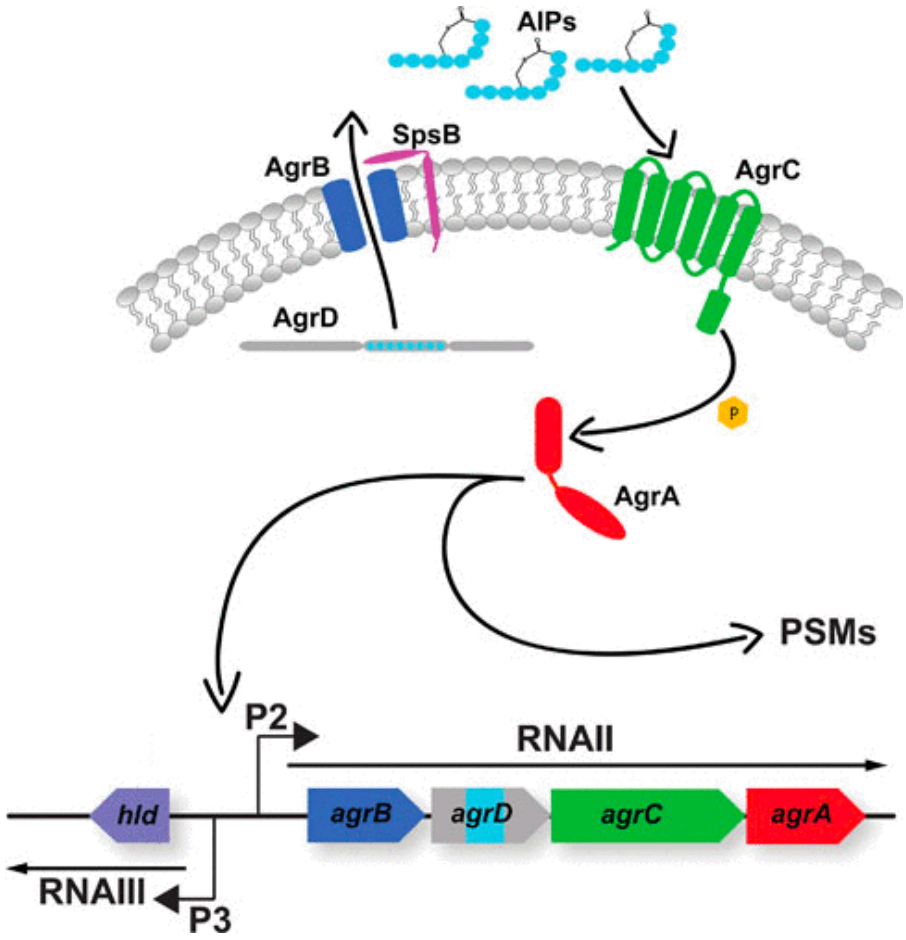

Figure 1.9. Schematic representation of Agr regulation and induction by AIPs

Quorum sensing Agr auto-inducing peptide (AIP) is encoded within *agrD*, transported into the envionment by AgrB and SpsB, and recognised by AgrC at the membrane. The production of AIPs at critical levels is achieved during post-exponential growth phase, wherein AgrC, a histidine kinase, binds AIPs. AgrC is autophosphorylated, and that phosphate is transferred to AgrA, which bind to *agr* promotors P2 and P3. This drives the expression of RNAII and RNAIII transcription, respectively. RNAII encodes the *agrBDCA* operon, responsible for AIP biosynthesis and the sensor-regulator machinary, while RNAIII regulates the expression of various secreted toxins and surface proteins. RNAIII also binds the *spa* transcript as antisense RNA to prevent *spa* translation, and thereby acts as a negative regulator. Taken from Jenul & Horswill, 2019.

1.11. Molecular Co-ordination of Precursor Peptides

Signal peptides are present at the N-terminus of many surface proteins and facilitate the secretion and translocation of proteins in bacteria (DeDent *et al*, 2008). The signal peptide functions as a binding site for chaperone enzymes and a recognition sequence for the secretion machinery, such as SecYEG (Section 1.10.1.; Briggs & Gierasch, 1986). Work done by Bae and Schneewind in 2003 shows that a motif within many of *S. aureus*' surface protein signal sequences, YSIRK G/S, plays an important role in the processing and secretion of surface protein A (SpA). Their work also reports that, while SpA processing and secretion were significantly reduced because of various YSIRK G/S mutations, the covalent attachment of SpA to the cell wall and the prevalence of SpA displayed on the bacterial surface was unaffected. Subsequent work done by DeDent *et al* (2008) showed that recombination of the YSIRK G/S motif into the signal peptide sequence of surface proteins that naturally lack YSIRK G/S, alter their sites of secretion. Clumping factor A (ClfA) possess the YSIRK G/S motif and displays a ring-like distribution around the *S. aureus* cell, while another surface protein, SasF, which lacks this sequence, is secreted onto the surface of the cell at distinct and punctate sites. The group has not only shown that recombinant SasF with the YSIRK G/S sequence is secreted across the whole cell surface, but also that removal of YSIRK G/S from ClfA caused it to be secreted at distinct foci on the bacterial surface. This suggests that the YSIRK G/S motif is important in the molecular co-ordination of precursor peptides and potentially impacts the localisation dynamics of surface proteins.

The possession of a YSIRK signal sequence motif at the hydrophobic N-terminal domain of surface exposed proteins is a shared characteristic across many Gram-positive bacterial species (Bai *et al*, 2020). The association between the YSIRK motif and the SecYEG translocon regarding key virulence determinant proteins in *S. aureus* and other Gram-positive organisms highlights some of the coordinated and dynamic pathways involved in *S. aureus*' ability to cause disease. To understand more about the importance and localisation of these essential virulence elements, further study is required using both a model organism and a model virulence determinant.

1.11.1. SecYEG

The translocation of many of *S. aureus*' surface proteins across the bacterial membrane from the cytoplasm, including IsdAB, ClfA, and SpA, is achieved by the SecYEG translocon (Khoon & Neela, 2010). In fact, all MSCRAMM surface proteins have been associated with the SecYEG translocon (Bartlett, A. H., & Hulten, 2010; Figure 1.10.). This association between MSCRAMM surface proteins and the SecYEG translocon has been shown via alterations in the N-terminal YSIRK signal sequence motif causing SpA to co-purify with SecA, as well as the lipoteichoic acid synthesis protein LtaS (Ye *et al*, 2018). Indeed, SecYEG is an essential translocation machinery in all bacteria, and is comprised of the cytosolic ATPase and translocase motor protein, SecA, and the protein channel complex SecYEG (Prabudiansyah & Driessen, 2016). While SecYEG is essential as an overall translocation machinery, it has been shown that SecG can be lost without effecting viability in *Escherichia coli* (Nishiyama *et al*, 1996). A chaperone protein associated with the SecYEG translocon, termed SecB (Rapoport, 2007), has been shown to guide cytoplasmic polypeptide precursors to the SecYEG complex for translocation across the bacterial membrane in *E. coli* and *B. subtilis*, but not in *S. aureus* (Mazmanian *et al*, 2001). Instead, *S. aureus* possesses SecA-2 and SecY-2 however, which are thought to perform a similar function in facilitating the translocation of preproteins. Additionally, SecDF are accessory factors to the SecYEG complex, despite acting as drivers for the proton motor force of SecA. SecDF has also being shown to impair both growth, division, antibiotic resistance, and SpA display in *S. aureus* (Quiblier *et al*, 2011).

While the SecYEG translocon has homology to the mammalian Sec61 pathway (Park & Rapoport, 2012), it is unique and essential to all bacteria. As such, the SecYEG translocon, including the SecA motor protein, which has no mammalian analogue, and SecDF accessory factors, are all considered valuable target for the development of antibiotic strategies against a range of bacterial species, including *S. aureus* (Jin *et al*, 2018).

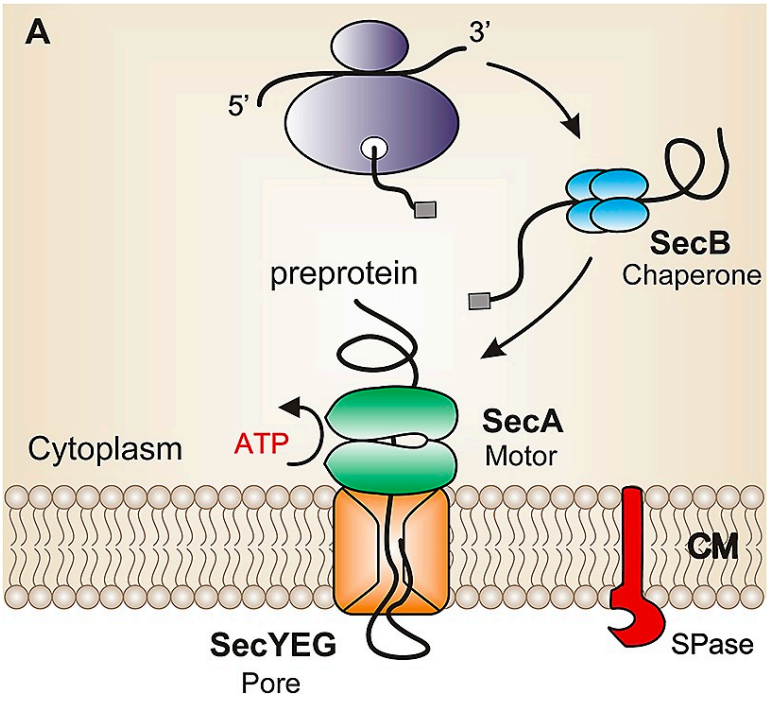

Figure 1.10. Schematic representation of SecYEG-mediated translocation of preproteins

Preproteins are chaperoned to the SecA motor protein by SecB in *E. coli* and *B. subtilis*, and by an unknown mechanism in *S. aureus*. Proteins are then translocated across the phospholipid bilayer membrane by SecYEG, where their signal sequence is recognised and cleaved by a membrane-bound signal peptidase prior to surface display. Adapted from Prabudiansyah *et al*, 2015.

1.12. Localisation Methods

Fluorescence microscopy is a frequently used technique to visualise cellular structures, molecules, proteins, nucleic acids, and lipids, both intracellularly and extracellularly in a range of cell types (Sanderson *et al*, 2014). In fluorescence microscopy, samples are typically stained with a fluorescent dye or probe that binds specifically to the structure or molecule of interest. The sample is then excited by light of a specific wavelength, which causes the fluorescent dye or probe to emit light of a different wavelength. This phenomenon is also known as photoluminescence (Shinde *et al*, 2012). The emitted light is detected by the microscope's objective lens, and a digital image of the sample is generated (Herman, 2020). Fluorescence microscopy has several advantages over other microscopy techniques. It is sensitive, allowing the detection of low levels of fluorescently labelled molecules, and has high spatial resolution, allowing the visualization of small structures within cells. Fluorescence microscopy is also relatively fast and easy to use, making it a widely used technique in research and clinical settings. There are several different types of fluorescence microscopy, including epifluorescence, confocal, immunofluorescence, and super resolution microscopy. These techniques differ both in their methods of sample preparation, in the way that they generate images, and in the level of detail that they can provide (Agard *et al*, 1989). Therefore, it is important to understand the benefits and limitations of microscopy techniques to better determine the most appropriate methodology for specific applications and objectives.

Fluorescence microscopy has elucidated many important cellular structures in bacteria whose localisations were previously unknown, which has enabled the further study of these proteins and structures in relation to the various processes of the bacterial cell cycle. For example, the localisation of key proteins involved in *S. aureus* cell division – FtsZ and EzrA – were achieved using fluorescence microscopy of these proteins conjugated to Yellow Fluorescent Protein (YFP) (Lund *et al*, 2018). Additionally, Red Fluorescent Protein (RFP) has been used to identify conditions in which *S. aureus* forms biofilms, as well as genes that contribute to biofilm formation (Boles & Horswill, 2008).

Immunofluorescence microscopy is a technique that uses fluorescently labelled antibodies to visualise proteins in a range of cell types and tissue cultures. It is widely used for the specific localisation of proteins due to the nature of immunogens, or antibodies, being highly specific to their target antigens. Due to the specificity of antibodies to bind antigens, antibodies can be produced in animal host species in response to a purified protein of interest. Once harvested, these antibodies can then be conjugated to fluorophores and used for research purposes. Typically, a combination of primary antibodies that are specific to a protein of interest, and a secondary antibody raised against the primary antibody are used, where the secondary antibody is conjugated to a fluorophore. Additionally, primary, and secondary antibodies can be used in isolation for localisation studies, where primary antibodies would then be conjugated to fluorophores. However, this is generally considered a less efficient method, as multiple secondary antibodies are capable of binding to primary antibodies – thereby providing increased intensities of fluorescence that more easily allow the user to localise their molecule of interest (Im *et al*, 2019). Immunofluorescence microscopy has been used to localise a variety of surface exposed antigens of methicillin resistant *S. aureus* (MRSA) previously, both *in vitro* and within mammalian infection models. These include localising capsular polysaccharide type 5 (CP5), manganese transporter C (MntC) and clumping factor A (ClfA) (Timofeyeva *et al*, 2014).

Light microscopy, including immunofluorescence microscopy, is limited by the optical diffraction limitation of light – also known as Abbe's diffraction limit – which is resolved at 200 nm (Klar *et al*, 2001). Traditional optical methods are unable to spatially resolve fluorescent reporters within 200 nm of one another. Diffraction limited fluorescence microscopy is constrained by this limitation, demonstrated by the appearance of "airy disks". The simultaneous excitation of fluorophores creates an airy disk of 200 nm in diameter. Therefore, other fluorophores emitting light within that diameter are impossible to spatially separate from one another (Rivolta, 1986). To circumvent this obstacle, various super resolution microscopy techniques are available, and have previously been used in the localisation of proteins in *S. aureus* (Lund *et al*, 2018). These super resolution microscopy techniques include, but are not limited to, structured illumination microscopy (SIM) and stochastic optical reconstruction microscopy (STORM) (Jensen *et al*, 2020; Li *et al*, 2018; Lund *et al*, 2022).

Work done by DeDent *et al* in 2007 illustrates both the usefulness of immunofluorescence and the diffraction limitation of fluorescence microscopy well. Although fluorescently conjugated antibodies bound to SpA are clearly visible in figure 1.11., precise localisation of individual proteins is impossible at this resolution. While diffraction limited fluorescence microscopy allows the user to visualise the presence of proteins tagged with fluorescent reporters, the precise localisation and identification of single surface proteins is not achievable via this technique. Nevertheless, fluorescence microscopy is a powerful technique in localising proteins, specifically in identifying patterns of localisation. While many biotechnologies exist that are compatible with fluorescence microscopy, such as GFP and YFP, they also come with their own advantages and disadvantages. For example, GFP has been reported to misfold, weakening its fluorescent signal (Cabantous *et al*, 2005). Additionally, YFP is sensitive to pH, has poor photostability, and is expressed poorly at 37°C (Griesbeck *et al*, 2001). For the investigation into the localisation of various surface proteins of *S. aureus* within this work, an alternative biotechnology was chosen called SNAP tag (Section 1.13).

Super resolution microscopy techniques exist which allow the precise molecular localisation of both intracellular and surface exposed proteins (Schermelleh *et al*, 2019). Super resolution microscopy can circumvent the limitations of conventional fluorescence microscopy – namely the elucidation and spatial separation of fluorescent molecules within 200 µm of one another (Yamanaka *et al*, 2014). One such example of a super resolution microscopy technique is Super Resolved Structured Illumination microscopy (SR-SIM), which surpasses the optical diffraction limitation by incorporating scattering light and moiré patterns to illuminate smaller sections of a given sample at a time, thereby preventing the accidental excitation of neighbouring fluorophores and avoiding the production of air disks (Heintzmann *et al*, 2017). Stochastic Optical Reconstruction Microscopy (STORM) achieves a similar effect in avoiding airy disk production by using highly focused, short bursts of excitation, to prevent the excitation of neighbouring fluorophores (Codron *et al*, 2021). However, an important limitation of super resolution microscopy techniques is the requirement of particularly sensitive and stable fluorophores, as these techniques employ higher excitation intensities and exposure times than their conventional counterparts (Tosheva *et al*, 2020).

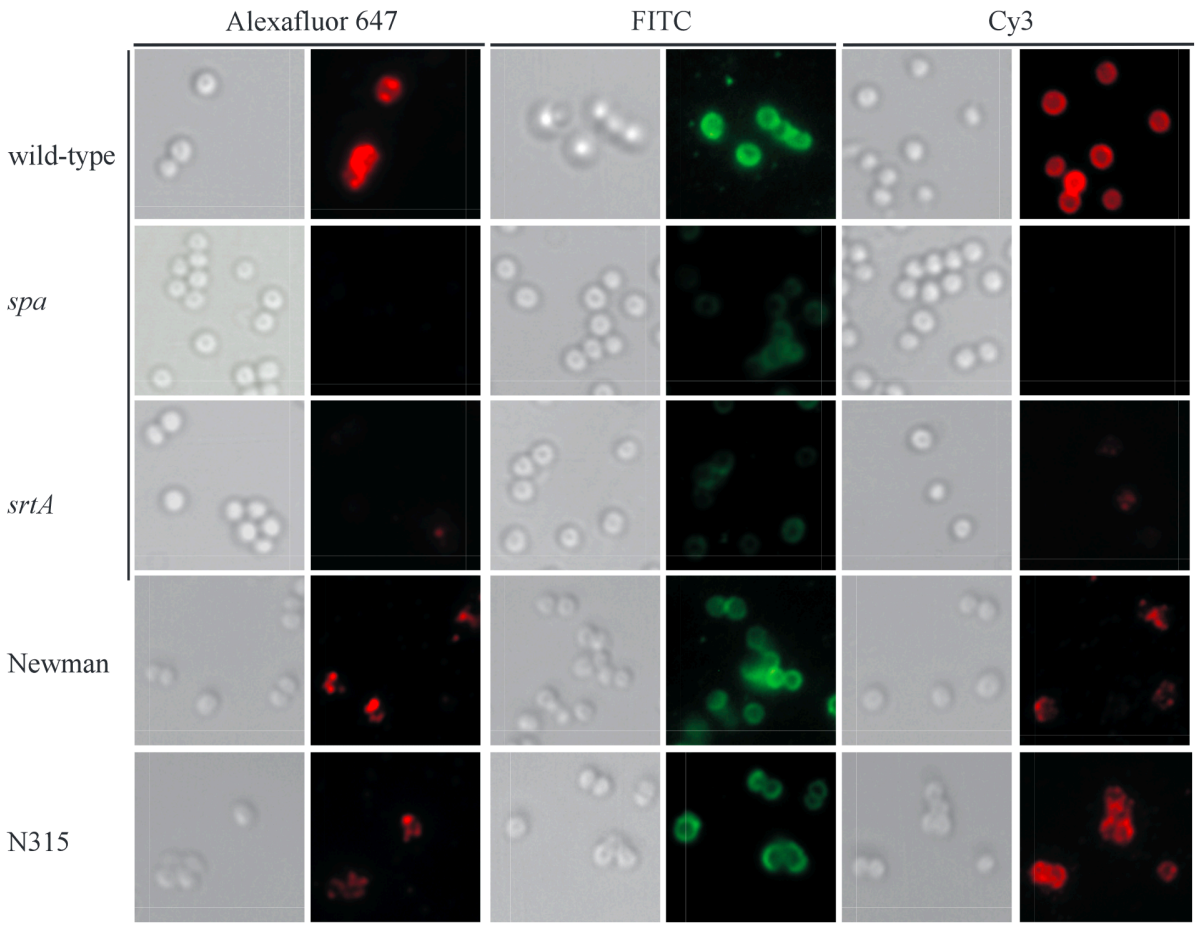

Figure 1.11. Antibody efficiency screen for SpA immunofluorescence of *S. aureus* strains

S. aureus RN4220, RN4220 deletion mutants of *spa*, *srtA*, and clinical strains Newman and N315 were used for immunofluorescence. *S. aureus* strains were fluorescently labelled with Alexa fluor 647-IgG, FITC-IgG, and Cy3-IgG conjugated antibodies as a comparison of antibody efficacy for the localisation of SpA. Taken from DeDent *et al*, 2007.

1.13. SNAP Tag

SNAP tag (Single Nucleotide Affinity Purification) is the product of directed evolution of the human O^6-alkylguanine-DNA-alkyltransferase (AGT) enzyme; a DNA repair enzyme that removes alkyl groups from DNA-guanine (Mollwitz *et al*, 2012). The result is O^6-benzylguanine-DNA-benzyltransferase, known as SNAP tag (Figure 1.12.). SNAP can be conjugated to proteins via a flexible, short oligo linker, where it can then be used to covalently and irrevocably bind to benzylguanine derivative substrates that contain fluorescent molecules (Juillerat *et al*, 2003). The benzylguanine substrate can also be conjugated to various functional groups, depending on the intended investigation, for various functions like protein purification. The 1:1 stoichiometry of SNAP and benzylguanine substrates means that this reaction does not interfere with other biological processes (Hoelzel & Zhang, 2020). The availability of multiple fluorophore-benzylguanine derivative dyes also allows for multicoloured labelling of SNAP, while the use of SNAP-Block prevents SNAP from binding benzylguanine derivatives, thereby affording a range of flexibility and versatility to the user. Additionally, CLIP tag was also developed, which functions identically to SNAP tag, but covalently binds benzylcytosine derivative dyes instead of benzylguanine. This allows not only the labelling of either SNAP or CLIP with multiple derivative dyes conjugated to a range of fluorophores, but also the use of both SNAP and CLIP together, wherein both can be labelled separately using their respective derivative substrates to localise multiple proteins of interest simultaneously without interfering with one another (Sun *et al*, 2011). The versatile nature of SNAP-tag makes it a useful and biotechnological approach to establish both the localisation of proteins in *S. aureus*, and their dynamic spatial and temporal development.

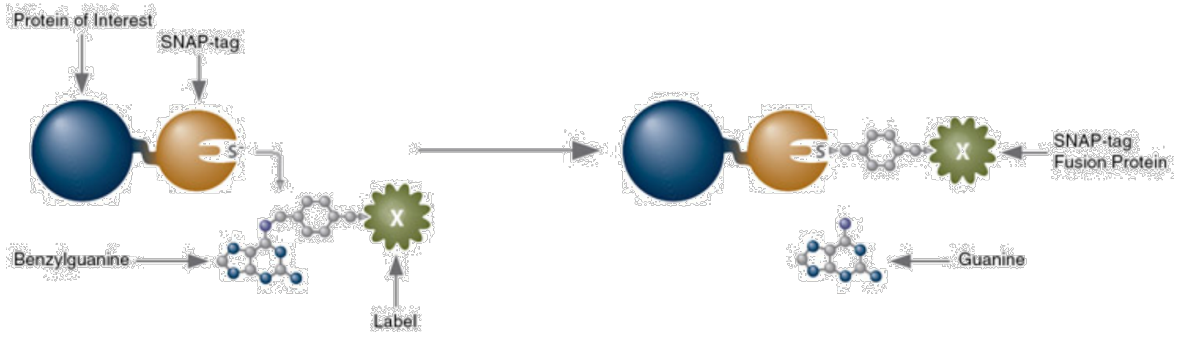

Figure 1.12. Schematic representation of SNAP tag functionality

SNAP covalently binds benzylguanine derivate substrates which, when conjugated to fluorophores, can be used to localise proteins of interest. Adapted from International.neb.com.

1.14. Aims

Proteins displayed on the surface of *S. aureus* cells are known to mediate colonisation and infection in humans and other mammals. While the function of many of these proteins have been investigated, their localisation on the surface is poorly understood. Therefore, the aims of this study include:

- Localisation of IsdAB, ClfA, and SpA on the surface of *S. aureus* using SNAP-tag and fluorescence microscopy
- Elucidate the molecular organisation of these proteins on the cell surface of *S. aureus*
- Investigate the development of surface protein display spatially and temporally using Trypsin cell shaving
- Investigate the regulation of surface protein display
- Correlate the localisation of these surface proteins to the newly discovered architecture of the *S. aureus* cell wall by AFM
- Create a nano-scale map of these surface proteins using gold-conjugated antibodies and AFM

Chapter 2

Materials & Methodology

2.1. Growth Media

All media was prepared using distilled water (dH_2O) and sterilised by autoclaving for 20 minutes at 121°C unless otherwise stated.

2.1.1. Lysogeny broth (LB)

Yeast extract (Oxoid)	10 g L^{-1}
Tryptone (Oxoid)	5 g L^{-1}
NaCl	5g L^{-1}

2.1.2. LB agar

Tryptone (Oxoid)	5 g L^{-1}
Yeast extract (Oxoid)	19 g L^{-1}
NaCl	5 g L^{-1}
Bacteriological agar	1.5% (w/v)

2.1.3. Lysogeny potassium broth (LK)

Tryptone (Oxoid)	5 g L^{-1}
Yeast extract (Oxoid)	19 g L^{-1}
KCl	5 g L^{-1}

2.1.4. LK agar

Tryptone (Oxoid)	5 g L^{-1}
Yeast extract (Oxoid)	19 g L^{-1}
KCl	5 L^{-1}
Bacteriological agar	1.5% (w/v)

2.1.5. Tryptic soy broth (TSB)

Tryptic soy broth (Oxoid)	30 g L^{-1}

2.1.6. TSB agar (TSA)

Tryptic soy broth (Oxoid) 30 g L^{-1}

Bacteriological agar 1.5% (w/v)

2.2. Antibiotics

The Antibiotics used in this study were filter sterilised through 0.2 µm pores and stored at -20°C. Stock solutions of antibiotics were thoroughly thawed where necessary, and diluted to their respective working concentrations in sterilized media, cooled at 55°C.

Table 2.1. Antibiotic stock solutions and working concentrations

Antibiotic	**Stock Concentration (mg mL^{-1})**	***S. aureus* working concentration (µg mL^{-1})**	***E. coli* working concentration (µg mL^{-1})**	**Solvent**
Ampicillin (Amp)	100	-	100	dH_2O
Erythromycin (Erm)	5	5	-	95% (v/v) ethanol
Kanamycin (Kan)	50	50	-	dH_2O
Lincomycin (Lin)	25	25	-	50% (v/v) ethanol
Methicillin (Meth)	10	10	-	dH_2O
Tetracycline (Tet)	5	5	-	50% (v/v) ethanol

2.3. Bacterial Strains and Plasmids

2.3.1. *Staphylococcus aureus* Strains

S. aureus strains used in this work were grown on TSA and in TSB with the appropriate antibiotic selection where necessary. Strains were stored at -80°C in Microbank bead tubes

(Pro-lab Diagnostics). Liquid cultures were grown in 10 mL TSB in sterilized Falcon tubes and in sterilized glass conical flasks at 37°C, shaking at 250 rpm. Agar plates were incubated at 37°C and stored at -4°C. Overnight liquid cultures were sub-cultured the following day to an OD_{600} of 0.05 and grown to exponential phase (OD_{600} of 0.5-0.8) for experimentation.

Table 2.2. *S. aureus* strains used in this study

Strain	Relevant genotype & selection markers	Source
SJF 57	8325-4 cured of pro-phages 011, 012, and 023	O'Neill, 2010
SJF 62	RN4220, a restriction deficient modification efficient intermediary transformation strain	Kreiswirth *et al*, 1983
SJF 315	COL, a methicillin resistant strain of *S. aureus*	Mahmud Masalha
SJF 426	SH1000 with *agr* locus deleted, Tet^R	Liz Cooper
SJF 682	SH1000 wild type, an *rsbU* $^+$ derivative of 8325-4	O'Neill, 2010
SJF 2181	SH1000 *isdA*::*kan* / Kan^R	Howard Crossley
SJF 2507	SH1000 *isdB*::ery / Erm^R	Howard Crossley
SJF 2978	SH1000 *spa*::*kan* / Kan^R	Girbe Buist
SJF 4996	SH1000 *lysA*::p*mecA* / Erm^R	Viral Panchal
SJF 5003	SH1000 *lysA*::p*mecA rpoB*^{H929Q} / Erm^R	Viral Panchal
SJF 5010	SH1000 *rpoB*^{H929Q}	Viral Panchal
SJF 5276	RN4220 *lysA*::*isdB-SNAP* / Erm^R	This study
SJF 5277	RN4220 *lsyA*::*isdA-SNAP* / Kan^R	This study
SJF 5278	RN4220 *lysA*::*clfA-SNAP* / Tet^R	This study
SJF 5281	RN4220 *lysA*::*spa-SNAP* / Erm^R	This study
SJF 5329	SH1000 *spa*::*kan lysA*::*spa-SNAP* / Kan^R, Erm^R	This study
SJF 5363	SH1000 *isdB*::*tet lysA*::*isdB-SNAP* / Tet^R, Erm^R	This study
SJF 5390	SH1000 *clfA*::*erm lysA*::*clfA-SNAP* / Erm^R, Tet^R	This study
SJF 5602	SH1000 *spa*::*kan lysA*::*spa-SNAP agr*::*tet* / Kan^R, Erm^R, Tet^R	This study
NE 453	JE2 bursa aurealis Tn insertion in *sbi* / Erm^R	Fey *et al*, 2013
SJF 5633	SH1000 transduced with NE 453 lysate (*sbi*::*erm*) / Erm^R	This study
SJF 5634	SH1000 *spa*::*kan* transduced with NE 453 lysate (*sbi*::*erm*) / Kan^R, Erm^R	This study
SJF 5737	SH1000 *lysA*::p*mecA agr*::*tet* / Erm^R, Tet^R	This study
SJF 5738	SH1000 *lysA*::p*mecA rpoB*^{H929Q} *agr*::*tet* / Erm^R, Tet^R	This study
SJF 5749	SH1000 *rpoB*^{H929Q} *agr*::*tet* / Tet^R	This study
SJF 5771	SH1000 *spa*::*kan agr*::*tet* / Kan^R, Tet^R	This study
SJF 5772	COL *agr*::*tet* / Tet^R	This study
SJF 5813	SH1000 *lysA*::p*mecA rpoB*^{H929Q} *sarA*::*kan* / Erm^R, Kan^R	This study
SJF 5814	SH1000 *rpoB*^{H929Q} *sarA*::*kan* / Kan^R	This study

2.3.2. *Escherichia coli* Strains

Escherichia coli strains were grown under the same conditions as *S. aureus*, using LB and LK media instead of TSB. Liquid *E. coli* cultures were incubated at 37°C, 200 rpm.

Table 2.3. *E. coli* strains used in this study

Strain	Relevant genotype & selection markers	Source
NEB5α	*fhuA2* Δ*(argF-lacZ) U169 phoA glnV44* Φ80 Δ*(lacZ) M15 gyrA96 recA1 relA1 endA1 thi-1 hsdR17*	New England Biolabs
SJF 5270	NEB5α transformed with pTH002 / Amp^R	This study
SJF 5271	NEB5α transformed with pTH004 / Amp^R	This study

2.3.3. Plasmids

Table 2.4. List of plasmids used in this study

Plasmid	Description	Source
pTH002	*isdA-SNAP* in pGM072	Kasia Wacnik
pTH003	*isdB-SNAP* in pGM068	Kasia Wacnik
pTH004	*clfA-SNAP* in pGM069	Kasia Wacnik
pTH005	*spa-SNAP* in pGM068	Kasia Wacnik

2.4. Buffers and Solutions

2.4.1. Phage Buffer

$MgSO_4$	1 mM
$CaCl_2$	4 mM
Tris-HCl pH7.8	50 mM
NaCl	0.6% (w/v)

2.4.2. Phosphate Buffered Saline (PBS)

NaCl	8 g L^{-1}
Na_2HPO_4	1.4 g L^{-1}
KCl	0.2 g L^{-1}
KH_2PO_4	0.2 g L^{-1}

2.4.3. TAE (50x)

Tris base	242 g L^{-1}
Glacial acetic acid	5.7% (v/v)
Na_2EDTA pH 8	50 mM

TAE (50x) was diluted to working concentration (1x) using dH_2O for experimental use.

2.4.4. TBSI

Tris-HCl pH 7.5	50 mM
NaCl	100 mM

EDTA-free protease inhibitor (Roche) was dissolved in buffer to make TBSI, as per manufacturer's instructions.

2.4.5. Fixing Solution Preparation

2.4.5.1. 100 mM Sodium Phosphate Buffer (pH 7)

1 M NaH_2PO_4	42.3 mL
1M Na_2HPO_4	57.7 mL

2.4.5.2. 16% (w/v) Paraformaldehyde (PFA)

Paraformaldehyde	8 g
100 mM Sodium Phosphate buffer pH 7	50 mL

2.4.5.3. Fixing Solution

PBS	2 mL
16% (w/v) Paraformaldehyde	0.5 mL

2.4.6. SDS-PAGE Solutions

2.4.6.1. SDS-PAGE Running Buffer (10x)

Tris	30.3 gL^{-1}
Glycine	144 gL^{-1}
SDS	10 gL^{-1}

10x SDS-PAGE buffer was diluted to working concentration (1x) with dH_2O for experimental conditions.

2.4.6.2. SDS-PAGE Loading Buffer (5x)

Glycerol	50% (v/v)
Tris-HCl pH6.8	250 mM
SDS	10% (w/v)
DTT	500 mM
Bromophenol blue	0.5% (w/v)

2.4.6.3. Coomassie Blue Stain

Coomassie blue	0.1% (w/v)
Glacial acetic acid	10% (v/v)
Methanol	5% (v/v)

2.4.6.4. Coomassie Blue De-stain

Glacial acetic acid	10% (v/v)
Methanol	5% (v/v)

2.4.7. Western Blotting Solutions

2.4.7.1. Blotting Buffer

Glycine	11.26 gL^{-1}
Tris	2.4 gL^{-1}
Ethanol	20% (w/v)

2.4.7.2. TBST (10x)

Tris	24.2 gL^{-1}
Tween-20	2% (v/v)
NaCl	20 gL^{-1}

TBST (10x) was diluted to working concentration (1x) with dH_2O.

2.4.7.3. Blocking Buffer

5% (w/v) powdered semi-skimmed milk was dissolved in 1x TBST buffer for experimental use.

2.5. Chemicals & Enzymes

All chemicals and enzymes used in this study were of analytical grade quality. All restriction enzymes, polymerases, and appropriate buffers were purchased from New England Biolabs or Fischer Scientific.

Table 2.5. Chemicals and stock solutions used in this study

Stock Solution	Concentration	Solvent	Storage
HADA (hydroxycoumarin 3-amino-D-alanine; Department of Chemistry, University of Sheffield)	100 mM	DMSO	-20°C in dark
IPTG (isopropyl-β-D-1-thigalactopyranoside) (Sigma)	1 M	dH_2O	-20°C
Lysostaphin (Sigma)	5 mg mL^{-1}	20 mM sodium acetate pH 5.2	-20°C
SNAP-Cell TMR-Star (New England Biolabs)	1 mM	DMSO	-20°C in dark
SNAP-Surface Alexafluor 647 (NEB)	1 mM	DMSO	-20°C in dark

2.6. Blocking buffer for Immunofluorescence Microscopy

Bovine Serum Albumin (BSA) 2% (w/v) in 1x PBS

2.7. Centrifugation

The following centrifuges were used to harvest bacterial samples:

- Eppendorf microcentrifuge 5418, maximum speed of 16,783 rcf (14,000 rpm)
- Sigma centrifuge 4K15C, maximum speed of 5,525 rcf (5,100 rpm)
- Avanti High Speed J25I, maximum speed of 75,600 rcf (25,000 rpm)

All centrifugation was carried out at room temperature unless otherwise stated.

2.8. Determination of Bacterial Cell Density

2.8.1. Optical Density

To determine bacterial yield from overnight liquid cultures, the cell solution was diluted 1:10 in sterile media and analysed via spectrophotometry at 600 nm (OD_{600}) (Biochrom WPA Biowave DNA spectrophotometer). The reading was multiplied by 10 to determine the OD_{600} of the overnight cell culture, which serves as a proxy measurement for CFU and growth phase.

2.9. DNA Purification

2.9.1. Genomic DNA Purification

S. aureus genomic DNA was purified using Qiagen DNeasy Blood and Tissue kit. 1 mL of overnight cell culture was centrifuged at 17,000 x g at room temperature for 3 minutes. The cell pellet was re-suspended in 180 µL dH_2O. 5 µL of 5 mg/mL lysostaphin was added to the re-suspended pellet and incubated at 37°C on a rotary shaker until the solution was clear (approximately 1 hour). 25 µL of proteinase K and 200 µL buffer AL (without ethanol) were added. The solution was vortexed briefly and incubated at 70 °C for 30 minutes. 200 µL of 99% (v/v) ethanol were added and the solution was briefly vortexed. The solution was then transferred to a column and centrifuged at 17,000 x g for 1 minute. The collection tube was replaced and 500 µL buffer AW1 (with ethanol) was added. The tube was centrifuged at 8000 rpm for 1 minute. The collection tube was replaced and 500 µL of buffer AW2 (with ethanol)

was added. The tube was centrifuged at 17,000 x g for 3 minutes. 100 µL of dH_2O was added directly to the tube's filter and incubated at room temperature for 2 minutes. Genomic DNA was eluted via centrifugation at 17,000 x g for 1 minute into an Eppendorf.

2.9.2. Plasmid Purification

Plasmids were purified from *E. coli* using the GeneJet Plasmid Miniprep kit as per the manufacturer's instructions.

2.10. *In vitro* Genetic Manipulation Techniques

2.10.1. Primer Design

Primers for PCR protocols were ordered from Sigma Aldrich and typically consisted of 18-29 nucleotides, ending in a G-C cap. These primers were designed against the genome sequence of *S. aureus* SH1000 and plasmid sequences used in this study to verify integration into the *S. aureus* chromosome. All primers were reconstituted in sterilised MQ dH_2O upon reception to 100 µM concentrations and stored at -20°C for long term use. Aliquots were made of 10 µM primers for use in this work and were also stored at -20°C for long term use.

2.10.2. PCR Amplification

PCR amplification was performed using ThermoFisher Scientific's Phusion High Fidelity Master Mix. A 25 µL reaction mix contained:

Phusion High Fidelity Maser Mix (2x)	12.5	µL
Forward primer (10 µM)	1.25	µL
Reverse primer (10 µM)	1.25	µL
Template DNA	>100	ng
MQ dH_2O	up to 25 µL	

PCR protocols were carried out using the Veriti Thermal Cycler (Applied Biosystems) with a pre-heated lid at 105°C. PCR reactions ran according to the following variables:

1x	Initial denaturation	98°C	30s
30x	Denaturation	98°C	10s
30x	Annealing	55-62°C	10s
30x	Extension	72°C	15-30s/kb
1x	Final extension	72°C	3-5 mins

All PCR products were analysed by 1% (w/v) agarose gel electrophoresis (2.10.4.). Concentration of DNA was measured using the NanoDrop 3300 spectrophotometer. 1.5 µL of MQ H_2O was used as a blank measurement. 1.5 µL of DNA eluted in MQ H_2O was loaded onto the platform and measured at 260 nm.

Table 2.6. List of primers used in this study

Primer	Sequence (5'- 3')	Source
SNAP R	GGTACGTTTCATTTCGCAATC	This study
lysA 5' F	ATGGCGAATTAACAATGGATG	This study
amp F	TAGATAACTACGATACGGGAG	This study
agr 2 F	ATTCGATGGTAACACAGAATATG	This study
agr 2 R	CGTATATGATTACACAATTAGG	This study
sbi F	GATACCTACAAACATAATGAC	This study
sbi R	GTTCTAGAGCTAATGAAG	This study
sarA F	AACATTCAGGACATGCACCG	This study
sarA R	GGTGGTTTGCTTGGGGTTAG	This study

2.10.3. Restriction Endonuclease Digestion

Restriction digestion of DNA was done using enzymes from New England Biosciences (NEB), following manufacturer's instructions. Reactions were incubated at 37 °C for 1 – 2 hours. Digested DNA was observed and measured via 1% agarose gel electrophoresis.

2.10.4. Agarose Gel Electrophoresis

1% (w/v) agarose gel was made using 1 x TAE buffer. 4 µL of Midori Green (GeneFlow) was added to small gels (~50 mL) and 8 µL Midori Green was added to large gels (~100 mL) for DNA visualisation as per the manufacturer's instructions. DNA fragments were mixed with 6x loading buffer (Thermofisher) prior to gel electrophoresis. A current of 120 V was applied for 30 minutes to separate DNA fragments according to size. Size of DNA fragments was determined by comparison to a 1 Kb DNA ladder run on the same gel (Thermofisher).

2.10.5. Transformation of Chemically Competent *E. coli* cells

A 50 µL aliquot of chemically competent *E. coli* NEB5α cells were defrosted on ice (New England Biolabs). 1 ng of plasmid DNA was added to the cell solution and mixed gently by pipetting, before being incubated on ice for 30 minutes. The cells were then heat shocked at 42°C for 45 seconds and placed on ice for 5 minutes. Cells were recovered by the addition of 500 µL LB and incubated at 37°C, shaking at 250 rpm, for 1 hour. 100 µL aliquots were spread on selected LB agar plates and incubated at 37°C for 16-18 hours, until colonies appeared. Chemically competent *E. coli* NEB5α were incubated with the equivalent volume of water and processed following the same method as negative controls.

2.10.6. Preparation of Electrocompetent *S. aureus*

A single colony of *S. aureus* RN4220 was grown in 5 mL TSB liquid culture overnight at 37°C, 250 rpm. 1 mL of the overnight culture was transferred into 99 mL fresh TSB in a 250 mL conical flask. The subculture was incubated at 37°C for 2 hours, or until an OD_{600} of 0.4 – 0.6 was reached. The flask was placed on ice for 20 minutes, the cell culture was transferred into two 50 mL Falcon tubes, then centrifugated at 5,000 rcf for 10 minutes at 4°C. 10 mL of pre-cooled 0.5M sterilised sucrose solution was added to gently re-suspend cells, before topping up to a total volume of 45 mL. The re-suspended cell solution was placed on ice for 30

minutes. Afterwards, the culture was centrifugated at 5,000 rcf for 10 minutes at 4°C. The supernatant was discarded, and the cell pellet was re-suspended in 1 mL pre-cooled 0.5M sucrose solution. Aliquots of 100 µL were transferred into Eppendorf tubes and were flash frozen in liquid nitrogen before being stored at -80°C.

2.10.7. Transformation of *S. aureus* by Electroporation

100 µL of electrocompetent *S. aureus* RN4220 cells were thawed on ice. 5 µL of plasmid DNA >100 ng was added to the thawed cells and incubated on ice for 20 minutes. Cells were then transferred to a pre-cooled electroporation cuvette (Bio-Rad) and pulsed with 2.9 kV, 100 Ω, and 25 uF using a Gene Pulser Xcell Electroporation system (Bio-Rad). 1 mL of pre-warmed TSB was immediately added to the cells, which were then incubated in Eppendorf tubes at 37°C for 2 hours. 100 µL of transformed cells were then plated onto selective media. Electrocompetent *S. aureus* RN4220 cells were also incubated with 5 µL MQ H_2O and were processed following the same methods as negative controls.

2.11. Bacteriophage Techniques

2.11.1. Bacteriophage

Bacteriophage Φ11 was used for phage transduction of genes into *S. aureus* (Mani *et al*, 1993).

2.11.2. Preparation of Phage Lysate

Donor strains of *S. aureus* were grown overnight in 5 mL TSB at 37°C, 250 rpm. In a Universal tube, 5 mL phage buffer, 5 mL TSB, 150 µL of the overnight culture, and 100 µL of phage lysate were mixed. The cell and phage mixture were incubated at room temperature overnight or until the solution was clear, indicating bacterial lysis. The mixture was then filter sterilised through a 0.45 µm filter and stored at 4°C for transduction of donor DNA.

2.11.3. Bacteriophage Transduction

The recipient strain of *S. aureus* was grown in 50 mL LK in a 250 mL conical flask overnight at 37°C, 250 rpm. The culture was then transferred into a 50 mL Falcon tube for centrifugation

at 5,000 rpm for 10 minutes at room temperature. The harvested cells were re-suspended in 3 mL LK. 500 µL of recipient cells, 1 mL of LK, 10 µL of 1M $CaCl_2$, and 500 µL of donor lysate were mixed in a Universal tube. The mixture was incubated for 25 minutes at 37°C without shaking, before being incubated at 37°C for 15 minutes, shaking at 250 rpm. 1 mL of ice cold 0.02M sodium citrate (NaCit) was added, and the mixture was incubated for 5 minutes on ice. The solution was centrifugated at 5,000 rpm for 10 minutes at 4°C and the supernatant was discarded. The bacterial pellet was resuspended in 1 mL ice cold 0.02M NaCit and incubated on ice for a further 45 minutes. 100 µL of the suspended cells were spread onto selection LK plates with 0.05% (v/v) NaCit and were incubated at 37°C for at least 24 hours, or until colonies grew. A mixture of recipient cells without donor phage lysate were used as a control.

2.12. Protein Analysis

2.12.1. Protein Extraction

An overnight culture of *S. aureus* was set up by inoculating a colony into 5 mL TSB in a universal tube which was then incubated at 37°C, 250 rpm, for 16 – 18 hours. A 1:10 dilution was made from this overnight culture the following day and the OD_{600} was read using a spectrophotometer. This was then used to calculate the volume of overnight liquid culture needed to obtain a 50 mL cell suspension at an OD_{600} 0.05 in TSB. Once the desired starting OD_{600} was achieved, the cells were incubated in TSB at 37°C, 250 rpm, for 2 hours to reach an OD_{600} of ~0.5. Once the cells had reached an OD_{600} of 0.5, the 50 mL cell solution was transferred to a 50 mL Falcon tube and centrifuged at 4,700 rcf, 4°C, for 15 minutes. The supernatant was discarded.

EDTA-free protease inhibitor cocktail tablets (Thermofisher) were dissolved in PBS as per the manufacturer's instructions to make the PBSI solution, which was kept on ice throughout this protocol. Cell pellets, also kept on ice, were re-suspended in 1 mL PBSI, and transferred to FastPrep tubes for cell lysis. Tubes were placed in an MP Biomedicals Fast Prep machine and run using the "Peptidoglycan" setting with the QuickPrep adapter at 7 m/sec for 35 seconds, 10 times. Tubes were kept on ice between each run for 2 minutes.

2.12.2. Preparation of cell wall and cell membrane fractions

S. aureus cells were grown in TSB to an OD_{600} of 1 and harvested by centrifugation at 5,000 rcf for 10 minutes at 4°C. Cells were washed twice by resuspension in PBS and centrifugation at 5,000 rcf for 10 minutes at 4°C. The cell pellet was resuspended in 1.5 mL PBSI and transferred to a chilled FastPrep tube for cell lysis. Tubes were placed in an MP Biomedicals Fast Prep machine and run using the "Peptidoglycan" setting with the QuickPrep adapter at 7m/sec for 35 seconds, 10 times. Tubes were kept on ice between each run for 2 minutes. The supernatant was recovered and transferred to a 15 mL falcon tube. To remove any beads in the supernatant, the sample was centrifuged at 2,000 rcf for 10 minutes at 4°C. The supernatant was then centrifuged twice at 15,000 rcf for 10 minutes at 4°C to sediment the cell wall material. The cell wall fraction was either used immediately for experimentation, or stored at -20°C. The supernatant was transferred to a fresh centrifuge tube and the membrane fraction was sedimented by centrifugation at 70,000 rcf for 60 minutes at 4°C. The pellet containing the membrane fraction was suspended in PBS and either used immediately for experimentation or stored at -20°C.

2.12.3. Bradford Protein Assay

To determine protein concentration of samples, a standard curve of set concentrations of bovine serum albumin (BSA) was generated (Figure 2.1.). 0, 1.6, 4, 8, and 12 µg of BSA in 800 µL PBS were transferred into a semi-micro-PS spectrophotometer cuvette (Fisherbrand). 200 µL of Bio-Rad Protein Assay Dye was added to each sample and mixed by pipetting. After 5 minutes at room temperature, the absorbance was measured at 595 nm.

To determine the concentration of a protein sample, the sample was diluted in 800 µL PBS and transferred to a spectrophotometer cuvette. 200 µL of Bio-Rad Protein Assay Dye was added to the sample. After 5 minutes at room temperature, the absorbance of the sample was read at 595 nm and measured against the Bradford Assay standard curve to determine the concentration of the sample. Otherwise, protein content of samples was normalised by optical density of the samples.

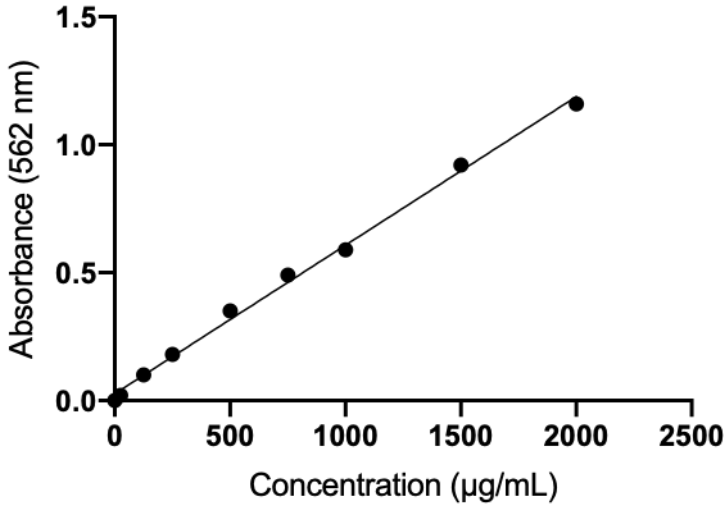

Figure 2.1. Standard curve of the Bradford Assay

Absorbance of different BSA concentrations at 595 nm. The line of linear regression is used to calculate the concentration of a protein sample.

2.12.4. SDS-PAGE

Proteins were separated by molecular weight using 12% (w/v) Mini-PROTEAN TGX Precast Gels, prepared as per the manufacturer's instructions (Bio-Rad). Samples were run in 1x SDS-PAGE running buffer at 150 V for 60 minutes, on ice.

2.12.5. Coomassie Staining

Following electrophoresis of the SDS-PAGE, the gel was submerged in Coomassie Blue stain for a minimum of 30 minutes at room temperature to visualise protein content. The size of proteins was estimated by comparing them to the standard "ladder" of known molecular weights.

2.12.6. Western Blot Analysis

Protein samples were separated based on molecular weight as described previously (section 2.11.4.). Amersham Hybond ECL Nitrocellulose Membrane (GE Healthcare) was cut to cover the size of the SDS gel and activated in methanol. Both the gel and membrane were equilibrated in blotting buffer for 20 minutes. Proteins were transferred from the gel to the membrane by wet transfer in blotting buffer, on ice, at 100 V for 1 hour. Following the transfer of protein from the gel to the membrane, the membrane was washed with TBST. The membrane was blocked in blocking buffer at room temperature for 1 hour, shaking gently. The membrane was washed 3 times for 10 minutes each time in TBST, shaking gently. The membrane was then incubated with primary antibodies diluted in blocking buffer, either for 2 hours at room temperature or at 4°C overnight, shaking gently. The membrane was washed again 3 times for 10 minutes each time in TBST, before the membrane was incubated with secondary antibodies conjugated to horseradish peroxidase (HRP) diluted in blocking solution for 2 hours at room temperature or overnight at 4°C, shaking gently. After a final 3 washes with TBST, the membrane was covered and incubated with Amersham Hyperfilm ECL solution (GE Healthcare) and imaged.

2.13. Sample Preparation for Fluorescence Microscopy

All steps involving fluorophores or otherwise light-sensitive compounds were exposed to light as little as possible during experimentation to minimise photobleaching.

2.13.1. Labelling Nascent Peptidoglycan Synthesis with HADA

5 mL of cell culture was grown overnight at 37°C, 250 rpm. The culture was diluted 1:10 and the OD_{600} was read via spectroscopy. This measurement was used to calculate the volume of overnight culture required to achieve a subculture at an OD_{600} of 0.05. This subculture was grown for 2 hours, or until an OD_{600} of 0.5 – 0.8 was reached. 10 mL of subculture was centrifugated at 5,000 rpm for 5 minutes at room temperature. The cell pellet was re-suspended in 1 mL TSB in an Eppendorf tube. 10 µL of 100 mM HADA was added to the cell suspension and the culture was incubated at 37°C, rotating, for 5 minutes. Cells were washed twice with PBS by centrifugation at 17,000 rcf.

2.13.2. Fixing Cells

Cells were re-suspended in 2 mL PBS and 0.5 mL of fixative was added (section 2.4.5.3.). Cells were fixed for 30 minutes at room temperature, rotating. Fixed cells were washed twice with MW dH_2O and centrifugation at 17,000 rcf for 1 minute at room temperature.

2.13.3. Labelling of SNAP-tag Fusion Proteins

S. aureus strains containing SNAP-tag fusion constructs were grown to and OD_{600} of 0.5-0.8. 10 mL of the cell culture was centrifugated at 5,000 rcf and re-suspended in 1 mL TSB supplemented with a compatible SNAP-tag substrate dye at 5 µM concentration, unless otherwise stated. Cells expressing SNAP-tag were incubated with SNAP substrate at 37°C, rotating, for 30 minutes. Cells were washed and incubated with HADA as described previously.

2.13.4. Immunolabelling & Antibodies

S. aureus cells were grown to an OD_{600} of 0.5-0.8. 10 mL of the cell culture was centrifugated at 5,000 rcf and re-suspended in 1 mL TSB supplemented with 10 µL of 100 mM HADA, and incubated at 37°C, rotating, for 5 minutes. Cells were washed twice with PBS by centrifugation at 17,000 rcf. Cells were then fixed with PFA for 30 minutes, rotating, at room temperature and washed twice with MQ H_2O. Fixed cells were then blocked with 2% (w/v) BSA for 1 hour, rotating, at room temperature. Cells were then incubated with monoclonal primary mouse α-SpA antibodies at a dilution factor of 1:250, either for 2 hours, rotating, at room temperature,

or overnight, rotating, at 4°C. Cells were then washed twice with MQ dH_2O before being incubated with polyclonal secondary rabbit α-mouse Alexafluor 488 conjugated antibodies, either for 2 hours, rotating, at room temperature, or overnight, rotating, at 4°C. Cells were then washed twice with MQ dH_2O and mounted on glass microscopy slides as detailed in section 2.13.5. Antibodies used for immunofluorescence were acquired from ThermoFisher. Primary antibodies used herein were monoclonal, raised in mice against purified surface protein A. The epitope which these antibodies bind to SpA are not detailed in the ThermoFisher product information. Polyclonal secondary antibodies were raised against primary antibodies in alternative hosts, such as goat and rabbit.

2.13.5. Sample Preparation for Fluorescence Microscopy

10 µL of fixed and labelled sample was dried onto a poly-L-lysine coated glass slide (Sigma) using air. The slide was washed with dH_2O and dried with air. A high precision 1.5H coverslip glass (Sigma) was mounted onto of the sample using SlowFade gold (Thermo Fischer) as a buffer. The coverslip was sealed to the glass slide with transparent nail varnish.

2.13.6. Fluorescence Microscopy Settings

Fluorescence microscopy images were acquired using a DeltaVision deconvolution microscopy (GE Healthcare). Images were deconvoluted and channels were aligned using SoftWoRx v.3.5.1. software. Contrast and brightness adjustment and cell measurements were performed using Fiji (ImageJ).

Table 2.7. Deltavision filter sets and fluorophores

Filter	Excitation filter (nm)	Emission filter (nm)	Fluorophores
DAPI	360/40	457/50	HADA
FITC	492/20	528/38	SNAP-Surface Alexafluor 488, rabbit α-mouse secondary antibody conjugated to Alexafluor 488
Cy5	640/20	685/40	SNAP-Surface Alexafluor 647

Chapter 3

Use of SNAP-tag Fusion Constructs to Localise Surface Proteins in *Staphylococcus aureus*

3.1. Introduction

S. aureus expresses and displays over 30 proteins on its cell surface, many of which contribute to the bacterium's ability to cause disease (Solis *et al*, 2014; Mazmanian *et al*, 2001). Surface proteins, also called cell wall associated / anchored (CWA) proteins, are generally characterised by the presence of a Sec-dependent N-terminal signal sequence, as well as a C-terminal sorting signal (Foster, 2019). Examples include the iron-regulated surface determinant proteins (IsdAB), clumping factor A (ClfA), and surface protein A (SpA), where IsdB, ClfA, and SpA possess an N-terminal YSIRK signal sequence motif. IsdA however has no YSIRK signal sequence. All have an LPXTG sorting signal at their C-termini (Clarke *et al*, 2004; Torres *et al*, 2006; McDevitt *et al*, 1997; Hasman *et al*, 2010). The presence of a YSIRK signal sequence – which is highly conserved among staphylococci – is thought to direct the translocation of these surface proteins across the cell membrane and into nascent cell wall material at the developing septum (Carlsson *et al*, 2006). The LPXTG sorting signal is recognised by the membrane-bound enzyme Sortase A (SrtA), which incorporates CWA proteins into the cell wall peptidoglycan via Lipid II, a peptidoglycan pre-cursor molecule (Chapter 1, Section 1.4.) (Mazmanian *et al*, 1999).

Previous studies have employed different techniques to localise various key virulence factors of *S. aureus*, including plasmid-based fluorescent protein fusion constructs, such as mCherry, and immunofluorescence microscopy (Zhang *et al*, 2021; DeDent *et al*, 2007). The results from these studies are incongruent however, despite working to localise the same surface protein – in this case Surface Protein A. DeDent *et al* favoured the use of the far-red Cy3 fluorophore conjugated to IgG to localise SpA. They observed SpA labelling as distinct and punctate foci diagonal to the developing septum, and thereby propose a model of distribution of SpA over time. Zhang *et al*, by contrast, use a plasmid borne, chemically inducible SpA construct to modulate expression, then immunostained with SpA-specific primary antibodies and fluorescently conjugated secondary antibodies. They show that SpA localises exclusively to

the cross wall of dividing cells. Additionally, both groups use the *S. aureus* strain RN4220 to study SpA display. RN4220 is a heavily mutated, cloning intermediate strain originally isolated to methylate foreign DNA for subsequent transfer into other *S. aureus* strains without restriction (Monk *et al*, 2015). It also lacks a functional *agr* locus, which therefore affects the expression and regulation of many virulence determinants (Nair *et al*, 2011). As such, a more robust and reliable approach to localise surface proteins is required in a well characterised strain of *S. aureus*, such as the SH1000 background, to establish a representation of wild type and clinically relevant SpA display and development, both temporally and spatially (O'Neill, 2010).

SNAP-tag is an increasingly popular biotechnological approach for the localisation of proteins, both in bacteria and mammalian cell lines (Kolberg *et al*, 2013). SNAP is the result of a directed evolution experiment on the human DNA repair protein O^6-Alkylguanine-DNA-Alkyltransferase, where instead of recognising alkylguanine, SNAP covalently binds to benzylguanine. Subsequent benzylguanine derivatives have been produced, conjugated to a variety of functional groups – including fluorophores – for localisation and purification studies using SNAP-tag. Much like the popular Green Fluorescent Protein (GFP), SNAP can be fused to a protein of interest via a short oligo linker (Cole, 2013). Unlike GFP however, which is constitutively fluorescent, SNAP can be labelled at a 1:1 stoichiometry with benzylguanine derivative dyes, which are otherwise inert *in vivo*. This allows for the selective labelling of SNAP, fused to a protein of interest, for localisation or purification without interfering with other biomolecules or pathways. Critically for this work, SNAP-tag can be used with non-cell permeable dyes to specifically label surface proteins and is resistant to fixative agents. Additionally, the variety of SNAP dyes and blocking substrates available allows for the dynamic labelling of fusion constructs over time, using different fluorophores which can be excited by different wavelengths. Therefore, SNAP provides the user with a variety of approaches at their disposal without the need for additional cloning, as SNAP-tag function is multi-faceted and subject to the benzylguanine substrates used. These characteristics make SNAP-tag an attractive biotechnological tool for the localisation of *S. aureus* surface proteins. Previous work carried out in the Foster lab has previously shown SNAP-tag to be an effective tool for localising a variety of cytoplasmic proteins in *S. aureus* (Lund *et al*, 2018).

3.1.2. Aims of the Chapter

The aim of this chapter was to evaluate the use of SNAP-tag fusions to localise surface proteins of *S. aureus*. Specifically, the aims were to:

i. Construct a suite of SNAP-tag protein fusions

ii. Create *S. aureus* SH1000 strains containing SNAP-tag fusions to *isdA*, *isdB*, *clfA*, and *spa* in their respective deletion mutant strains

iii. Visualise SNAP-surface proteins constructs using fluorescence microscopy.

3.2. Results

3.2.1. *isdA-SNAP* Suicide Vector Design and Chromosomal Integration

All suicide vectors used in this study were either synthesised by GeneWiz or constructed by Kasia Wacnik in the Foster lab as part of previous work. The *isdA-SNAP* suicide vector was designed for a single homologous recombination crossover event into the chromosome of *S. aureus* SH1000 (Figure 3.1.). Specifically, SH1000 *isdA*::*erm* (SJF 2181) was chosen as the intended final recipient of the pTH002 *isdA-SNAP* suicide vector to ensure that the *isdA-SNAP* fusion is the only copy of *isdA* stably expressed within the chromosome. *isdA-SNAP* lies under the native *isdA* promotor and is preceded by its native signal peptide sequence. *SNAP* is encoded after the 138 bp signal sequence of *isdA* and is followed by a short flexible oligo-linker. This was designed to enable the continued recognition of the IsdA signal peptide and to observe IsdA localisation as close to wild type SH1000 as possible. Iron-regulated surface determinant proteins, including IsdA and IsdB, are controlled by the ferric uptake regulator protein (Fur) and PerR and are expressed under iron-limited conditions (Clarke *et al*, 2004).

First, endonuclease restriction digestion using NsiI was performed to verify the plasmid size. The expected band sizes of 1 Kb for the insert containing *isdA-SNAP*, and 9 Kb for the plasmid backbone were separated by gel electrophoresis (Figure 3.1.). The 3' end of the *lysA* gene was chosen for homologous recombination due to its size (approximately 1 Kb) and previous use as a site of homologous recombination (Panchal *et al*, 2020). The integration of DNA into this site was designed in such a way that the *lysA* gene, encoding a diaminopimelate decarboxylase, would remain intact. Transformation into the restriction-deficient, modification-efficient RN4220 strain for DNA methylation was successful (SJF 5276) (Figure 3.1.). However, bacteriophage transduction into the SH1000 *isdA*::*erm* strain for further study could not be achieved. Wild type *S. aureus* SH1000 genomic DNA was used as a negative control for chromosomal integration screening owing to the lack of *SNAP* in its chromosome. No bands were seen for wild type SH1000 as a negative control, which lacks *SNAP* DNA for the *SNAP* R primer to bind to. Expected band size of 1.6 Kb was seen in the genomic DNA of transformed RN4220 cells (Figure 3.1.).

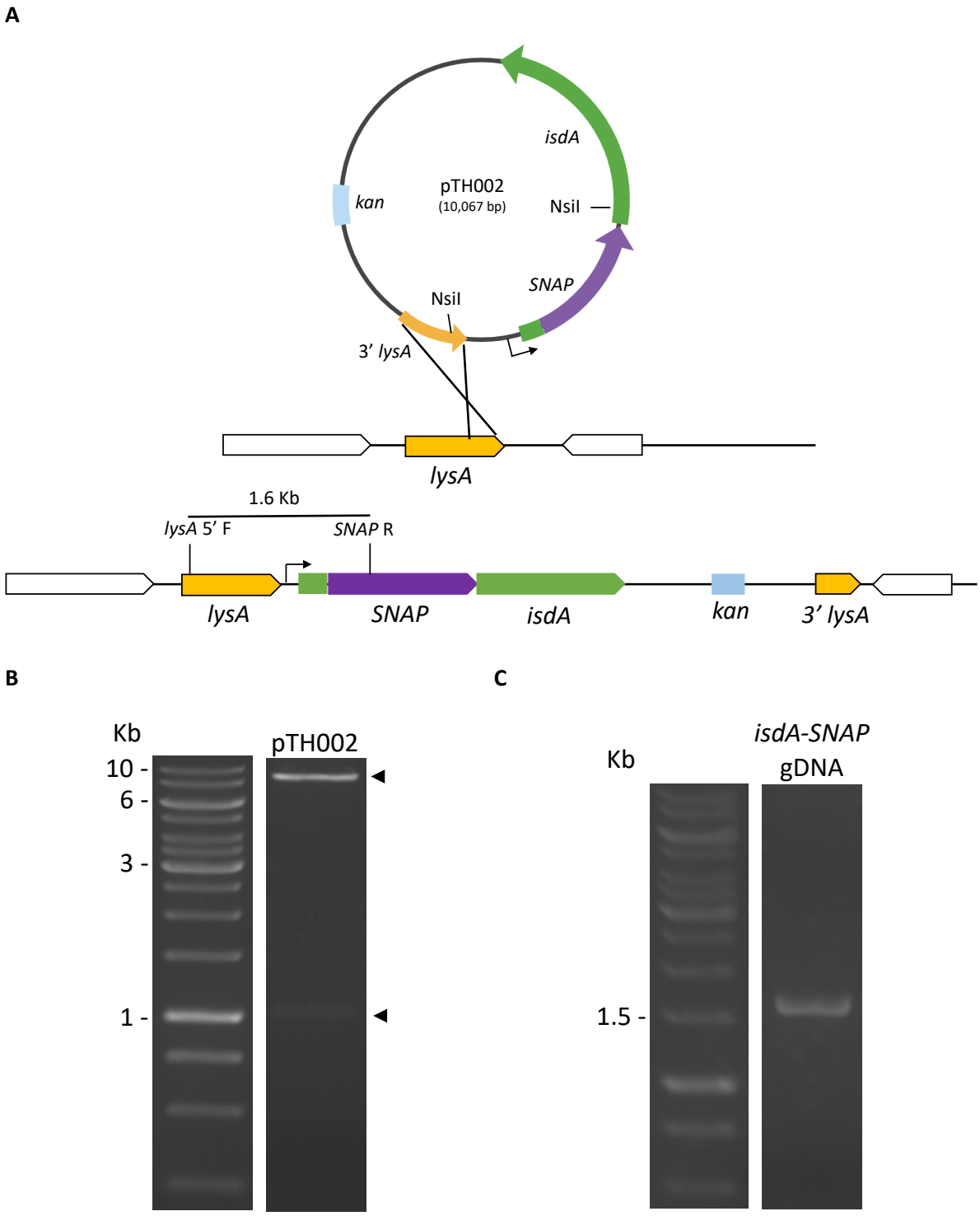

Figure 3.1. *isdA-SNAP* suicide vector and integration

(A) Schematic representation of pTH002 suicide vector showing homologous *lysA* 3' recombination into the *S. aureus* chromosome. **(B)** Endonuclease restriction digest of pTH002 was performed using NsiI to verify plasmid size. Insert = 1 Kb, plasmid backbone = 9 Kb. **(C)** Genomic DNA was purified from RN4220 *lysA*::*isdA-SNAP* and amplified using *lysA* 5' F and *SNAP* R primers to verify integration of pTH002 into the chromosome of *S. aureus* RN4220. Expected band size of 1.6 Kb was observed.

3.2.2. *isdB-SNAP* Suicide Vector Design and Chromosomal Integration

The *isdB-SNAP* suicide vector is identical to that of *isdA-SNAP*, except for an erythromycin resistance cassette (erm) for selection in the recipient strain. The *isdB-SNAP* vector was designed for a single homologous recombination crossover event into the chromosome of *S. aureus* SH1000 via the 3' end of *lysA* as described previously (Section 3.2.1.). Specifically, SH1000 *isdB*::*tet* (SJF 2507) was chosen as the intended final recipient of the pTH003 *isdB-SNAP* suicide vector to ensure that the *isdB-SNAP* fusion is the only copy of *isdB* stably expressed within the chromosome. *isdB-SNAP* lies under the control of its native promotor and is preceded by its native signal peptide sequence composed of 120 bp, followed by a flexible oligo-linker sequence connecting *SNAP* to the remainder of *isdB*. This was designed to retain the function of the IsdB signal peptide recognition and cleavage, and to enable the observation of IsdB localisation as close to wild type SH1000 as possible. Therefore, *isdA-SNAP* expression requires iron-limited conditions to be expressed (Chapter 1, Section 1.3.2.1.; Section 3.2.1.).

To verify the size of pTH003 an endonuclease restriction digest was performed using HindIII. Plasmid DNA was separated by gel electrophoresis and band sizes of the 2.8 Kb insert of *isdB-SNAP* and 7.6 Kb plasmid backbone were both observed (Figure 3.2.). Transformation into the restriction-deficient, modification-efficient RN4220 strain for DNA methylation was achieved using *lysA* 5' F and *SNAP* R primers, amplified and separated by PCR gel electrophoresis showing the expected band size of 1.6 Kb (SJF 5276) (Figure 3.2.). Bacteriophage lysates were generated of *S. aureus* RN4220 *isdB-SNAP* and were used to transduce *isdB-SNAP* into *S. aureus* SH1000 *isdB*::*tet* via horizontal gene transfer and subsequent homologous recombination of the 3' end of *lysA* into the chromosome of *S. aureus* SH1000 *isdB*::*tet*. The same *lysA* 5' F and *SNAP* R primers were used to amplify 1.6 Kb of genomic DNA purified from colonies successfully grown on selective media containing 5 μg mL^{-1} erythromycin (Section 3.2.1.; Figure 3.2.). The expected band size of 1.6 Kb was observed by gel electrophoresis, confirming the construction of *S. aureus* SH1000 *isdB*::*tet lysA*::*isdB-SNAP* (SJF 5363).

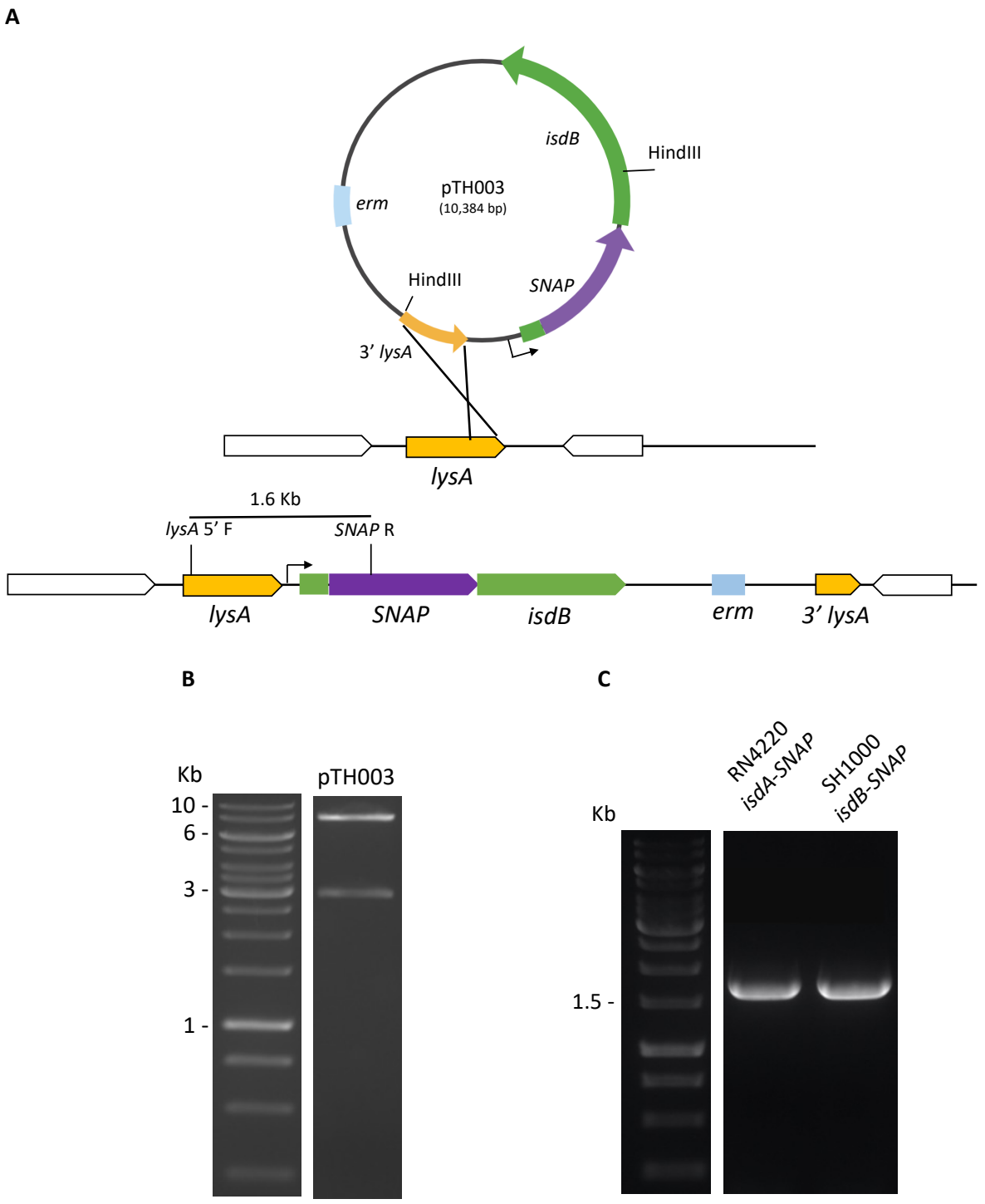

Figure 3.2. *isdB-SNAP* suicide vector and integration

(A) Schematic representation of pTH003 suicide vector showing homologous *lysA* 3' recombination into the *S. aureus* chromosome. **(B)** Endonuclease restriction digest of pTH003 with HindIII showing expected 2.8 Kb and 7.6 Kb bands **(C)** Genomic DNA amplified using *lysA* 5' F and *SNAP* R primers to verify integration of methylated *isdB-SNAP* into the chromosome of *S. aureus* SH1000. Genomic DNA from RN4220 *isdA-SNAP* used as a positive control. Expected band sizes of 1.6 Kb were observed for both samples.

3.2.3. *clfA-SNAP* Suicide Vector Design and Chromosomal Integration

The *clfA-SNAP* suicide vector was designed for a single homologous recombination crossover event into the chromosome of *S. aureus* SH1000 via *lysA* recombination, as described previously (Sections 3.2.1., 3.2.2.). Specifically, SH1000 *clfA*::*erm* was chosen as the intended final recipient of the pTH004 *clfA-SNAP* suicide vector to ensure that the *clfA-SNAP* fusion is the only copy of *clfA* stably expressed within the chromosome. *clfA-SNAP* lies under its native promotor, is preceded by its native 117 bp signal peptide sequence and is linked to the remainder of the *clfA* gene by a sequence encoding a short, flexible oligo-linker. This was designed to enable the observation of ClfA localisation as close to wild type SH1000 as possible. ClfA is known to be predominantly expressed during stationary growth phase (Entenza *et al*, 2005; Crosby *et al*, 2016).

An endonuclease restriction digest was performed to confirm the size of the pTH004 plasmid. The DNA was separated by gel electrophoresis and the expected band sizes of 2.1 Kb and 10.2 Kb were observed for both the *clfA-SNAP* insert and plasmid backbone respectively (Figure 3.3). Successful transformation into the restriction-deficient, modification-efficient RN4220 strain for DNA methylation was achieved as shown by gel electrophoresis separation of purified DNA, amplified using *lsyA* 5' F and *SNAP* R primers. A band of 1.6 Kb was observed, indicating successful integration of methylated pTH004 into the SH1000 chromosome at *lysA* (SJF 5278). Phage lysates were generated of *S. aureus* RN4220 *clfA-SNAP* and used to transduce *clfA-SNAP* into *S. aureus* SH1000 *clfA*::*erm* via horizontal gene transfer and homologous recombination (Figure 3.3.). Purified gDNA of the transduced strain was amplified using *lsyA* 5' F and *SNAP* R primers and separated by gel electrophoresis. A band of 1.6 Kb confirmed the successful creation of *S. aureus* SH1000 *clfA*::*erm lysA*::*clfA-SNAP* (SJF 5390).

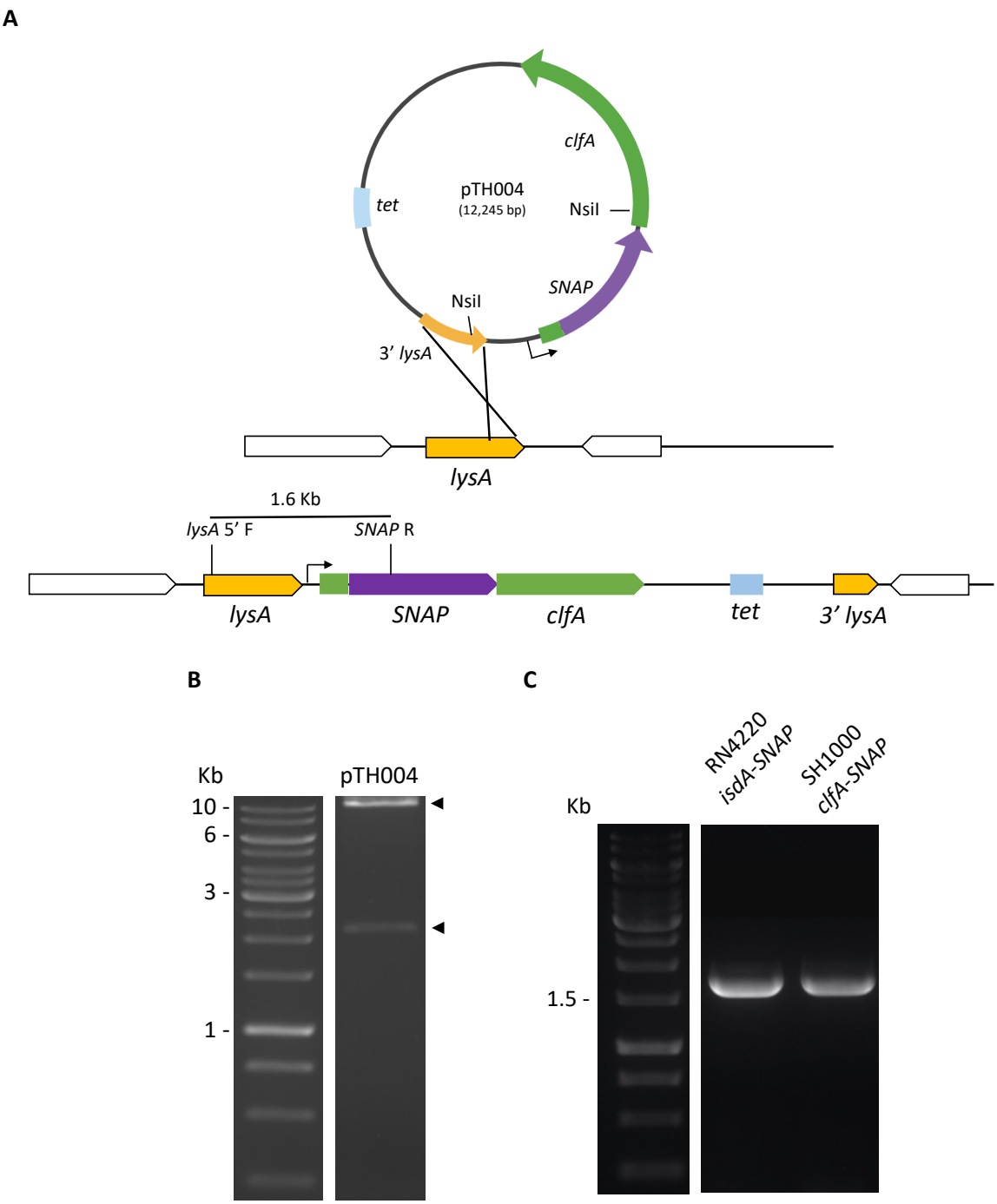

Figure 3.3. *clfA-SNAP* suicide vector and integration

(A) Schematic representation of pTH004 suicide vector showing homologous *lysA* 3' recombination into the *S. aureus* chromosome. **(B)** Endonuclease restriction digest of pTH004 with NsiI showing expected 2.1 Kb and 10.2 Kb bands. **(C)** Genomic DNA amplified using *lysA* 5' F and *SNAP* R primers to verify integration of methylated *clfA-SNAP* into the chromosome of *S. aureus* SH1000. Genomic DNA from RN4220 *isdA*-SNAP used as a positive control. Both show amplified bands of 1.6 Kb, indicating successful recombination into the chromosome.

3.2.4. *spa-SNAP* Suicide Vector Design and Chromosomal Integration

The *spa-SNAP* suicide vector was designed for a single homologous recombination crossover event into the chromosome of *S. aureus* SH1000 via the 3' end of *lysA*. Specifically, SH1000 *spa*::*kan* was chosen as the intended final recipient of the pTH005 *spa-SNAP* suicide vector to ensure that the *spa-SNAP* fusion is the only copy of *spa* stably expressed within the chromosome. *spa-SNAP* lies under its native promotor, is preceded by its native signal peptide sequence, composed of 108 bp, if followed by a sequence encoding a short, flexible oligo-linker connecting *SNAP* to the remainder of the *spA* gene. This was designed to enable the observation of SpA localisation as close to wild type SH1000 as possible. SpA is known to be regulated by both Agr and SarA (Paulander *et al*, 2018). Therefore, SpA-SNAP expression is regulated by mid-exponential growth phase via the alleviation of Agr mediated repression by RNAIII (Figure 1.8.).

An endonuclease restriction digest was performed on pTH005 using HindIII to verify the size of the plasmid prior to electroporation into RN4220 for DNA methylation. The expected band sizes of 2.3 Kb for the *spa-SNAP* insert and 7.6 Kb for the plasmid backbone were observed by gel electrophoresis (Figure 3.4.). Successful transformation into the restriction-deficient, modification-efficient RN4220 strain for DNA methylation was achieved, shown by gDNA PCR using *lysA* 5' F and *SNAP* R primers which amplified 1.6 Kb of the recombined DNA. Phage lysates were generated of *S. aureus* RN4220 *spa-SNAP* (SJF5281) and used to transduce methylated *spa-SNAP* into *S. aureus* SH1000 *spa*::*kan* via horizontal gene transfer and homologous recombination into *lysA*. Genomic DNA from the SH1000 *spa*::*kan* strain transduced with phage lysate containing methylated *spa-SNAP* was purified and amplified using *lysA* 5' F and *SNAP* R primers. The 1.6 Kb band was separated and observed by gel electrophoresis, confirming the generation of *S. aureus* SH1000 *spa*::*kan lysA*::*spa-SNAP* (SJF 5329) (Figure 3.4.).

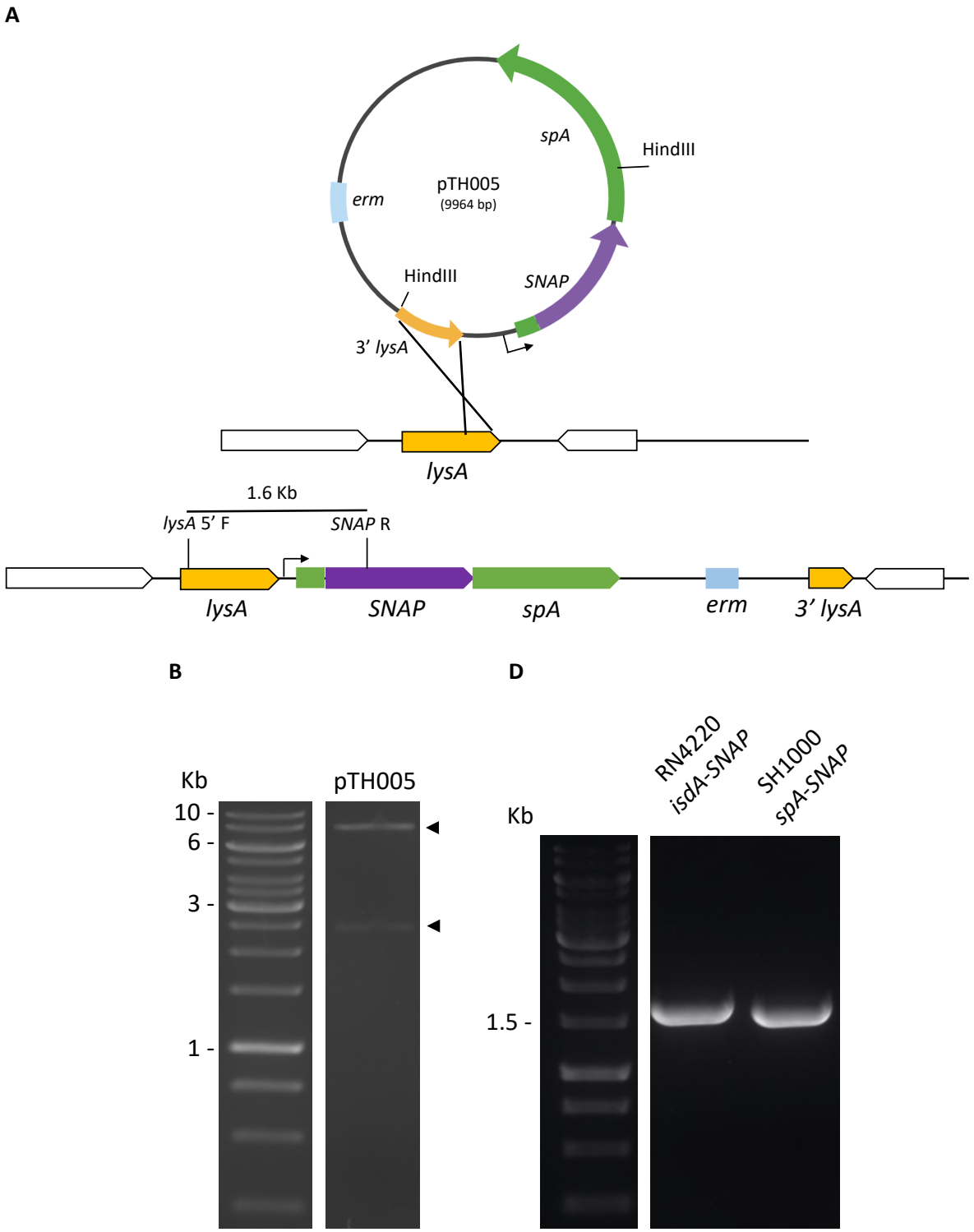

Figure 3.4. SpA-SNAP suicide vector and integration

(A) Schematic representation of pTH005 suicide vector showing homologous *lysA* 3' recombination into the *S. aureus* chromosome. **(B)** Endonuclease restriction digest of pTH005 cut with HindIII, showing expected 2.3 Kb and 7.6 Kb bands. **(C)** Genomic DNA amplified using *lysA* 5' F and *SNAP* R primers to verify integration of methylated SpA-SNAP into the chromosome of *S. aureus* SH1000. Genomic DNA from RN4220 *isdA*-SNAP used as a positive control. The expected band size of 1.6 Kb was observed.

3.3. Proteomic verification of SH1000 SpA-SNAP and ClfA-SNAP

Because the transduction of methylated *isdA-SNAP* from RN4220 into SH1000 was unsuccessful, the remaining SH1000 strains containing SNAP-tag fusions were prioritised for further analysis. Additionally, iron-limited conditions are required to produce IsdB (Torres *et al*, 2010). As such, it was determined that the *clfA-SNAP* and *spa-SNAP* strains would be simpler to grow and assess for SNAP expression and subsequent fluorescent labelling. For simplicity, the SH1000 strains containing recombinant *SNAP* fusions will be referred to by their associated proteins throughout (i.e. SH1000 *spa*::*kan lysA*::*spa-SNAP* will be referred to simply as SpA-SNAP).

S. aureus SH1000 SpA-SNAP and ClfA-SNAP were chosen for further analysis because of their ease of use. SpA-SNAP was grown to mid exponential phase for expression, while ClfA-SNAP was grown to stationary phase. Proteomic analysis was performed by Western blot with whole cell lysates of *S. aureus* SH1000 SpA-SNAP and ClfA-SNAP, using the chemically inducible, plasmid-based *ftsZ-SNAP* as a positive control (Lund *et al*, 2018). *ftsZ-SNAP* lies under the Pspac promotor and is repressed by LacI. The addition of 1 mM Isopropyl β-d-1-thiogalactopyranoside (IPTG) alleviates LacI repression of Pspac and induces the expression of the genes downstream (*ftsZ-SNAP*) (Sun *et al*, 2009).

To verify the presence of SNAP-tag in the cell wall of *S. aureus* SH1000 SpA-SNAP, samples were grown and fractionated as described in Chapter 2, Section 2.12.2 for Western blot analysis using α-SNAP antibodies. SNAP is a 20 kDa protein, and Western blot analysis shows both SpA-SNAP and FtsZ-SNAP bands at ~70kDa, as expected. Additionally, no SNAP specific binding was seen in the wild type control sample, nor the ClfA-SNAP sample, where a band of 111 kDa was expected. As such, further analysis of SNAP constructs was performed using SpA-SNAP only. SNAP was detected in both the cell wall and membrane fractions of SpA-SNAP at approximately 70 kDa (Figure 3.5.). A growth curve of SpA-SNAP against the wild type SH1000 strain of *S. aureus* shows that the mutant grows slightly quicker during mid-exponential and stationary phase.

A

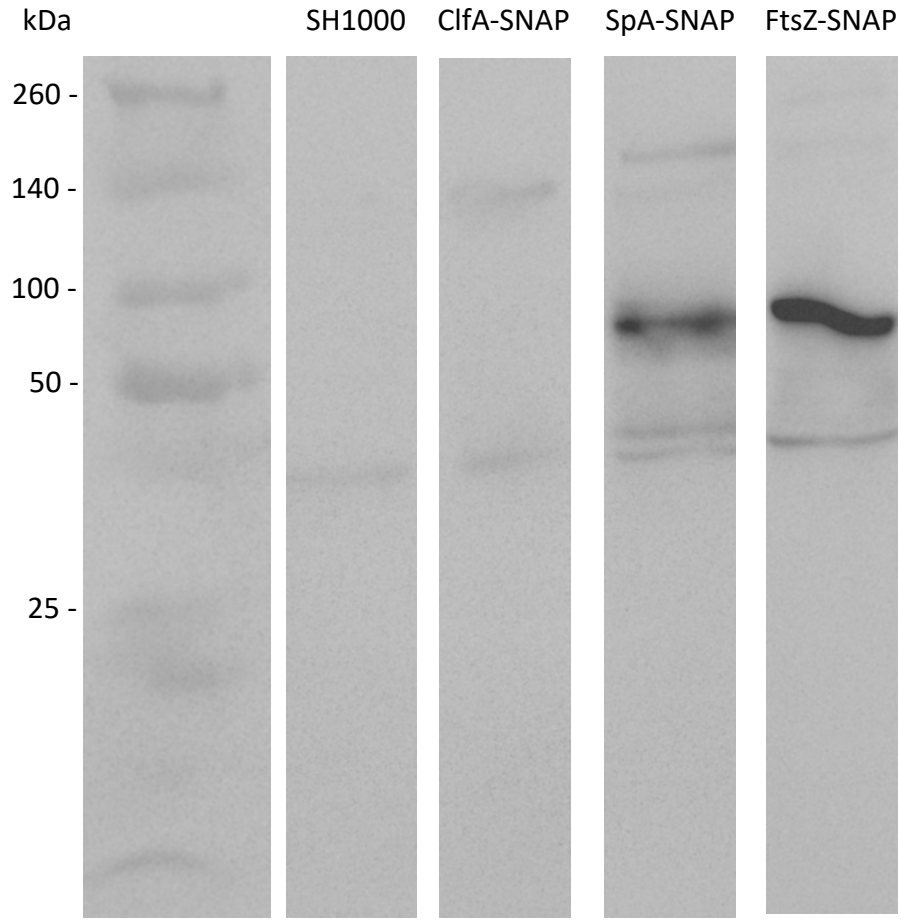
kDa
SH1000
ClfA-SNAP
SpA-SNAP
FtsZ-SNAP
260 -
140 -
100 -
50 -
25 -

B

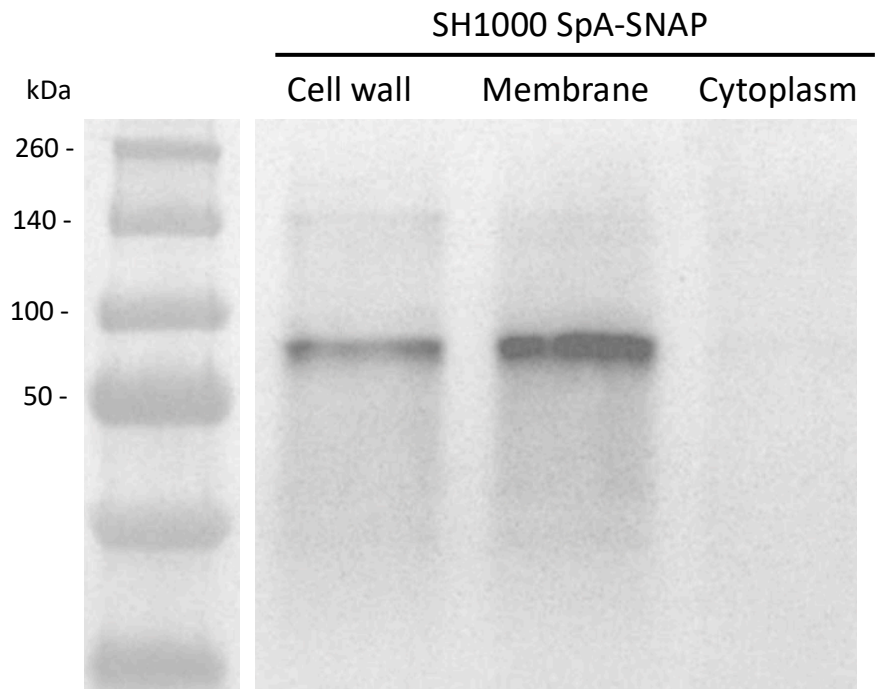
SH1000 SpA-SNAP
kDa
Cell wall
Membrane
Cytoplasm
260 -
140 -
100 -
50 -

C

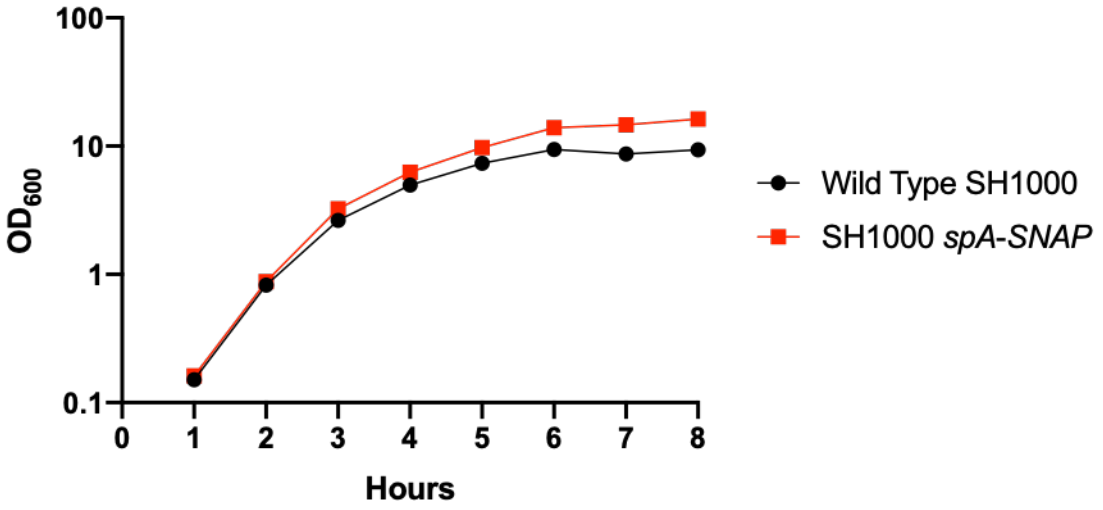

Figure 3.5. Expression of SpA-SNAP fusion protein in SH1000

(A) Whole cell lysates of SH1000 wild type, ClfA-SNAP, SpA-SNAP, and FtsZ-SNAP were seperated by a 12% (w/v) SDS-PAGE and transferred to an activated membrane for α-SNAP Western blot analysis. Samples were normalised to an OD_{600} of 2 prior to lysis. Wild type sample shows binding around 50 kDa, which is consistant throughout all sample and is likely native SpA binding to the Fc region of the α-SNAP antibodies. The expected band for ClfA-SNAP of 111 kDa was not observed. Expected band sizes of both SpA-SNAP and FtsZ-SNAP were observed at ~70 kDa. **(B)** α-SNAP Western blot analysis on cell wall, membrane, and cytoplasmic fractions of SpA-SNAP. Expected band sizes of SpA-SNAP were observed in the cell wall and membrane fractions at ~70 kDa. No band was observed in the cytoplasmic fraction. **(C)** Growth curve of *S. aureus* SH1000 wild type SH1000 compared to SpA-SNAP, measured by optical density at 600 nm. Error bars are too small to show. n = 3.

3.4. Fluorescence Microscopy of SpA Localisation Using SpA-SNAP Protein Fusion

Diffraction-limited fluorescence microscopy was used to visualise the surface display of SpA-SNAP. To juxtapose nascent cell wall synthesis to SpA localisation, samples were incubated with a 1mM fluorescent D-Alanine derivative (HADA) for 5 minutes in TSB at 37°C. HADA is incorporated as a fluorescent terminal D-Ala in the peptide stem of peptidoglycan when supplemented into growth media. Incorporation can take as little as 15 seconds to visualise nascent cell wall synthesis (Lund *et al*, 2018). Samples were then washed twice in PBS and fixed with 4% (v/v) paraformaldehyde for 30 minutes at room temperature. Samples were washed twice in PBS, and SNAP was labelled using a range of concentrations of benzylguanine derivative Alexa Fluor 647 conjugated dye (BG-AF 647; magenta) in TSB, at 37°C for 5 minutes (Sun *et al*, 2011). Labelled and fixed samples were mounted on poly-L-Lysine coated Poly-Prep slides and buffered with SlowFade gold anti-fade reagent. Nascent septum synthesis and cell wall was visualised with HADA (cyan) (Kuru *et al*, 2012). Images were captured on an OMX DeltaVision Imagine System using conventional settings. Excitation wavelengths used were 405 nm for HADA, and 647 nm for BG-AF 647. Excitation time for all wavelengths was 200 ms. Laster intensity was set to 10% for HADA channels and 30% for objective channels as an optimum setting to observe fluorescence while minimising fluorophore bleaching. Analysis of microscopy images was performed on convoluted images. Data shown herein are deconvoluted for clarity.

The visualisation of SpA-SNAP required a substantial amount of method development and optimisation for use in the localisation of SpA in *S. aureus*. These include microscope setting configuration, substrate concentration, labelling time, labelling media, bacterial growth phase, the use of cell permeable dyes, and the effect of chemical fixation (Figures 3.6. – 3.13.). Ultimately, experimentation with these variables did not uncover a reliable method with which to visualise SpA-SNAP. Immunofluorescence microscopy was also used as an alternative method, which showed heterogenous SpA display in the population (Figure 3.14.). This was unexpected, as SpA is considered a rather ubiquitous protein (Frankel *et al*, 2010). As such, further investigation into SpA display using immunofluorescence microscopy was required in the wild type strain of *S. aureus* SH1000 (Chapter 4).

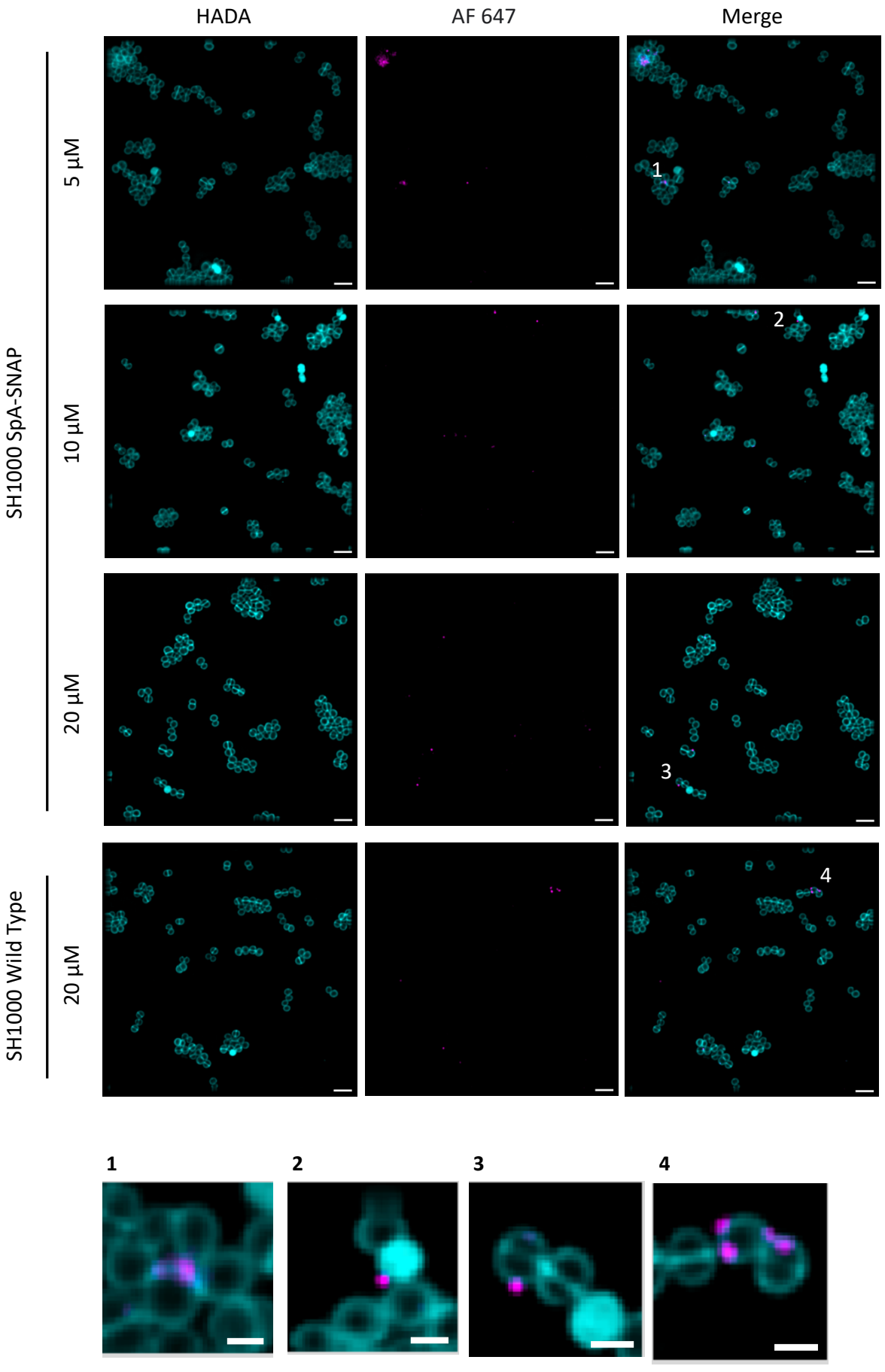
HADA
AF 647
Merge
SH1000 SpA-SNAP
5 µM
10 µM
20 µM
SH1000 Wild Type
20 µM
1
2
3
4
1
2
3
4

Figure 3.6. Effect of SNAP dye concentrations on SpA-SNAP labelling by fluorescence microscopy

Samples of *S. aureus* SH1000 *spa*::*kan lysA*::*spa*-SNAP were incubated with HADA (cyan) to visualise peptidoglycan synthesis, fixed with PFA, incubated with 5, 10, and 20 µM BG-AF 647 SNAP-Surface dye (magenta) in TSB, and mixed at 37°C for 30 minutes. Wild type *S. aureus* SH1000 not expressing SNAP-tag was used as a negative control. Inset numbers are enlarged to show punctate fluorescent signal associated with cells. Scale bars = 3 µm. Inset scale bars = 1 µm. n = 3.

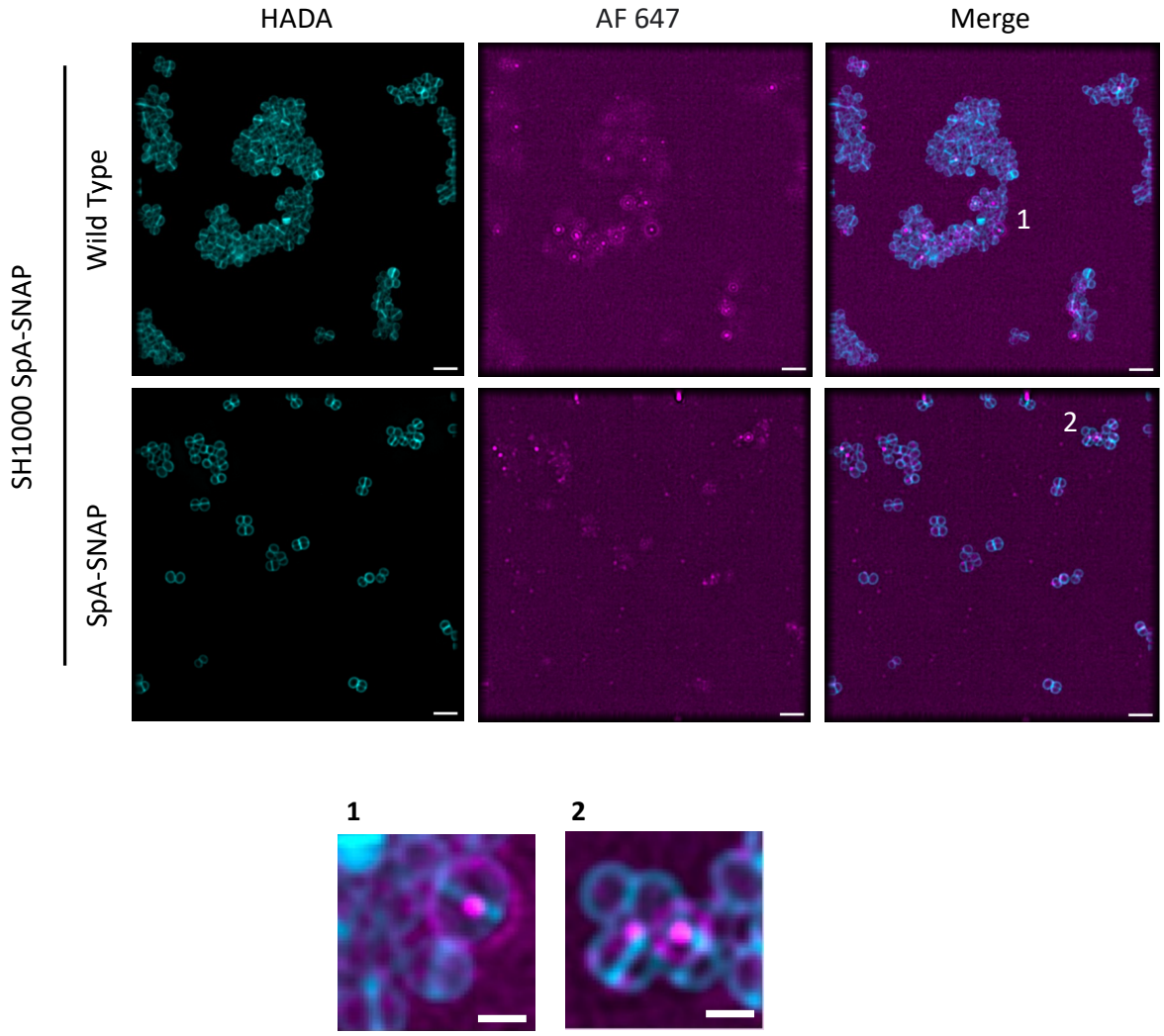

Figure 3.7. Effect of no contrast manipulation on SpA-SNAP localisation

Samples of *S. aureus* SH1000 SpA-SNAP were incubated with HADA (cyan) to visualise peptidoglycan synthesis, fixed with 4% (v/v) PFA, incubated with 5µM BG-AF 647 SNAP-Surface dye (magenta) in TSB, and rotated at 37°C for 30 minutes. Wild type *S. aureus* SH1000 not expressing SNAP-tag was used as a negative control. Contrast settings are typically altered to account for background fluorescence, such that the fluorescence seen is representative of viable signal (Figure 3.6.). Without appropriate contrast manipulation, background fluorescence is prominent and obscures potentially viable signal. Inset numbers 1 and 2 are enlarged below. Scale bars = 3 µm. Inset scale bars = 1 µm. n = 3.

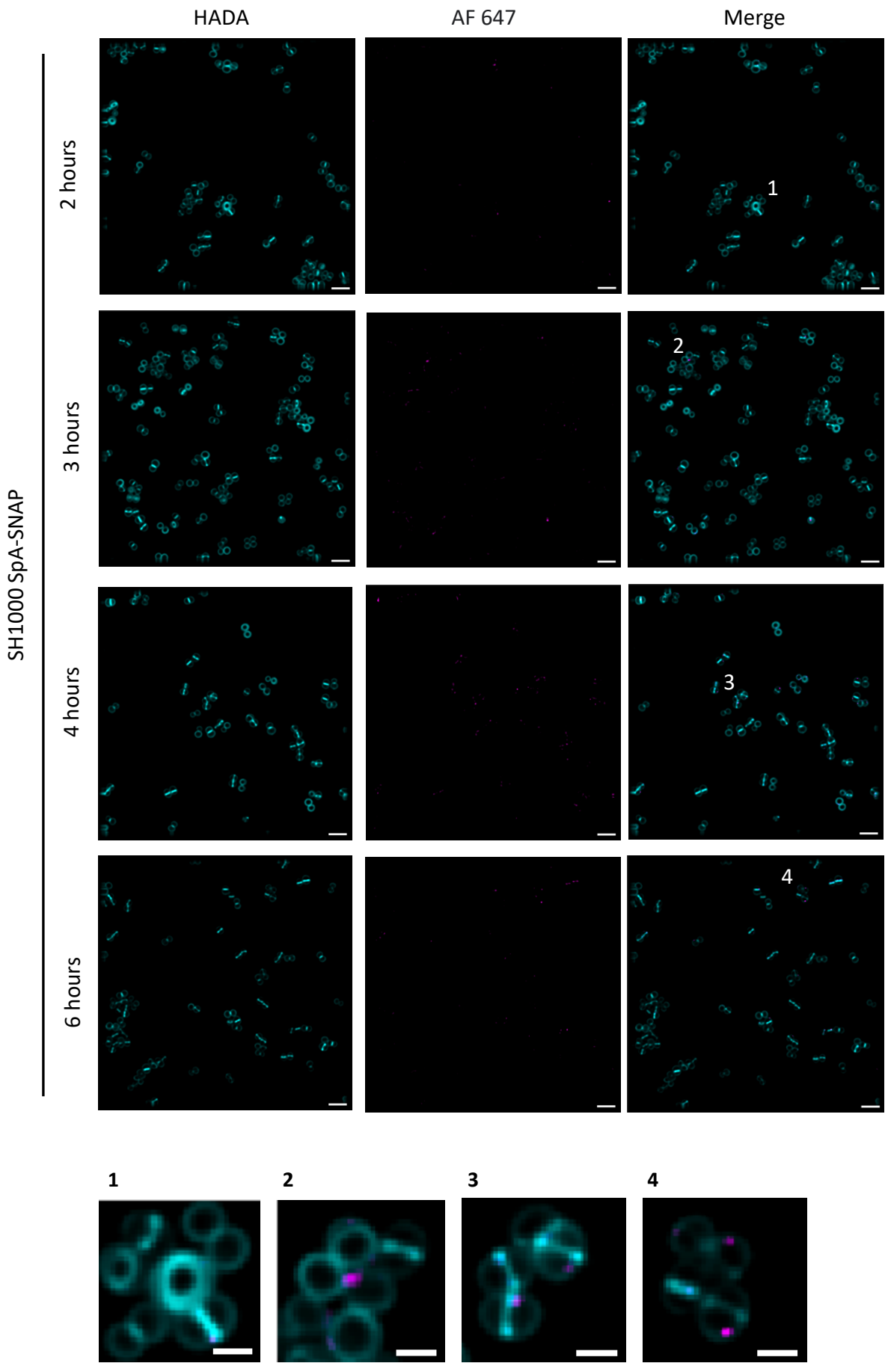
HADA
AF 647
Merge
SH1000 SpA-SNAP
2 hours
3 hours
4 hours
6 hours
1
2
3
4
1
2
3
4

Figure 3.8. Effect of growth phase on SpA-SNAP labelling by fluorescence microscopy

Samples of *S. aureus* SH1000 *spa*::*kan lysA*::*spa-SNAP* were incubated with HADA (cyan) to visualise septal synthesis, fixed with PFA, incubated with 5 µM BG-AF 647 SNAP-Surface dye (magenta) in TSB, and rotated at 37°C, for 30 minutes. Samples were taken throughout exponential growth phase to observe SpA-SNAP display (Figure 3.5.). Inset numbers are enlarged below. Scale bars = 3 µm. Inset scale bars = 1 µm. n = 3.

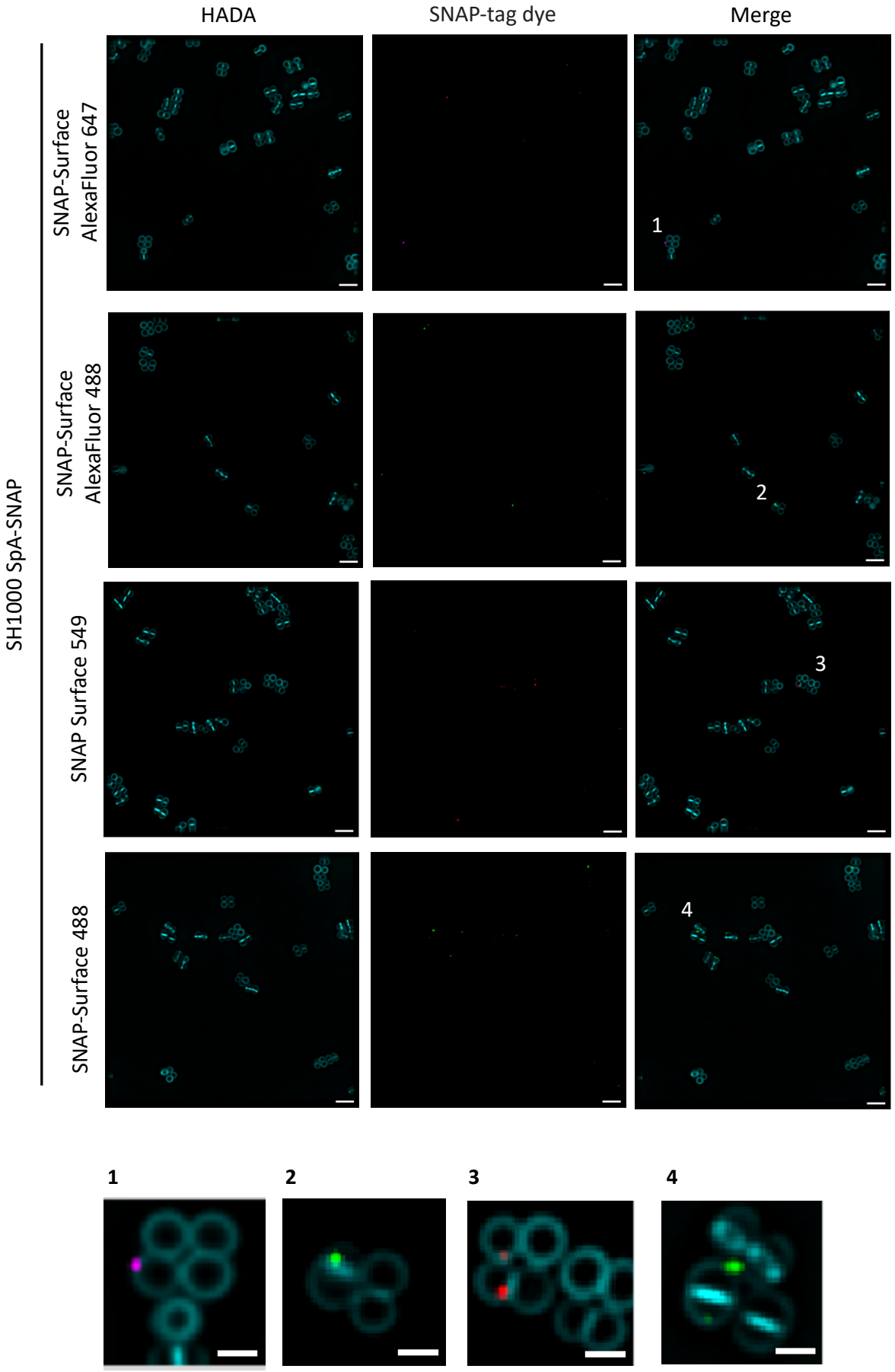
HADA
SNAP-tag dye
Merge
SH1000 SpA-SNAP
SNAP-Surface AlexaFluor 647
SNAP-Surface AlexaFluor 488
SNAP Surface 549
SNAP-Surface 488
1
2
3
4
1
2
3
4

Figure 3.9. Use of alternative SNAP labelling substrates for fluorescence microscopy

Samples of *S. aureus* SH1000 *spa*::*kan lysA*::*spa-SNAP* were incubated with HADA (cyan) to visualise septal synthesis, fixed with PFA, incubated with BG-AF 647 SNAP-Surface dye (magenta), BG-AF 488 (green), BG 549 (red), and BG 488 (green) in TSB, and rotated at 37°C, for 30 minutes. Inset numbers are enlarged below. Scale bars = 3 µm. Inset scale bars = 1 µm. n = 3.

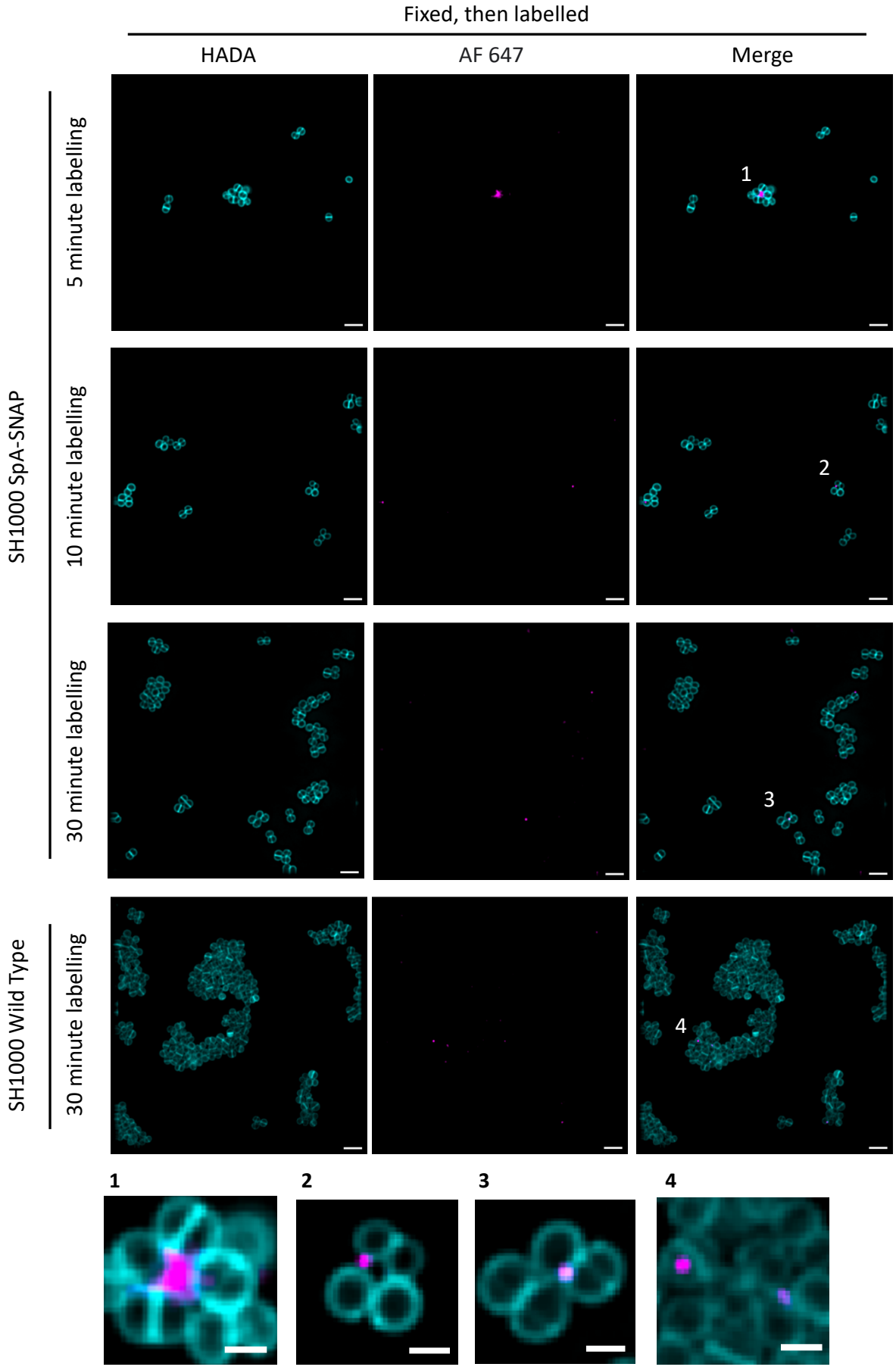
Fixed, then labelled
HADA
AF 647
Merge
SH1000 SpA-SNAP
5 minute labelling
10 minute labelling
30 minute labelling
SH1000 Wild Type
30 minute labelling
1
2
3
4
1
2
3
4

Figure 3.10. Effect of increased SNAP dye incubation time on SpA-SNAP labelling for fluorescence microscopy

Samples of *S. aureus* SH1000 *spa*::*kan lysa*::*spa-SNAP* were incubated with HADA (cyan) to visualise septal synthesis, fixed with PFA, incubated with BG-AF 647 SNAP-Surface dye (magenta) in TSB, and rotated at 37°C, for 5, 10, and 30 minutes to ascertain the optimum SNAP-tag labelling time. Wild type *S. aureus* SH1000 not expressing SNAP-tag was used as a negative control. Inset numbers are enlarged below. Scale bars = 3 µm. Inset scale bars = 1 µm. n = 3.

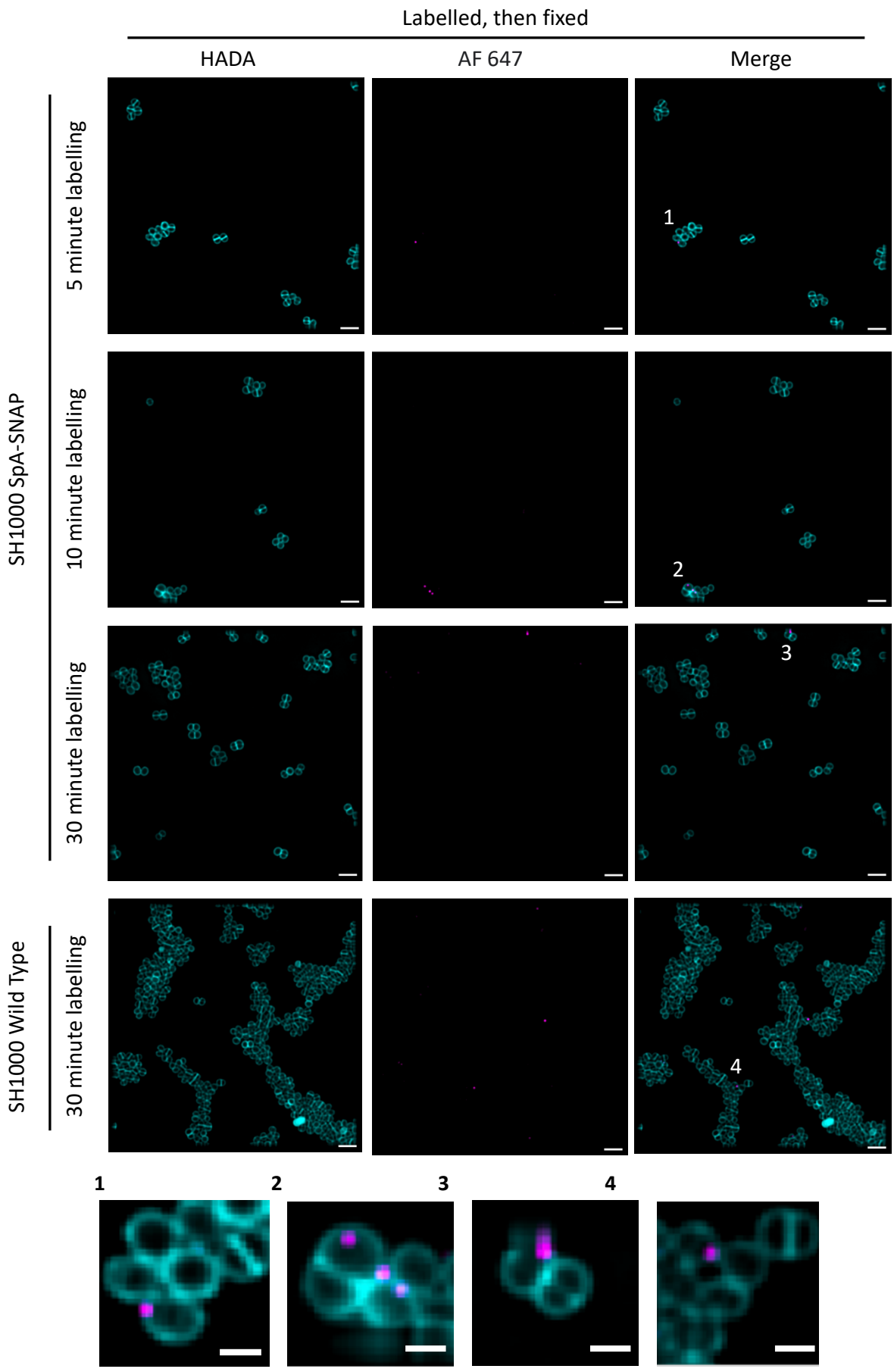
Labelled, then fixed
HADA
AF 647
Merge
SH1000 SpA-SNAP
5 minute labelling
10 minute labelling
30 minute labelling
SH1000 Wild Type
30 minute labelling
1
2
3
4
1
2
3
4

Figure 3.11. Effect of labelling SpA-SNAP prior to chemical fixation for fluorescence microscopy

To investigate the potential for PFA fixation interfering with the ability of SNAP-tag to bind the BG-AF 647 substrate, samples were labelled with HADA, incubated with the dye for 5, 10, and 30 minutes before fixation. Wild type *S. aureus* SH1000 not expressing SNAP-tag was used as a negative control. Inset numbers are enlarged below. Scale bars = 3 µm. Inset scale bars = 1 µm. n = 3.

A

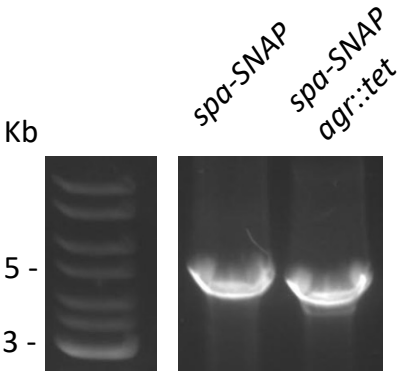
spa-SNAP
spa-SNAP agr::tet
Kb
5 -
3 -

B

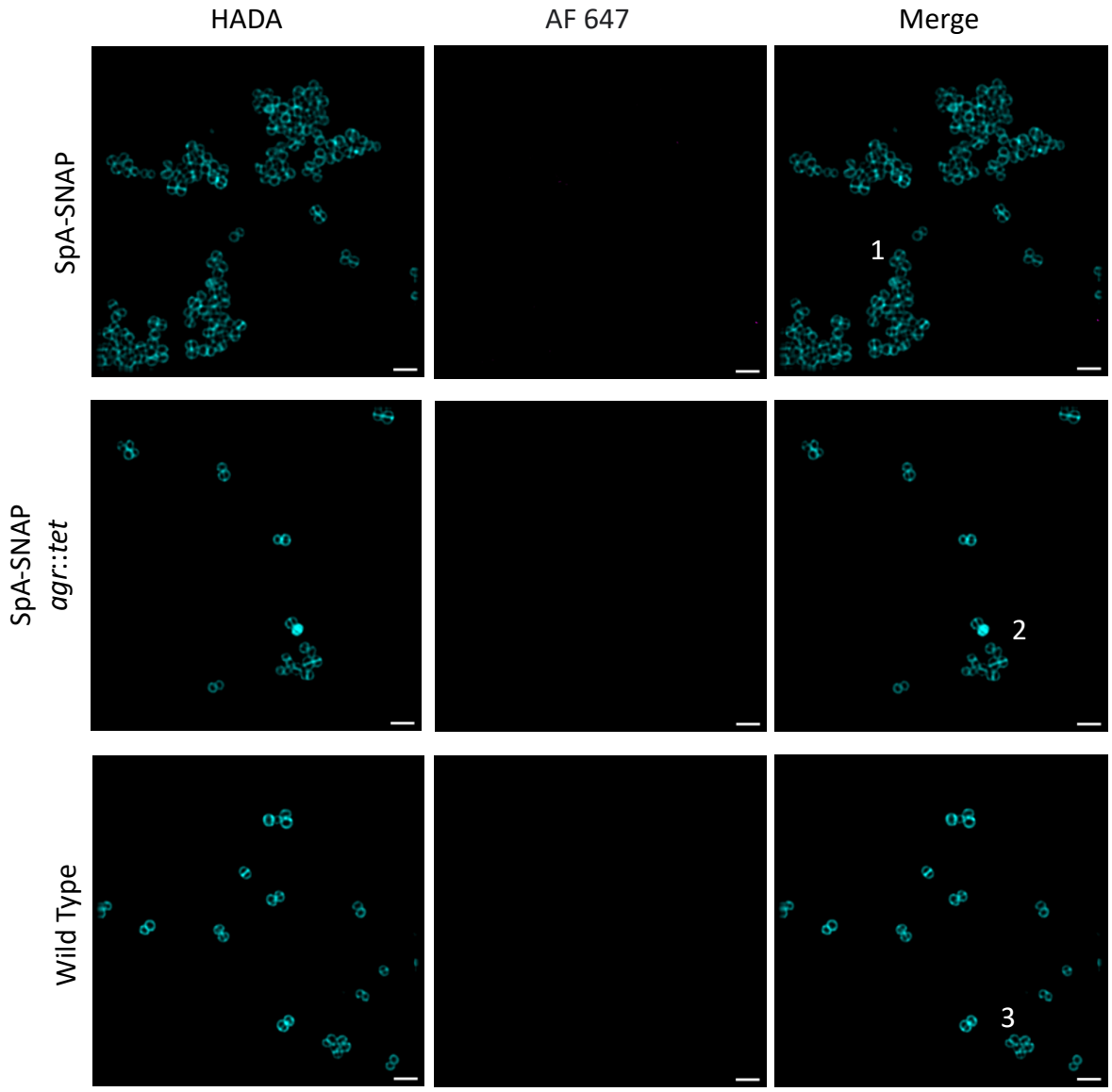
HADA
AF 647
Merge
SpA-SNAP
SpA-SNAP agr::tet
Wild Type
1
2
3

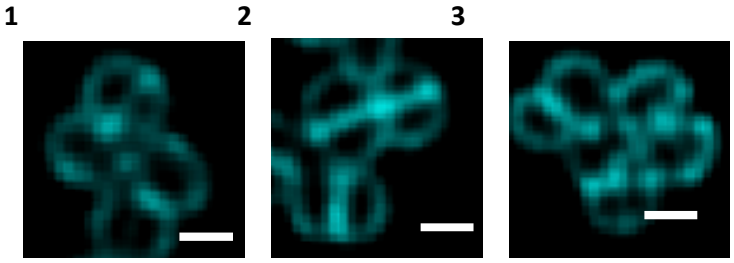

Figure 3.12. Effect of an *agr* mutation on SpA-SNAP labelling using fluorescence microscopy

(A) Genomic DNA of *spa-SNAP* and *spa-SNAP agr*::*tet* was amplified using *agr* 2 F and *agr* 2 R primers and verified by PCR and gel electrophoresis. The exact size difference of the *agr* mutation compared to the mutant is unknown. Thus, the slight difference in amplified DNA size was assumed to be representatie of a successful transduction of *agr*::*tet* into SpA-SNAP. **(B)** Samples of *S. aureus* SH1000 *spa*::*kan lysA*::*spa-SNAP* and *spa*::*kan lysA*::*spa-SNAP agr*::*tet* were incubated with HADA (cyan) to visualise peptidoglycan synthesis, fixed with PFA, incubated with 5 µM BG-AF 647 SNAP-Surface dye (magenta) in TSB, and rotated at 37°C for 30 minutes. Wild type *S. aureus* SH1000 not expressing SNAP-tag was used as a negative control. Inset numbers are enlarged below. Scale bars = 3 µm. Inset scale bars = 1 µm. n = 3.

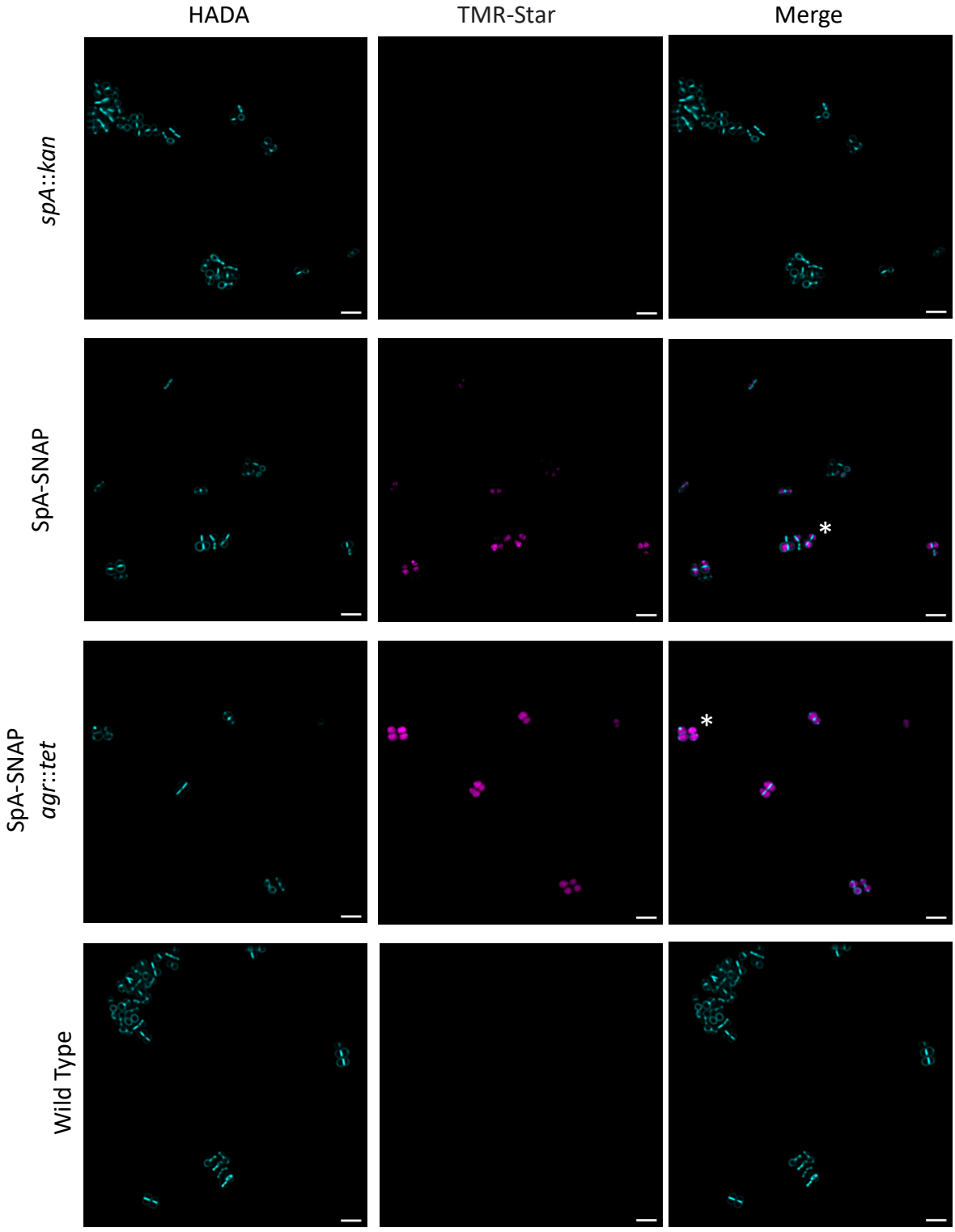
HADA
TMR-Star
Merge
spA::kan
SpA-SNAP
SpA-SNAP
agr::tet
Wild Type
*
*

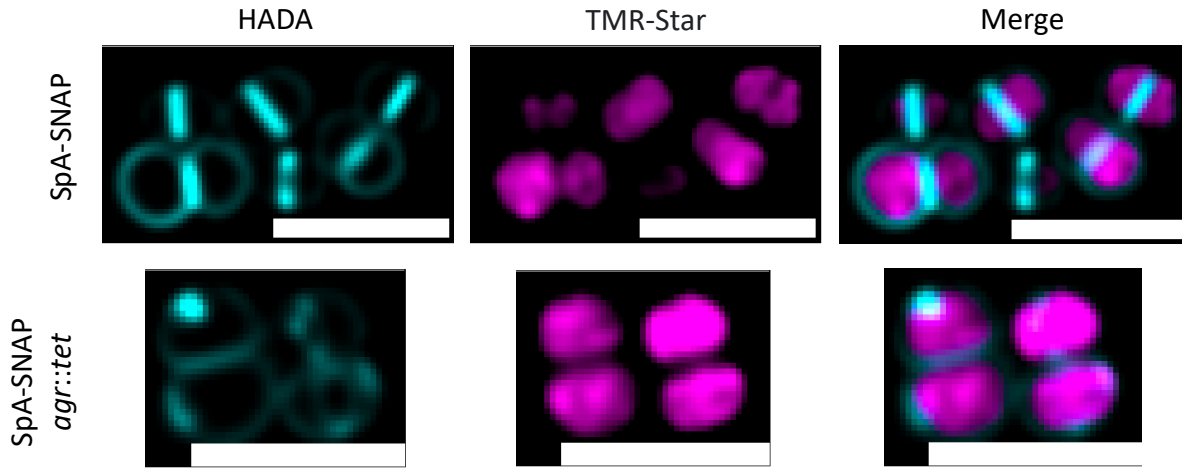

Figure 3.13. Effect of cell-permeable SNAP dye using fluorescence microscopy

Samples of *S. aureus* SH1000 *spa*::*kan lysA*::*spa-SNAP* and *spa-SNAP agr*::*tet* were incubated with HADA (cyan) to visualise septal synthesis, fixed with PFA, incubated with BG-AF 647 SNAP-Surface dye (magenta) in TSB, and rotated at 37°C, for 5 minutes. Wild type *S. aureus* SH1000 and SH1000 *spa*::*kan* not expressing SNAP-tag were used as negative controls. Cells marked with an asterisk are enlarged below. Cell permeable SNAP dye is retained in the cytoplasm of cells expressing SNAP-tag SpA fusions. Scale bars = 3 µm. n = 3.

New England Biosciences (NEB), the suppliers of both SNAP-tag biotechnology and its substrate benzylguanine derivative dyes, recommend a concentration of 5 µM for their non-cell permeable dyes. However, these recommendations are for cell and tissue cultures, not bacteria. Therefore, a variety of labelling concentrations, times, and media were tested to optimise and achieve SNAP-tag labelling in *S. aureus* cells expressing SNAP-tag fused to surface protein A (SpA) (Figures 3.6 – 3.7.). No reliable or distinct labelling of *S. aureus* expressing SNAP-tag conjugated SpA was observed on the cell surface under any of the conditions tested. Instead, each sample shows a small degree of fluorescence in punctate spots which, in some samples, were associated with cells, while others were not associated with any cells. As such, these signals could not be considered representative of SpA localisation.

To assess whether the process of chemical fixation affected SNAP-tag's ability to covalently bind the benzylguanine substrate, cells were incubated with the recommended 5 µM SNAP-Surface Alexafluor 647 (BG-AF 647) for varying periods of time before and after fixation with 4% (v/v) paraformaldehyde (Figures 3.10. and 3.11.). No difference in labelling was observed between cells incubated with BG-AF 647 before or after chemical fixation. The amount of time samples were subcultured prior to labelling and microscopy also appeared to have no impact on the degree of fluorescence observed (Figure 3.8.). Additionally, other benzylguanine derivative dyes from NEB were tested, including SNAP-Surface Alexafluor 488, SNAP-Surface 549, and SNAP-Surface 488 (Figure 3.9.). No new labelling patterns were observed in these samples aside from the punctate points of fluorescence observed previously.

SNAP-tag fusions to SpA were designed downstream of the native *spa* promotor to observe surface protein A localisation in conditions that are as close to the wild type *S. aureus* phenotype as possible. To assess whether native levels of expression of *spa* were insufficient for successful SNAP-tag labelling, a knockout mutation of *agr* was generated in SH1000 SpA-SNAP (Figure 3.12.). The Accessory Gene Regulator (Agr) is a negative regulator of multiple virulence factors – including SpA – and is comprised of five distinct *agr* genes. When functional, Agr-regulated RNAIII binding of *spa* mRNA is alleviated during exponential growth phase and is bound by RNAIII in lag and stationary phase, preventing *spa* translation (Robinson *et al*, 2005). Phage lysates were generated from *S. aureus* SH1000 *agr*::Tn551, in

which the *agr* locus is absent and a tetracycline resistance cassette is present as a selectable marker. Lysates from this strain were used to transduce the *agr* mutation into the SpA-SNAP recipient strain as described by Wu *et al*, 1999. The loss of *agr* did not appear to affect the level of SNAP-tag labelling in the SpA-SNAP strain, as no fluorescence could be observed in either sample (Figure 3.12.). However, incubating SpA-SNAP and SpA-SNAP *agr*::*tet* strains with a cell permeable benzylguanine derivative dye – SNAP-Cell TMR Star – shows either cytoplasmic SNAP binding, or cytoplasmic retention of the cell permeable dye (Figure 3.13.).

The punctate foci of SNAP labelling observed throughout figures 3.6. – 3.11. appears similar to findings from DeDent *et al*, 2007, in which they report using immunofluorescence microscopy to localise SpA in *S. aureus* RN4220. Therefore, to verify whether the punctate fluorescence observed throughout this chapter is representative of SpA localisation, Immunofluorescence microscopy was used as an alternative approach to localise surface protein A (Figure 3.14.). The immunolabelling protocol used in Figure 3.14. was adapted from DeDent *et al*, 2007 and uses mouse monoclonal α-SpA primary antibodies and rabbit α-mouse polyclonal secondary antibodies conjugated to Alexafluor 488. Labelling of surface protein A is observed in *S. aureus* SH1000 SpA-SNAP, SpA-SNAP *agr*::*tet*, and the wild type SH1000. No labelling is observed in the negative control *S. aureus* SH1000 *spa*::*kan*, which suggests that the fluorescence seen is specific to and representative of SpA localisation. Fluorescent signal observed via this protocol was consistent in a subset of each population, with the exception of SH1000 *spa*::*kan*, which showed a lack a fluorescence altogether. Therein, single cells display SpA over the whole surface, while diplococcal cells demonstrate a “horseshoe” like pattern of fluorescence, where no SpA is observed at developing septa.

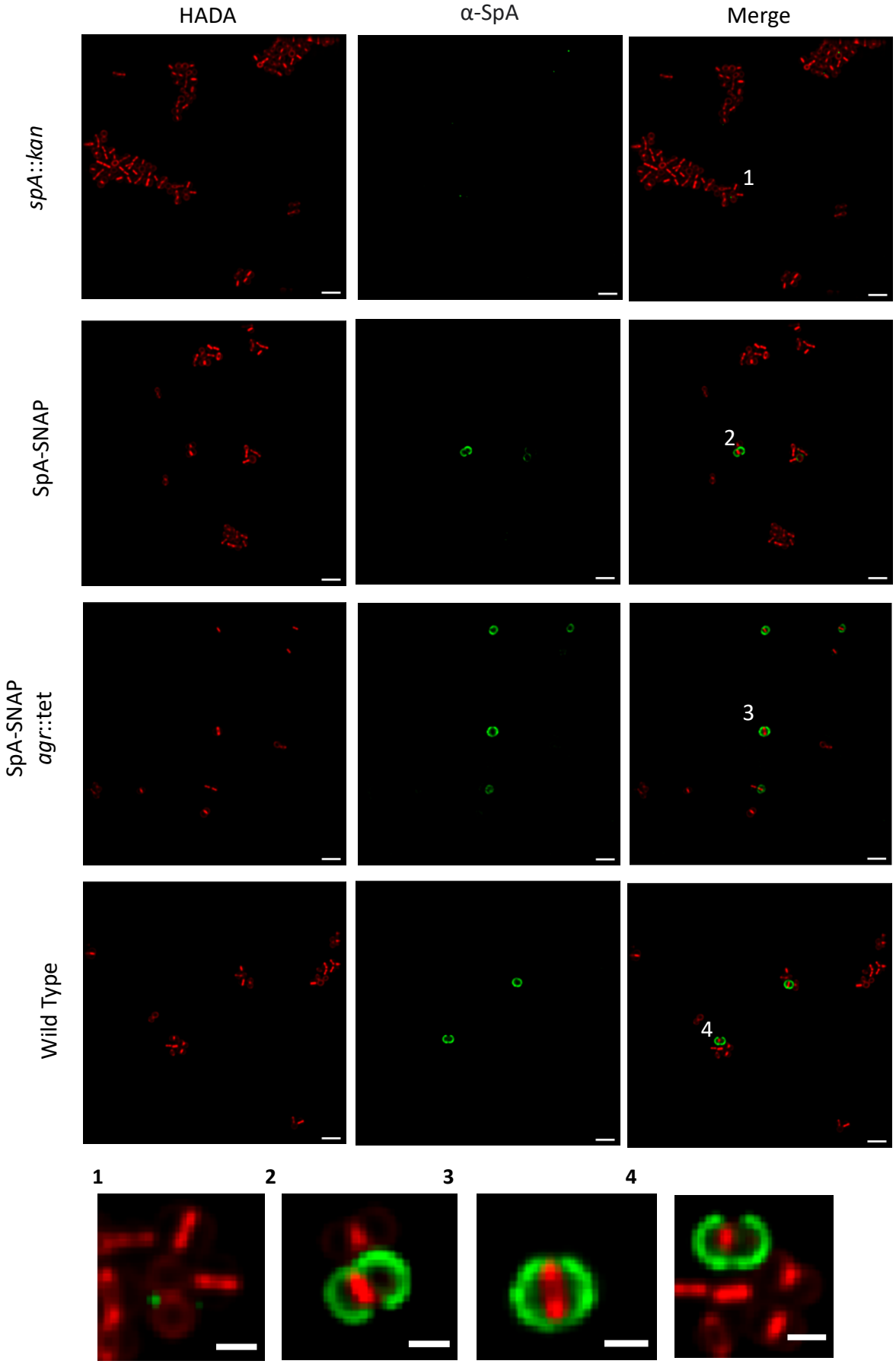
HADA
α-SpA
Merge
spA::kan
SpA-SNAP
SpA-SNAP agr::tet
Wild Type
1
2
3
4
1
2
3
4

Figure 3.14. Effect of α-SpA immunofluorescence microscopy on SpA localisation

Samples of *S. aureus* SH1000 *spa*::*kan lysA*::*spa-SNAP* and *spa*::*kan lysA*::*spa-SNAP agr*::*tet* were incubated with HADA (red) to visualise septal synthesis, fixed with PFA, blocked with 2% (w/v) BSA for 1 hour, and incubated with primary mouse α-SpA monoclonal antibody for 2 hours RT, rotating. Samples were then incubated with rabbit α-mouse secondary antibody (green) for 2 hours RT, rotating. Samples were mounted on poly-prep slides with slow-fade buffer and 22 x 22 mm high precision microscope cover glass. *S. aureus* SH1000 *spa*::*kan* was used as a negative control. Inset numbers are enlarged below. Scale bars = 3 μm. Inset scale bars = 1 μm. n = 3.

3.5. Discussion

Previous work from our lab has shown SNAP-tag to be an effective self-labelling tool to localise both essential and non-essential cytoplasmic proteins of *S. aureus* (Wacnik, 2016; Lund *et al*, 2018). Surface Protein A (SpA) is a well-studied virulence determinant of *S. aureus* and other staphylococcal species, known to be expressed during exponential growth phase, both as a cell wall-anchored surface protein, and as a secreted protein (Movitz, 1976; Becker *et al*, 2014). Experiments reported in this chapter have shown that SpA-SNAP fusion proteins are expressed under the native *spa* promotor in a *spa*$^-$ strain of *S. aureus* SH1000, such that *spa-SNAP* is the only copy of *spa* being stably expressed from the chromosome. This study also demonstrates the presence of SpA-SNAP in the both the cell wall and membrane fractions of *S. aureus* SH1000. The presence of SpA-SNAP in the membrane fraction is likely a consequence of a percentage of the population actively translocating SpA-SNAP at the time of lysis. Unfortunately, SpA localisation via SNAP-tag labelling could not be achieved using SNAP-Cell Surface benzylguanine derivative dyes, despite the range of dyes tested. This, along with the range of variables tested, suggests that the lack of labelling can be attributed to the SNAP-tag enzyme or SpA-SNAP construct in general. Issues of misfolded protein fusions used in localisation studies has also been reported previously (Evanko, 2006). Instead, it appears as though the expression of SNAP-tag causes *S. aureus* to either retain cell-permeable dye or is indicative of cytoplasmic SpA-SNAP labelling. However, as Western blot analysis using α-SNAP primary antibodies shows no SNAP-tag in the cytoplasmic fraction of lysed cells, this is unlikely (Figure 3.5.). Additionally, Figure 3.5. shows the SpA-SNAP is present in the cell wall fraction, which suggests that it is being translocated and displayed on the cell surface. Therefore, as *S. aureus* SH1000 did not retain cell permeable dye, it is assumed that the production of SpA-SNAP may affect secretion in these strains. Additionally, it may be that SNAP used in these experiments was not sensitive enough for consistent labelling.

Interestingly, issues using SNAP-tag have been reported in bacterial systems in oxidative environments (Veggiani & de Marco, 2011). The functionality of SNAP-tag is dependent on its active-site Cysteine residue, which is known to be highly susceptible to reactive oxygen species such as hydroxyl radicals. A study on the effects of reactive oxygen species on the growth of *E. coli* has shown that hydroxyl radicals are present in both liquid TSB and TSB agar

(Kameya *et al*, 2019); both of which have been used to grow *S. aureus* SH1000 SpA-SNAP in this study. It is well established that *S. aureus*, a facultative anaerobe, is efficient in dealing with oxidative stress – including reactive oxygen species (Clauditz *et al*, 2006). Therefore, the presence of hydroxyl radicals in the growth media used in this study may be insufficient to affect the growth or noticeable function of *S. aureus* during these studies but could be sufficient to render SNAP-tag non-functional when displayed on the cell surface. This too may explain the discrepancy between this work and others from the Foster lab where SNAP-tag was successfully used to localised cytoplasmic proteins, as the presence of hydroxyl radicals or other reactive oxygen species in the extracellular milieu is unlikely to affect the activity of subcellular enzymes directly (Wacnik, 2016; Weihs, 2016).

Previous efforts to localise both endogenous and chemically inducible plasmid-based *spa* have been undertaken using protein fusions constructs and immunofluorescence microscopy in a variety of background strains of *S. aureus* (DeDent *et al*, 2018; Yu *et al* 2018). Each study reports different SpA localisation patterns for different background strains, as well as different SpA localisation in RN4220 with and without plasmid-inducible *spa*. While SpA localisation using SNAP-tag has been unsuccessful, initial α-SpA immunofluorescence microscopy with *S. aureus* SH1000 in this study shows a heterogeneity in the population for SpA surface display (23%; Chapter 4, Figure 4.2.). Cells that are labelled by immunofluorescence appear to display SpA across the whole cell, except for noticeable gaps that colocalise with the leading edges of developing septa. To investigate this phenomenon further, an α-SpA immunofluorescence microscopy approach was used to screen a variety of mutants in the Foster lab collection that are known to be involved in *spa* expression and regulation (Chapter 4). Additionally, it is important to conduct further immunofluorescence experiments in cells not expressing SNAP, as this may result in artifacts or anomalous signals.

3.6. Main Findings in this Chapter

- Surface Protein A fused to SNAP-tag can be expressed under the native *spa* promotor and localises to the *S. aureus* membrane and cell wall
- SNAP-tag exposed on the surface of cells is unable to be visualised using benzylguanine derivative dyes
- Cells expressing SNAP-tag SpA fusions show cytoplasmic fluorescence when using cell permeable dyes, but no detectable cytoplasmic SNAP by Western blot analysis
- Membrane associated SNAP localisation may cause cytoplasmic retention of cell permeable SNAP dye
- Immunofluorescence microscopy localises SpA on the surface of a subset of the bacterial population

Chapter 4

Use of Immunofluorescence Microscopy to Localise *Staphylococcus aureus* Surface Protein A

4.1. Introduction

Surface proteins are key virulence determinants that enable bacteria to colonise a host and establish disease. Their functions range from adhesion to mammalian extracellular matrices and sequestering iron from the host, to evading the innate and adaptive immune systems. Staphylococcal Surface Protein A (SpA) and its analogues are known to bind the constant (Fc) domain of mammalian immunoglobulin G (IgG), as well as other antibodies, to prevent opsonisation, phagocytosis, and subsequent clearing from the host system (Balachandran et al, 2018; Foster and Höök, 1998). Regulation of *spa* in *Staphylococcus aureus* is achieved primarily by the accessory gene regulator (Agr), which in turn is regulated by the staphylococcal accessory regulator (SarA) (Cheung *et al*, 2008). Agr is a negative regulator of *spa* and many other virulence factors with its own complex regulation pathways. AgrC is a two-component histidine kinase that recognises AgrD auto-inducing peptides as part of a quorum sensing regulation system, which activates AgrA by a phosphorylation event (Canovas *et al*, 2016). Together, these proteins form a two-component regulatory system. In the transition between exponential and post-exponential phase of growth, SarA becomes active (Cheung *et al*, 2008). SarA upregulates *agr* expression, which in turn inhibits the production of surface proteins, and initiates the secretion of various toxins (Crossley *et al*, 2009).

The structure and function of surface protein A is well understood (Kim *et al*, 2012) (Chapter 1; Section 1.4.3.). As a prominent and vital virulence factor of *S. aureus*, SpA is used as a marker to characterise the potential virulence capacity of clinical isolates by a technique called SpA typing (Hallin *et al*, 2009). SpA typing is also used as the standard for the epidemiological comparison of unrelated *S. aureus* strains by comparing the polymorphisms within variable 24 base pair repeats found in the *spa* gene. This enables the characterisation of strains and the prediction of multilocus sequence typing across independent isolates globally, while also contributing to the control and prevention of *S. aureus* outbreaks

(Asadollahi *et al*, 2018; Strommenger *et al*, 2008). Given the widespread use of SpA as a tool in epidemiological surveying, protein analysis, and virulence studies, its localisation and display over time on the surface of *S. aureus* is of paramount importance. Many methods exist with which to localise proteins. The most common among them is fluorescence microscopy. Fluorescence microscopy is a widely used technique in the localisation of molecules that traditionally takes advantage of the inherent fluorescent properties of various proteins, such as green fluorescent protein (GFP), yellow fluorescent protein (YFP) and mCherry (Lichtman, 2005). When expressed as fusion constructs, these proteins can be excited by specific wavelengths of light to fluoresce, and in so doing, can be used to localise the molecules they are fused to. However, issues of fluorescent protein misfolding and insufficient fluorescence capabilities have been reported previously (Jensen, 2012). To circumvent the limitations of inherently fluorescent proteins, self-labelling enzymes have been developed, such as Halo-tag and SNAP-tag (Stagge *et al*, 2013). These enzymes can also be expressed as fusion constructs to proteins for localisation. The main difference between self-labelling enzymes and fluorescent proteins is the former's dynamic ability to be labelled with a variety of fluorophore conjugate substrates. This provides the user with more control over the fluorescence and subsequent labelling of fusion constructs and allows the use of multiple colour labelling for the same fusion construct. Despite the many advantages of self-labelling enzymes including SNAP-tag, there are conditions in which such enzymes can also present complications, as shown throughout Chapter 3. As such, an alternative labelling method for the localisation of SpA is required.

Immunolabelling, or immunofluorescence microscopy, is one of the most well-established methodologies in fluorescence microscopy (Zinchuk *et al*, 2007; Miller & Shakes, 1995). The technique revolves around the use of antibodies conjugated to various fluorophores to localise proteins and molecules both within cells and on the cell surface (Borek, 1961). This occurs as a specific binding event when primary antibodies are used, which are antibodies raised against the protein of interest in an animal host, such as rabbits or mice. These hosts are typically injected with a purified protein of interest to generate antibodies against that protein. The host is then exsanguinated to varying degrees and the antibodies are purified from the blood (Griffiths & Lucocq, 2014). Additionally, recombinant antibodies can be generated and stored in cell libraries through techniques such as mammalian and phage

display (Ho & Pastan, 2009). Antibodies are then employed in immunolabelling techniques to specifically bind the protein of interest in a bacterial population. Secondary antibodies which have been raised in a different host animal against the primary antibodies are conjugated to a fluorophore. These secondary antibodies fluoresce and can be used to bind to the primary antibodies used in experimentation– thereby localising the protein of interest.

The structure, function, and regulation of SpA has been well studied by various groups in a range of background strains of *S. aureus*. However, the localisation of this surface exposed protein is poorly understood. While efforts have been made to localise SpA by different groups, the results not only conflict across strains of *S. aureus*, but also within the same strains (DeDent *et al*, 2007; Yu *et al*, 2018). DeDent reports that SpA is displayed in punctate foci adjacent to the developing septum in *S. aureus* RN4220 and proceeded to formulate a model by which this translocation pattern develops over time to display SpA across the whole cell, though images of whole-cell SpA are not shown therein. While Yu reports, also in *S. aureus* RN4220, that SpA is exclusively localised at the developing septum of cells following treatment with the protease Trypsin and shows whole-cell SpA localisation of plasmid-based *spa* variants without Trypsin treatment. However, RN4220 is a restriction deficient strain of *S. aureus* that contains many additional mutations – including in the *agr* locus which, when functional, negatively regulates *spa* expression (Jenul *et al*, 2019). This strain is primarily used for the methylation of foreign DNA to facilitate the transformation or transduction of such DNA into a more stable strain for study (Nair *et al*, 2011).

Based on these works, immunolabelling was employed to investigate the localisation of SpA in the well characterised and genetically amenable *S. aureus* SH1000 background, as well as strains containing mutations relevant to the regulation and / or display of SpA in the SH1000 background. Monoclonal primary antibodies were chosen for their specificity in binding SpA, such that the binding of fluorophore-conjugated secondary antibodies would be representative of SpA localisation. However, as an antibody binding protein, SpA is also capable of binding secondary antibodies that are not bound to primary antibodies. For this reason, working in strains in which SpA is the only surface exposed antibody binding protein is important to ensure the most accurate representation of SpA localisation possible (Figure 4.1.; Figure 4.2.).

4.1.2. Aims of this Chapter

- Use immunofluorescence microscopy to investigate the localisation of SpA in *S.* aureus SH1000
- To investigate how various mutations in genes associated with *spa* regulation and surface display affect the localisation of surface protein A
- Use the protease Trypsin to investigate the development of SpA surface display both spatially and temporally

4.2. Results

4.2.1. Generation of Controls for α-SpA Immunofluorescence Microscopy

To ensure that signals observed using immunofluorescence microscopy for surface protein A (SpA) were truly representative of SpA localisation, positive and negative controls were generated. A positive control of *S. aureus* SH1000 *sbi*::*erm* was made by transducing the bursa aurealis transposable element from the NARSA library (Fey, *et al*, 2013) into the SH1000 background. An *sbi* knockout was chosen as a positive control because this gene encodes for the only other known surface-exposed antibody binding protein of *S. aureus*, besides SpA (Smith *et al*, 2011). As such, this ensures that any signal in this mutant is representative of SpA localisation exclusively. A negative control of *spa*::*kan sbi*::*erm* was also made in the SH1000 background via transduction to ensure that no surface exposed antibody binding proteins are displayed on the cell surface of *S. aureus*. Mutant strains generated for use as positive (*sbi*::*erm*) and negative (*spa*::*kan sbi*::*erm*) controls in the localisation of SpA were verified by PCR and immunofluorescence microscopy (Figure 4.1.; Figure 4.2.). The insertion of the bursa aurealis transposable element into *sbi* can be observed via PCR as an increase in band size by 3.2 Kb from the positive control amplification of 500 bp. Therefore, bands around 3.7 kb suggest successful recombination of the transposon into *sbi*.

Immunofluorescence microscopy of the wild type *S. aureus* SH1000 shows approximately 20% of the population displaying SpA on the cell surface (Figure 4.2.). The few single cells in this population with immunolabelled SpA on the surface show labelling over the whole cell, while immunolabelled diploids typically display a horseshoe pattern of SpA, with little to no labelling at the site of division between two daughter cells. SpA labelling can however be observed between a diploid pair when HADA incorporation into the next plain of division is also evident in these cells (Figure 4.2). HADA is incorporated into the cell wall as nascent peptidoglycan is being synthesised. Therefore, juxtaposing HADA labelling to SpA localisation enables the correlation of SpA display dynamics to the cell cycle.

The morphology of SH1000 was not affected by the loss of *sbi*, as shown in Figure 4.2. via HADA incorporation. A negligible difference in the amount of fluorescent cells was seen between SH1000 wild type (20%) and SH1000 *sbi*::*erm* (23%). Thus, the loss of Sbi surface

display does not affect the IgG binding of SpA, nor does its presence appear to obstruct the labelling patterns of SpA via IgG binding. Despite its negligible interference with SpA labelling, SH1000 *sbi*::*erm* was chosen as the primary sample for further investigation into SpA localisation to ensure that the signal observed is strictly representative of SpA. SH1000 *spa*::*kan sbi*::*erm* was used as a negative control (Figure 4.2.). Background and autofluorescence was removed when analysing the negative control strain, and those values were used as the minimum parameters for fluorescence signal in both the positive control and all samples to ensure that the signals observed therein are representative of SpA immunofluorescence. As shown previously in Figure 3.14. (Chapter 3), SpA immunofluorescence in a *spa*$^{-}$ strain shows no immunolabelling, which further suggests that the presence of Sbi on the cell surface does not bind the SpA specific primary antibodies used therein. Regardless, and for added clarity, a double knockout strain of *spa* and *sbi* were used throughout this chapter as a negative control.

A heterogeneity of SpA display was observed in the SH1000 population, wherein 20% of cells were successfully labelled with fluorescently conjugated antibodies (Figure 4.2.). A standard dilution of 1:250 primary / secondary antibody to 2% (w/v) BSA PBS was used. To assess whether this concentration was insufficient in labelling a larger percentage of the population, higher concentrations of both primary and secondary antibodies were tested. No significant increase in the percentage of SH1000 *sbi*::*erm* populations was observed (data not shown). Therefore, the heterogeneity of SpA display observed in Figure 4.2. is likely a feature of the *S. aureus* population. To investigate this phenomenon further, and to screen for the impact of the removal of genes involved in the regulation and surface display of SpA, a variety of background strains and mutants were tested via immunofluorescence microscopy.

A

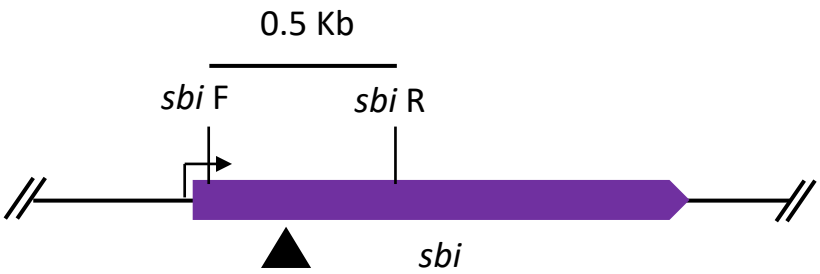

B

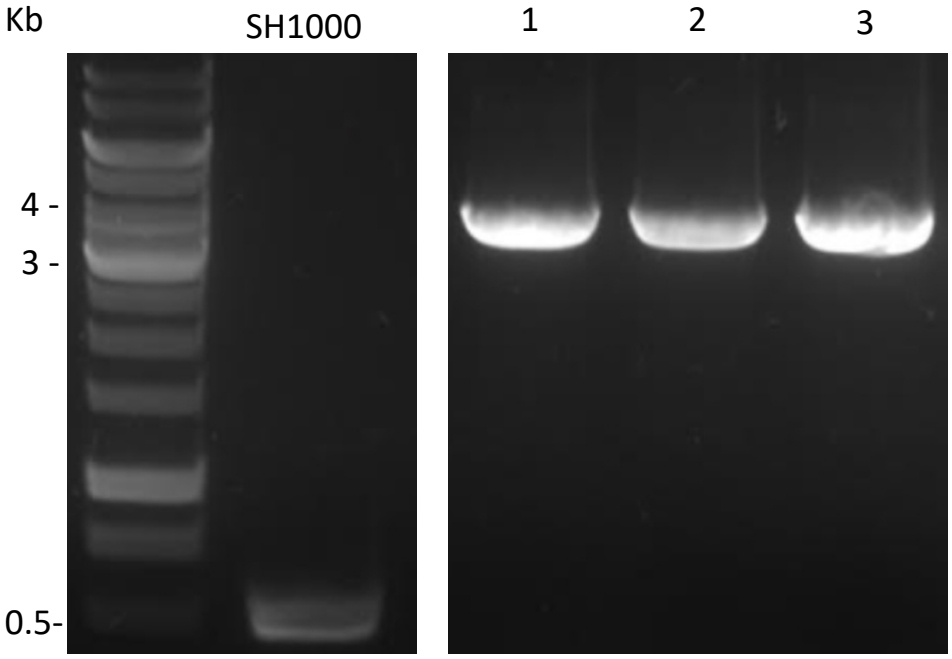

Figure 4.1. Verification of *sbi* knockout mutation in *S. aureus* strains

(A) Schematic representation of *sbi* in *S. aureus* SH1000. Highlighted region represents sequence amplified using *sbi F* and *sbi R* primers, which produce a band of 511 bp in the wild type *S. aureus* SH1000. Black arrow represents the insertion of the Bursa aurealis transposon within this region. The Bursa aurealis transposon is 3.2 Kb. Successful insertion of the transposon within this region will produce a 3.7 Kb band when amplifies using *sbi* F and *sbi* R primers **(B)** PCR amplification of *sbi* knockout transduction using *sbi* F and *sbi* R primers. Samples were seperated on a 1% (w/v) gel by electrophoresis. Bursa aurealis transposon insertion observed via 3.7 Kb PCR products. Samples 1, 2, and 3 represent JE2 *sbi*::*erm*, SH1000 *sbi*::*erm*, and SH1000 *spa*::*kan sbi*::*erm*, respectively. SH1000 wild type gDNA was used as a negative control at 0.5 Kb.

A

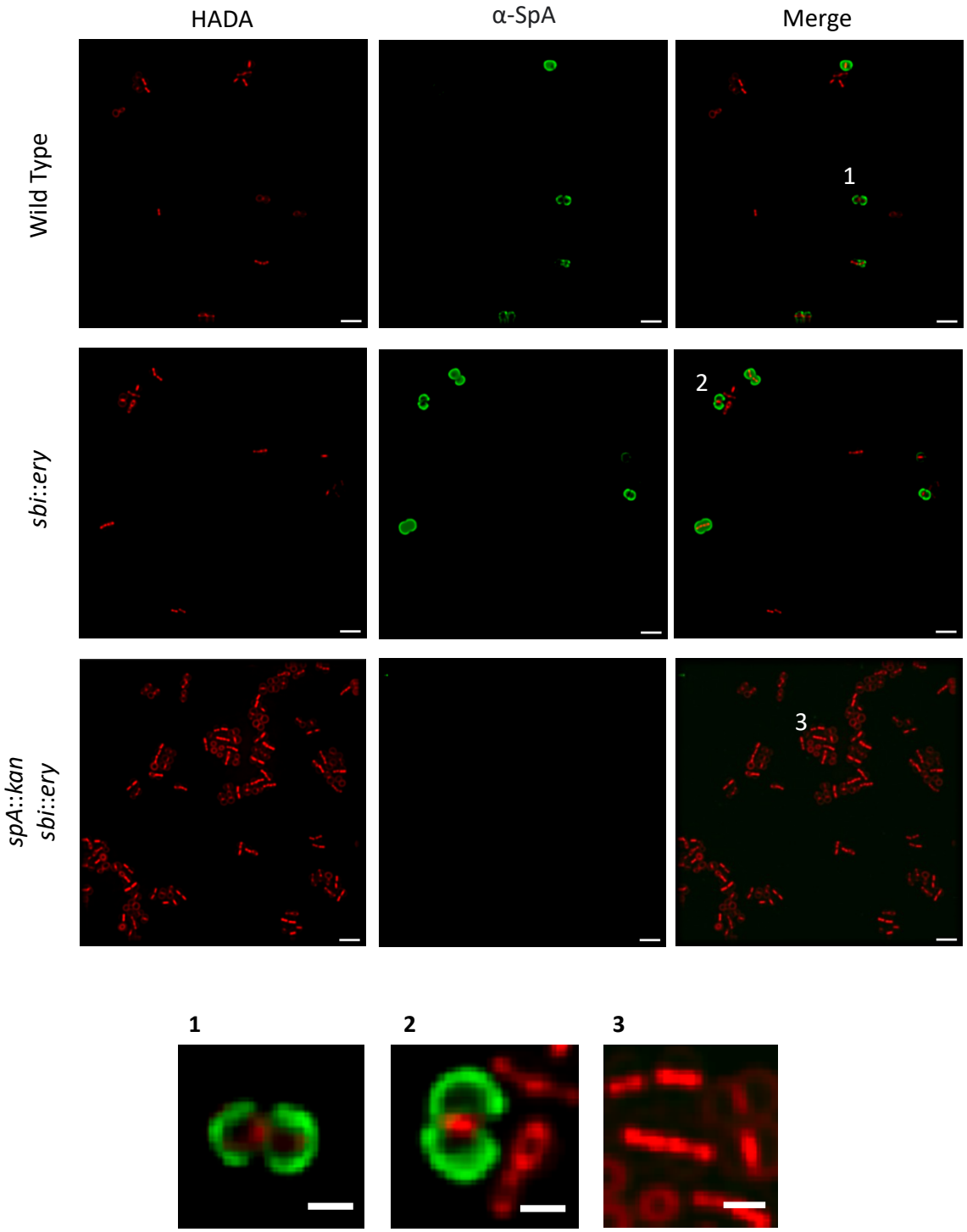

B

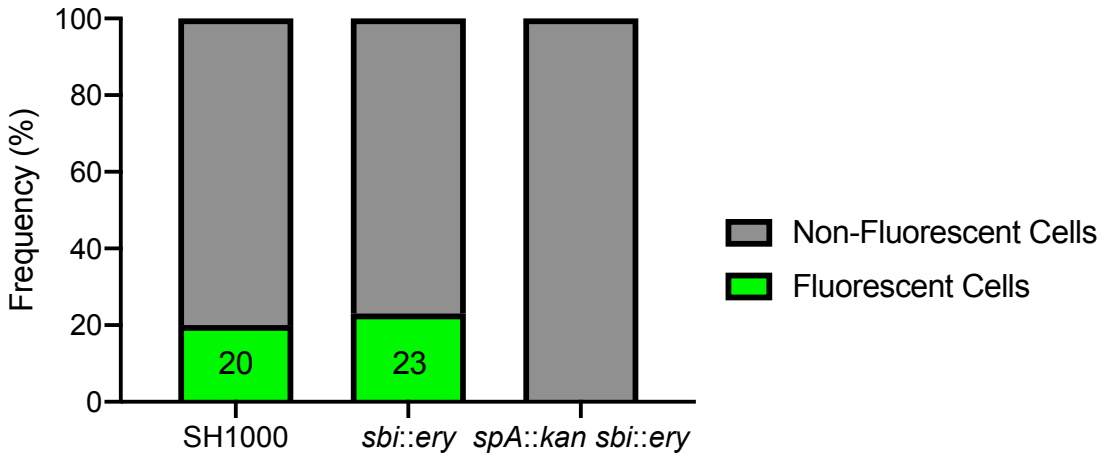

Figure 4.2. Positive and negative controls for SpA localisation by immunofluorescence microscopy

(A) α-SpA Immunofluorescence microscopy of *S. aureus* SH1000 *sbi*::*erm*. HADA (red) shows nascent peptidoglycan synthesis. α-SpA (green) shows SpA localisation on cell surface. Inset numbers are enlarged below. Scale bars = 3 µm. Inset scale bars = 1 µm. **(B)** Quantification of percentage of SH1000 wild type (20%; n=1380), SH1000 *sbi*::*erm* (23%; n=1364), and SH1000 *spa*::*kan sbi*::*erm* (0%; n=1284) cells with fluorescently labelled *spa*. Samples shown are representative of three biological repeats.

4.2.2. Subcellular Localisation of Surface Protein A by Immunofluorescence Microscopy

HADA was used to identify the stages of division in the subcellular population and to juxtapose SpA fluorescence to the development of nascent peptidoglycan. Growth media was supplemented with HADA for 5 minutes, unless otherwise stated. Conventional fluorescence microscopy using α-SpA Immunofluorescence microscopy identifies a subset of the population displaying SpA over on the surface of single cells (Figure 4.3.). This appears to encompass the entire cell. In addition, *S. aureus* cells that have recently split into daughter cells typically display a horseshoe like pattern of SpA fluorescence, where the newly exposed cell wall material between the two daughter cells does not appear to have SpA on the surface (Figure 4.3.; inset 2). Faint fluorescence can occasionally be seen in this area – referred to as the previous division site (PDS) – of recently split cells. As daughter cells develop septal plates in the next plane for division, SpA can be seen more readily at the PDS (Figure 4.3.; inset 3). The intensity of fluorescent signals from cells displaying SpA varies. As such, the contrast of immunofluorescence microscopy images was adjusted to ascertain the presence of fluorescence at the PDS in diplococcal cells displaying a horseshoe pattern of SpA localisation. Cells that display a horseshoe SpA motif do not in fact display any SpA fluorescence in this region that is not apparent in the images shown, despite further contrast manipulation. This suggests that recently exposed cell wall at the PDS does not possess cell wall-anchored SpA at the surface level immediately following septation.

To investigate the effect of immunofluorescence labelling methods on SpA localisation in *S. aureus* SH1000, a range of approaches adapted from published works were tested. These include labelling with a secondary fluorescent antibody only (DeDent *et al* 2007), incubating samples with a fluorescent primary antibody only (Tan *et al*, 2012), and varying incubation times and temperatures with both primary and secondary monoclonal and polyclonal antibodies. There was no different observed between incubation times and temperatures tested (2-hour incubation at room temperature vs overnight incubation at 4°C), while using α-SpA primary antibodies and fluorescently conjugated secondary antibodies provided consistent and clear results (data not shown). As such, this methodology was used for further experimentation.

A

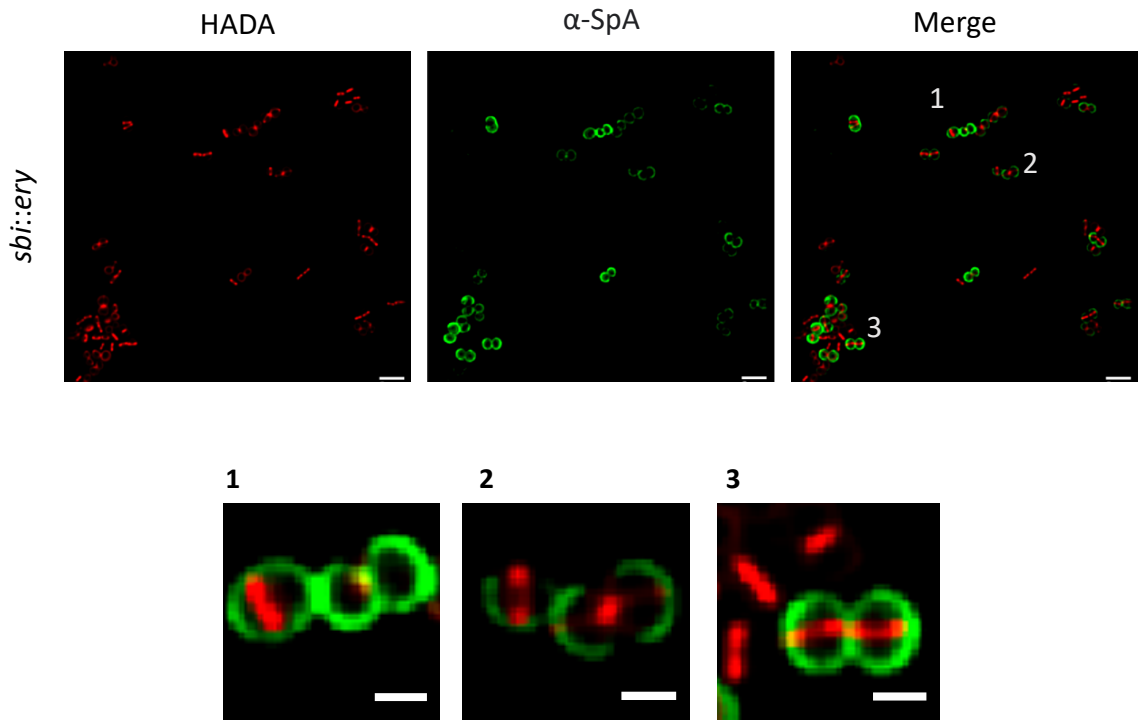

Figure 4.3. SpA localisation by immunofluorescence microscopy

(A) HADA was used to label nascent peptidoglycan synthesis (red). α-SpA immunofluorescence microscopy of SH1000 *sbi*::*erm* (green) shows whole cell labelling and horseshoe patterns. Inset numbers are enlarged below. Scale bars = 3 µm. Inset scale bars = 1 µm. Insets enlarged below are representative examples of SpA localisation in the SH1000 background. **(1)** Single and diplococcal cells with SpA over the whole surface. **(2)** Diplococcal cells with a new round of division initiated. Newly exposed cell wall material lacks surface-exposed SpA detectable by immunofluorescence microscopy. **(3)** Diplococcal cells with partial septum formation in a new plane of division. SpA is detectable over the whole surface and between two daughter cells. Sample shown is representative of three biological repeats.

To simplify our current understanding of SpA display over time, a schematic representation of SpA temporal evolution with reference to the *S. aureus* cell cycle is shown in Figure 4.4. As *S. aureus* initiates cell division, represented by HADA incorporation at the mid cell (red), such that the prominent incorporation of peptidoglycan takes place at the cross wall, SpA can be observed in a horseshoe pattern at the periphery of the burgeoning diplococcal pair. No SpA is observed at the division site at this stage. This motif of SpA display persists as the bacteria continue to grow and differentiate into daughter cells. As the next cycle of cell division begins to take place, the horseshoe pattern of SpA localisation remains. However, as the cells continue to incorporate nascent cell wall material as part of the next round of cell division, SpA can be observed at the previous division site (PDS) as the current division site is being synthesised. This emergence of SpA display at this site is currently hypothesised to be the result of cell wall hydrolysis as a natural part of the cell cycle. (Chapter 5; Chapter 6). This hypothesis is based on data generated by Pasquina-Lemonche et *al*, 2020, wherein it is shown that there is an additional dense ring-like structure of peptidoglycan at the septum of dividing cells that covers the mesh structure of peptidoglycan beneath it. This could explain why no SpA can be immunolabelled at the active division site of recently divided cells, as the ring structure is either too dense to allow sufficient immunolabelling of SpA present within that structure, or that SpA is incorporated into the mesh layer beneath the rings, and so obfuscates its localisation until the dense ring-like structure is hydrolysed sufficiently.

To assess whether this pattern of SpA display is consistent among background strains of *S. aureus* besides SH1000, a range of clinically relevant strains were assessed for SpA display using immunofluorescence microscopy.

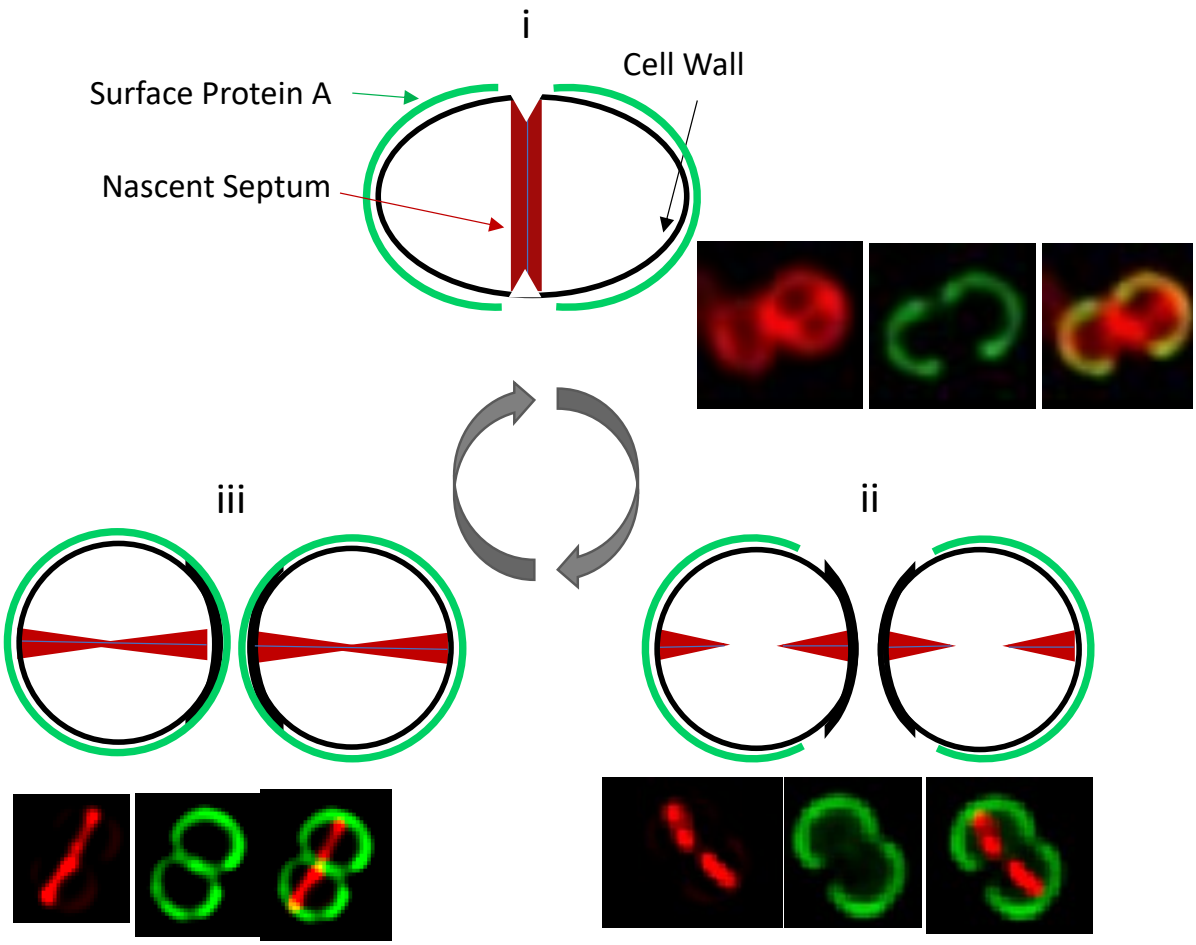

Figure 4.4. Schematic representation of SpA localisation in *S. aureus* SH1000

(i) Cells in the process of septation from one another, observed by HADA labelling (red), show a horseshoe pattern of SpA fluorescence at the periphery of cells, where no labelling is observed at the current site of division. **(ii)** The horseshoe motif of SpA diplay persists at the periphery of the cells, as the diplococcal pair develop septa in the next plain of division. Surface exposed nascent cell wall is shown as thicker, black region between diplococci, representative of the previous division site (PDS). **(iii)** As diplococcal cells complete the septal plate for the next round of division, SpA can be observed at the region between cells where the previous division occurred, as well at at the periphery of both cells. As those cells septate further, the horseshoe motif is observed again in the next plane of division.

4.2.3. Effect of Strain Backgrounds on SpA Localisation

Strain-dependent variation is known to occur with regards to *S. aureus* gene expression (Geisinger *et al*, 2012; Lindsay *et al*, 2006). Therefore, it is important to compare the SpA surface localisation seen in the SH1000 background against other strains. *S. aureus* 8325-4 is the parental strain of the widely studied SH1000 background strain used primarily in this study. 8325-4 contains three prophages and contains a non-function *rsbU* gene (Horsburgh *et al*, 2002). SH1000, by contrast, has a functional *rsbU* gene.

S. aureus RN4220 is a commonly utilised intermediary strain for the horizontal transfer of genetic elements into other background strains (Schenk & Laddaga, 1992). RN4220 is derived from 8325-4 and has been subjected to chemical mutagenesis employing nitrosoguanidine (MNNG) to inactivate its restriction enzymes. This enables the uptake of foreign DNA which is then methylated in an *S. aureus* specific manner. AgrA is also inactivated in this strain, which alters the regulation and expression of numerous virulence factors. For these reasons, RN4220 is primarily used as a subcloning host strain (Berscheid, *et al*, 2012).

S. aureus Newman is a human clinical isolate containing four siphoviridae prophages known to contribute to organ-specific virulence capabilities in murine models of infection (Bae *et al*, 2006). Newman was chosen primarily due to its clinical relevance as a nosocomial pathogenic strain. *S. aureus* NewHG (Newman HG) is a repaired derivative of Newman, with a functional *saeS* gene. *saeS* encodes one part of a two-component regulatory system for a range of virulence factors in *S. aureus*, with its counterpart being *saeR* (Mainiero *et al*, 2010). However, NewHG has also been reported to lack the production of certain extracellular proteins including coagulase, Sbi, gamma-haemolysin, and fibrinogen-binding proteins (Herbert *et al*, 2010). Similarly, COL is a methicillin resistant *Staphylococcus aureus* (MRSA) strain first identified in the 1960s as part of the first MRSA lineage (Harkins *et al*, 2017). Another globally recognised MRSA background strain was screened for SpA localisation, *S. aureus* USA300. While the characterisation of USA300 for its resistance to methicillin was first identified in the 1990s, it has since been found to have developed resistance to many non- β-lactams (Enström *et al*, 2018).

A

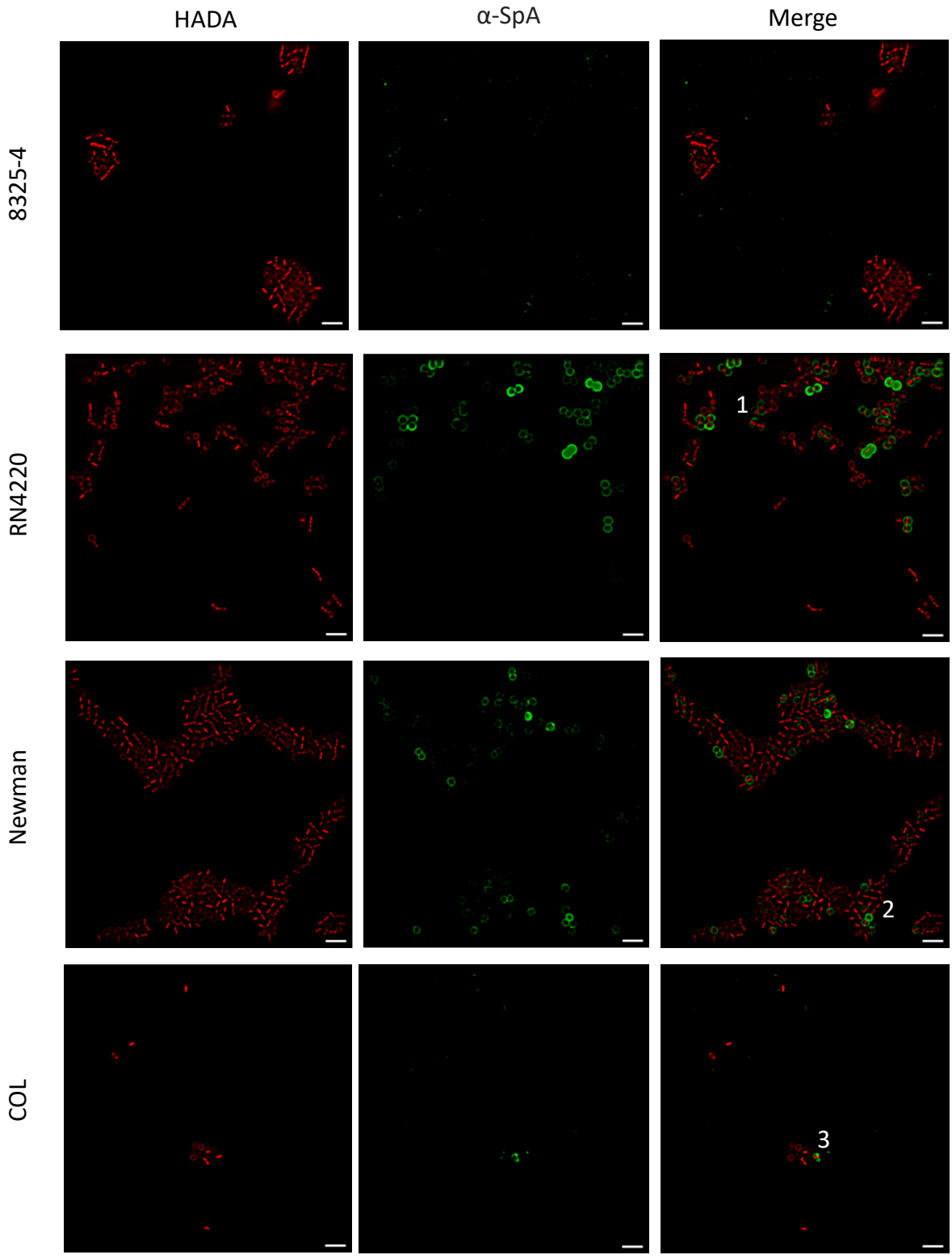

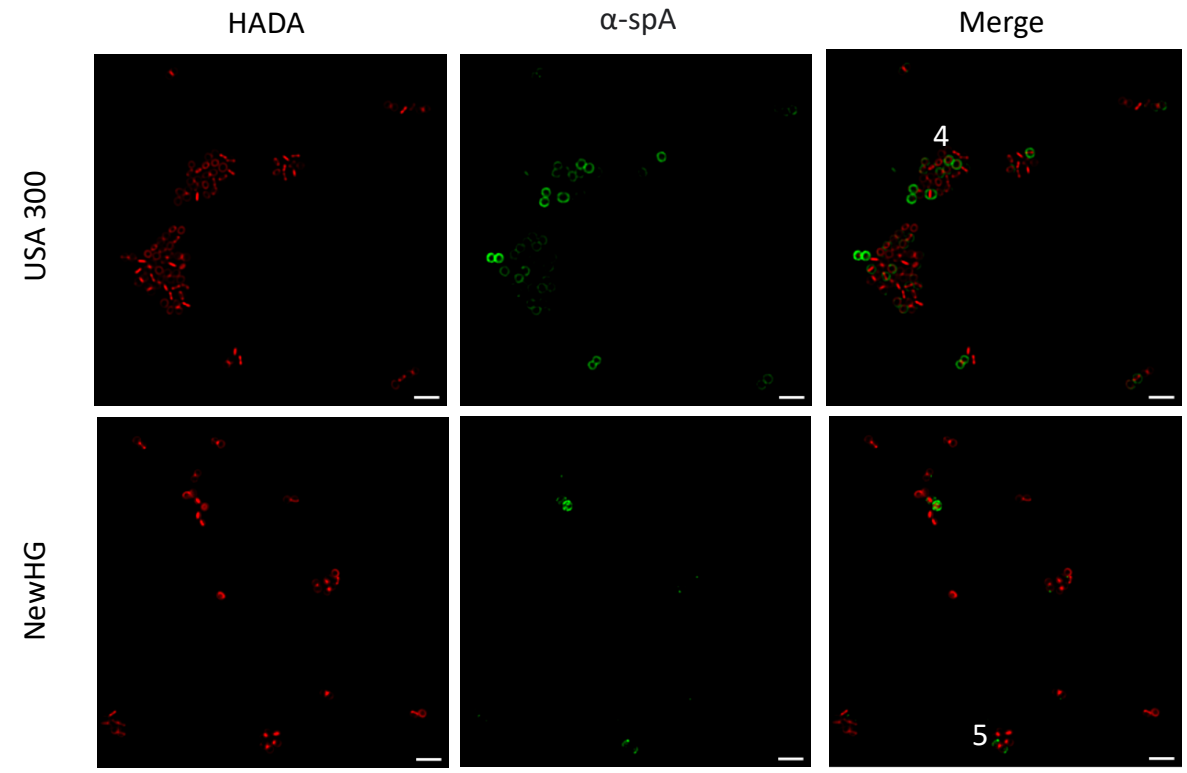
HADA
α-spA
Merge
USA 300
NewHG
4
5

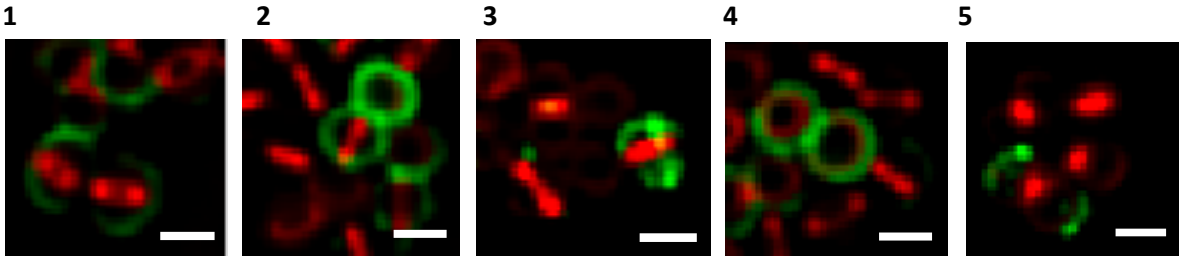
1
2
3
4
5

B

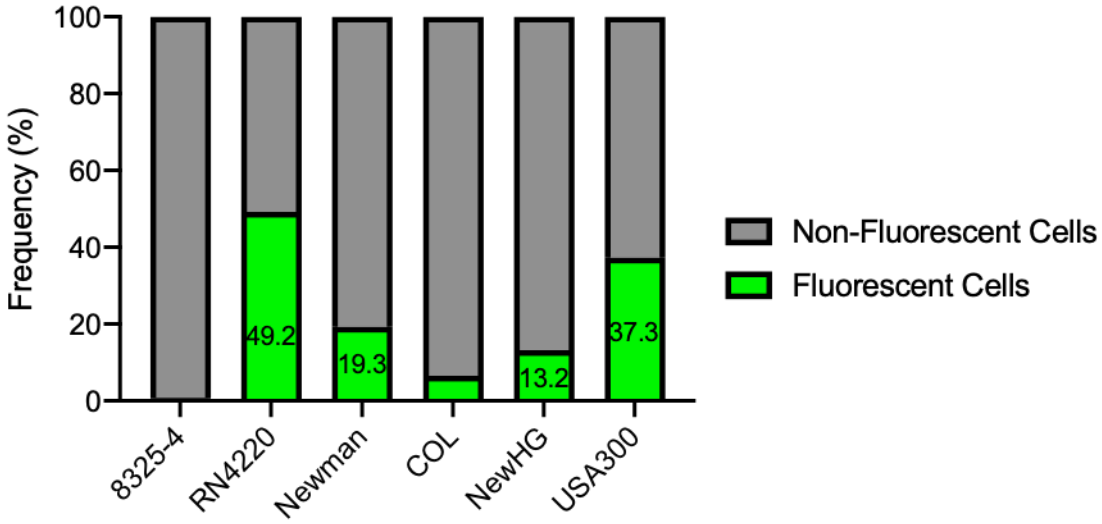
Frequency (%)
100
80
60
40
20
0
49.2
19.3
13.2
37.3
8325-4
RN4220
Newman
COL
NewHG
USA300
Non-Fluorescent Cells
Fluorescent Cells

Figure 4.5. SpA localisation in background strains of *S. aureus* by immunofluorescence microscopy

(A) α-SpA Immunofluorescence microscopy of *S. aureus* 8325-4, RN4220, Newman, COL, USA300 and NewHG. Inset numbers are enlarged below. Scale bars = 3 µm. Inset scale bars = 1 µm. **(B)** Quantification of percentage of 8325-4 (1%; n=472), RN4220 (49%; n=503), Newman (19%; n=596), COL (7%; n=182), NewHG (13%; n=486) and USA300 (37%; n=522) population with fluorescently labelled SpA. Frequencies under 10% are not labelled. Samples shown are representative of one biological repeat.

Results from Figure 4.5. show a reduction in the number of cells with fluorescently labelled SpA between *S. aureus* SH1000 (20%) and its parental strain 8325-4 (1%) (Figure 4.2.). The possession of prophages has been known to enhance a range of virulence capabilities between strains, and previous work to sequence the genomes of SH1000 and 8325-4 have speculated on the altered virulence capabilities of the genetic polymorphisms that differ between *S. aureus* 8325-4 and SH1000 (O'Neill *et al*, 2010). As such, the regulation of *spa* may differ between these strains due to the presence of functional *rsbU* in SH1000 (Horsburgh *et al*, 2002).

Unsurprisingly, RN4220 shows a higher percentage of cells labelled through α-SpA Immunofluorescence microscopy (49.2%) than SH1000 (20%), likely due to its non-functional *agrA* gene as one of the key response regulator elements of *spa* expression (Koenig *et al*, 2004). As such, increased transcription, and therefore display, of SpA was expected. Newman shows a comparable percentage of the population displaying SpA on the cell surface as SH1000 (19.3%), while the number of COL cells in the sample were lower than other strains (n = 182). COL grew much slower than the other strains shown in Figure 4.5. (data not shown) and has noticeably smaller cells. Furthermore, COL cells displaying SpA were as low as 7%. SpA labelling patterns in these strains is similar to that observed with SH1000 and SH1000 *sbi*::*erm*, albeit at altered frequencies of display within the population. RN4220, Newman, NewHG and USA300 each display SpA in similar patterns as observed previously; horseshoe localisations of SpA can be observed, as can whole cell labelling. However, COL had not only a substantially lower percentage of the population displaying SpA, but its localisation appeared different. Instead of whole cell display in single cells and a horseshoe motif in diplococcal cells, COL shows SpA labelling that appears to be perpendicular to the developing septum (Figure 4.5., inset 3). However, due to the small size of these cells compared to other strains shown here, it is unclear if this is due to the size difference or a facet of the genetic variation between strains (Lindsay, 2010).

4.2.4. Use of Defined Mutations to Analyse the Regulation of SpA Surface Localisation

The discovery of a subpopulation of cells demonstrating surface exposed SpA suggests that a mechanism relating to SpA regulation is involved in its expression or subsequent display on the surface of cells. The lack of SpA at the septal surface of newly divided cells also hints at further levels of control. To investigate these hypotheses, various *S. aureus* strains containing genetic mutations involved in teichoic acid synthesis and display (Section 4.2.4.1.), cell wall associated protein regulation (Section 4.2.4.2.), and SpA regulation (Section 4.2.4.3.) were assessed for SpA localisation by immunofluorescence microscopy in an effort to elucidate additional factors contributing to SpA surface display.

4.2.4.1. Effect of Teichoic Acid Biosynthesis Gene Mutations on SpA Surface Localisation

Associations have been made by previous works between the functionality of both wall teichoic acid (WTA) and lipoteichoic acid (LTA) synthesis and display with the coordination and subsequent cross-linking of the peptidoglycan cell wall (Atilano *et al*, 2010). Additional correlations have been made between the septal secretion of surface proteins, including SpA, and the synthesis of teichoic acids (Yu *et al*, 2018). Among the genes investigated in these works was the lipoteichoic acid synthase *ltaS*.

LtaS is a synthase that catalyses the polymerisation of lipoteichoic acid (LTA) glycerol phosphate and is considered essential for the growth of *S. aureus* under normal conditions (Hesser *et al*, 2020). The growth of non-functional LtaS strains requires the supplementation of media with osmoprotectants and presents with mis-coordinated cell division sites. However, strains that were able to grow under regular conditions without LTA (i.e. without osmoprotectants to prevent cell lysis) were found to possess a mutation in the gene encoding cyclic-di-AMP-phosphodiesterase, *gdpP* (Corrigan *et al*, 2011). Mutations in the *gdpP* gene have also been linked to certain MRSA strains which lack the traditional penicillin binding protein 2a (PBP2a) encoded by *mecA* yet demonstrate increased resistance to methicillin (Ba *et al*, 2019). Mutation is *gdpP* have been shown to increase the degree of peptidoglycan cross-linking in *S. aureus* and is thought to prevent the bacterium from lysing in the absence of LtaS.

LcpB is a pyrophosphatase responsible for the synthesis and ligation of WTA to the cell wall and has been shown to regulate virulence independently of Agr activity, while LcpC is known to bind various polysaccharides to the peptidoglycan cell wall (Pan *et al*, 2021; Li *et al*, 2020). Loss of the LcpC has also been associated with an increased sensitivity to β-lactam antibiotics, while the deletion of all three *lcp* genes (*lcpABC*) results in the lack of WTA on the surface of *S. aureus* entirely (Chan *et al*, 2013).

tarO by contrast is one of the few non-essential genes in the biosynthetic pathway of WTA synthesis. Many other genes involved in the biosynthesis pathway of WTA are essential, as their abrogation causes a build-up of toxic intermediates (Suzuki *et al*, 2011). TarO is responsible for the transfer of N-acetyl-glucosamine (Glc*N*Ac) to membrane-anchored undecaprenyl carrier lipid (Brown et al, 2008). The loss of TarO has been shown to abrogate WTA expression in *S. aureus* and is not essential for viability (Weidenmaier et al, 2004). Teichoic acid synthesis initiated by TarO has also been shown to aid in the localisation of PBP4 to the cross-wall of *S. aureus*, which contributes to the degree of peptidoglycan cross-linking (Atilano *et al*, 2010).

Given the relationship between covalently bound surface exposed proteins like SpA to the peptidoglycan cell wall and its degree of peptide stem cross-linking, strains lacking crucial genes involved in the biosynthesis pathway of wall teichoic acids were assessed via α-SpA immunofluorescence microscopy. To assess the effect of the loss of LcpB, LcpC and TarO on SpA display in *S. aureus* SH1000, α-SpA Immunofluorescence microscopy was performed on knockout mutants of the encoding genes in SH1000, generated by the insertion of the bursa aurealis transposon from the NARSA library (Fey *et al*, 2013). Signals observed in the SpA objective channel for LcpB and LcpC strains were considered to be artifacts of immunofluorescence as they were not always associated with cells; appearing as punctate signals. Only 2% of the *tarO* mutant strain showed SpA localisation. Together these results suggest that the synthesis and cell wall associated display of LTA and WTA are required for the display of covalently bound surface proteins like SpA.

A

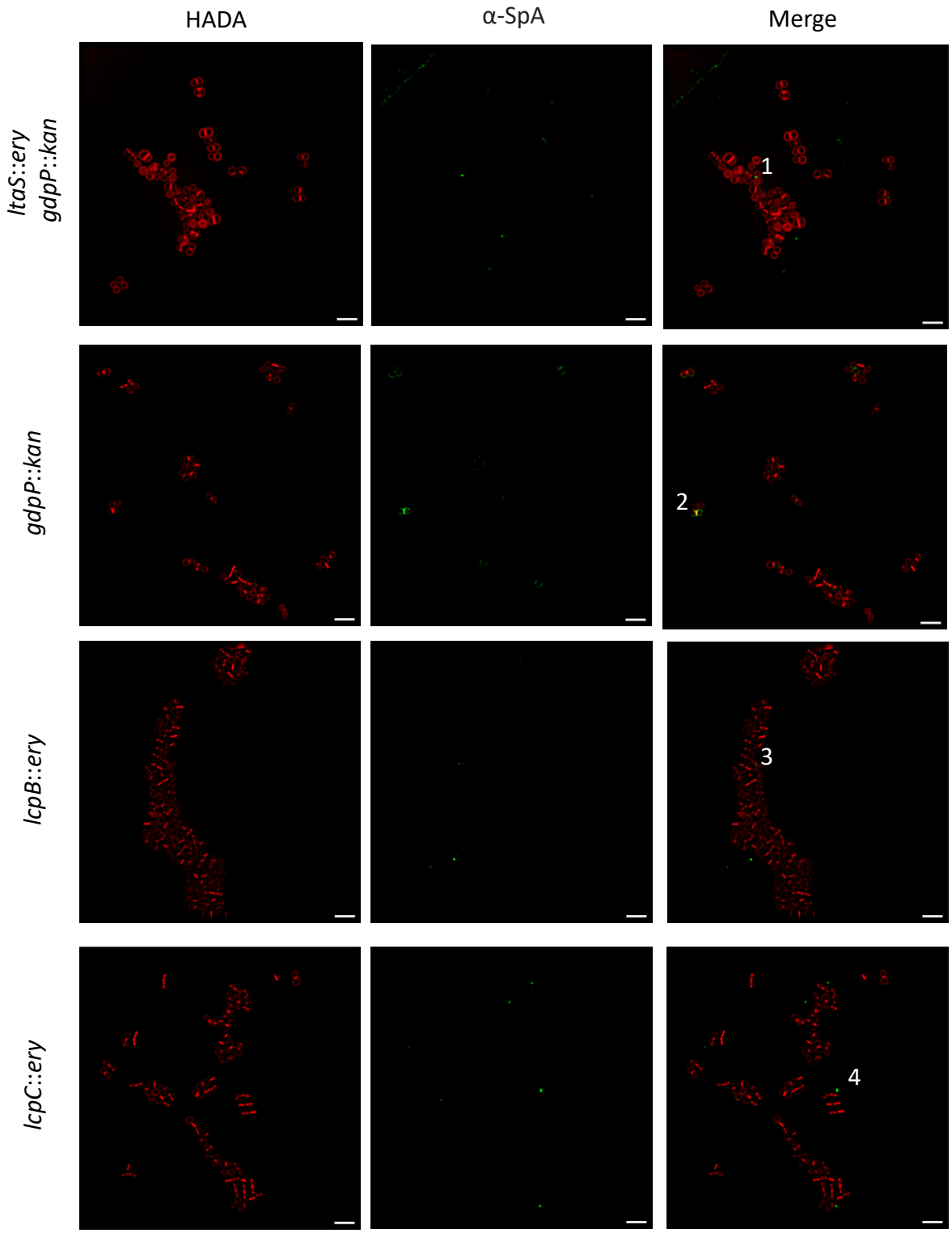
HADA
α-SpA
Merge
ltaS::ery gdpP::kan
gdpP::kan
lcpB::ery
lcpC::ery
1
2
3
4

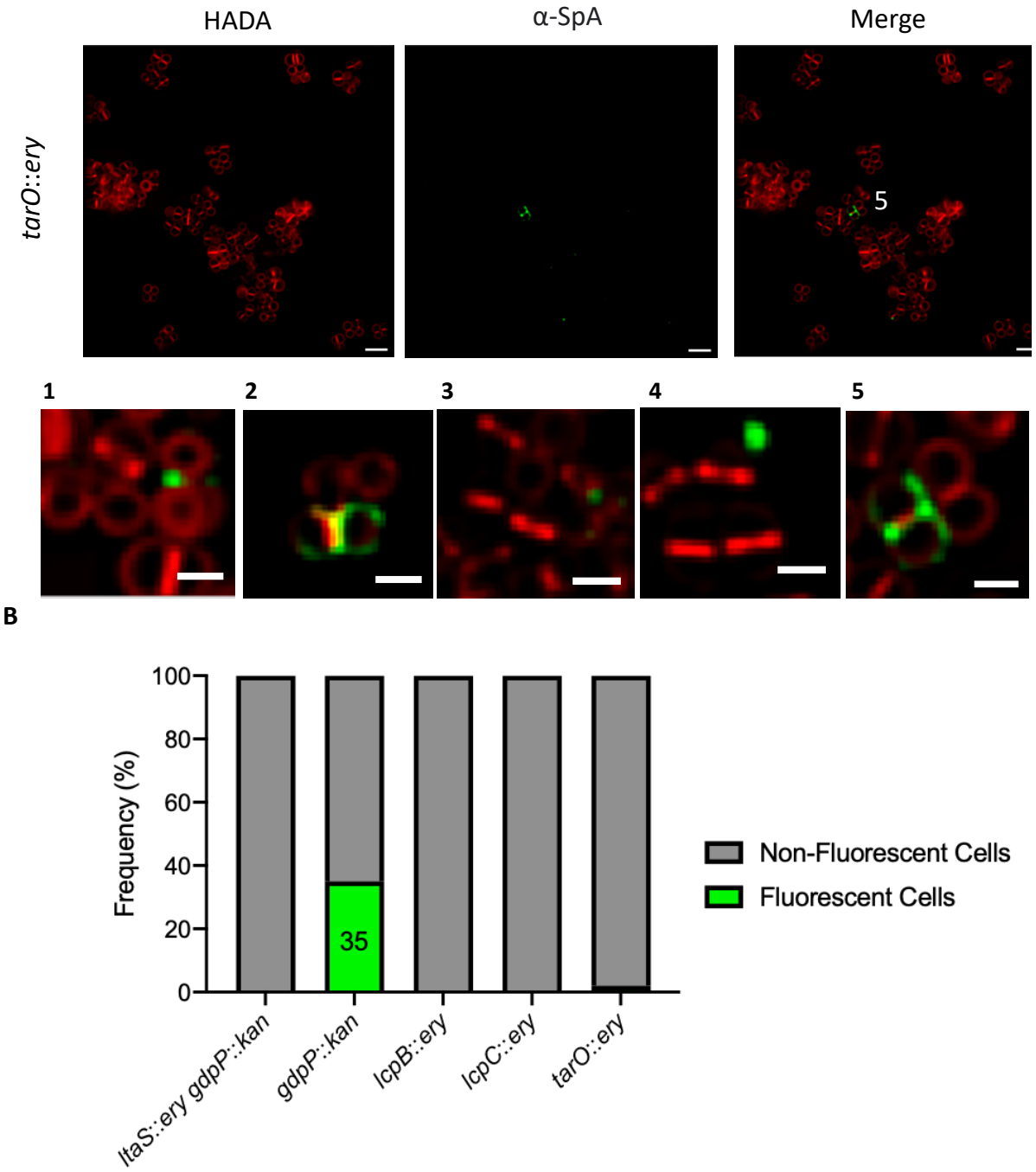

Figure 4.6. The role of lipteichoic acid and wall teichoic acid synthesis in SpA localisation

(A) HADA was used to observe nascent peptidoglycan synthesis (red). α-SpA Immunofluorescence microscopy of *S. aureus ltaS*::*erm gdpP*::*kan*, *gdpP*::*kan*, *lcpB*::*erm*, *lcpC*::*erm*, and *tarO*::*erm*. Inset numbers are enlarged below. Scale bars = 3 µm. Inset scale bars = 1 µm. **(B)** Quantification of percentage of *ltaS*::*erm gdpP*::*kan* (0%; n=184), *gdpP*::*kan* (35%; n=216), *lcpB*::*erm* (0%; n=220), *lcpC*::*erm* (0%; n=277), and *tarO*::*erm* (2%; n=198) populations with fluorescently labelled SpA. Frequencies under 10% are not labelled. Samples shown are representative of one biological repeat.

The loss of phosphodiesterase activity and subsequent increase in secondary messenger cyclic-di-AMP alone (Sommer *et al*, 2021) in the SH1000 *gdpP*::*kan* mutant does not appear to affect SpA localisation. The loss of lipoteichoic acid synthesis in the SH1000 *ltaS*::*erm gdpP*::*kan* strain not only abrogates SpA display on the cell surface, but also presented morphological defects, including cells with multiple septa and swollen cells. This strain also grew slowly, as expected (Oku *et al*, 2009). Similarly, the interruption of genes involved in both WTA (LcpB) and LTA (LcpC) synthesis and display results in the abrogation of SpA display on the surface of *S. aureus*. Previous work has shown that teichoic acids contribute to the regulation of peptidoglycan cross-linking (Atilano *et al*, 2010), which may affect the display of surface proteins in *S. aureus*, as the results shown in Figure 4.6. might suggest.

4.2.4.2. Effect of Cell Wall Protein Associated Processes on SpA Surface Localisation

The regulation of *S. aureus* virulence factors is a complex and layered process. One level of the regulation of surface exposed virulence factors involves the production of proteases. These enzymes proteolytically cleave cell wall associated proteins on the surface of *S. aureus*, including SpA, as well as inhibit clearance by the host immune system by cleaving some immunoglobulins (Pietrocola *et al*, 2017). Most notable of *S. aureus*' extracellular proteases are: Aur, SspAB, ScpA, and Spl (Wörmann *et al*, 2011).

Aureolysin (Aur) is a metalloprotease which inhibits components of the mammalian immune response by proteolytic cleavage (Laarman *et al*, 2011). Aur also cleaves proteins from the surface of *S. aureus* cells, provoking the immune response further by the subsequent divestment of surface proteins into the host's environment and contributing to the pathogenesis of osteomyelitis (Cassat *et al*, 2013). Aureolysin is upregulated by Agr and is also co-expressed with SspB and ScpA – a cysteine protease B and a serine protease, respectively (Mootz *et al*, 2013). Both SspB and ScpA are staphopain enzymes. Staphopains catalyse a range of endopeptidase reactions on proteins such as elastin, as well as the hydrolysis of many small molecules. Also co-regulated with Aur, SspB, and ScpA is SspA, a V8 protease which cleaves the carbonyl group of aspartate and glutamate residues (Tam & Torres, 2019).

The *spl* operon encodes six serine proteases: SplA, B, C, D, E, and SplF (Stach *et al*, 2021). This operon is currently thought to be exclusive to *S. aureus*, found within the vSaβ pathogenicity island (Jin *et al*, 2021). While the substrates for these proteases are still poorly understood, studies have shown that this group of proteases have immunogenic effects in both rabbit infection models and human infections (Paharik *et al*, 2016; Rieneck *et al*, 1997; Reed *et al*, 2001; Nordengrün *et al*, 2021). To assess the contribution of these proteases to the display of surface exposed SpA, a mutant lacking SplA, B, C, D , E, F, and Aur ("Protease Mutant") was screened for SpA display by immunofluorescence, along with its parental strain ("LAC"; Boles *et al*, 2010) which produces functional copies of those proteases.

Sortase A (SrtA) is a membrane-bound enzyme that recognises the LPXTG motif of certain surface proteins (Chapter 1, Section 1.4.). SrtA forms an acyl-enzyme intermediate between the threonine and glycine residues of the protein's C-terminus, which is then resolved covalently by the free amine group of the pentaglycine bridge's terminal glycine (Ton-That *et al*, 1999). The pentaglycine bridge typically cross-links the Gram-positive peptidoglycan cell wall between the 4^{th} D-ala and the 3^{rd} L-lysine of two peptide stems. Through the action of SrtA, this bridge serves to anchor, and subsequently display, surface proteins possessed of the LPXTG motif on the cell wall (Huang *et al*, 2003). To investigate the impact of SrtA in the population frequency of SpA display, an SH1000 ΔSrtA strain was assessed.

The increased percentage of the protease mutant population displaying SpA on the surface (79%) compared with both its parental strain (33%) and the wild type SH1000 (20%) suggests that the proteolytic turnover of surface exposed virulence factors contributes to the population heterogeneity of SpA localisation observed previously (Section 4.2.3.) (Boles *et al*, 2010). Interestingly, 13% of cells lacking functional SrtA displayed SpA on the cell surface, though the localisation was less well defined (Figure 4.7.). This suggests that an alternative method was used in this strain to display SpA – likely the ionic binding of SpA's LysM domain. Each strain in Figure 4.7. grew similarly to their wild type background strain SH1000 and displayed no morphological abnormalities. SpA localisation for each strain shown in Figure 4.7. remains consistent with SH1000, with the exception of Δ*srtA*, which displayed a less well-defined SpA fluorescence compared to SH1000. It's possible that some SpA signal in the ΔSrtA strain is membrane-associated at the time of fixation and immunofluorescence.

A

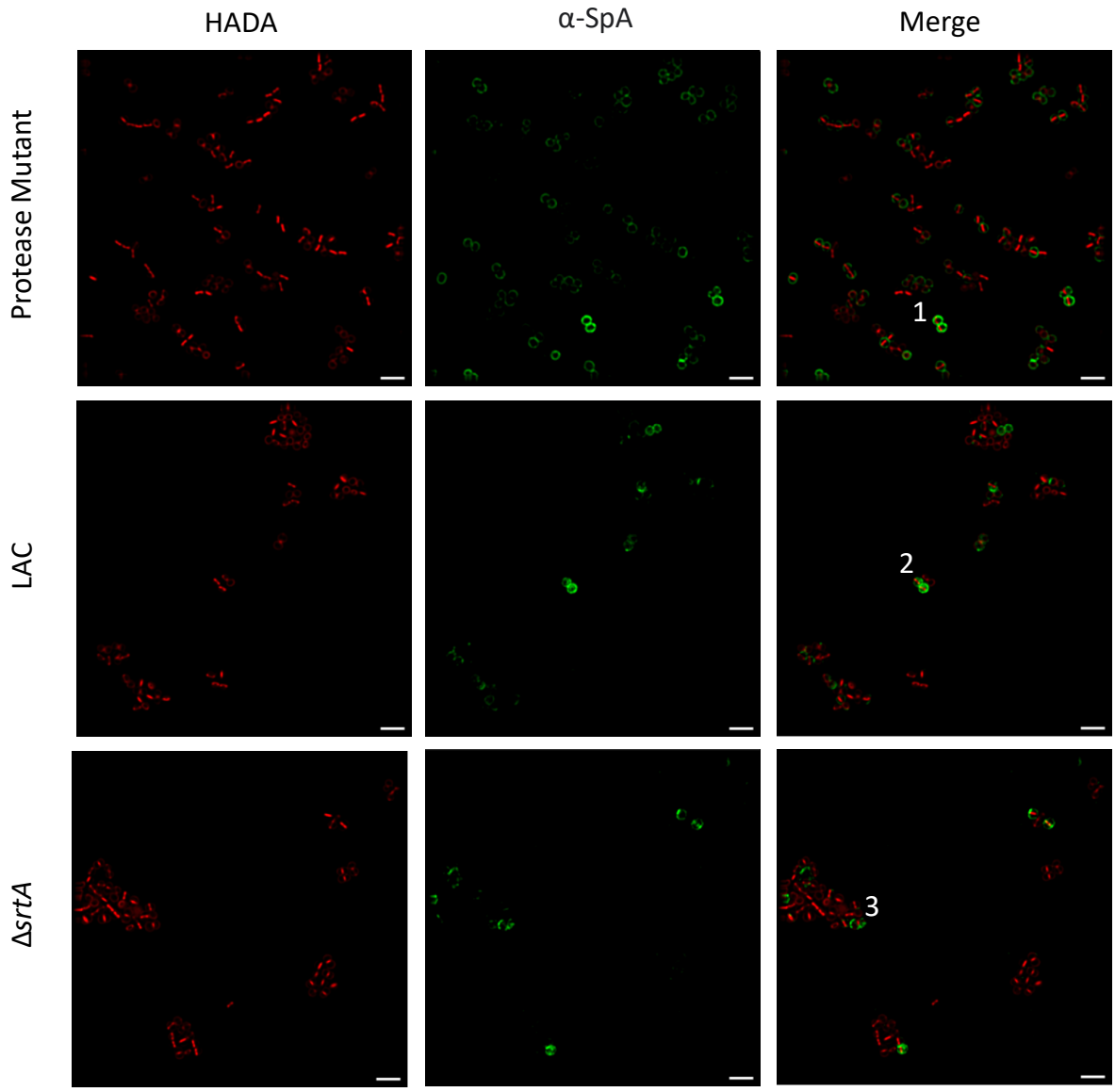

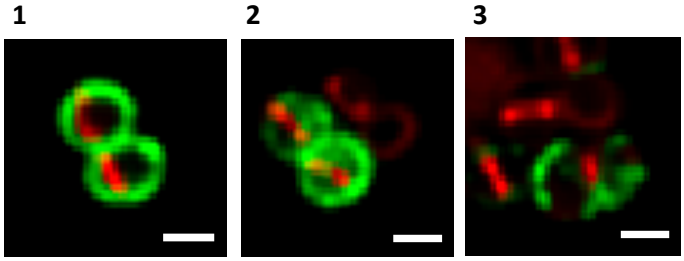

B

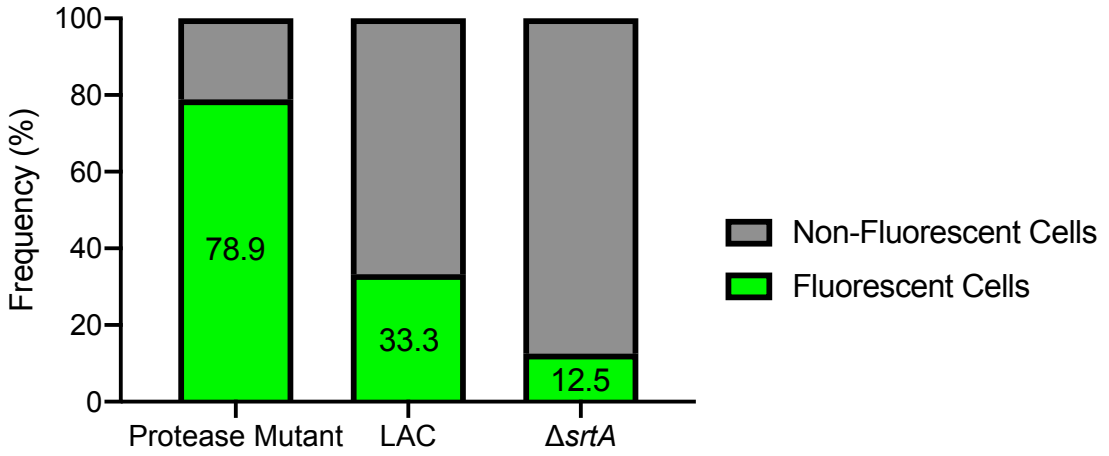

Figure 4.7. The role of proteases and SrtA in SpA localisation by immunofluorescence microscopy

(A) HADA was used to label nascent peptidoglycan (red). α-SpA Immunofluorescence microscopy of *S. aureus* protease mutant (Δ*aur*, Δ*sspAB*, Δ*scpA*, *spl*::*erm*), its parental strain LAC (Boles *et al*, 2010), and Δ*srtA*. Inset numbers enlarged below. Scale bars = 3 µm. Inset scale bars = 1 µm. **(B)** Quantification of percentage of protease mutant (79%; n=389), its parental strain (33%; n=228), and Δ*srtA* (13%; n=332) populations with fluorescently labelled SpA. Samples shown are representative of one biological repeat.

4.2.4.3. The Effect of SDS Treatment on SH1000 Δ*srtA* to Extract Ionically Bound Surface Proteins

In addition to its LPXTG sorting signal motif, SpA possesses a Lysin Motif (LysM) which is known to enable the binding of surface exposed proteins to the cell wall of *S. aureus* (Buist *et al*, 2008). This binding is ionic, as opposed to covalent binding that anchors LPXTG surface proteins to the *S. aureus* cell wall, typically via SrtA. To test whether this ionic binding is responsible for the presence of SpA seen in the SH1000 Δ*srtA* strain, *S. aureus* SH1000 wild type, and SH1000 Δ*srtA* were boiled in a 4% (v/v) sodium dodecyl sulphate (SDS) solution prior to α-SpA Immunofluorescence microscopy (Figure 4.8.). In the presence of SDS, proteins form negatively charged SDS-protein complexes which releases non-covalently bound proteins from their ionically bound substrate.

A slight reduction of the percentage of the SH1000 wild type population displaying SpA was observed when boiled in 4% (v/v) SDS (20% reduced to 17%). This is likely representative of a minority of SpA being ionically incorporated into the cell wall architecture. Conversely, treatment of SH1000 Δ*srtA* with 4% (v/v) SDS removed all detectable SpA from the cell surface of this strain. This suggests that SpA observed previously in this strain is ionically bound to the cell wall, likely via LysM (Zhang *et al*, 2021). However, some of the signal observed in

A

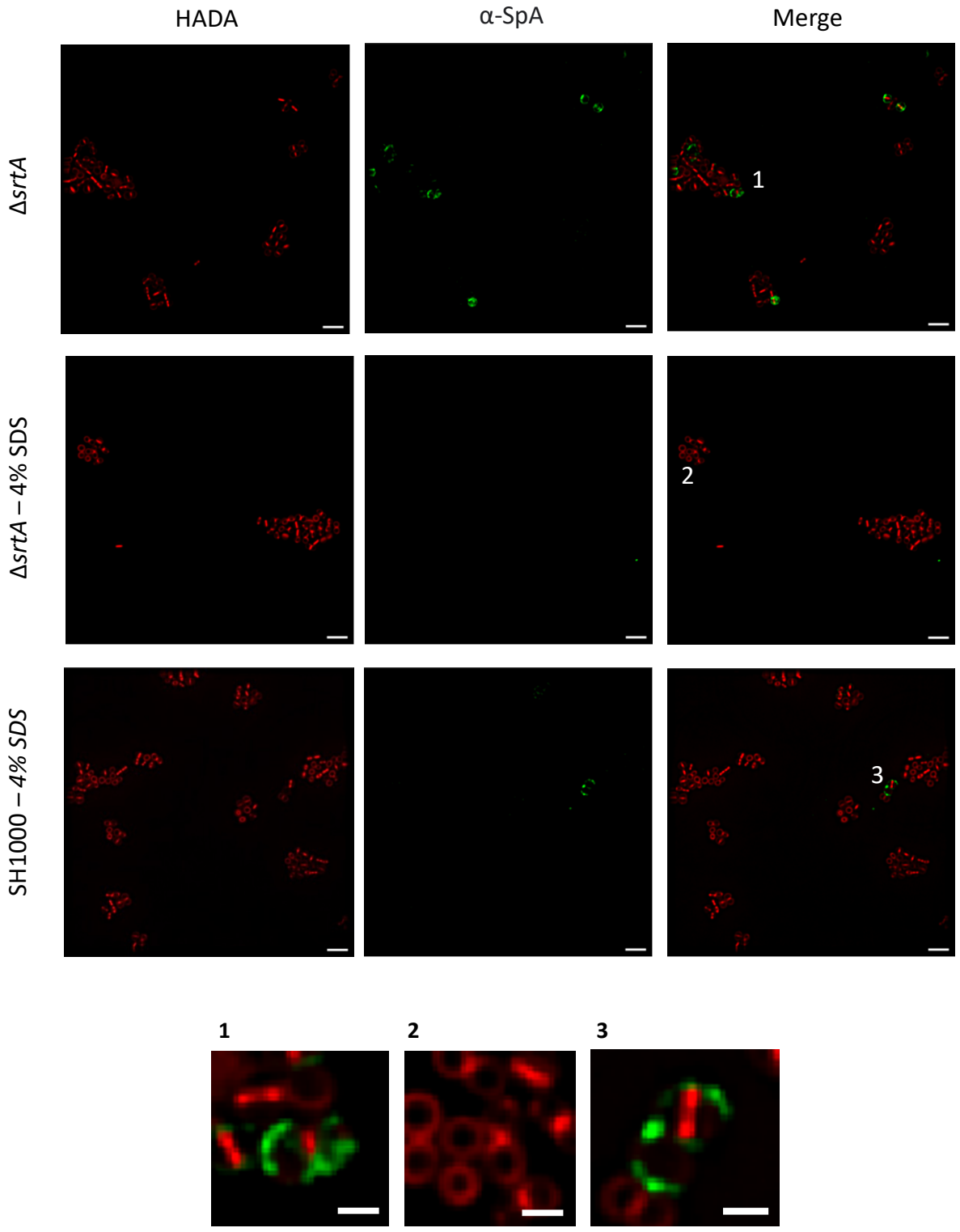

B

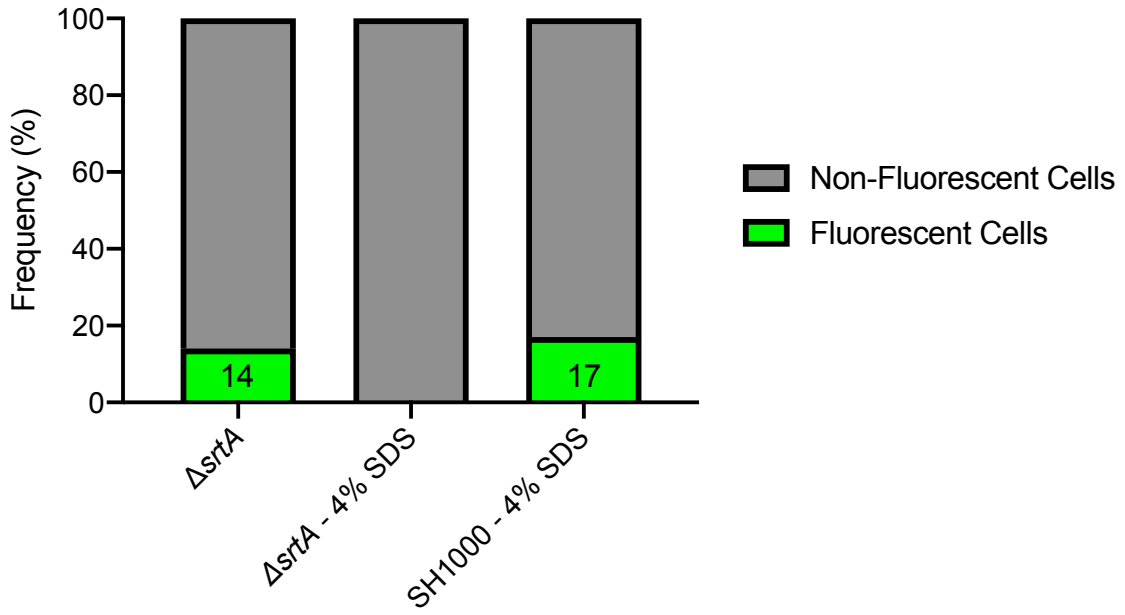

Figure 4.8. Effect of SDS treatment on SpA localisation by immunofluorescence microscopy

(A) HADA was used to observe nascent peptidoglycan synthesis (red). α-SpA Immunofluorescence microscopy of *S. aureus* Δ*srtA*, SH1000 wild type and *agr*::*tet* treated with 4% (v/v) SDS solution. Inset numbers are enlarged below. Scale bars = 3 µm. Inset scale bars = 1 µm. Loss of SpA display is observed in Δ*srtA* strain treated with SDS, while SpA display remains in SH1000 wild type and *agr*::*tet*. **(B)** Quantification of percentage of Δ*srtA* (14%; n=112), Δ*srtA* – 4% SDS (0%; n=128), SH1000 – 4% SDS (17%; n=136) cells with fluorescently labelled SpA. Frequencies under 10% are not labelled. Samples shown are representative of one biological repeat.

4.2.4.4. The Role of Regulatory Components on SpA Surface Localisation

Two-component systems are an effective mechanism by which many prokaryotes regulate genes and protein function (Mitrophanov *et al*, 2008). The SaeRS two-component system in *S. aureus* is known to regulate the of production of more than 20 virulence factors, which include but are not limited to: leukocidins, haemolysins, proteases, and surface proteins (Jenul & Horswill, 2019). *saeR* encodes a response regulator, which responds to levels of the kinase activity of the histidine kinase *saeS*. The expression of the *spa* gene is repressed by the Agr regulated RNAIII. During post-exponential growth phase, Agr negatively regulates *spa* at the transcriptional and translational level, mediated by a quorum sensing system which involves the two-component histidine kinase AgrC and the response regulator AgrA (Xu *et al*, 2017). A high cell density, such as in post-exponential growth phase of *S. aureus*, results in an abundance of RNAIII, also encoded within the *agr* locus, as a result of the recognition of AgrD-derived autoinducing peptides. RNAIII binds to the *spa* transcript and prevents its translation (Pailander *et al*, 2018). Another gene involved in the regulation of *agr*, and therefore the regulation of *spa* is *sarA*. SarA upregulates the transcription of RNAII and RNAIII within the *agr* locus and negatively regulates the expression of a range of virulence associated RNA such as *spa*, as well as various genes involved in antibiotic resistance and biofilm formation (Valle *et al*, 2003). SarA is activated in the transition between exponential growth phase and stationary phase, wherein the production of surface protein A is halted by SarA – Agr regulation, and the secretion of toxins is increased (Cheung *et al*, 2008). While the exact regulatory mechanisms are still unknown, the SarA family of proteins (SarA, SarR, SarS, and MgrA) each possess a helix-turn-helix conformation, which is characteristic of DNA-binding proteins. This has led to the supposition that the SarA protein family physically interact with the chromosome to regulate transcription (Liu *et al*, 2006).

While the percentage of cells with fluorescently labelled SpA in the *agr*::*tet* strain increased (85%), the same patterns of SpA localisation could be observed (Figure 4.9.). Therefore, a non-functional Agr strain is a useful tool for the further study of SpA localisation due to the vastly increased number of cells displaying SpA. Disrupting the function of SarA causes 100% of cells to fluorescence for SpA labelling. In addition, the horseshoe like pattern observed previously is much less frequent in this strain, though it can still be observed within the population.

A

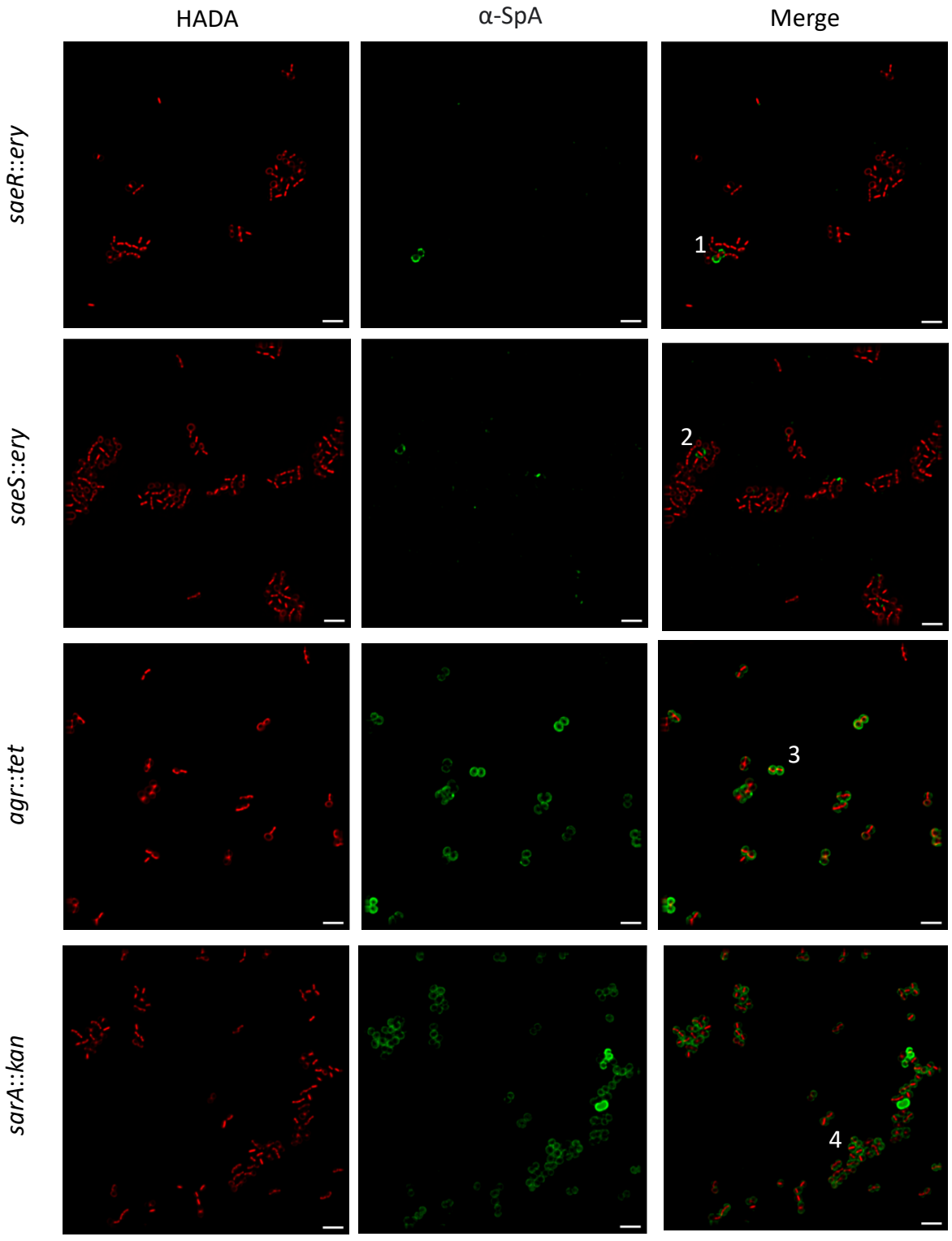

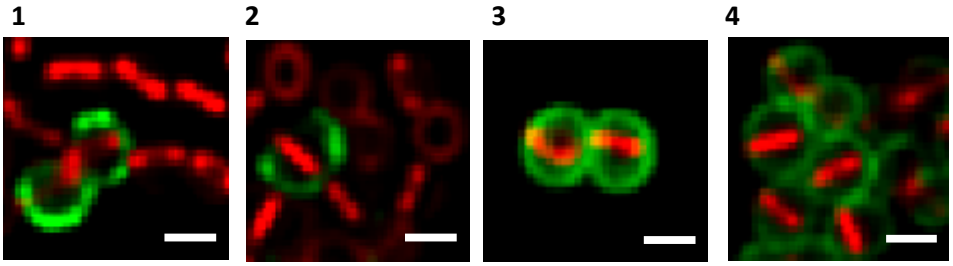

B

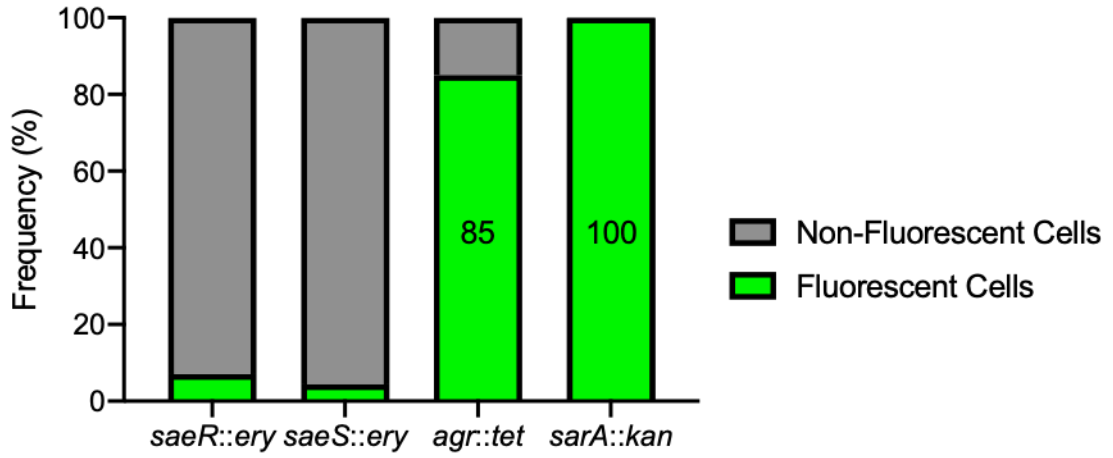

Figure 4.9. Effect of virulance regulation genes on SpA localisation by immunofluorescence microscopy

(A) HADA was used to label nascent peptidoglycan (red). α-SpA Immunofluorescence microscopy of *S. aureus saeR*::*erm*, *saeS*::*erm, agr*::*tet,* and *sarA*::*kan*. Inset numbers are enlarged below. Scale bars = 3 µm. Inset scale bars = 1 µm. **(B)** Quantification of percentage of *saeR*::*erm* (7%; n=211), *saeS*::*erm* (4%; n=238), *agr::tet* (85%; n=207) and *sarA*::*kan* (100%; n=266) cells with fluorescently labelled SpA. Frequencies under 10% are not labelled. Samples shown are representative of one biological repeat.

4.2.5. Dynamics of SpA Surface Display

4.2.5.1. Shaving of Surface Proteins using Trypsin

Previous work on the localisation of SpA in RN4220 has shown that SpA is first displayed on the cell surface at the developing septum of dividing cells (Yu *et al*, 2018). However, the localisation of SpA in SH1000 and other strains tested in my work have shown that SpA is absent from the developing septum of cells until the next cycle of cell division is underway. So to investigate where SpA is initially displayed on the cell wall of SH1000, samples of SH1000 *sbi*::*erm* were treated with the protease trypsin to cleave off surface exposed proteins (DeDent *et al*, 2007). Taking samples at various time points after recovery from trypsin treatment – via washing with trypsin inhibitor solution – allows for the observation of the emergence of SpA over time.

Treatment of *S. aureus* with trypsin did not affect growth rate following recovery or HADA incorporation. However, cells in Figure 4.10. did appear smaller than normal, though they were not specifically measured. Cells that were fixed and incubated with primary α-SpA and fluorescently conjugated secondary antibodies immediately after recovery from trypsin display no SpA on the cell surface. Samples taken after 10 minutes of additional growth following trypsin recovery (T_{10}) show punctate foci of SpA localisation at the developing septum of cells. After 30 minutes of growth following trypsin recovery (T_{30}) SpA is localised both at the most recent site of septation of two daughter cells as well as at the periphery of a cell. After an hour of growth (T_{60}), cells in the process of septation demonstrate the typical horseshoe like pattern of fluorescence seen in non-trypsin treated cells, while single cells display SpA over the whole cell (Figure 4.10.). This suggests that, while cells appear to translocate SpA at the developing septum, as previously suggested by Yu *et al*, 2018, additional translocation also occurs at the periphery of the cells, albeit to a lesser extent. Then, as cells continue to grow and divide further, SpA becomes distributed over the whole of the cell. Alternatively, SpA may be present at the septum but not exposed on the surface at the time of treatment. Therefore, over time, SpA is incorporated at the septum during cell growth and subsequent cell wall hydrolysis is required to fully expose underlying SpA (Figures 4.10. – 4.13.).

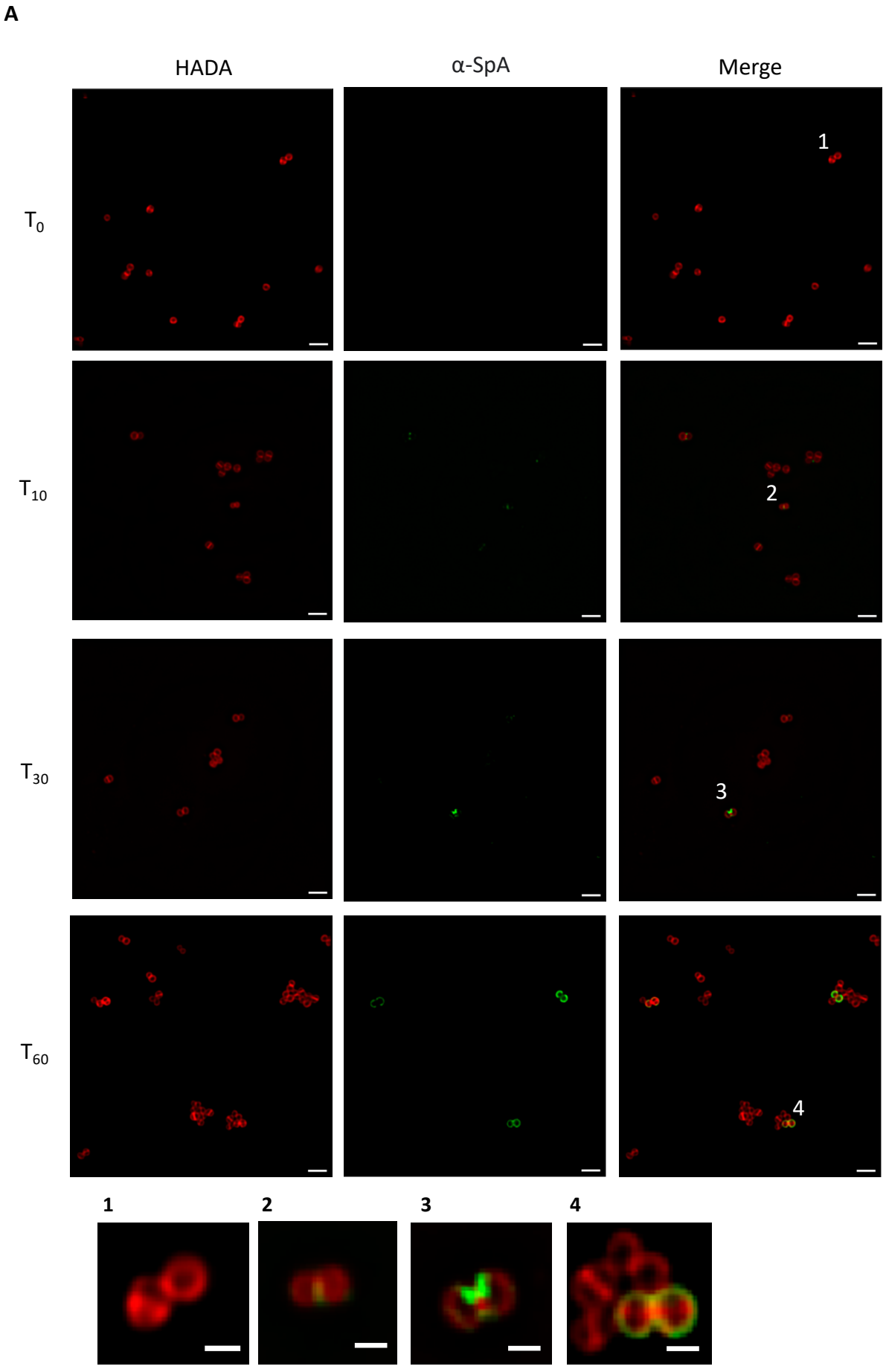
A
HADA
α-SpA
Merge
T0
T10
T30
T60
1
2
3
4
1
2
3
4

B

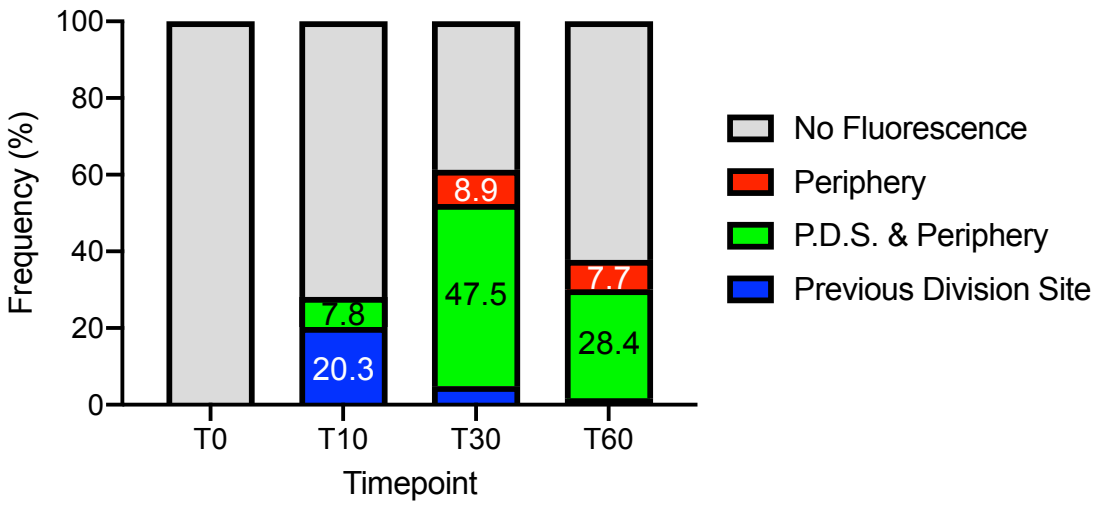

Figure 4.10. Trypsin treatment of SH1000 *sbi*::*erm* & SpA localisation by immunofluorescence microscopy

(A) HADA was used to visualise nascent peptidoglycan synthesis (red). α-SpA Immunofluorescence microscopy of *S. aureus* SH1000 *sbi*::*erm*. Inset numbers are enlarged below. Scale bars = 3 µm. Inset scale bars = 1 µm. **(B)** Quantification of percentage of *sbi*::*erm* at time point 0 (0%; n=97), 10 (28% n=92), 30 (61%; n=101), and 60 (38%; n=116). Percentages in bars represent that group's percentage fluorescence according to the key (right) based on morphological characterisations detailed in Figure 4.4. Categories with no percentage shown are under 5%. Keys denoting SpA localisation are detailed in Figure 4.4. Samples shown are representative of three biological repeats.

Due to the low percentage of the SH1000 *sbi*::*erm* population that display surface exposed SpA (Figure 4.10.), an SH1000 *agr*::*tet sbi*::*erm* strain was generated by transduction for use in the trypsin treatment experiment (Figure 4.11.). A non-functional Agr strain was chosen due to the increased percentage of the population displaying SpA on the cell surface without altering the display pattern observed in the wild type strain (Figure 4.9.). This enables the quantification of more cells and more examples of SpA localisation to analyse the display and development of SpA over time, while the Sbi mutation is maintained in this strain to ensure that what is observed via α-SpA immunofluorescence microscopy is representative of only SpA and not Sbi antibody binding activity, despite previous results suggesting that Sbi plays little to no role in inhibiting SpA immunolabelling (Figures 4.2. and 4.3.).

SpA localisation patterns observed using the *agr*::*tet sbi*::*erm* strain are comparable to those seen in the *sbi*::*erm* strain alone, as well as the *agr*::*tet* strain (Figures 4.2., 4.3., and 4.9.). Specifically, single cells displaying SpA show whole-cell surface display, while cells undergoing division demonstrate the characteristic horseshoe motif. Diplococcal cells undergoing division display SpA at the PDS as well as the periphery of cells (Figures 4.4. and 4.10.) There is no observable SpA on the cell surface immediately following recovery from trypsin treatment in the *agr*::*tet sbi*::*erm* strain. At ten minutes post-recovery, the majority of SpA is localised at the septum of cells that have partially divided, with slight peripheral fluorescence as well. After thirty minutes of growth following recovery from trypsin treatment, most of the SpA fluorescence can be seen between daughter cells at the PDS (Figure 4.4.), with an increasing amount of peripheral localisation on some cells. By an hour after recovery from trypsin, cells display SpA across their entire cell wall, with the notable re-emergence of the horseshoe like pattern seen in dividing cells.

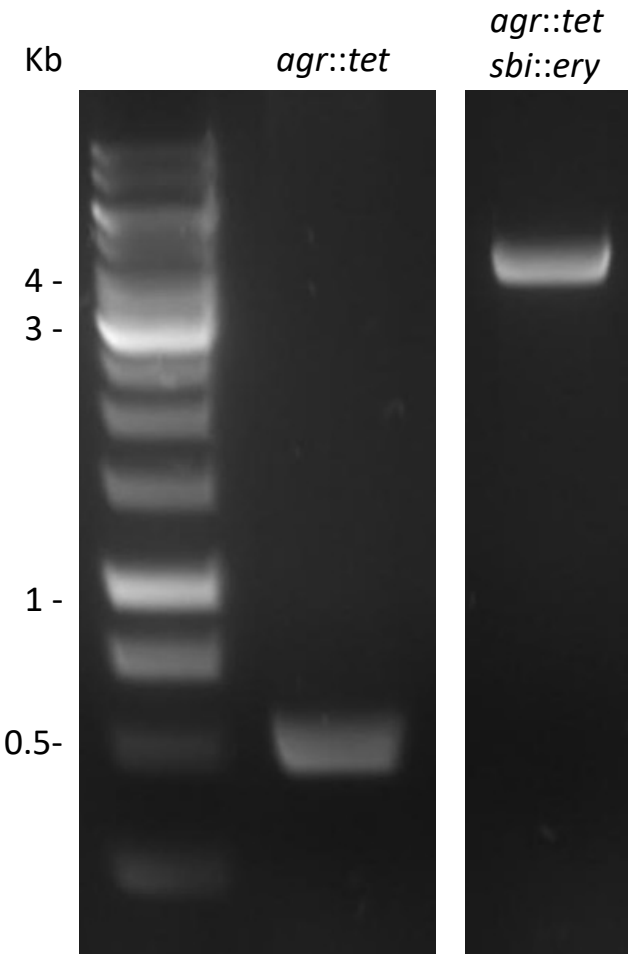

Figure 4.11. Creation of *S. aureus* SH1000 *agr*::*tet sbi*::*erm* by bacteriophage transduction

PCR amplification of *sbi*::*erm* transduction using *sbi* F and *sbi* R primers (Figure 4.1.). Samples were seperated by 1% (w/v) agarose gel electrophoresis. Bursa aurealis transposon insertion was observed by a 4.2 Kb PCR product. SH1000 *agr*::*tet* gDNA was used as a negative control, with a PCR product of 500 bp.

A

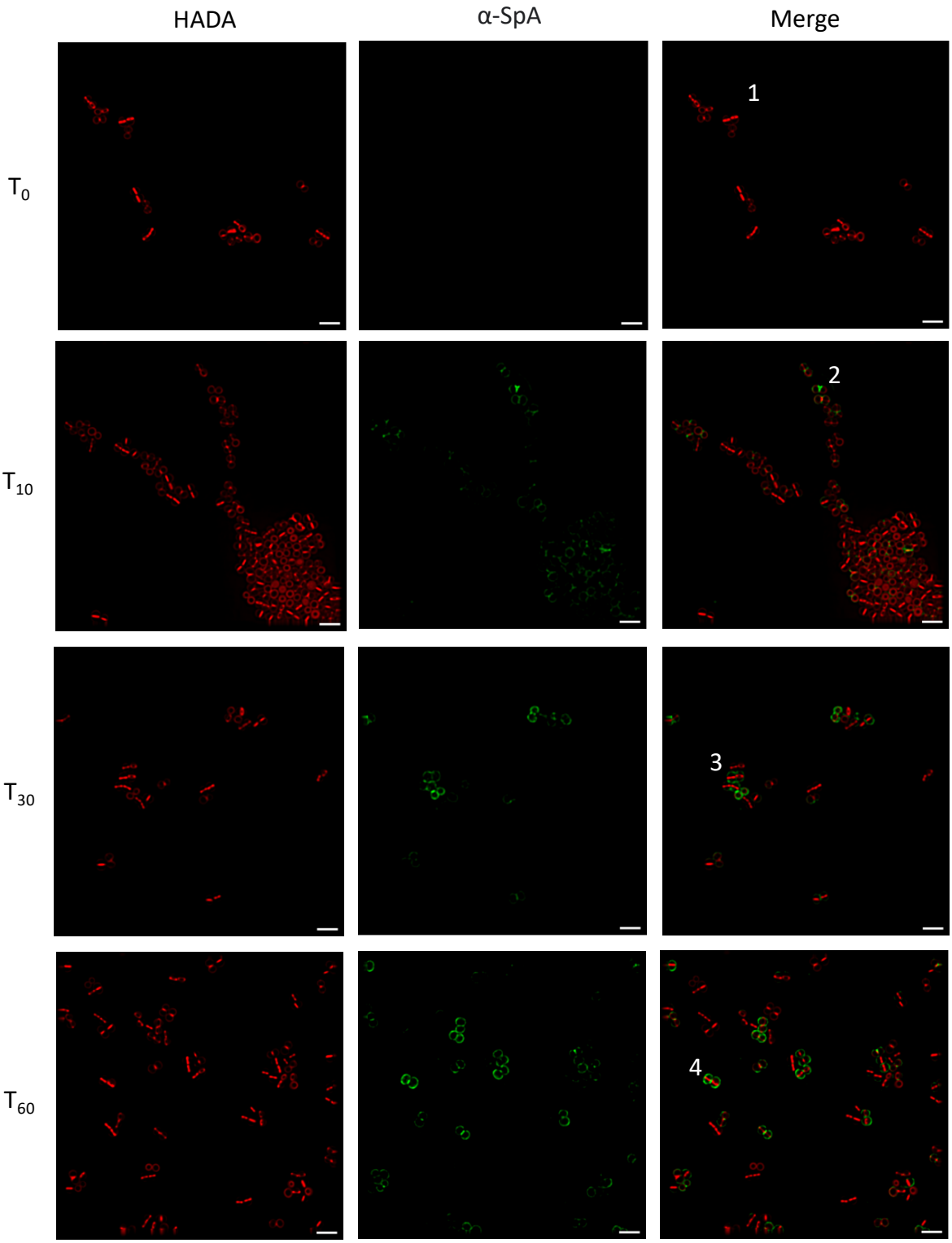

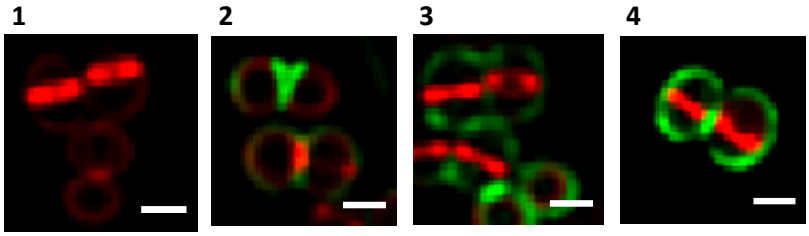

B

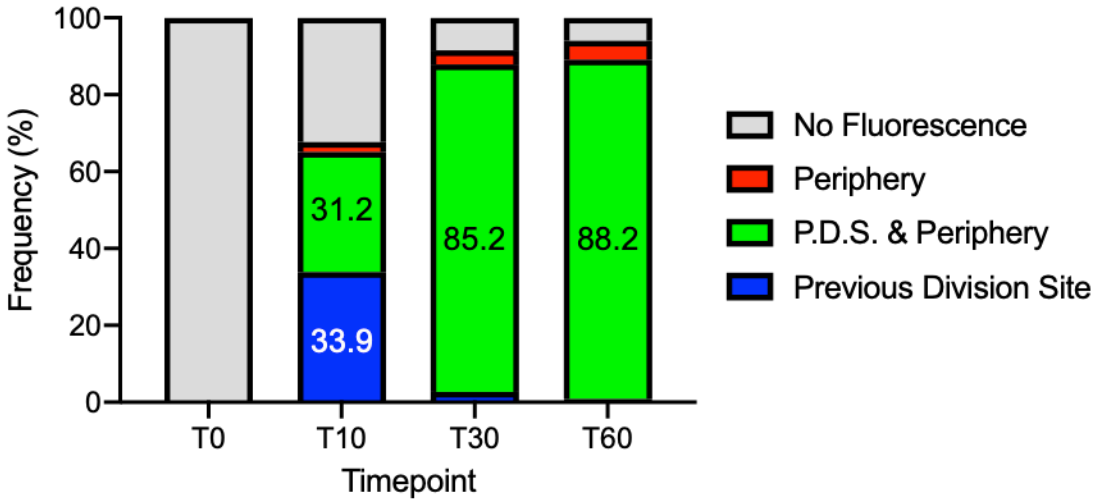

Figure 4.12. Trypsin treatment of SH1000 *agr*::*tet sbi*::*erm* and subsequent SpA display by immunofluorescence microscopy

(A) Trypsin treated SH1000 *agr*::*tet sbi*::*erm* cells showing SpA emergence after recovery from trypsin with trypsin inhibitor solution. Inset numbers are enlarged below. Scale bars = 3 µm. Inset scale bars = 1 µm. **(B)** Quantification of percentage of SH1000 *agr*::*tet sbi*::*erm* T_0 (0%; n=102), T_{10} (68%; n=109), and T_{30} (92%; n=108) and T_{60} (94%; n=102) cells with fluorescently labelled SpA. Keys denoting SpA localisation are detailed in Figure 4.4. Categories with no percentage shown are under 5%. Samples shown are representative of three biological repeats.

4.2.5.2. Relationship of SpA Surface Display to the Cell Cycle

The association with SpA localisation in *S. aureus* to the developing septum has been observed in previous work, primarily using either trypsin treatment of cells, or by the chemical induction of SpA expression (DeDent *et al*, 2007; Yu *et al*, 2018). Surface protein A can be observed by immunofluorescence in as little as 10 minutes following the treatment of cells with trypsin and is almost exclusively associated with the most recently observable, completed septation event, or the "previous division site" (Figures 4.4., 4.10., and 4.12.). However, the presence of SpA embedded in the cell wall, which is not exposed on the surface and is therefore inaccessible to trypsin, has not been investigated to date. As such, it is unclear whether the SpA localisation seen in timepoints ten and thirty following recovery from trypsin are the result of the production of SpA, or if the hydrolysis of the cell wall as part of the natural cell cycle exposes SpA that was previously inaccessible to trypsin and detection by immunofluorescence.

To juxtapose peptidoglycan synthesis with SpA localisation, cells were pulsed with the fluorescently conjugated D-alanine derivative TADA (red) for 5 minutes, treated with trypsin for 1 hour, washed with trypsin inhibitor, then chased with HADA (cyan) for 5 minutes, before chemical fixation and α-SpA immunofluorescence microscopy. Performing a pulse-chase with two different fluorescent D-alanine derivitives enables the correlation of SpA display with peptidoglycan synthesis that occurred prior to trypsin treatment (red), and nascent cell wall synthesis that took place after cells were recovered from trypsin (cyan). This serves to establish a potential correlation between SpA emergence and nascent cell wall synthesis. Samples taken immediately following trypsin treatment show no SpA on any cell in the population. HADA could not be added to time point 0 (T_0) samples because HADA incorporation requires cell growth. Therefore, only TADA was used to label nascent peptidoglycan synthesis prior to trypsin treatment in this sample (Figure 4.13.). At T_{10}, SpA is observed exclusively between diplococcal cells where a completed septation event would have previously occurred. At T_{30}, this pattern persists, with some cells displaying SpA at the currently developing septa, juxtaposed between TADA incorporation prior to trypsin treatment, and HADA incorporation prior to chemical fixation. Finally, at T_{60} SpA was exclusively co-localised with TADA, which suggests that the SpA visible in this sample was

incorporated into the cell wall prior to treatment with trypsin, when TADA was used in septal synthesis.

To assess whether SpA is present in the cell wall of trypsin-treated *S. aureus* immediately following recovery, the cells were fractionated and the cell wall fraction was purified for α-SpA Western blot analysis. The trypsin treated cell wall fraction showed a much fainter SDS-PAGE product compared to the non-treated sample, implying a reduced amount of SpA in this fraction. Quantification of Western blot band intensity, run in triplicate, shows an average of 22% of SpA remains in the cell wall of trypsin treated cells, compared to control cells incubated in PBS (Figure 4.14.). The presence of SpA in the cell wall of trypsin treated cells immediately following recovery suggests that not all cell wall associated surface proteins are fully exposed on the surface of cells and are therefore protected from the effects of trypsin. This in turn implies that there is SpA incorporated into the cell wall of these samples which is also not accessible to immunolabelling, which could explain the emergence of the horseshoe motif seen in actively dividing cells.

The treatment of *S. aureus* with trypsin and the subsequent localisation of SpA by immunofluorescence microscopy has shown that SpA localises to the most recently completed septation event between diplococcal cells. This localisation can be observed within ten minutes of growth in the absence of trypsin (Figure 4.13.). The remaining 22% of SpA in the trypsin treated cell wall compared to the same *S. aureus* sample without trypsin treatment suggests that some SpA is incorporated into the cell wall that is not fully exposed on the surface and is therefore protected from the effects of trypsin. It follows then, that SpA observed at T_{10} in trypsin treated samples was likely incorporated into the cell wall prior to the treatment, as opposed to actively incorporated SpA since the cells were recovered from trypsin. The exposure of SpA over time co-localising with cell wall material synthesised prior to trypsin treatment could be due to hydrolysis of the cell wall as part of the cell cycle.

A

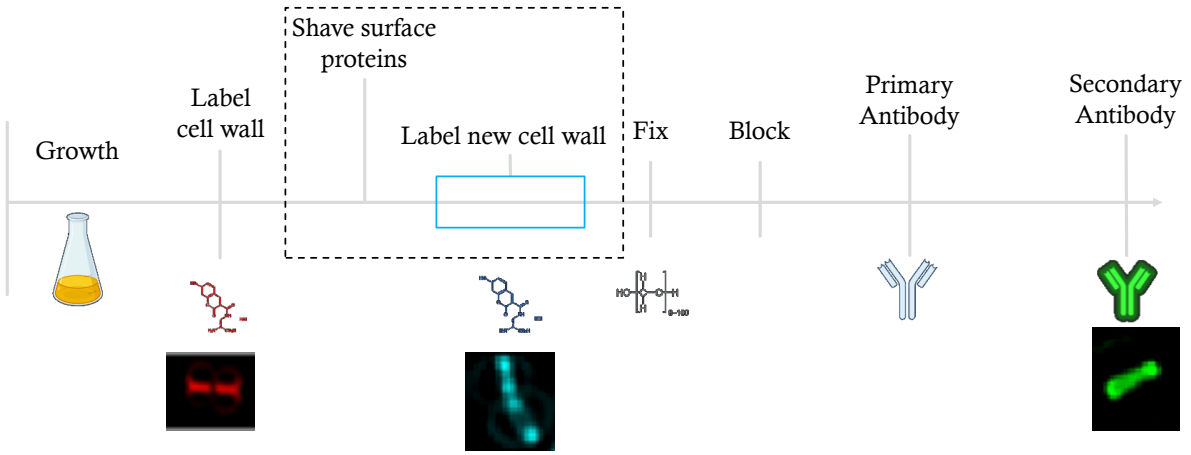
Shave surface proteins
Label cell wall
Growth
Label new cell wall
Fix
Block
Primary Antibody
Secondary Antibody

B

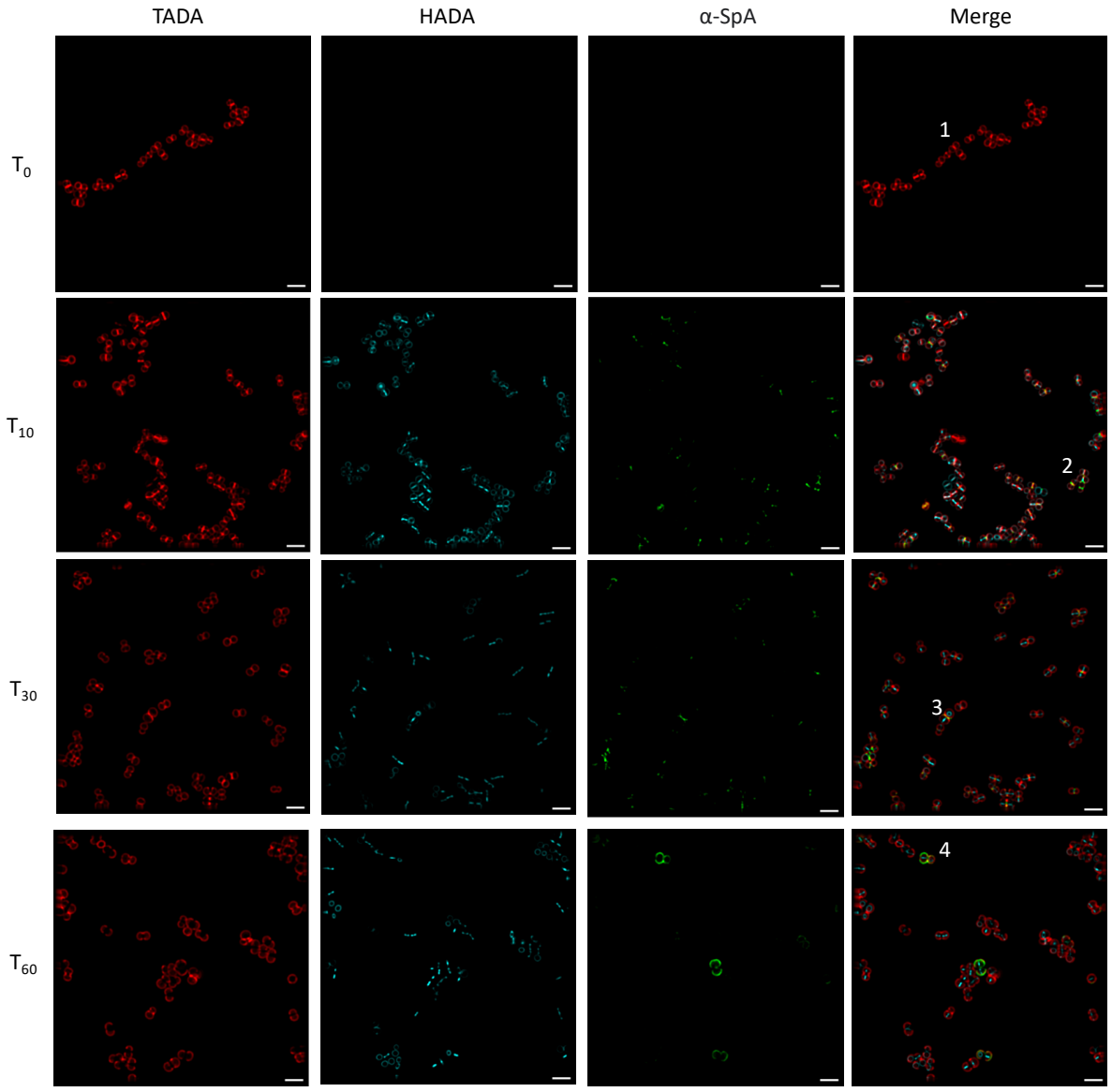
TADA
HADA
α-SpA
Merge
T0
T10
T30
T60
1
2
3
4

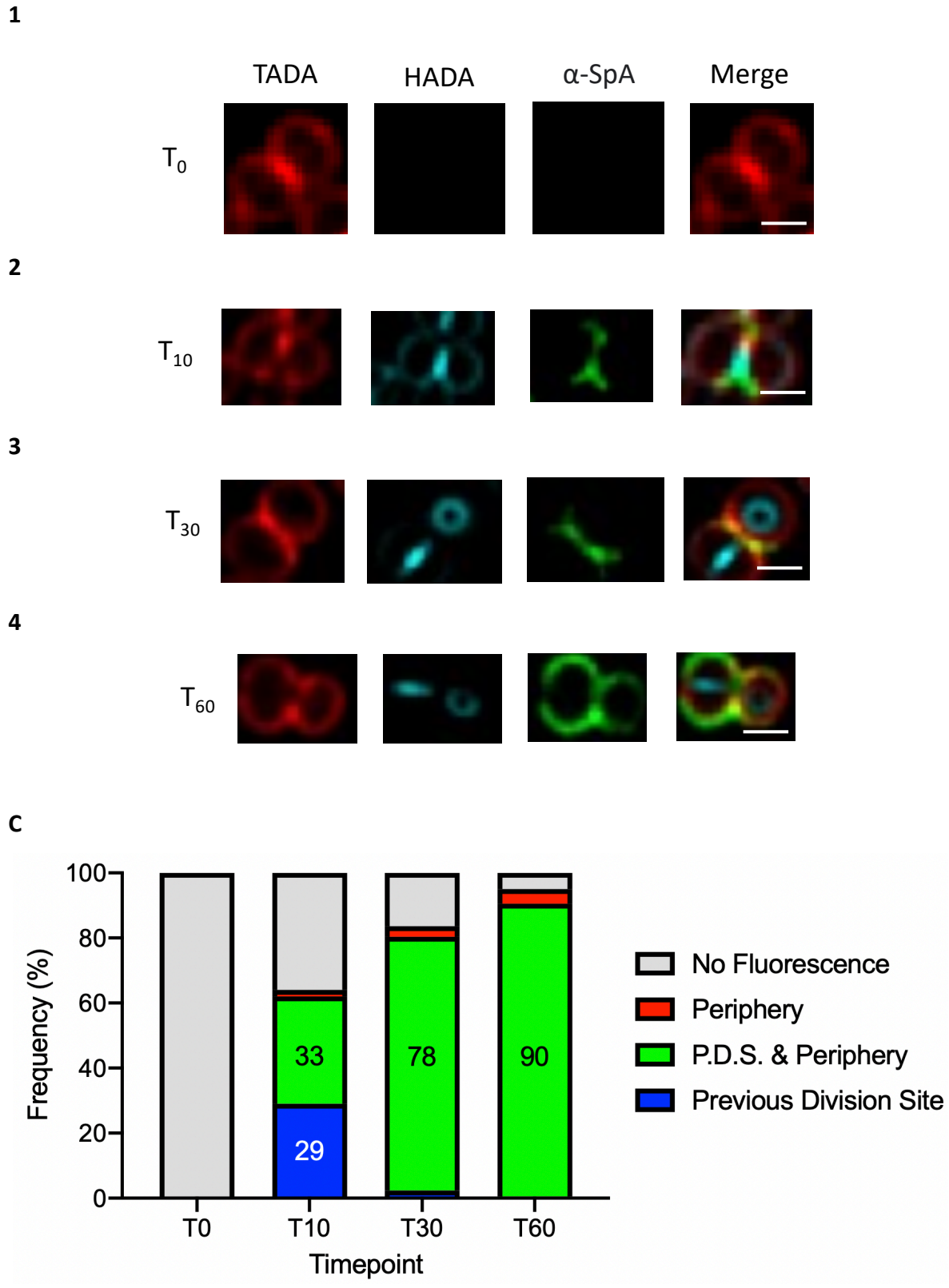
1
TADA
HADA
α-SpA
Merge
T0
2
T10
3
T30
4
T60
C
100
80
60
40
20
0
Frequency (%)
33
29
78
90
T0
T10
T30
T60
Timepoint
No Fluorescence
Periphery
P.D.S. & Periphery
Previous Division Site

Figure 4.13. TADA-HADA pulse chase & trypsin treatment of SH1000 *agr*::*tet sbi*::*erm* by α-SpA immunofluorescence microscopy

(A) Schematic representation of pulse-chase experiment steps. Initial fluorescent amino acid derivitive TADA (red) is incorporated into the cell wall prior to trypsin treatment. Dashed box highlights trypsin treatment and subsequent HADA incorporation (cyan). Chemical fixation was achieved using PFA. Blocking was achieved using 2% (v/v) BSA in PBS. Samples were incubated with primary α-SpA and conjugated secondary fluorescent antibodies for two hours, rotating, at room temperature. **(B)** α-SpA Immunofluorescence microscopy of trypsin-treated SH1000 *agr*::*tet sbi*::*erm*. Inset numbers enlarged below. Scale bars = 3 µm. Inset scale bars = 1 µm. **(C)** Quantification of percentage of SH1000 *agr*::*tet sbi*::*erm* T_0 (n=112), T_{10} (n=100), and T_{30} (n=98) and T_{60} (n=105) cells with fluorescently labelled SpA. Keys denoting SpA localisation are detailed in Figure 4.4. Frequencies under 10% are not labelled. Samples shown are representative of three biological repeats.

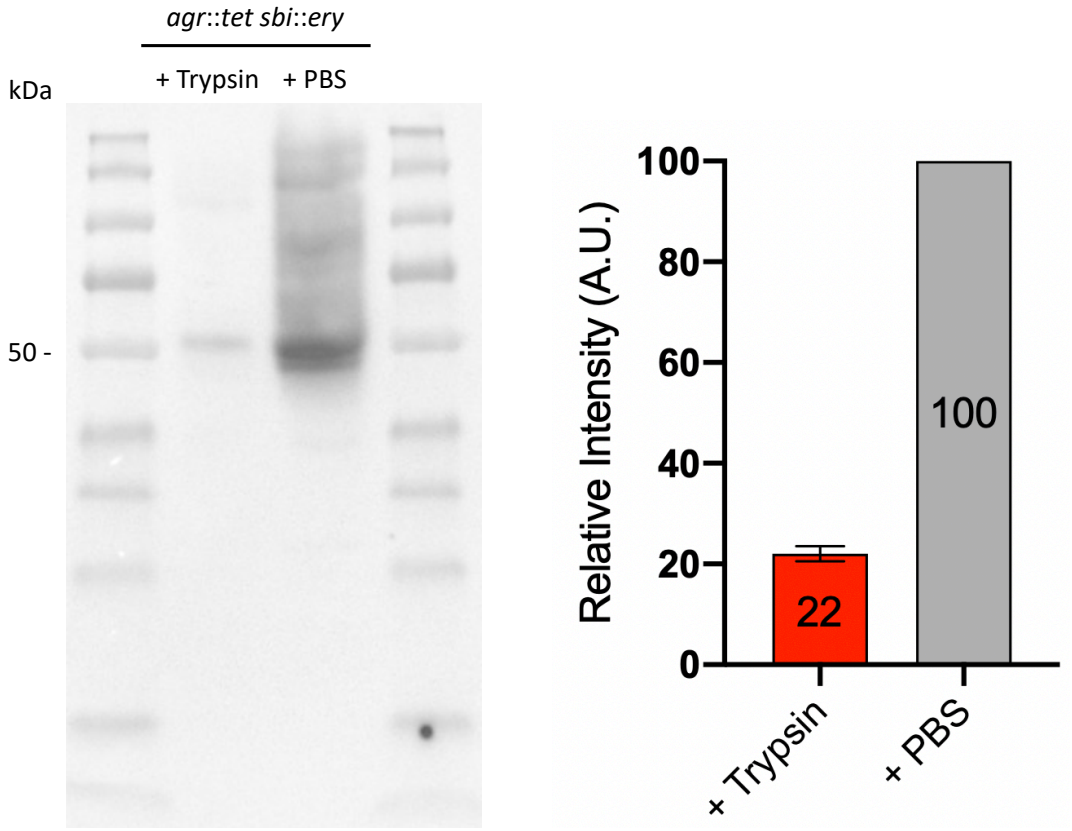

Figure 4.14. Proteomic comparison of cell wall associated SpA in trypsin treated cell wall fractions

α-SpA western blot of *S. aureus* SH1000 *agr*::*tet sbi*::*erm* trypsin treated cell wall. Quantification shows 22% SpA present in the cell wall of trypsin treated samples compared to the SpA content of samples incubated with PBS as a control. n = 3. Error bars represent standard deviation.

4.4. Discussion

Previous work by different groups has shown conflicting localisation patterns of SpA in *S. aureus*. Work done by DeDent *et al* (2007) demonstrates the emergence of SpA in trypsin-treated *S. aureus* RN4220 at two to four distinct foci across the cell, and thus proposed a model of SpA distribution over time based on these findings. The group also states that SpA is unevenly distributed over the cells surface, and that this localisation requires the presence and function of Sortase A (SrtA). Most recently, Scaffidi *et al* (2021) have summarised their work using immunofluorescence microscopy to localise chemically inducible plasmid-based SpA on the surface of *S. aureus* RN4220, demonstrating whole cell surface display of SpA for every cell shown. The group also treated cells with the protease trypsin to visualise cross-wall localisation of SpA on a subset of the population, which they show exclusively to emerge at the cross wall of dividing cells.

The immunofluorescence protocol used in this study to localise SpA was based on that described by DeDent *et al* (2007). However, instead of using Cy5-conjugated goat α-rabbit IgG at a dilution factor of 1:1000, my work has utilised mouse α-SpA monoclonal primary antibody, and an Alexafluor 488 conjugated rabbit α-mouse IgG, both at a dilution factor of 1:250. Using only a fluorescently conjugated secondary antibody for SpA localisation was tested, as described in DeDent *et al*, 2007, at varying dilution factors but was found to be insufficient to localise SpA beyond the observation of a few punctate foci in any given population (data not shown). Initially, this was thought to be an indication of consolidation with DeDent's findings. However, the use of specific primary antibodies raised against purified SpA from *S. aureus* has improved the localisation of SpA, enabling the consistent observation of SpA localisation across strains as described throughout this chapter. This has shown both whole cell display of SpA and a horseshoe like localisation in dividing cells, compared to inconsistent and distinct foci of SpA labelling shown previously. This could also account for the disparity in signal intensity between the work of DeDent, Yu, and my own, as multiple polyclonal secondary antibodies can also bind to both SpA and a single primary antibody, thereby amplifying the immunofluorescent signal further.

The occurrence of the horseshoe motif of SpA localisation is interesting, as the developing septum is thought to be the primary location of SpA incorporation into the cell wall (Yu *et al*, 2018). Yet the lack of SpA immunolabelling at this site in currently dividing cells is what gives rise to this horseshoe pattern of fluorescence. This could be in part due to the lack of complete separation between daughter cells, as is a characteristic morphology of *S. aureus* (Saraiva *et al*, 2020). Alternatively, this could be due to the presence of multiple layers of peptidoglycan cell wall at the developing septum, as shown by AFM (Pasquina-Lemonche *et al*, 2020). Whether this additional ring structure of cell wall material is too dense to observe SpA at this site, or whether this architecture obfuscates SpA incorporated into the porous mesh structure of peptidoglycan below is an interesting question that requires further investigation (Chapter 5).

Despite the supposed ubiquitous nature of SpA in exponentially growing *S. aureus* cells (Hao *et al*, 2021), only a small percentage of the population of SH1000 cells were labelled by immunofluorescence (Figure 4.2.). The heterogeneity of SpA expression in the population was unexpected, considering that translational regulation of *spa* is known to be controlled, at least in part, by Agr mediated RNAIII antisense RNA binding to *spa* transcript, which is also a global regulator of virulence factors. Specifically, Agr mediated translational repression of *spa* is alleviated during exponential growth phase. As such it was expected that most of the population would display SpA during exponential growth phase. Ultimately, the use of an Agr deficient strain enabled the analysis of SpA localisation in a much higher frequency than was possible in both the wild type SH1000 and the *sbi* mutant strains alone, without altering the localisation patterns observed in these strains. This made the *agr* mutant strain a useful tool for investigating not only the natural display patterns of SpA, but also in elucidating the localisation patterns of emerging SpA in cells treated with trypsin (Figures 4.10., 2.12., and 4.13.).

The role of proteases in the turnover of bacterial cell surface proteins is an important facet of *S. aureus*' ability to cause disease (Singh *et al*, 2019). This is predominantly due to the release of virulence factors into the host environment (Bien *et al*, 2011). The shedding of *S. aureus* surface proteins as a natural part of the cell cycle acts as another layer of modulation to the display of surface proteins over time. As such, the effect of the deletion of multiple genes

encoding proteases was assessed by immunofluorescence for the localisation of SpA. A multiple protease mutant (Δ*aur*, Δ*sspAB*, Δ*scpA*, *spl*::*erm*) was chosen to investigate their collective contribution to the display of SpA. The parental strain of this mutant, LAC, was also used as a control (Boles *et al*, 2010). Unsurprisingly, the multiple protease mutant exhibited an increased percentage of the population displaying SpA, though no additional localisation patterns were observed beyond the characteristic horseshoe and whole cell localisation. These same motifs of SpA immunolabelling were also observed in the LAC parental strain, though only 33% of the LAC population were found to be displaying SpA on the surface. This suggests that these proteases are indeed vital in the turnover of SpA, and likely contribute to the heterogeneity of display observed across these *S. aureus* populations.

A deletion strain of *srtA* was also screened for SpA localisation, with the expectation that there would be no SpA displayed on the cell surface. This work not only found that there was SpA on the surface of this strain, but that the localisation of surface protein A was similar to the wild type and other mutants expressing SpA, albeit at a slightly lower frequency. Treatment of this strain with SDS showed the SpA present on the cell surface was ionically bound to the cell wall, likely via its C-terminal LysM domain. Therefore, these findings not only suggest that SrtA is not the sole method by which surface proteins containing the LPXTG sorting signal may be incorporated into the cell wall, but also that SrtA may not play a role in directing the site at which these proteins are translocated and subsequently displayed on the cell surface. Conducting a trypsin treatment experiment with this strain may provide additional information regarding the emergence of SpA without covalent binding facilitated by SrtA.

Previous work has found that both wall teichoic acids (WTA) and lipoteichoic acids (LTA) play an important role in the modulation of Gram-positive cell wall crosslinking (Atilano *et al*, 2010). Given that the highly crosslinked cell wall of *S. aureus* acts as the framework for the display of key surface exposed virulence determinants, like SpA, mutant strains lacking a variety of genes contributing to the display of teichoic acids to the cell wall were assessed. SpA-specific immunofluorescence microscopy of *S. aureus* strains lacking important functional genes involved in both WTA and LTA synthesis shows that SpA display is abrogated when the synthesis of teichoic acids is disrupted (Figure 4.6.). Both LcpC and LcpB deficient

strains of *S. aureus* SH1000 display no SpA immunolabelling, suggesting that the attachment of capsular polysaccharides and the ligation of WTA to the cell wall are important for the display of SpA and potentially other key surface exposed virulence factors (Li *et al*, 2020). Additionally, LtaS appears to also be required for SpA surface display, as a mutant without the capacity to produce this protein shows no immunolabelled SpA. Investigating SpA immunofluorescence in the *gdpP*::*kan* strain, which is a mutation required for survival in an LtaS deficient mutant, shows that more of the population display SpA when compared to the wild type SH1000 (35% compared to 20%, respectively). This suggests that the loss of GdpP does not negatively affect SpA surface display, and that LtaS activity is required for the display of SpA in the cell wall of *S. aureus*.

Many genes involved in the biosynthesis of WTA are considered essential as, without them, *S. aureus* strains produce toxic intermediates of WTA that are detrimental to cell viability (Suzuki, 2011). *tarO* is the first gene in the biosynthetic pathway of WTA and is one of the few that is considered non-essential, as its abrogation does not appear to impact the viability of *S. aureus* under standard laboratory conditions (D'Elia *et al*, 2006). The inhibition of TarO by both chemical and genetic means has recently been shown to down-regulate *spa* (Lu *et al*, 2023). Because teichoic acid synthesis has been shown to play a role in various aspects of the cell wall of *S. aureus*, assessing a *tarO* mutant strain for SpA localisation was necessary. Findings reported in Figure 4.6. show that only 2% of the population deficient in TarO production display SpA on the cell surface. This further corroborates findings within the literature that both the biosynthesis and display of teichoic acids are vital pathways that contribute to surface protein display.

The mutant library screening also found that SarA plays a significant role in the display of SpA. The knockout strain of this gene showed 100% of cells quantified to fluoresce under immunofluorescence microscopy for SpA. Furthermore, the frequency of the horseshoe motif of SpA surface display was reduced. This could suggest that the horseshoe pattern of SpA localisation seen in other strains is the result of a lower amount of SpA incorporation into the cell wall, compared to wild type, which could be investigated by RNA transcription analysis. Alternatively, a *sarA* mutant strain could express a greater amount of SpA compared to the wild type such that minimal cell wall hydrolysis of the most recently completed and exposed

septum is required to fully expose SpA between two daughter cells – thus making the horseshoe pattern rarer to observe.

Additionally, data shown in figures 4.13. and 4.14. show that SpA is colocalised with cell wall material synthesised prior to treatment with trypsin, as opposed to colocalising with nascent cell wall synthesis at the time of analysis. This suggests that SpA may be present in the cell wall, which is not accessible to trypsin, for a time. A subsequent Western blot analysis of the cell wall fraction of a trypsin treated sample compared to a non-trypsin treated sample supports this hypothesis, as 22% of SpA remains in the cell wall following treatment. Together, these data suggest that further processes beyond translocation are required for the display of SpA on the cell surface, such that interaction with extracellular components can be achieved.

In summary, it is clear from these data that the display of SpA on the surface of *S. aureus* is a complex and multi-faceted process. Not only does the amount of SpA displat on the surface vary between strains of *S. aureus*, but it also requires multiple other biosynthetic pathways and regulatory processes, such as teichoic acid synthesis and protease activity. Surface protein display is an important virulence strategy of *S. aureus* that depends on the proper synthesis and display of teichoic acids to decorate the cell wall and lies under strict control by both genetic and translational regulation, as well as by mechanistic regulation achieved by multiple proteases and various cell wall associated components. Additionally, it has been found that *S. aureus* can display the key virulence factor SpA without membrane bound SrtA to covalently bind SpA to the cell wall. The presence of alternative methods of cell wall incorporation, and subsequently surface display, exemplifies the important of surface proteins like SpA to *S. aureus*' capacity for virulence. As such, surface protein display dynamics warrant further study – particularly in clinically relevant strains – to elucidate alternative treatment strategies and the management of antibiotic resistance.

4.5. Main Findings in this Chapter

- SpA-specific immunofluorescence microscopy provides consistent localisation of surface exposed SpA
- Mutants not producing the antibody binding protein Sbi do not appear to have altered SpA display patterns
- *S. aureus* demonstrates a population heterogeneity of SpA display, seemingly due to regulation factors such as Agr and SarA
- The horseshoe pattern of SpA labelling is likely due to the requirement of cell wall hydrolysis at the site of septation to display SpA on the cell surface
- A *sarA* mutant strains of *S. aureus* rarely displays the horseshoe localisation of SpA, presumably due to increased SpA content incorporated into the cell wall
- Treatment of cells with SDS shows that the majority of SpA localisation is covalently bound to the cell wall via SrtA

Chapter 5

Localisation of Surface Protein A in Methicillin Resistant *Staphylococcus aureus*

5.1. Introduction

5.1.1. β-lactam Resistance in *S. aureus*

Penicillin, and other β-lactam antibiotics, function by the formation of an acyl-enzyme intermediate with PBPs as they act as analogues of D-ala-D-ala (Lima *et al*, 2020). Transpeptidation is an essential step in the synthesis of the cell wall peptidoglycan whereby peptide stems are crosslinked. As such, its inhibition is fatal for *S. aureus* (Hobby *et al*, 1942; Craft *et al*, 2019). Resistance to the antibiotic effects of β-lactams in *S. aureus* were observed within just two years of the initial and widespread use of penicillin in 1940 (Lowy, 2003). The evolution of resistance to penicillin is attributed to the production of a penicillinase, also known as β-lactamase, which binds to and cleaves the β-lactam ring of penicillin (Sabath, 1982). As a result of the development of resistance to penicillin, a new β-lactam antibiotic was synthesised and named methicillin, which was unaffected by penicillinase activity (Thomas *et al*, 2022). However, *S. aureus* strains became resistant to the effects of methicillin by an alternative mechanism. This was discovered to be the acquisition of a modified penicillin binding protein 2, called PBP2a (Fergestad *et al*, 2020). PBP2a possesses transpeptidase activity only – as opposed to the bifunctionality of PBP2 – and is the only functional PBP in *S. aureus* in the presence of inhibitory concentrations of methicillin. The production of PBP2a is encoded by the exogenous *mecA* gene, which has since been found to confer resistance to other β-lactam antibiotics like oxacillin as well as methicillin and penicillin (Goering *et al*, 2019; Liang *et al*, 2022).

The *mecA* gene is part of the exogenously acquired staphylococcal cassette chromosome (SCCmec) which contains not only the gene conferring resistance to most β-lactam antibiotics, but also regulatory elements responsible for the expression of *mecA* encoded PBP2a (Liu *et al*, 2016; Katayama *et al*, 2000). Specifically, the self-contained regulation of *mecA* is often orchestrated by *mecI* and *mecR1* (Archer & Bosilevac, 2001). There are many configurations of SCCmec that confer a variety of resistance capabilities to *S. aureus*, though the general

composition of SCCmec remains the same: a *mec* complex encoding PBP2a and the regulators of its expression, the cassette chromosome recombinase (*ccr*) which allows SCCmec to remain mobile, and the three joining regions (J region) (Ito *et al*, 2009). The size and content of the three joining regions vary across individual SCCmec elements, which has given rise to the classification of the cassette into thirteen different types (I – XIII) (Turlej *et al*, 2011; Liu *et al*, 2016; Urushibara *et al*, 2020). Typical examples of variant SCCmec complexes include type I, which, like types II and III, are larger genetic elements that confer resistance to multiple antibiotics, while types IV and V are more commonly associated with clinically acquired MRSA (Bal *et al*, 2016). Two clinically derived strains possessing type I and types IV SCCmec complexes used in this study are COL and USA300, respectively (Chapter 4, Figure 4.5.; Chongtrakool *et al*, 2006; Fey *et al*, 2013).

While the variety of SCCmec elements afford strains of *S. aureus* resistance to many β-lactams and other clinically relevant antibiotics, there are genes in the chromosome of *S. aureus* known to contribute to the bacteria's ability to maintain its resistance. These are referred to as auxiliary genes (*aux*), and many are known to encode proteins involved in the synthesis of cell wall peptidoglycan (Bilyk *et al*, 2022). However, there are also *aux* genes that encode proteins involved in nitrogen metabolism (GlnR) and various surface proteins like FmtB and MprF (Gustafson *et al*, 1994; Komatsuzawa *et al*, 2000; Komatsuzawa *et al*, 2001). The mechanisms by which the proper expression and function of these proteins contributes to antibiotic resistance are unclear, though the expression of surface proteins is also known to contribute to virulence in *S. aureus*. The interplay between antibiotic resistance and virulence has been alluded to previously, though the significance of this relationship is still largely unknown (Cameron *et al*, 2011).

Similarly, there are genes which, when mutated or rendered non-functional, make *S. aureus* more resistant to β-lactam antibiotics (Figure 5.1.). These genes are known as potentiators (*pot*) (Bilyk *et al*, 2022). Though the mechanisms by which *aux* and *pot* genes contribute to β-lactam resistance are not known – as many of these genes play no part in cell wall synthesis or PBP functionality – they show that the acquisition of *mecA* encoding PBP2a is not solely responsible for the development of high-level methicillin resistance (Dordel *et al*, 2014).

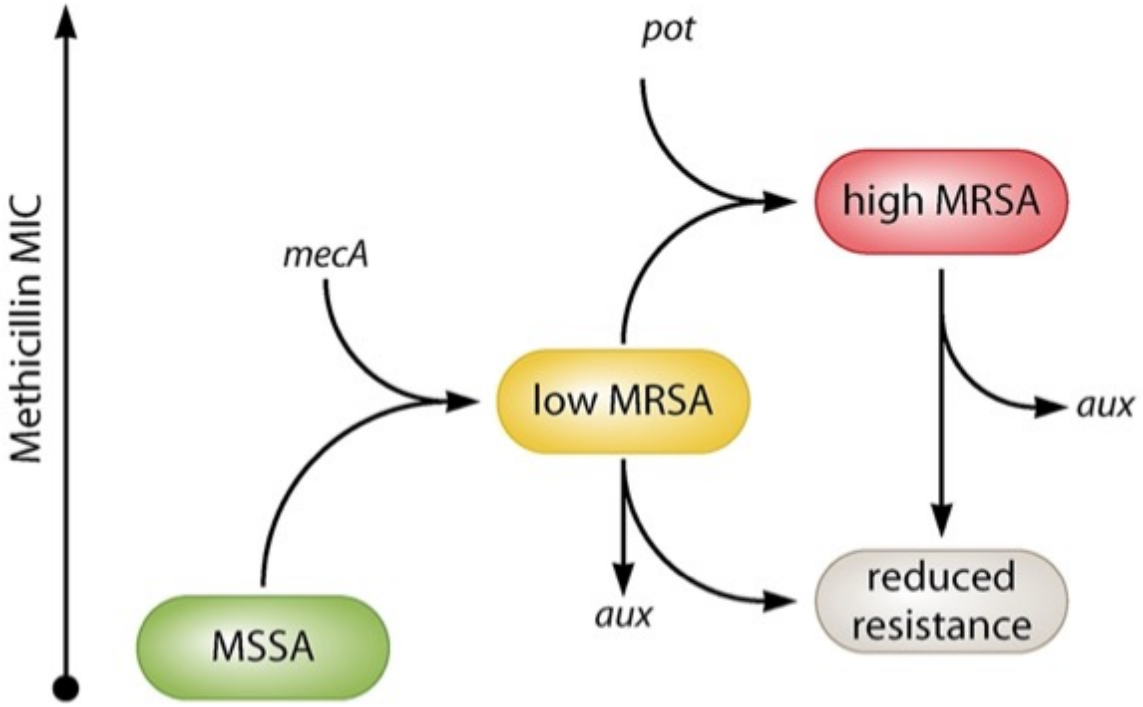

Figure 5.1. Model of mechanisms for the development of methicillin resistance in *Staphylococcus aureus*

Contributing factors associated with the development of low and high level methicillin resistance in *S. aureus*. Genetic elements such as *mecA* provide methicillin resistance. Potentiators (*pot*) are genes which, when mutated or lost, increase *S. aureus*' resistance to methicillin further. Converesely, auxillary genes (*aux*) are those which, when non-functional, render *S. aureus* more succeptable to the effects of methicillin. Adapted from Bilyk *et al*, 2022.

5.1.2. Evolution of High-Level Methicillin Resistance in *S. aureus*

Recent work has shown that single copy, chromosomal *mecA* in *S. aureus* is sufficient to confer methicillin resistance in an otherwise methicillin susceptible strain of *S. aureus* SH1000 (Panchal *et al*, 2020). To elucidate the molecular mechanisms underpinning high-level methicillin resistance, a directed evolution study was performed to generate high-level MRSA to elucidate the genetic factors contributing to methicillin resistance (Panchal *et al*, 2020). Therein, it was established that the minimum inhibitory concentration (MIC) of MSSA SH1000 to oxacillin is 0.12 μg mL^{-1}, while the expression of *mecA* more than doubles the MIC to 0.25 μg mL^{-1}. These MRSA strains were also grown on methicillin gradient agar at increasing concentrations to develop highly resistant MRSA (>50 μg mL^{-1}). *S. aureus* colonies were isolated from this experiment where the MIC had increased to ≥256 μg/mL, as determined using oxacillin E-test diffusion strips. Sequencing of these highly resistant *S. aureus* isolates showed various mutations; the acquisition of a point mutation in RNA polymerase B (*rpoB*), substituting the histidine at position 929 of RpoB with a glutamine residue ($RpoB^{H929Q}$; *rpoB**) was the most common. Mutations in RpoB have been reported previously regarding the protein's contribution to altered methicillin resistance (Matsuo *et al*, 2011). The observation of RpoC mutations from clinical isolates has also been made previously (Dordel *et al*, 2014; Hiramatsu *et al*, 2013). The correlation between the precise amino acid substitution of RpoB, predominantly at its C-terminus, and the alteration to a strain's resistance to antibiotics has also been previously observed (Aiba *et al*, 2013). This suggests that RNA polymerases play a crucial role in *S. aureus*' ability to withstand various antibiotics, presumably due to altered RNA-mediated regulation, such as transcription pausing (James *et al*, 2017).

Recent work using atomic force microscopy has elucidated the architecture of the Gram-positive cell wall of *S. aureus* (Chapter 1; Section 1.2.; Figure 1.2.; Pasquina-Lemonche *et al*, 2020). Therein, two distinct architectures of the cell wall were observed: a porous, mesh-like structure of older cell wall material, and a concentric ring-like structure of nascent septal peptidoglycan (Figure 5.2.). The cell wall of *S. aureus mecA rpoB** has since been detailed using AFM. In the absence of methicillin, the cell wall architecture of this strain remains consistent with the organisation of the SH1000 wild type cell wall, where concentric rings make up the cell wall architecture at the nascent septum, while older cell wall material

presents a dense mesh-like structure. However, in the presence of 25µg mL^{-1} methicillin, the concentric ring-like architecture is absent in the *mecA rpoB** strain (Figure 5.2., Panel B). This extraordinary finding demonstrates that the acquisition of *mecA* in high-level resistant strains allows *S. aureus* to divide without one of its characterising peptidoglycan architectural features. This has important consequences for many other features of the cell wall, including the display and subsequent localisation of surface proteins.

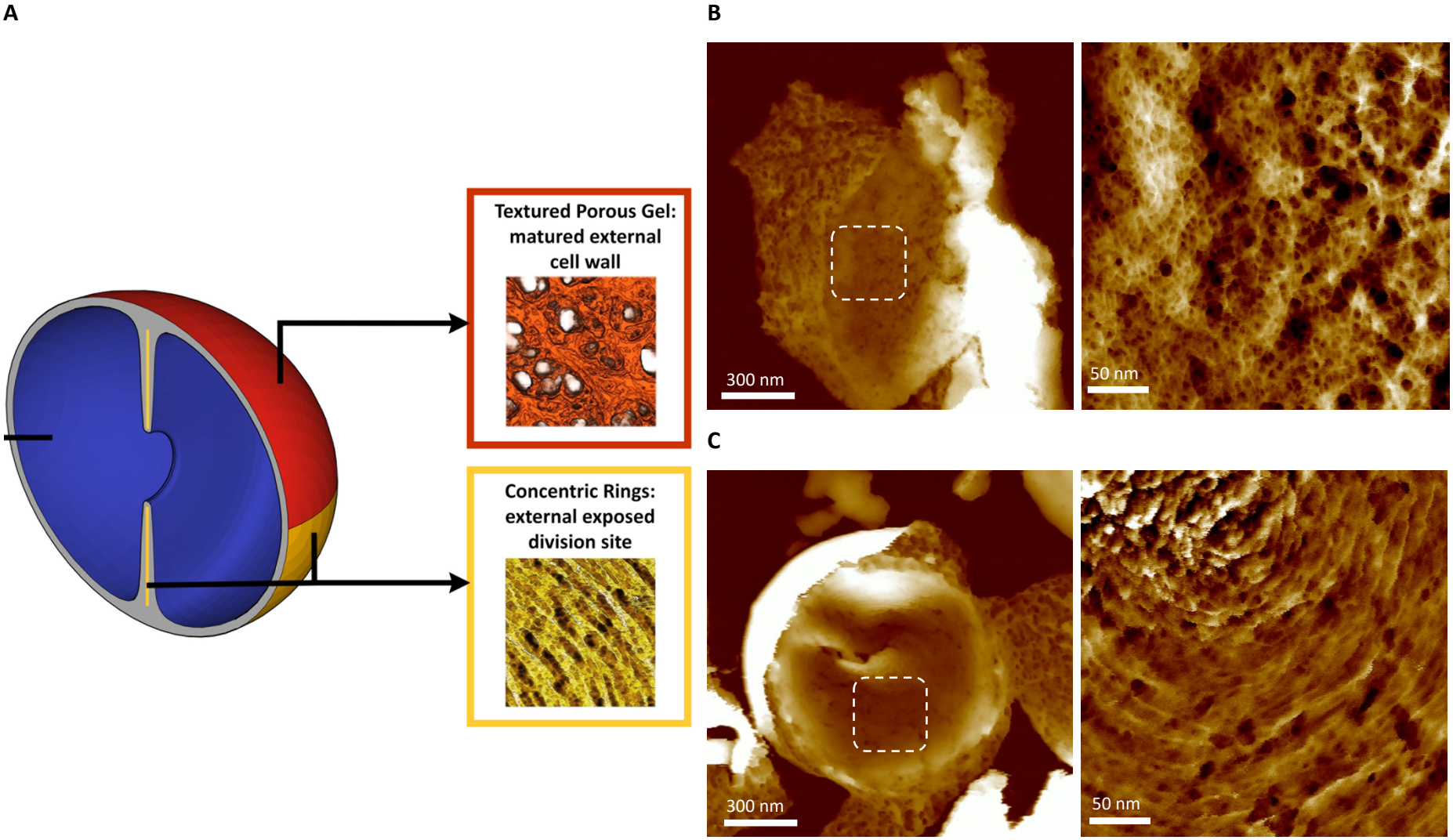
A
Textured Porous Gel: matured external cell wall
Concentric Rings: external exposed division site
B
300 nm
50 nm
C
300 nm
50 nm

Figure 5.2. Atomic force micrograph of *S. aureus mecA rpoB external sacculus surface without and with methicillin**

(A) Schematic representation of cell wall architecture at the cell surface of *S. aureus*. Adapted from Pasquina-Lemonche, 2020. **(B)** *S. aureus mecA rpoB** external surface sacculus. Samples were grown in TSB supplemented with 25 µg mL^{-1} methicillin. Dashed box in the left image is magnified on the right hand side, showing the absence of ring architecture of nascent septal cell wall. **(C)** *S. aureus mecA rpoB** external sacculus surface imaged by AFM. Sample was growth without methicillin. Dashed box region in the middle image is magnified on the right hand side, showing concentric ring architecture of nascent cell wall material. Adapted from Abimbola Olulana, unpublished.

5.1.3. SpA Localisation in MRSA

SpA localisation in the methicillin susceptible *S. aureus* SH1000 background has been elucidated in Chapter 4. It was found that several genes, including *agr* and *sarA*, have a distinct effect on the frequency of SpA display within the *S. aureus* population. Single cells display SpA over the whole cell surface. When single cells divide into diplococci, an absence of SpA at the division site becomes apparent, giving a horseshoe pattern of localisation. As those cells continue to grow and divide in a new plane, SpA becomes visible on the cell surface at the previous site of division, eradicating the horseshoe motif. These patterns of SpA localisation, and indeed SpA display altogether, are all but absent in strains lacking certain genes thought to play a role in cell wall component modulation and synthesis (i.e. *ltaS* and *tarO*), while SpA appeared at an increased frequency in strains with mutations in key regulatory genes (i.e. *agr* and *sarA*).

Surface protein A is not observed on newly exposed septal peptidoglycan, which contains the dense ring-like architecture of cell wall peptidoglycan. Therefore, the rings may not contain SpA, which could instead be embedded within the inner, mesh-like peptidoglycan layer, and is therefore inaccessible to immunolabelling. The ring architecture may therefore act as a layer which, only upon maturation of the rings into mesh via hydrolase activity, does SpA become observable using immunofluorescence microscopy. The discovery that high level MRSA strains lack this ring structure in the presence of methicillin affords the opportunity to investigate this hypothesis.

5.1.4. Aims of This Chapter

- Using α-SpA immunofluorescence microscopy, characterise the SpA display pattern in *S. aureus* SH1000 *mecA rpoB** in the presence and absence of methicillin

- Generate *agr* and *sarA* mutants in the *mecA rpoB** strain to assess and compare SpA display in MRSA against MSSA strains at comparable levels of expression within the population

5.2. Results

5.2.1. SpA Localisation in the MRSA Background Without Methicillin

To assess the localisation of SpA on the surface of *S. aureus* strains resistant to methicillin, *S. aureus* SH1000 *mecA* and *mecA rpoB** were used in the SpA immunofluorescence protocol detailed previously (Chapter 3; Chapter 4). The positive and negative controls used in these experiments are as described in Chapter 4.

Mutations in the *agr* locus were made in both the *mecA* and *mecA rpoB** strains of *S. aureus* SH1000 by bacteriophage transduction to generate increased display of SpA across the population, as described previously in Chapter 4 (Figure 5.2.). Successful colonies from the transduction protocol were selected on 5μg mL^{-1} tetracycline agar plates (1.5% w/v). Genomic DNA was extracted from these colonies and the *agr* locus was amplified by PCR. Wild type amplification of intact *agr* appear at 5 Kb on a 2% (w/v) agarose gel, while knockout mutants of *agr* appear closer to 4 Kb (Figure 5.3., panel B). The exact size of the tetracycline cassette used to mark the *agr* deletion is unknown but was constructed using bacteriophage 80α and has been used extensively since (Novick, 1990; Benson *et al*, 2011). However, these results in combination with the increased percentage of the *S. aureus* population immunolabelled for SpA in Figure 5.4. demonstrates that the transduction of *agr*::*tet* into the *mecA* and *mecA rpoB** strains were successful.

To investigate whether the loss of functional Agr affected the MIC of *mecA* and *mecA rpoB** on oxacillin resistance, antibiotic E-test diffusion tests were used. As shown in Table 5.1. the loss of functional Agr does not affect the MIC of the SH1000 wild type or *mecA rpoB**. However, the *mecA* strain becomes four time more susceptible to the effects of oxacillin when *agr* is mutated (Table 5.1.).

A

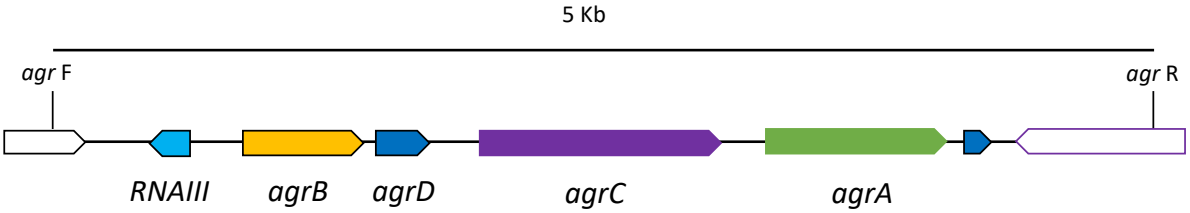

B

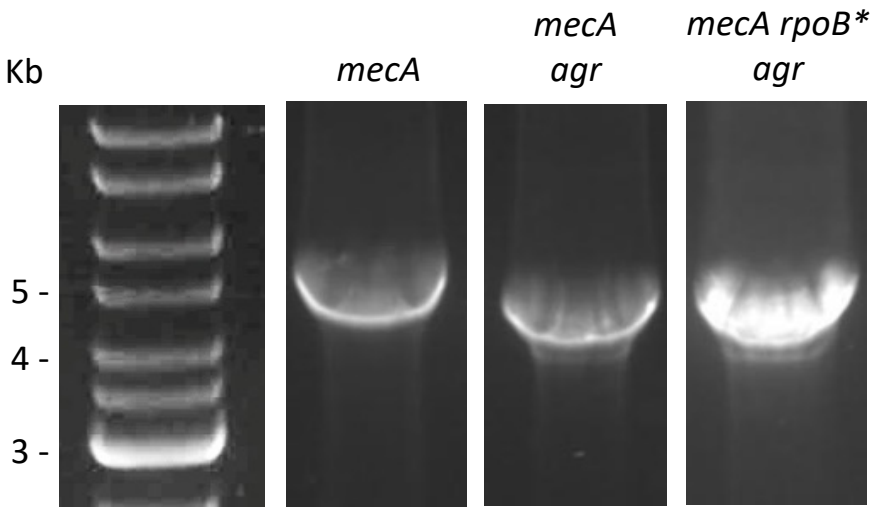

Figure 5.3. Transduction of *agr*::*tet* into the MRSA background

(A) Scematic representation showing *agr* F and *agr* R primers used to amplify the *agr* locus in *S. aureus* SH1000. Highlighted section shows the region amplified by *agr* primers, resulting in a 5 Kb PCR product in the wild type SH1000. **(B)** 2% (w/v) Gel electrophoresis of gDNA from *S. aureus* SH1000 *mecA* with intact *agr*, *mecA* transduced with *agr*::*tet* lysate, and *mecA rpoB** transduced with *agr*::*tet* lysate.

Table 5.1. E-test MIC comparing the change in resistance to oxacillin between MRSA strains with and without functional Agr

Strain	Oxacillin MIC (µg mL^{-1})
SH1000 Wild Type	0.38
SH1000 *agr*::*tet*	0.38
mecA	2
mecA agr*::*tet	0.5
mecA rpoB*	≥256
mecA rpoB** agr*::*tet	≥256

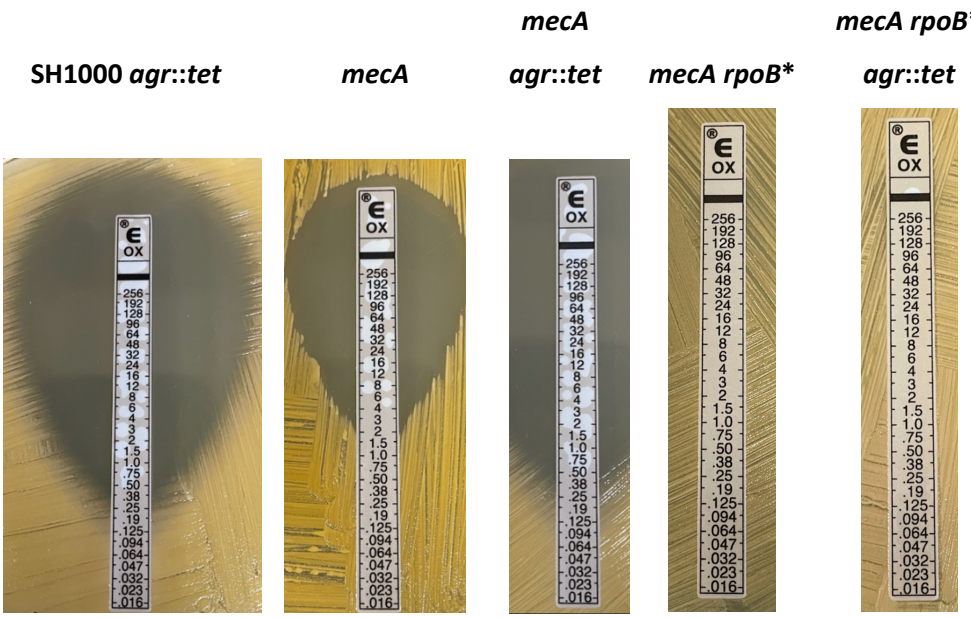

A

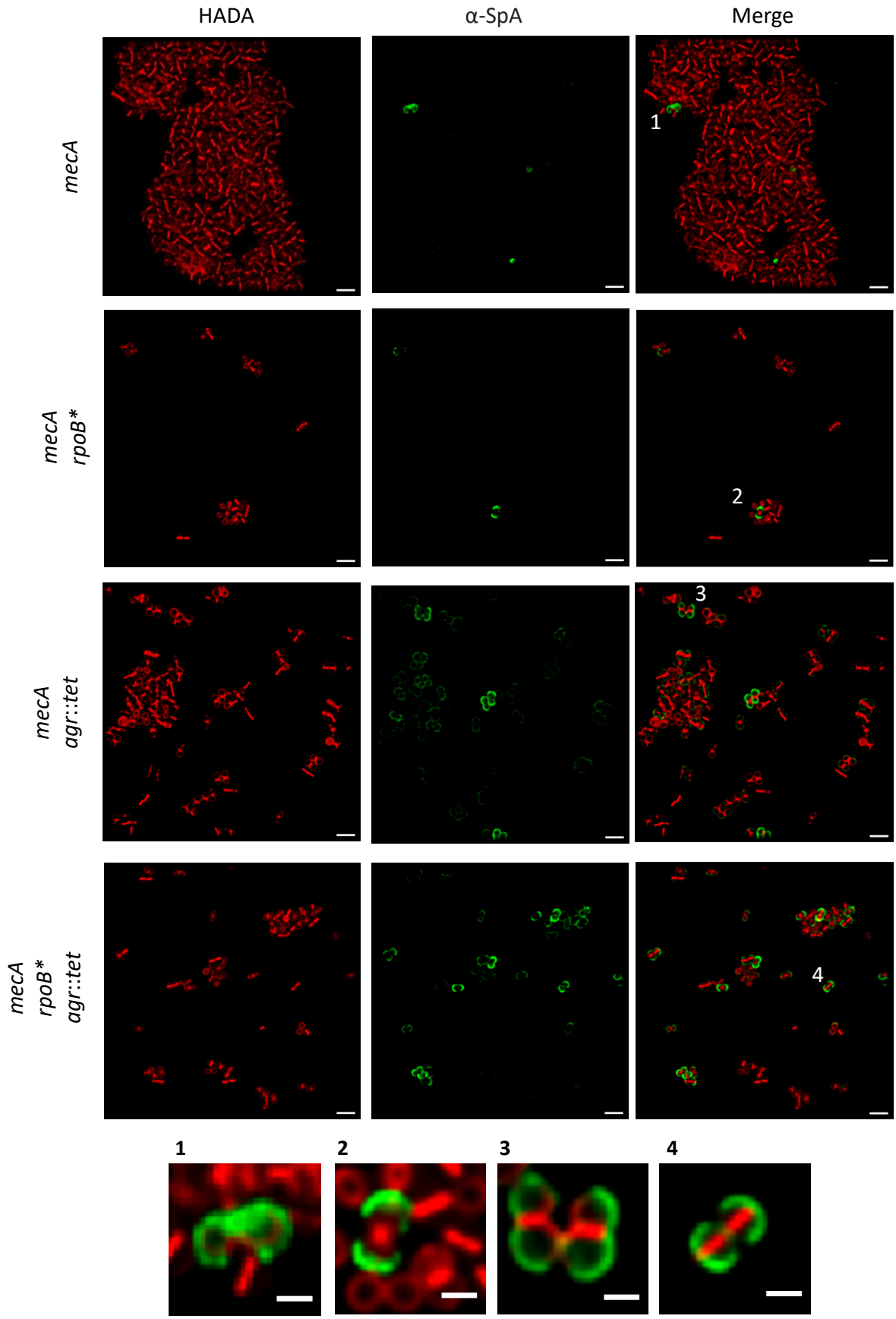
HADA
α-SpA
Merge
mecA
mecA rpoB*
mecA agr::tet
mecA rpoB* agr::tet
1
2
3
4
1
2
3
4

B

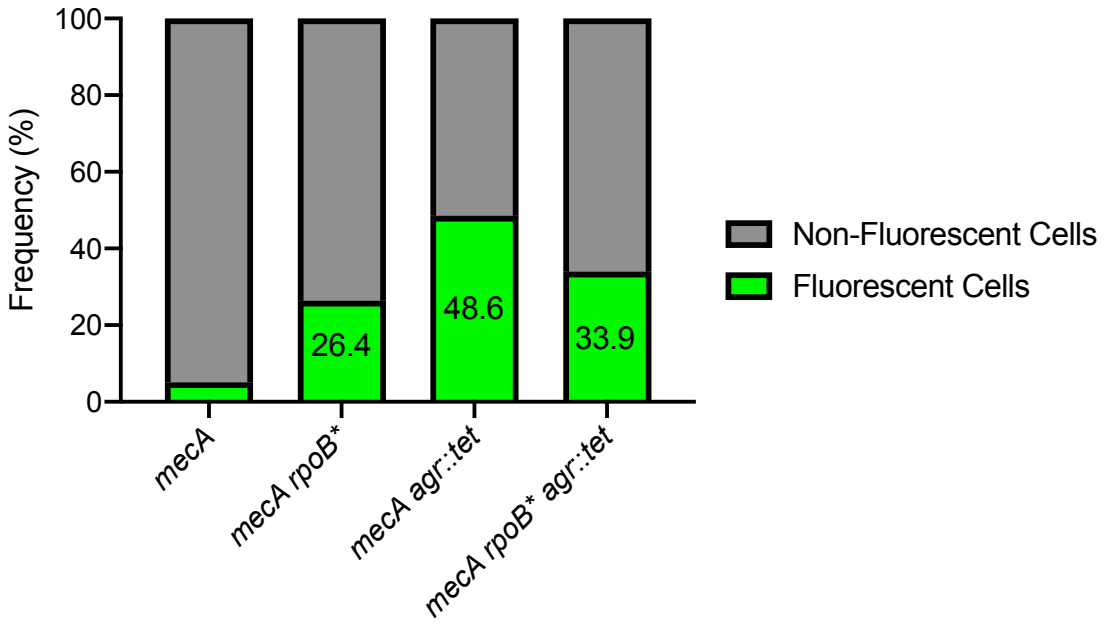

Figure 5.4. Analysis of SpA localisation in the MRSA background without methicillin by immunofluorescence microscopy

(A) HADA was used to visualise nascent peptidoglycan synthesis (red). SpA localisation in *S. aureus* SH1000 *mecA*, *mecA rpoB**, *mecA agr*::*tet*, and *mecA rpoB** *agr*::*tet* in the absence of methicillin. Inset numbers are enlarged below. Scale bars = 3 µm. Inset scale bars = 1 µm. **(B)** Percentage of *S. aureus* SH1000 *mecA* (5%; n=123), *mecA rpoB** (26%; n=108), *mecA agr*::*tet* (49%; n=144), and *mecA rpoB** *agr*::*tet* (34%; n=162) cells showing SpA localisation. Frequencies under 10% are not labelled. Samples shown are representative of three biological repeats.

Figure 5.4., panel A, shows the characteristic horseshoe pattern of SpA fluorescence in the *mecA* and *mecA rpoB** strains, both with and without functional Agr, as seen previously (Chapter 4). The expression of *mecA* and *mecA rpoB** in the absence of methicillin does not appear to alter SpA localisation from those observed previously (Chapter 4). These MRSA strains, like the MSSA SH1000 strains, show whole cell SpA immunolabelling of single cells, while dividing diplococcal cells display a horseshoe pattern of fluorescence. The heterogeneity of SpA display in these populations grown in the absence of methicillin also remains consistent, with *S. aureus mecA* demonstrating lower levels of SpA than the wild type control, where 23% of the SH1000 population display SpA on the surface, whereas only 5% of the SH1000 mecA population display SpA (Chapter 4, Figure 4.2.). The inactivation of Agr increases the percentage of cells displaying SpA in both MRSA strains, as expected, with 49% of the population of *mecA* displaying SpA with non-functional Agr, compared to its Agr-functional counterpart at 5%. Similarly, the percentage of the population of *mecA rpoB** displaying SpA increased from 26% to 34% (Figure 5.4.).

5.2.2. Effect of Methicillin Treatment on SpA Localisation in the MRSA Background

To investigate what affect the alteration of the cell wall architecture due to methicillin has on the localisation of SpA in the *mecA rpoB** and *mecA rpoB** *agr*::*tet* strains, subcultures were grown in the presence of 25 μg mL^{-1} methicillin for 2 hours at 37°C, 250 rpm. This concentration of methicillin was chosen in accordance with data acquired previously in the lab, wherein growing *mecA rpoB** in the presence of 25 μg mL^{-1} methicillin results in a lack of the concentric ring structure of nascent peptidoglycan seen in strains grown without methicillin (Section 5.1.3.; Figure 5.2.). Figure 5.5. shows α-SpA immunofluorescence of *S. aureus mecA rpoB** and *mecA rpoB** *agr*::*tet* treated with methicillin. Both strains display a horseshoe pattern of SpA fluorescence on diplococcal cell surfaces and whole cell labelling on single cells, though the percentage of the population with functional Agr displaying SpA is only 11%. This is slightly higher than *mecA* without methicillin (5%) but lower than the wild type SH100 strain (23%). An increase in the percentage of the bacterial population displaying surface protein A in the Agr deficient strain of *mecA rpoB** was observed as expected.

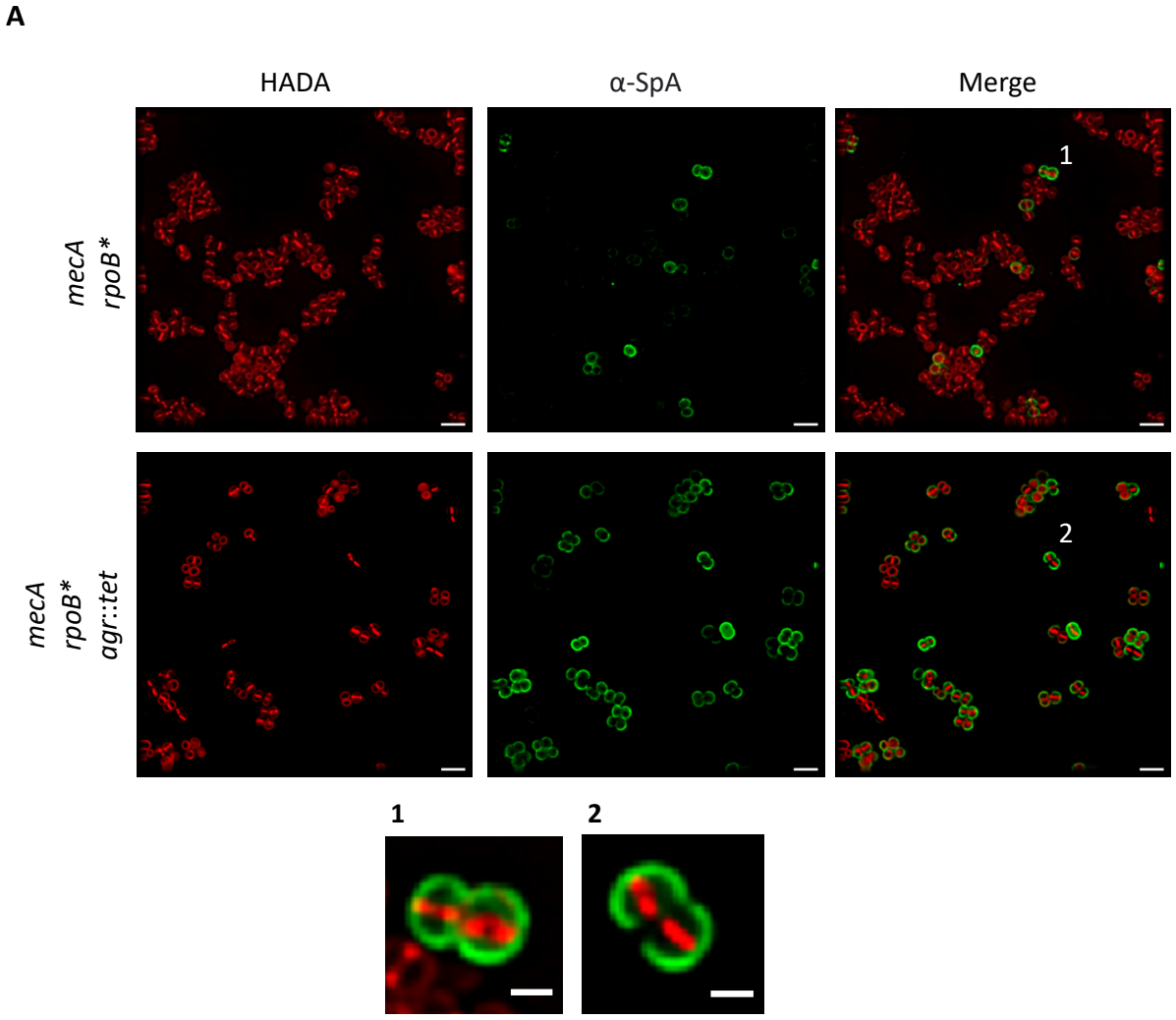
A
HADA
α-SpA
Merge
mecA rpoB*
mecA rpoB* agr::tet
1
2
1
2
B
Frequency (%)
100
80
60
40
20
0
10.7
54.6
mecA rpoB*
mecA rpoB* agr::tet
Non-Fluorescent Cells
Fluorescent Cells

Figure 5.5. SpA localisation in the MRSA background in the presence of methicillin

(A) HADA was used to visualise nascent peptidoglycan synthesis (red). SpA localisation in *S. aureus* SH1000 *mecA rpoB** and *mecA rpoB** *agr*::*tet* in the presence of 25 μg mL^{-1} methicillin. Inset numbers are enlarged below. Scale bars = 3 μm. Inset scale bars = 1 μm. **(B)** Percentage of *S. aureus* SH1000 *mecA rpoB** (11%; n=103) and *mecA rpoB** *agr*::*tet* (55%; n=108) cells showing SpA localisation. Samples shown are representative of three biological repeats.

To determine the role of SarA on the localisation of SpA in the MRSA background, *sarA*::*kan* was transduced into *S. aureus mecA* and *mecA rpoB**. Verification of the successful transduction of *sarA*::*kan* was achieved by PCR using *Kan* F and *sarA* R primers, growth on 50 μg mL^{-1} kanamycin, and α-SpA immunofluorescence microscopy (Figure 5.6.). The knockout of *sarA* is expected to increase the percentage of the *mecA rpoB** population displaying SpA on the cell surface as seen previously (Chapter 4, Figure 4.8.).

α-SpA immunofluorescence microscopy of the *sarA* mutant in the MRSA background demonstrates every cell in the population displaying SpA on the surface, albeit with varying intensity (Figure 5.7.). The display patterns observed in the MRSA *sarA*::*kan* strains are similar to *sarA*::*kan* strain in the SH1000 MSSA background, in that every cell appears to be displaying SpA, almost always around the whole cell, with few cells displaying the horseshoe pattern described previously. Attempts to grow these MRSA *sarA* mutant strains in the presence of 25 μg mL^{-1} methicillin, as shown in Figure 5.5. was unsuccessful. Subsequent oxacillin E-test diffusion revealed that, whilst the mutation of *sarA* increased the resistance of *S. aureus mecA* from 2 μg mL^{-1} to 4 μg mL^{-1}, it also reduced the resistance of *S. aureus mecA rpoB** from ≥256 μg mL^{-1} to 4 μg mL^{-1}. This made it impossible to assess the SpA localisation pattern in MRSA strains with non-functional SarA under the same conditions as explored previously (Figure 5.5.). As such, the role of SarA in MRSA on the localisation of SpA remains unknown, as does its apparent role in antibiotic resistance as an auxiliary gene.

A

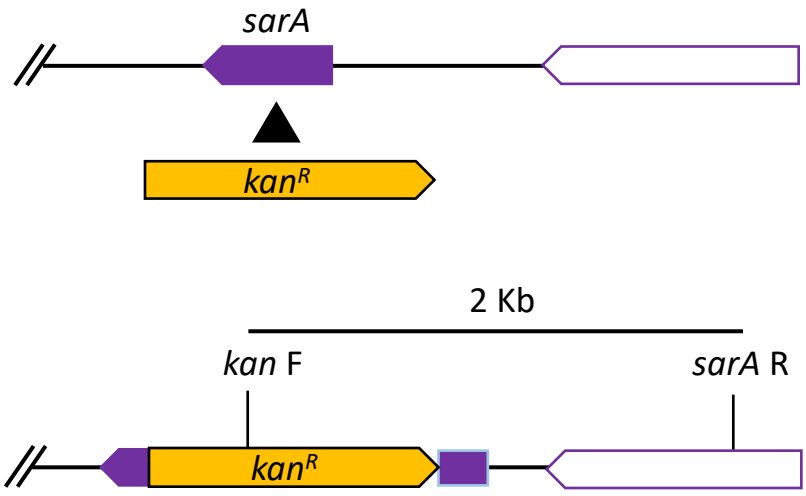

B

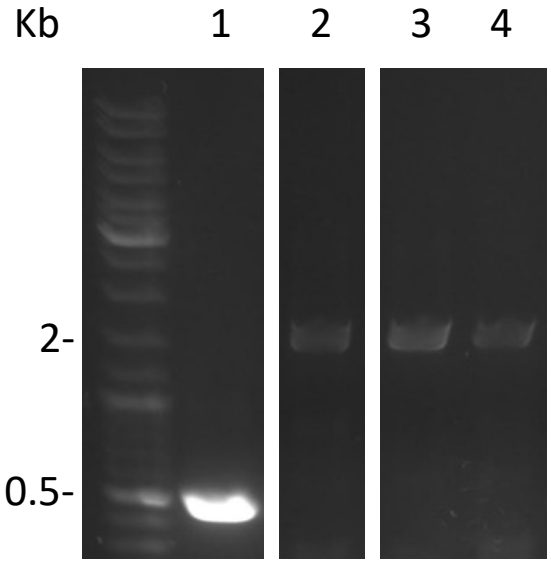

C

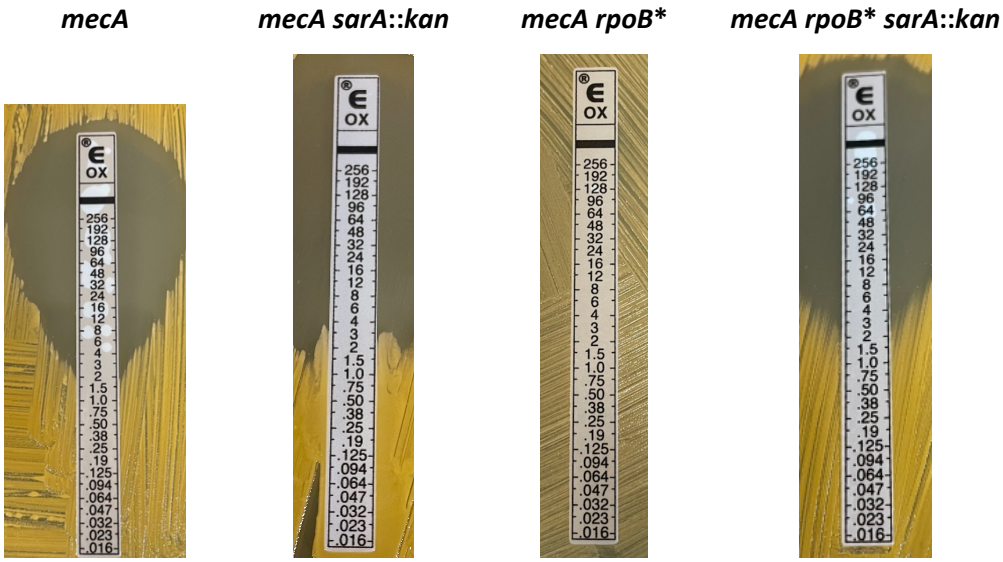

Figure 5.6. Construction of *sarA* mutant in the MRSA background

(A) Schematic representation of the insertion of *kan*^{R} antibiotic resistance cassette into chromosomal *sarA* (black triangle). **(B)** Agarose gel (2% w/v) electrophoresis of *sarA* knockout PCR verification. **(1)** Control band at 0.5 Kb is the amplification of the *sarA* in the SH1000 genome using *sarA* F (not shown) and *sarA* R (shown) primers. Expected PCR product size of 0.5 Kb is shown. **(2)** *S. aureus* SH1000 *sarA*::*kan* gDNA at 2 Kb shows interruption of *sarA*. **(3)** *S. aureus mecA sarA*::*kan* gDNA at 2 Kb shows interruption of *sarA*. **(4)** *S, aureus mecA rpoB* sarA*::*kan* gDNA at 2 Kb shows interruption of *sarA*. Markers are of sizes shown. **(C)** Oxacillin E-test strips showing change in antibiotic resistance as a result of *sarA* mutation in the MRSA background. The MIC of *mecA* increased from 2 µg mL^{-1} to 4 µg mL^{-1}, while the MIC of *mecA rpoB** decreased from ≥256 µg mL^{-1} to 4 µg mL^{-1}.

A

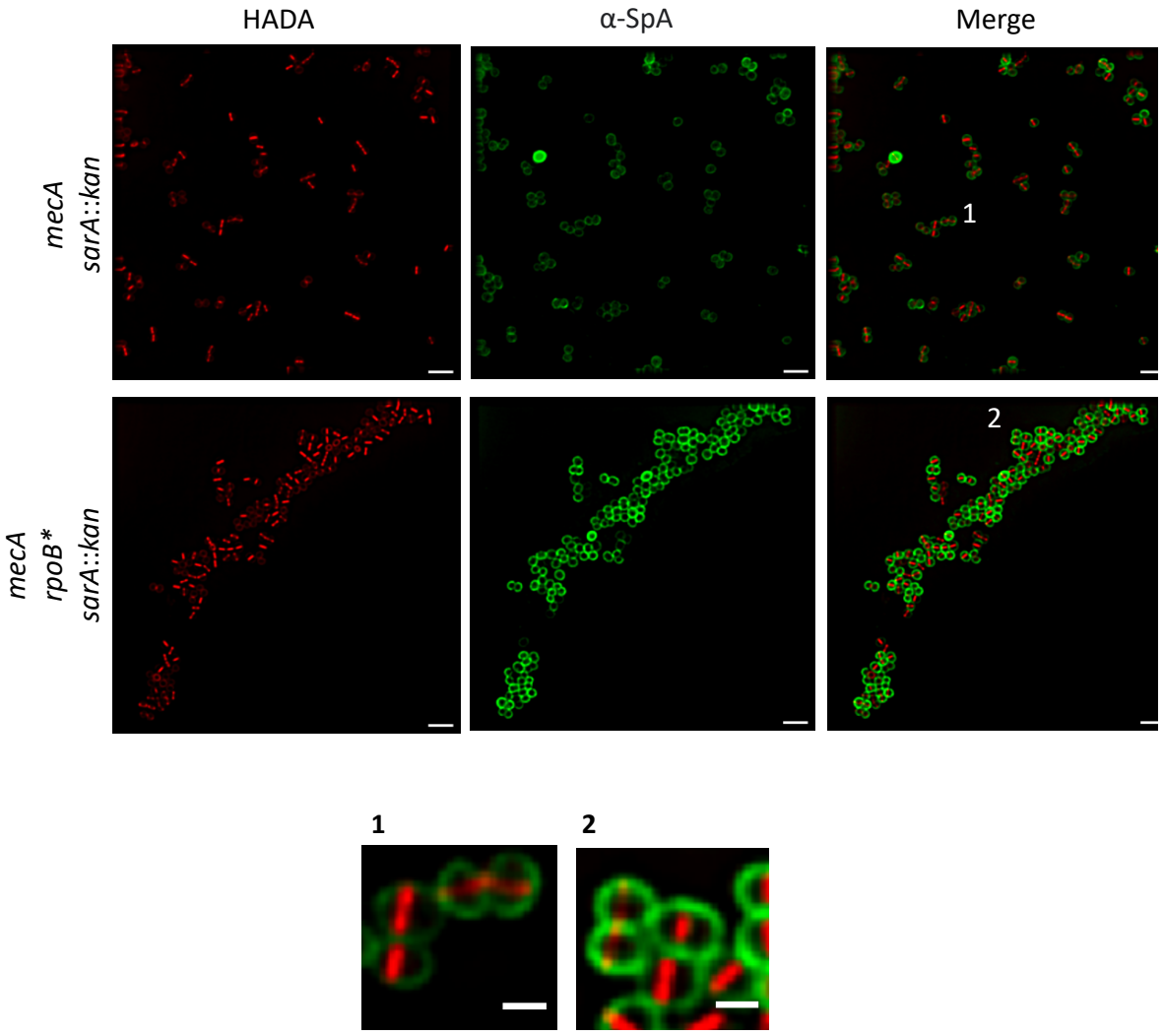
HADA
α-SpA
Merge
mecA sarA::kan
mecA rpoB* sarA::kan
1
2
1
2

B

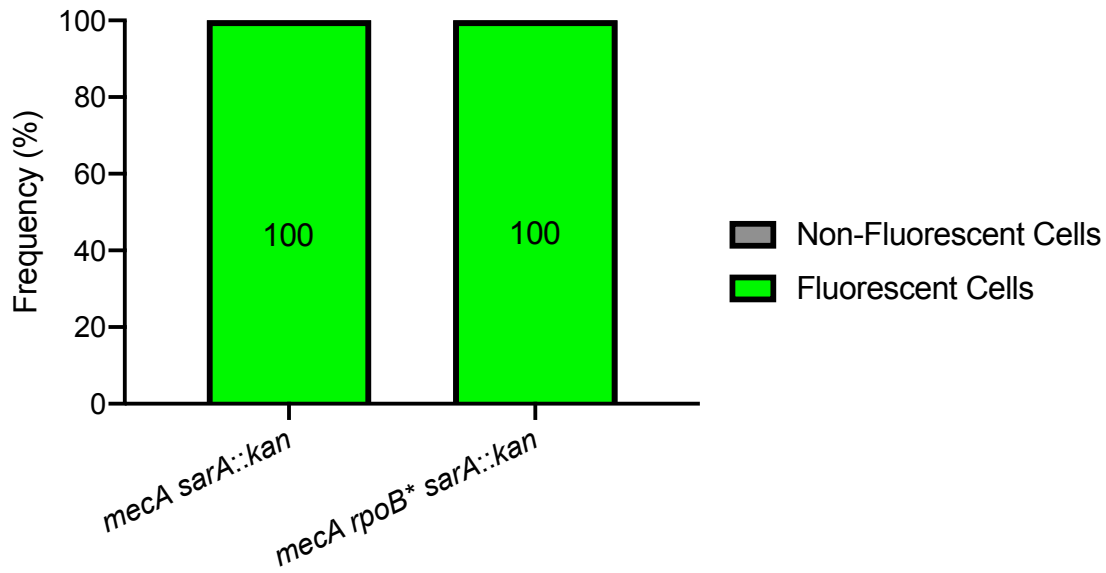
Frequency (%)
100
80
60
40
20
0
100
100
mecA sarA::kan
mecA rpoB* sarA::kan
Non-Fluorescent Cells
Fluorescent Cells

Figure 5.7. Effect of SarA on SpA localisation in the MRSA background without methicillin **(A)** HADA was used to visualise nascent peptidoglycan synthesis (red). SpA localisation in *S. aureus* SH1000 *mecA sarA*::*kan* and *mecA rpoB** *sarA*::*kan* in the absence of methicillin. Inset numbers are enlarged below. Scale bars = 3 µm. Inset scale bars = 1 µm. **(B)** Percentage of *S. aureus* SH1000 *mecA sarA*::*kan* (100%; n=128) and *mecA rpoB** *sarA*::*kan* (100%; n=157) cells showing SpA localisation. Samples shown are representative of three biological repeats.

5.3. Discussion

Immunofluorescence microscopy has been shown to be a reliable method for investigating the localisation of proteins, both in the literature, and in this work (DeDent *et al*, 2007; Yu *et al*, 2018). As a result of its reliability, immunofluorescence microscopy was used to investigate the display pattern and distribution of surface protein A in methicillin resistant *Staphylococcus aureus*, conferred by the exogenous *mecA* gene encoding PBP2a.

Additional screening of SpA localisation was done in a *mecA* strain which had also acquired an amino acid substitution in the *rpoB* gene, replacing the histidine at position 929 with a glutamine residue. This substitution conferred significant resistance to methicillin in the strain via an unknown mechanism (Panchal *et al*, 2020). This highly methicillin resistant strain has been used previously to investigate the architecture of the cell wall, via atomic force microscopy, of *S. aureus* grown in the presence of methicillin. While wild type SH1000 and subsequent mutant strains demonstrate a combination of dense mesh-like older cell wall material and a concentric ring-like structure of nascent peptidoglycan around developing septa, the cell wall of the *mecA rpoB** strain, when grown in 25 µg mL^{-1} methicillin, has no ring structure – only mesh. Figure 1.2. (Chapter 1) shows the localisation of these cell wall architectures, both surface exposed cell wall, and the membrane-facing cell wall – referred to as the internal sacculus. This new understanding of the cell wall of *S. aureus* raised some interesting questions that were addressed in this chapter. For example: how significant is the presence of this centric ring architecture in the display of surface proteins? Does a strain with no ring structure of peptidoglycan display surface proteins differently?

An attempt to address these questions was made using immunofluorescence microscopy on MRSA strains with and without methicillin to investigate the contribution of the ring-like architecture to surface protein display, using surface protein A as a model surface protein. Possessed of a YSIRK signal sequence motif, SpA is known to be translocated and subsequently displayed on the cell surface first at the developing septum (Carlsson *et al*, 2006; Chapter 4). SpA localisation in the SH1000 background of *S. aureus* in Chapter 4 has been shown to be displayed at the previously completed septum of diplococcal cells. As those cells continue to grow and divide, SpA becomes distributed over the whole cell prior to the next septation

event. The division of cells causes the appearance of a horseshoe like motif of SpA localisation, where the site of septation lacks surface exposed SpA at that time. As cells continue to develop septa in another plane of division, SpA becomes exposed at the previous site of division over time. Data in this chapter has shown that the localisation of SpA in MRSA strains of SH1000, conferred by exogenous *mecA* and the subsequent acquisition of $RpoB^{H929Q}$ does not appear to alter the localisation of SpA in the absence of methicillin. The addition of 25 µg mL^{-1} of methicillin to *mecA rpoB**, which is known to affect the architecture of the cell wall, does not alter the localisation of SpA. This implies that the ring structure of the cell wall at developing septa does not possess SpA, nor does the mesh-like architecture of peptidoglycan at the septum of *S. aureus mecA rpoB** in the presence of methicillin. Instead, these data suggest that the outermost cell wall of *S. aureus* at the septum acts as an additional layer, obfuscating SpA labelling by immunofluorescence, regardless of its architecture. Further, this implies that SpA incorporation into the cell wall may be associated with PBP2 activity, as PBP2 is responsible for synthesising the peptidoglycan layer closest to the bacterial membrane after the typical synthesis of ring structured peptidoglycan at the nascent cross wall (Wacnik *et al*, 2022). Treating MRSA strains with methicillin and trypsin could prove useful in testing this hypothesis, as a time course of SpA display could be observed using immunofluorescence microscopy, as shown previously, to elucidate the emergence of SpA over time (Chapter 4, Figure 4.10.; Figure 4.12.).

While the slight increase in susceptibility to oxacillin was unexpected when knocking out Agr in the *mecA* strain, the substantial increase in susceptibility of *mecA* and *mecA rpoB** with non-functional SarA was very surprising. The association and potential trade-off between virulence capacity and resistance to antibiotics has been discussed previously, which includes the global regulation of virulence factors by Agr and SarA (Mlynarczyk-Bonikowska *et al*, 2022; Bruce *et al*, 2022; Bilyk *et al*, 2022).

Recent work on the development of β-lactam resistance in *S. aureus* has shown that, while resistance to β-lactams is mediated by the acquisition of *mecA* encoding PBP2a, many genes that play no obvious role in the associated process of cell wall synthesis are required to maintain, and even improve upon, the bacterium's resistance to antibiotics. Genes that are required to maintain levels of resistance to β-lactams conferred by *mecA* are known as

auxiliary genes (*aux*). Other genes, known as potentiators (*pot*) undergo mutations which enable *S. aureus* to withstand much greater concentrations of β-lactam antibiotics (Bilyk *et al*, 2022). Of the genes investigated in this Chapter, as well as in Chapter 4, *sarA* is thought to be an *aux* gene (Li *et al*, 2016). Indeed, the loss of SarA in the high-level MRSA strains examined in this Chapter result in the sensitisation of *S. aureus* to oxacillin, dropping from an MIC of ≥256 μg mL^{-1} to 4 μg mL^{-1}, and thereby rendering the strain impossible to examine for SpA localisation in the presence of the requisite concentration of methicillin (25μg mL^{-1}) to abrogate the ring structure.

5.4. Main Findings in this Chapter

- SpA localisation in *mecA* mediated MRSA in the absence of methicillin is like that observed in the MSSA SH1000 background
- *mecA* MRSA strains grown in the presence of methicillin show the same SpA localisation as seen in SH1000 background
- The deletion of *agr* in the MRSA strain *mecA* sensitises the bacteria to oxacillin
- The interruption of *sarA* drastically sensitises *mecA rpoB** strains to oxacillin

Chapter 6

General Discussion

Staphylococcus aureus is an increasingly important human pathogen that places a huge burden on both global healthcare systems and agriculture (Kalayu *et al*, 2020). Carried on the skin of approximately one third of the population, *S. aureus* is particularly dangerous as a nosocomial pathogen, especially regarding individuals with ongoing disease progression as well as the immunocompromised (Sabbagh *et al*, 2019). *S. aureus* can cause a range of diseases, from cellulitis and impetigo to bacteraemia and toxic shock syndrome (Cheung *et al*, 2021). The ability of *S. aureus* to cause these diseases is in part attributed to its production and display of a variety of surface proteins. Surface exposed proteins enable *S. aureus* to interact with many molecules and to adhere to and colonise various mammalian hosts (Laux *et al*, 2019). One particularly important surface protein is Surface Protein A (SpA) which binds to the constant domain of mammalian immunoglobulins such as IgG and IgM (Kota *et al*, 2020). As such, the display of SpA on the surface of *S. aureus* allows the bacteria to evade opsonisation by mammalian antibodies. This in turn enables *S. aureus* to continue to colonise its host and persist as an agent of chronic infection (Schneewind *et al*, 2019).

As a result of its role in disease progression and conservation among global strains of *S. aureus*, SpA is a widely studied virulence factor. Much is known about its function, structure, and regulation, while its localisation on the surface of *S. aureus* remains poorly understood. However, studies have been performed to determine the localisation of SpA in *S. aureus* to understand more about where the protein is translocated, and how its display changes over time. DeDent *et al* (2007) used Alexa Fluor 647 conjugated antibodies to show the distribution of SpA in the RN4220 strain of *S. aureus*. Therein, they observe discrete foci of SpA display, and go on to propose a model by which SpA becomes distributed across the cell wall over time. Additionally, the use of trypsin to shave the surface proteins from the cells showed that SpA appears at distinct foci and that, over time, SpA can be observed across the whole cell. The group also state that the use of antibodies conjugated to FITC and Cy3 show a more uniform pattern of SpA localisation, and that the distinct patterns observed using Alexa Fluor 647 denote a higher level of detail and accuracy (Mazmanian *et al*, 2000; Schneewind *et al*, 1992). Conversely, Zhang *et al* (2021) show that SpA first becomes observable at the cross

wall of diplococcal cells in RN4220 following trypsin treatment. These experiments, while performed in the same strain used by DeDent *et al* (2007), use a chemically inducible plasmid version of SpA, such that its expression can be controlled. The immunofluorescence protocol used by Zhang also included SpA-specific antiserum, as well as Alexa Fluor 488 conjugated secondary antibodies, whereas DeDent *et al* (2007) used only fluorescent secondary antibodies. This might suggest that the data presented by Zhang *et al* (2021) provides a more accurate representation of SpA display under these conditions, as SpA-specific primary antisera ensures SpA-specific localisation. However, the use of chemically inducible SpA does not reflect wild type levels of expression, which may affect localisation. Additionally, the strain studied by both groups (RN4220) is already highly mutated, and is intended as an intermediary strain for genetic manipulation.

The original aim of this work was to improve upon what is currently known about SpA localisation using SNAP-tag biotechnology. SNAP is an enzyme that covalently binds to the benzyl group of benzylguanine derivative dyes, which can be expressed as a protein fusion via a short oligo link (Kolberg *et al*, 2013; Section 1.4.5.; Section 3.1.). Previous work in the lab has shown that SNAP is an effective tool for the localisation of intracellular proteins in *S. aureus* (Lund *et al*, 2018). However, after extensive troubleshooting – including growth conditions, labelling time, different substrates, substrate concentration, and temperature – SNAP could not reliably be used to localise SpA, despite confirming its expression as a fusion to SNAP in *S. aureus* (Chapter 3). It is possible that this lack of signal is due to a lack of SNAP sensitivity to benzylgunaine derivative dyes. To account for this, an *agr* mutation was transduced into SpA-SNAP to generate an increased percentage of the population displaying SpA-SNAP. However, this failed to elicit an increased signal within the population. Alternatively, the lack of SNAP-tag labelling may be due to the higher levels of oxygen and reactive oxygen species (ROS) which the surface of *S. aureus* – and therefore SpA-SNAP – are exposed to. The active site of SNAP contains a cysteine residue, which is known to readily react with oxygen and ROS (Veggiani & de Marco, 2011; Alcock *et al*, 2018; Kameya *et al*, 2019). This would also explain the discrepancy between the FtsZ-SNAP microscopy shown by Wacnik (2016) and this work, as FtsZ is an intracellular protein, and is therefore not exposed to ROS.

In an effort to replicate the data shown by DeDent *et al* (2007) and Zhang *et al* (2021), immunofluorescence microscopy was used to localise SpA in place of SNAP-tag. Both methodologies were tested using Alexa Fluor 488 conjugated secondary antibodies against wild type *S. aureus* SH1000 cells grown to mid-exponential phase. The only notable difference between these two methodologies tested in this work was that the combination of α-SpA primary and fluorescently conjugated secondary antibodies provided clearer localisation of SpA. In secondary-only samples, the pattern of fluorescence was less uniform (data not shown). So, to ensure the highest level of detail, a combination of SpA specific primary antibodies and fluorescent secondary antibodies were used. Additionally, even though no discernible difference was observed by strains producing Sbi – another antibody binding protein on the cell surface of *S. aureus* – immunofluorescence experiments were predominantly performed in an *sbi* mutant to ensure the most representative localisation of SpA as possible. Immunofluorescence microscopy was used to localise SpA in *S. aureus* and revealed three distinct localisation patterns. Firstly, SpA was localised over the entire surface of single cells. Then, cells undergoing septation demonstrated a horseshoe motif of SpA fluorescence. Lastly, diplococcal cells that had begun synthesising cross wall peptidoglycan in the next plane of division display SpA over the whole surface of both cells (Figure 4.3.). Interestingly only 20% of the wild type SH1000 population appear to display SpA on their cell surface under laboratory conditions (Figure 4.2.). This level of population heterogeneity was unexpected, especially as the samples in this work were all grown to exponential phase, wherein the negative regulation of SpA by Agr is alleviated (Gao & Stewart, 2004).

Surface protein A is considered a ubiquitous protein among *S. aureus* populations (Gao *et al*, 2004; Frankel *et al*, 2010; Hao *et al*, 2021). Because of this, SpA has been considered an ideal target for vaccine development which, to date, has only shown some success in mice models. However, this work has shown that as little as 7% to as much as 37% of clinically relevant *S. aureus* strains like COL and USA300, respectively, display SpA on the cell surface during exponential growth phase (Figure 4.5.). These findings suggests that SpA surface display may not be as common as previously thought. As part of the investigation to determine the cause of this heterogeneity of SpA display, a non-functional Agr mutant was generated by bacteriophage transduction, which proved to be a useful tool for the investigation of SpA localisation. In the Agr negative mutant, the frequency of the population displaying SpA on

the cell surface increased to 85% without introducing any new patterns of SpA localisation (Figure 4.8.). This suggests that the heterogeneity of SpA expression is largely controlled at the genetic level. Additionally, immunofluorescence microscopy of a non-functional SarA mutant showed that 100% of the *S. aureus* population display SpA on the cell surface. Though, in this mutant, the characteristic horseshoe pattern of fluorescence in dividing cells was all but abrogated. This is likely due to a substantial increase in expression such that the cell wall is saturated with SpA, though further investigation is required. Interestingly, a Sortase A (SrtA) mutant showed SpA localised to the cell surface as well (Figure 4.7.). This was surprising, as SrtA is known to incorporate SpA into the peptidoglycan cell wall by covalently binding the protein to Lipid II. Therefore, its abrogation was expected to result in no SpA on the bacterial cell surface in this strain. SpA possesses the LPXTG motif recognised by SrtA, but it also has a LsyM domain at its C-terminus. This domain has previously been theorised to facilitate the ionic binding of SpA into the cell wall (Buist *et al*, 2008). It was therefore hypothesised that this mechanism may be responsible for SpA display in the Δ*srtA* strain. To test this hypothesis, samples of this strain were boiled in 4% (v/v) SDS to strip ionically bound proteins from the cell surface, then subjected to SpA immunofluorescence microscopy. The result of this experiment showed that SDS treated *S. aureus* Δ*srtA* no longer displayed any SpA on the cell surface. Meanwhile, the SDS treatment of SH1000 wild type and *S. aureus agr*::*tet* showed a slight reduction in the percentage of the population displaying SpA: 17% and 82%, respectively (Figure 4.9.). This suggests that a minority of surface displayed SpA is ionically bound to the cell wall in these strains, presumably via the LysM domain.

Interestingly, mutant strains of *S. aureus* lacking functional genes involved in the synthesis and display of teichoic acids display little to no SpA at on the surface of *S. aureus* (Chapter 4, Figure 4.6.). The interplay between teichoic acid display and the spatial regulation of both cell wall cross linking and SpA display has been explored previously (Atilano *et al*, 2010; Yu *et al*, 2018). These data suggest that the co-ordination and regulation of cell wall synthesis, teichoic acid anchoring, and surface protein display are important and associated pathways that warrant further investigation.

To investigate the temporal evolution of SpA, a trypsin-based cell shaving protocol was adapted from the methodologies described by DeDent *et al* (2007) and Cheung *et al* (2021). Immediately following recovery from trypsin, *S. aureus* displays no SpA on the cell surface. The hour following trypsin recovery shows that SpA predominantly emerges at the previous division site of diplococcal cells. Then, the majority of SpA can be observed over the whole of cells displaying SpA, with a minority expressing the protein at the periphery of cells (Figure 4.10.). Due to the heterogeneity of *S. aureus* SpA expression in Agr functional strains, an Agr Sbi double mutant was generated to investigate this display pattern in a higher frequency (Figure 4.11.). Figure 4.12. shows that an Agr deficient *S. aureus* strain treated with trypsin displays SpA in the same pattern as seen with *S. aureus sbi*::*erm*, over the whole of single cells and as a horseshoe like pattern on the surface of a subset of dividing cells, albeit at a greater frequency. This suggests that SpA is initially translocated at the previous division site of diplococcal cells – or the active site of septation in single cells. To juxtapose the localisation of SpA with the bacterial cell cycle, *S. aureus agr*::*tet sbi*::*erm* was pulsed with TADA, treated with trypsin, chased with HADA, and assessed via immunofluorescence microscopy. Figure 4.13. shows that emerging SpA co-localises with the site of septation prior to trypsin treatment. A Western blot analysis of trypsin treated and non-trypsin treated cells shows that 22% of SpA remains in the cell wall of the Agr and Sbi deficient *S. aureus* strain following treatment with trypsin (Figure 4.14.). This implies that the co-localisation of SpA with the TADA fluorescent peptidoglycan, which was synthesised and incorporated prior to trypsin treatment, contains SpA that is inaccessible to trypsin. Therefore, SpA seen predominantly at the previous division site following trypsin treatment is already present in the cell wall at the time of treatment and is simply inaccessible to trypsin due to the extra layer of peptidoglycan, such as the ring structure mentioned previously and in Figure 6.1. However, when the findings of Cheung *et al*, 2021, are considered, wherein plasmid-borne, inducible SpA was localised at the septum in a SpA deletion strain, it's likely that SpA is predominantly translocated and subsequently displayed at the cross wall of dividing cells. As such, the current hypothesis is that the presence of an additional layer of peptidoglycan at the developing bacterial septum, regardless of its architecture, obscures SpA localisation by immunolabelling and, subsequently, its surface function immediately following septation (Figure 6.1.). This hypothesis is supported by the findings represented in Figures 5.4. and 5.5., where growing methicillin resistant *S. aureus* in the presence of methicillin to abrogate the ring structure of

peptidoglycan (Pasquina-Lemonche *et al*, 2020) did not alter the localisation of SpA. If the ring structure was simply too dense to immunolabel SpA, growing MRSA with methicillin should have enabled the localisation of SpA at the developing septum. However, no SpA was observed at the developing septum or the previous division site of cells. Therefore, the lack of SpA at this site of division in *S. aureus* is likely due to the presence of the ring-like architecture of peptidoglycan, which has recently been shown to require hydrolysis for the display of SpA (Leonard *et al*, 2023).

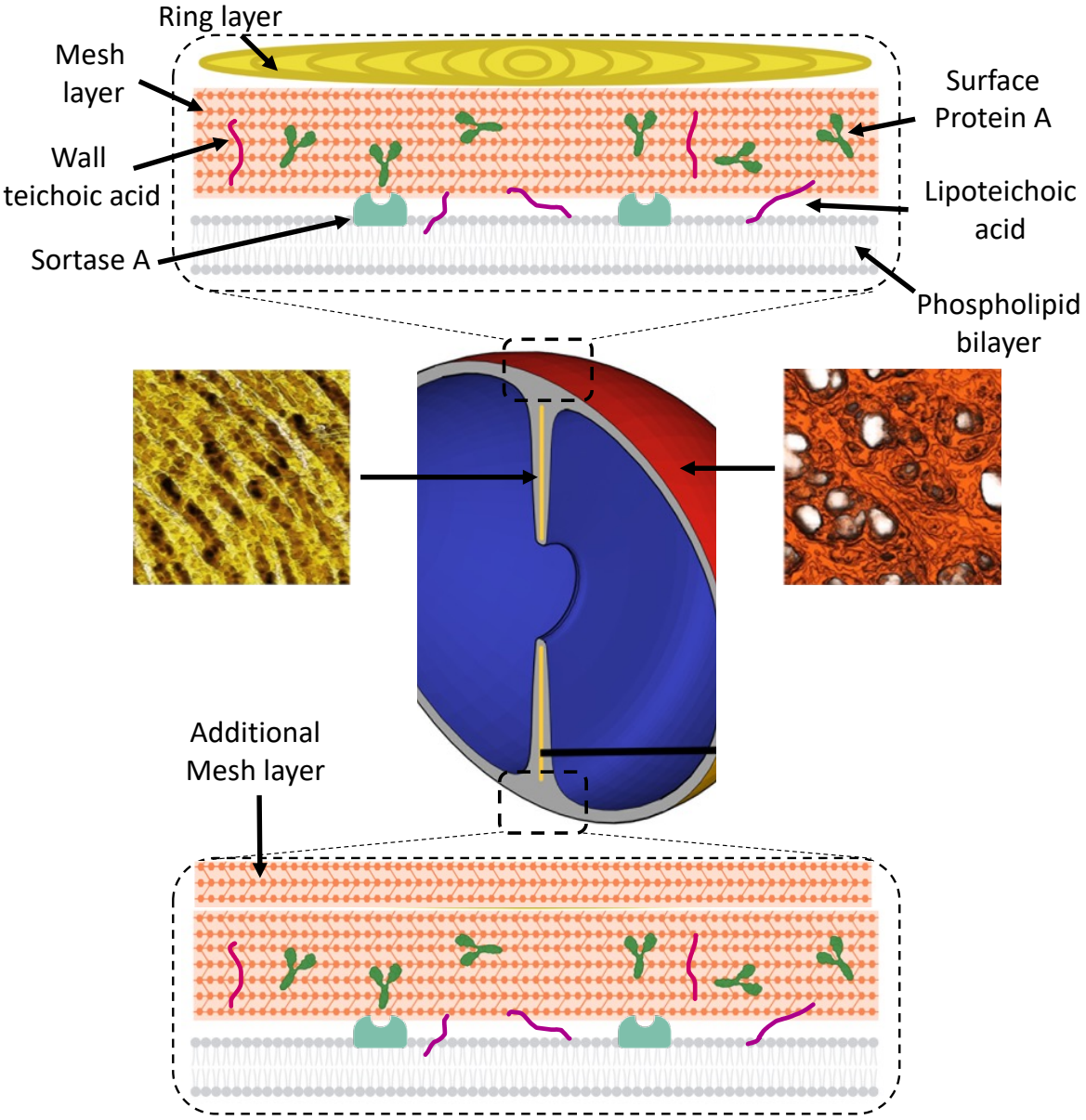

Figure 6.1. Model of peptidoglycan layers of the *S. aureus* cell wall and SpA display

(Top) As *S. aureus* builds a division septum, peptidoglycan is incorporated by PBP1 and arranged in a concentric ring like architecture (yellow) at the leading edge. Upon cell division, the ring structure becomes the outer most layer of the cell wall, and contains no SpA. Closer to the membrane where Sortase A is anchored (pale green), the mesh-like architecture of peptidoglycan (red) is more dense and contains SpA (green) as well as wall teichoic acid. Lipoteichoic acid is found in the exoplasm (purple). Immediately following cell division, SpA is inaccessable to antibodies, and therefore cannot be observed by immunofluorescence microscopy, nor function as an antibody binding protein. Over time,

the ring structure is matured, presumably by cell wall hydrolases as part of the natural cell cycle, making it more porous and thereby rendering the underlying SpA accessable. **(Bottom)** In the presence of methicillin, MRSA does not produce the concentric ring architecture of peptidoglycan as PBP1 is inhibited. Instead, PSP2a synthesises a mesh architecture in place of the rings, which continues to act as an additional layer of cell wall material that also lacks SpA.

The advent and subsequent proliferation of antibiotic resistance has had a devastating effect on global healthcare systems. As a result of the widespread use and misuse of antibiotics, many pathogenic microbes can persist in the presence of a range of frontline medical treatments (Foster, 2019). Methicillin resistant *Staphylococcus aureus* (MRSA) is one such example. The capacity of *S. aureus* to resist most β-lactam antibiotics is largely attributed to the possession of the *mecA* gene found within the staphylococcal cassette chromosome (SCCmec) (Liu *et al*, 2016). The *mecA* gene encodes a penicillin resistant PBP, dubbed PBP2a (Lim *et al*, 2002). The relationship between antibiotic resistance and virulence among pathogenic microbes has long since been a topic of discussion (Björkman & Andersson, 2000; Schroeder *et al*, 2017; Pan *et al*, 2020). The effect of methicillin resistance in *S. aureus* on SpA localisation and display was therefore of interest. As such, SpA localisation was assessed in MRSA (*S. aureus mecA*) and high-level MRSA (*S. aureus mecA rpoB**).

Only 5% of the population of *S. aureus mecA* was found to display SpA in the absence of methicillin, while 26% of the *mecA rpoB** strain display SpA on their cell surface under the same conditions. It's thought that the lack of SpA display in the *mecA* strain may be due to the upregulation of genes involved in anaerobic growth (Panchal *et al*, 2020). Similarly, the increased frequency of SpA display in the *mecA rpoB** strain is attributed to the correction of this dysregulation by RpoB* activity. The removal of the *agr* locus in these strains increases the frequency of the population displaying SpA as expected. However, the lack of Agr appears to sensitise the *mecA* strain to oxacillin (Table 5.1.). In the presence of 25 μg mL^{-1} methicillin, the percentage of the *mecA rpoB** population displaying SpA reduces from 26% to 10%, which the same strain without its *agr* locus shows 54% of the population displaying SpA (Figure 5.5). Despite the known association between the virulence capacities of bacteria and their ability to resist antibiotics, the *mecA rpoB** *agr*::*tet* strain shows no increased sensitivity to oxacillin. However, the strain is resistant to ≥256 μg mL^{-1} so any changes to sensitivity above that concentration cannot be observed using E-strip tests. Interestingly, while the persistence of bacteria in the presence of antibiotics is a concern to global healthcare systems, the reduction in the rate of SpA display on the surface of the population could potentially contribute to some attenuation of virulence capabilities under such conditions.

6.1. Future Perspectives

This work has elucidated the surface display of the key virulence factor Surface Protein A (SpA) in a well-studied, model lab strain of *Staphylococcus aureus*. The results herein have been used to develop a model for the development of SpA surface display within the context of cell wall dynamics during the cell cycle (Figure 6.1.). However, the observation of strain-dependent variation among *S. aureus* suggests that no one model in a single strain will be applicable to others, necessarily.

The heterogeneity of SpA expression in the bacterial populations studied was unexpected and made the elucidation of SpA display in more clinically relevant strains difficult. Attempts to generate *agr* mutant variants of clinically relevant strains, such as COL, Newman, and NewHG, to counter the lack of SpA display in these strains failed. However, the successful genetic manipulation of these strains – either by *agr* mutation or by the introduction of plasmid-borne SpA – could provide important detail regarding SpA display in more clinically relevant *S. aureus*, and could further elucidate the strain-dependent variation observed herein.

While the genes involved in the regulation of SpA expression are well known, such as *agr* and *sarA*, little is known about the transcriptional and translational regulation of SpA beyond the binding of antisense RNAIII (Zhu *et al*, 2019). Further investigation into factors involved in transcriptional and translational regulation of SpA expression may elucidate the cellular heterogeneity of SpA display in these bacterial populations. This may also explain the dramatic increase in population expression of SpA in the SarA mutant strain.

Although the investigation of SpA display in high level MRSA in the presence of methicillin showed no altered patterns – implying that the architecture of the outermost layer of peptidoglycan does not contribute to the lack SpA at the site of septation – it would be interesting to examine the emerging pattern of SpA display in a trypsin treated MRSA strain. This could provide more information regarding the role of the architecture of peptidoglycan at the septum. Specifically whether the arrangement of the peptidoglycan contributes to SpA display (or lack thereof at that site), or whether simply the possession of an “outer” layer of

peptidoglycan obscures cell wall associated SpA within the layer of peptidoglycan closer to the bacterial membrane. Also, the use of an exogenous peptidoglycan hydrolase could be used to strip off the septal ring / mesh architecture to determine if the underlying cell wall material contains SpA.

Lastly, the use of gold-conjugated antibodies to localise SpA at a nanometre scale using AFM may provide valuable insight into the dynamic display of protein A on the bacterial cell wall. As SpA appears to be primarily translocated to the surface at the developing septum, elucidating the precise organisation of these proteins could also reveal interesting information regarding the localisation of sortase A.

My work has revealed many new details as to the display of SpA across both varied populations and individual cells. Combining molecular analysis across those components that constitute the *S. aureus* cell wall will reveal where on the cell surface this key virulance protein is able to interact with its host, where it is able to cause such potentially devastating diseases.

References

Agard, D. A., Hiraoka, Y., Shaw, P., & Sedat, J. W. (1989). Fluorescence microscopy in three dimensions. *Methods in cell biology*, *30*, 353-377.

Aiba, Y., Katayama, Y., Hishinuma, T., Murakami-Kuroda, H., Cui, L., & Hiramatsu, K. (2013). Mutation of RNA polymerase β-subunit gene promotes heterogeneous-to-homogeneous conversion of β-lactam resistance in methicillin-resistant *Staphylococcus aureus*. *Antimicrobial agents and chemotherapy*, *57*(10), 4861-4871.

Ajayi, C., Åberg, E., Askarian, F., Sollid, J. U., Johannessen, M., & Hanssen, A. M. (2018). Genetic variability in the sdrD gene in *Staphylococcus aureus* from healthy nasal carriers. *BMC microbiology*, *18*, 1-13.

Alcock, L. J., Perkins, M. V., & Chalker, J. M. (2018). Chemical methods for mapping cysteine oxidation. *Chemical Society Reviews*, *47*(1), 231-268.

Archer, G. L. (1998). *Staphylococcus aureus*: a well-armed pathogen. *Reviews of Infectious Diseases*, *26*(5), 1179-1181.

Archer, G. L., & Bosilevac, J. M. (2001). Signaling antibiotic resistance in staphylococci. *Science*, *291*(5510), 1915-1916.

Asadollahi, P., Farahani, N. N., Mirzaii, M., Khoramrooz, S. S., Van Belkum, A., Asadollahi, K., & Darban-Sarokhalil, D. (2018). Distribution of the most prevalent SpA types among clinical isolates of methicillin-resistant and-susceptible *Staphylococcus aureus* around the world: a review. *Frontiers in microbiology*, *9*, 163.

Assadullah, S., Kakru, D. K., Thoker, M. A., Bhat, F. A., Hussain, N., & Shah, A. (2003). Emergence of low-level vancomycin resistance in MRSA. *Indian journal of medical microbiology*, *21*(3), 196-198.

Atilano, M. L., Pereira, P. M., Yates, J., Reed, P., Veiga, H., Pinho, M. G., & Filipe, S. R. (2010). Teichoic acids are temporal and spatial regulators of peptidoglycan cross-linking in *Staphylococcus aureus*. *Proceedings of the National Academy of Sciences*, *107*(44), 18991-18996.

Ba, X., Kalmar, L., Hadjirin, N. F., Kerschner, H., Apfalter, P., Morgan, F. J., & Holmes, M. A. (2019). Truncation of GdpP mediates β-lactam resistance in clinical isolates of *Staphylococcus aureus*. *Journal of Antimicrobial Chemotherapy*, *74*(5), 1182-1191.

Bae, T., & Schneewind, O. (2003). The YSIRK-G/S motif of staphylococcal protein A and its role in efficiency of signal peptide processing. *Journal of bacteriology*, *185*(9), 2910-2919.

Bae, T., Baba, T., Hiramatsu, K., & Schneewind, O. (2006). Prophages of *Staphylococcus aureus* Newman and their contribution to virulence. *Molecular microbiology*, *62*(4), 1035-1047.

Bai, Q., Ma, J., Zhang, Z., Zhong, X., Pan, Z., Zhu, Y., & Yao, H. (2020). YSIRK-G/S-directed translocation is required for Streptococcus suis to deliver diverse cell wall anchoring effectors contributing to bacterial pathogenicity. *Virulence*, *11*(1), 1539-1556.

Bal, A. M., Coombs, G. W., Holden, M. T. G., Lindsay, J. A., Nimmo, G. R., Tattevin, P., & Skov, R. L. (2016). Genomic insights into the emergence and spread of international clones of healthcare-, community-and livestock-associated methicillin-resistant *Staphylococcus aureus*: blurring of the traditional definitions. *Journal of Global Antimicrobial Resistance*, *6*, 95-101.

Balachandran, M., Bemis, D. A., & Kania, S. A. (2018). Expression and function of protein A in Staphylococcus pseudintermedius. Virulence, 9(1), 390-401.

Barbu, E. M., Mackenzie, C., Foster, T. J., & Höök, M. (2014). SdrC induces staphylococcal biofilm formation through a homophilic interaction. *Molecular microbiology*, *94*(1), 172-185.

Barbuti, M. D., Myrbråten, I. S., Morales Angeles, D., & Kjos, M. (2023). The cell cycle of *Staphylococcus aureus*: An updated review. *MicrobiologyOpen*, *12*(1), e1338.

Bartlett, A. H., & Hulten, K. G. (2010). *Staphylococcus aureus* pathogenesis: secretion systems, adhesins, and invasins. *The Pediatric infectious disease journal*, *29*(9), 860-861.

Bates, C. S., Montanez, G. E., Woods, C. R., Vincent, R. M., & Eichenbaum, Z. (2003). Identification and characterization of a Streptococcus pyogenes operon involved in binding of hemoproteins and acquisition of iron. *Infection and immunity*, 71(3), 1042-1055.

Becker, S., Frankel, M. B., Schneewind, O., & Missiakas, D. (2014). Release of protein A from the cell wall of *Staphylococcus aureus*. Proceedings of the National Academy of Sciences, 111(4), 1574-1579.

Beeby, M., Gumbart, J. C., Roux, B. & Jensen, G. J., (2013). Architecture and assembly of the Gram-positive cell wall. Mol. *Microbiol*. 88, 664-672.

Benson, M. A., Lilo, S., Wasserman, G. A., Thoendel, M., Smith, A., Horswill, A. R., & Torres, V. J. (2011). *Staphylococcus aureus* regulates the expression and production of the staphylococcal superantigen-like secreted proteins in a Rot-dependent manner. *Molecular microbiology*, *81*(3), 659-675.

Berscheid, A., Sass, P., Weber-Lassalle, K., Cheung, A. L., & Bierbaum, G. (2012). Revisiting the genomes of the *Staphylococcus aureus* strains NCTC 8325 and RN4220. *International Journal of Medical Microbiology*, *302*(2), 84-87.

Bien, J., Sokolova, O., & Bozko, P. (2011). Characterization of virulence factors of *Staphylococcus aureus*: novel function of known virulence factors that are implicated in activation of airway epithelial proinflammatory response. *Journal of pathogens*, *2011*.

Bierne, H., Garandeau, C., Pucciarelli, M. G., Sabet, C., Newton, S., Garcia-del Portillo, F., & Charbit, A. (2004). Sortase B, a new class of sortase in Listeria monocytogenes. *Journal of bacteriology*, *186*(7), 1972-1982.

Björkman, J., & Andersson, D. I. (2000). The cost of antibiotic resistance from a bacterial perspective. *Drug Resistance Updates*, *3*(4), 237-245.

Boles, B. R., & Horswill, A. R. (2008). Agr-mediated dispersal of *Staphylococcus aureus* biofilms. *PLoS pathogens*, *4*(4), e1000052.

Boles, B. R., Thoendel, M., Roth, A. J., & Horswill, A. R. (2010). Identification of genes involved in polysaccharide-independent *Staphylococcus aureus* biofilm formation. *PloS one*, *5*(4), e10146.

Borek, F. (1961). The fluorescent antibody method in medical and biological research. *Bulletin of the World Health Organization*, *24*(2), 249.

Bottomley, A. L., Kabli, A. F., Hurd, A. F., Turner, R. D., Garcia-Lara, J., & Foster, S. J. (2014). S taphylococcus aureus DivIB is a peptidoglycan-binding protein that is required for a morphological checkpoint in cell division. *Molecular Microbiology*, *94*(5), 1041-1064.

Bottomley, A. L., Liew, A. T., Kusuma, K. D., Peterson, E., Seidel, L., Foster, S. J., & Harry, E. J. (2017). Coordination of chromosome segregation and cell division in *Staphylococcus aureus*. *Frontiers in microbiology*, *8*, 1575.

Briggs, M. S., & Gierasch, L. M. (1986). Molecular mechanisms of protein secretion: the role of the signal sequence. In *Advances in protein chemistry* (Vol. 38, pp. 109-180). Academic Press.

Brown, S., Zhang, Y. H., & Walker, S. (2008). A revised pathway proposed for *Staphylococcus aureus* wall teichoic acid biosynthesis based on in vitro reconstitution of the intracellular steps. *Chemistry & biology*, *15*(1), 12-21.

Bruce, S. A., Smith, J. T., Mydosh, J. L., Ball, J., Needle, D. B., Gibson, R., & Andam, C. P. (2022). Shared antibiotic resistance and virulence genes in *Staphylococcus aureus* from diverse animal hosts. *Scientific Reports*, *12*(1), 1-11.

Buist, G., Steen, A., Kok, J., & Kuipers, O. P. (2008). LysM, a widely distributed protein motif for binding to (peptido) glycans. *Molecular microbiology*, *68*(4), 838-847.

Butaye, P., Argudín, M. A., & Smith, T. C. (2016). Livestock-associated MRSA and its current evolution. *Current Clinical Microbiology Reports*, *3*(1), 19-31.

Cabantous, S., Terwilliger, T. C., & Waldo, G. S. (2005). Protein tagging and detection with engineered self-assembling fragments of green fluorescent protein. *Nature biotechnology*, *23*(1), 102-107.

Cadieux, B., Vijayakumaran, V., Bernards, M. A., McGavin, M. J., & Heinrichs, D. E. (2014). Role of lipase from community-associated methicillin-resistant *Staphylococcus aureus* strain USA300 in hydrolyzing triglycerides into growth-inhibitory free fatty acids. *Journal of bacteriology*, *196*(23), 4044-4056.

Cameron, D. R., Howden, B. P., & Peleg, A. Y. (2011). The interface between antibiotic resistance and virulence in *Staphylococcus aureus* and its impact upon clinical outcomes. *Clinical Infectious Diseases*, *53*(6), 576-582.

Canovas, J., Baldry, M., Bojer, M. S., Andersen, P. S., Gless, B. H., Grzeskowiak, P. K., & Ingmer, H. (2016). Cross-talk between *Staphylococcus aureus* and other staphylococcal species via the agr quorum sensing system. Frontiers in microbiology, 7, 1733.

Carlsson, F., Stålhammar-Carlemalm, M., Flärdh, K., Sandin, C., Carlemalm, E., & Lindahl, G. (2006). Signal sequence directs localized secretion of bacterial surface proteins. Nature, 442(7105), 943-946.

Cassat, J. E., Hammer, N. D., Campbell, J. P., Benson, M. A., Perrien, D. S., Mrak, L. N., & Skaar, E. P. (2013). A secreted bacterial protease tailors the *Staphylococcus aureus* virulence repertoire to modulate bone remodeling during osteomyelitis. *Cell host & microbe*, *13*(6), 759-772.

Chan, P. F., & Foster, S. J. (1998). Role of SarA in virulence determinant production and environmental signal transduction in *Staphylococcus aureus*. *Journal of bacteriology*, *180*(23), 6232-6241.

Chan, Y. G., Frankel, M. B., Dengler, V., Schneewind, O., & Missiakas, D. (2013). *Staphylococcus aureus* mutants lacking the LytR-CpsA-Psr family of enzymes release cell wall teichoic acids into the extracellular medium. *Journal of bacteriology*, *195*(20), 4650-4659.

Chavakis, T., Wiechmann, K., Preissner, K. T., & Herrmann, M. (2005). *Staphylococcus aureus* interactions with the endothelium. *Thrombosis and haemostasis*, *94*(08), 278-285.

Chen, J., DU, X., Song, Y., Ruan, F., Lü, Y., & LI, M. (2012). The novel surface-anchored protein SasX promotes aggregation and colonization of *Staphylococcus aureus*. *Chinese Journal of Microbiology and Immunology, 519-524.*

Cheng, A. G., Kim, H. K., Burts, M. L., Krausz, T., Schneewind, O., & Missiakas, D. M. (2009). Genetic requirements for *Staphylococcus aureus* abscess formation and persistence in host tissues. *The FASEB Journal*, *23*(10), 3393.

Cheung, A. L., Nishina, K. A., Trotonda, M. P., & Tamber, S. (2008). The SarA protein family of *Staphylococcus aureus*. The international journal of biochemistry & cell biology, 40(3), 355-361.

Cheung, G. Y., Bae, J. S., & Otto, M. (2021). Pathogenicity and virulence of *Staphylococcus aureus*. *Virulence*, *12*(1), 547-569.

Chongtrakool, P., Ito, T., Ma, X. X., Kondo, Y., Trakulsomboon, S., Tiensasitorn, C., & Hiramatsu, K. (2006). Staphylococcal cassette chromosome mec (SCC mec) typing of methicillin-resistant *Staphylococcus aureus* strains isolated in 11 Asian countries: a proposal for a new nomenclature for SCC mec elements. *Antimicrobial agents and chemotherapy*, *50*(3), 1001-1012.

Clancy, K. W., Melvin, J. A., & McCafferty, D. G. (2010). Sortase transpeptidases: insights into mechanism, substrate specificity, and inhibition. *Peptide Science*, *94*(4), 385-396.

Clarke, S. R., Harris, L. G., Richards, R. G., & Foster, S. J. (2002). Analysis of Ebh, a 1.1-megadalton cell wall-associated fibronectin-binding protein of *Staphylococcus aureus*. *Infection and immunity*, *70*(12), 6680-6687.

Clarke, S. R., Wiltshire, M. D., & Foster, S. J. (2004). IsdA of *Staphylococcus aureus* is a broad spectrum, iron-regulated adhesin. Molecular microbiology, 51(5), 1509-1519.

Clauditz, A., Resch, A., Wieland, K. P., Peschel, A., & Götz, F. (2006). Staphyloxanthin plays a role in the fitness of *Staphylococcus aureus* and its ability to cope with oxidative stress. *Infection and immunity*, *74*(8), 4950-4953.

Codron, P., Letournel, F., Marty, S., Renaud, L., Bodin, A., Duchesne, M., & Chevrollier, A. (2021). STochastic Optical Reconstruction Microscopy (STORM) reveals the nanoscale organization of pathological aggregates in human brain. *Neuropathology and Applied Neurobiology*, *47*(1), 127-142.

Cole, N. B. (2013). Site-Specific Protein Labeling with SNAP-Tags. Current protocols in protein science, 73(1), 30-1.

Corrigan, R. M., Abbott, J. C., Burhenne, H., Kaever, V., & Gründling, A. (2011). c-di-AMP is a new second messenger in *Staphylococcus aureus* with a role in controlling cell size and envelope stress. *PLoS pathogens*, *7*(9), e1002217.

Corrigan, R. M., Rigby, D., Handley, P., & Foster, T. J. (2007). The role of *Staphylococcus aureus* surface protein SasG in adherence and biofilm formation. *Microbiology*, *153*(8), 2435-2446.

Cosgrove, S. E., Sakoulas, G., Perencevich, E. N., Schwaber, M. J., Karchmer, A. W., & Carmeli, Y. (2003). Comparison of mortality associated with methicillin-resistant and methicillin-susceptible *Staphylococcus aureus* bacteremia: a meta-analysis. *Clinical infectious diseases*, *36*(1), 53-59.

Courcol, R. J., Trivier, D., Bissinger, M. C., Martin, G. R., & Brown, M. R. (1997). Siderophore production by *Staphylococcus aureus* and identification of iron-regulated proteins. Infection and immunity, 65(5), 1944-1948.

Craft, K. M., Nguyen, J. M., Berg, L. J., & Townsend, S. D. (2019). Methicillin-resistant *Staphylococcus aureus* (MRSA): antibiotic-resistance and the biofilm phenotype. *MedChemComm*, *10*(8), 1231-1241.

Crivat, G., & Taraska, J. W. (2012). Imaging proteins inside cells with fluorescent tags. *Trends in biotechnology*, 30(1), 8-16.

Crosby, H. A., Schlievert, P. M., Merriman, J. A., King, J. M., Salgado-Pabón, W., & Horswill, A. R. (2016). The *Staphylococcus aureus* global regulator MgrA modulates clumping and virulence by controlling surface protein expression. *PLoS pathogens*, *12*(5), e1005604.

Crossley, K. B., Jefferson, K. K., Archer, G. L., & Fowler Jr, V. G. (Eds.). (2009). Staphylococci in human disease.

Cucarella, C., Solano, C., Valle, J., Amorena, B., Lasa, I., & Penadés, J. R. (2001). Bap, a *Staphylococcus aureus* surface protein involved in biofilm formation. *Journal of bacteriology*, *183*(9), 2888-2896.

D'Elia, M. A., Millar, K. E., Beveridge, T. J., & Brown, E. D. (2006). Wall teichoic acid polymers are dispensable for cell viability in Bacillus subtilis. *Journal of bacteriology*, 188(23), 8313-8316.

D'Elia, M. A., Pereira, M. P., Chung, Y. S., Zhao, W., Chau, A., Kenney, T. J., & Brown, E. D. (2006). Lesions in teichoic acid biosynthesis in *Staphylococcus aureus* lead to a lethal gain of function in the otherwise dispensable pathway. *Journal of Bacteriology*, *188*(12), 4183-4189.

Daniel, R. A., Noirot-Gros, M. F., Noirot, P., & Errington, J. (2006). Multiple interactions between the transmembrane division proteins of Bacillus subtilis and the role of FtsL instability in divisome assembly. *Journal of bacteriology*, *188*(21), 7396-7404.

De Kruijff, B., van Dam, V., & Breukink, E. (2008). Lipid II: a central component in bacterial cell wall synthesis and a target for antibiotics. Prostaglandins, Leukotrienes and Essential Fatty Acids, 79(3-5), 117-121.

DeDent, A. C., McAdow, M., & Schneewind, O. (2007). Distribution of protein A on the surface of *Staphylococcus aureus*. *Journal of bacteriology*, *189*(12), 4473-4484.

DeDent, A., Bae, T., Missiakas, D. M., & Schneewind, O. (2008). Signal peptides direct surface proteins to two distinct envelope locations of *Staphylococcus aureus*. *The EMBO journal*, *27*(20), 2656-2668.

Dmitriev, B., Toukach, F., & Ehlers, S. (2005). Towards a comprehensive view of the bacterial cell wall. *Trends in microbiology*, *13*(12), 569-574.

Do, T., Schaefer, K., Santiago, A. G., Coe, K. A., Fernandes, P. B., Kahne, D., & Walker, S. (2020). *Staphylococcus aureus* cell growth and division are regulated by an amidase that trims peptides from uncrosslinked peptidoglycan. *Nature microbiology*, *5*(2), 291-303.

Dordel, J., Kim, C., Chung, M., de la Gándara, M.P., Holden, M.T.J., Parkhill, J., de Lencastre, H., Bentley, S.D., and Tomasz, A. (2014). Novel determinants of antibiotic resistance: Identification of mutated Loci in Highly methicillin-resistant subpopulations of methicillin-resistant *Staphylococcus aureus*. MBio *5*, 1–9.

Drechsel, H., Freund, S., Nicholson, G., Haag, H., Jung, O., Zähner, H., & Jung, G. (1993). Purification and chemical characterization of staphyloferrin B, a hydrophilic siderophore from staphylococci. *Biometals*, *6*(3), 185-192.

Dziarski, R., & Gupta, D. (2010). Mammalian peptidoglycan recognition proteins (PGRPs) in innate immunity. *Innate immunity*, *16*(3), 168-174.

Egan, A. J., Errington, J., & Vollmer, W. (2020). Regulation of peptidoglycan synthesis and remodelling. *Nature Reviews Microbiology*, *18*(8), 446-460.

Enright, M. C., Robinson, D. A., Randle, G., Feil, E. J., Grundmann, H., & Spratt, B. G. (2002). The evolutionary history of methicillin-resistant *Staphylococcus aureus* (MRSA). *Proceedings of the National Academy of Sciences*, *99*(11), 7687-7692.

Enström, J., Fröding, I., Giske, C. G., Ininbergs, K., Bai, X., Sandh, G., & Fang, H. (2018). USA300 methicillin-resistant *Staphylococcus aureus* in Stockholm, Sweden, from 2008 to 2016. *PloS one*, *13*(11), e0205761.

Entenza, J. M., Moreillon, P., Senn, M. M., Kormanec, J., Dunman, P. M., Berger-Bächi, B., & Bischoff, M. (2005). Role of σB in the expression of *Staphylococcus aureus* cell wall adhesins ClfA and FnbA and contribution to infectivity in a rat model of experimental endocarditis. *Infection and immunity*, *73*(2), 990-998.

Evanko, D. (2006). Training GFP to fold. *Nature Methods*, *3*(2), 76-76.

Fergestad, M. E., Stamsås, G. A., Morales Angeles, D., Salehian, Z., Wasteson, Y., & Kjos, M. (2020). Penicillin-binding protein PBP2a provides variable levels of protection toward different β-lactams in *Staphylococcus aureus* RN4220. *Microbiologyopen*, *9*(8), e1057.

Fey, P. D., Endres, J. L., Yajjala, V. K., Widhelm, T. J., Boissy, R. J., Bose, J. L., & Bayles, K. W. (2013). A genetic resource for rapid and comprehensive phenotype screening of nonessential *Staphylococcus aureus* genes. *MBio*, *4*(1), e00537-12.

Fey, P. D., Endres, J. L., Yajjala, V. K., Widhelm, T. J., Boissy, R. J., Bose, J. L., & Bayles, K. W. (2013). A genetic resource for rapid and comprehensive phenotype screening of nonessential *Staphylococcus aureus* genes. *MBio*, *4*(1), e00537-12.

Figshare. (2015). *Model of protein secretion.* [online] Available at: https://plos.figshare.com/articles/figure/_model_of_protein_secretion_/1438232. Accessed 4 April 2023.

Foster, S. J. (1995). Molecular characterization and functional analysis of the major autolysin of *Staphylococcus aureus* 8325/4. *Journal of Bacteriology*, *177*(19), 5723-5725.

Foster, T. J. (2019). Can β-lactam antibiotics be resurrected to combat MRSA?. *Trends in microbiology*, *27*(1), 26-38.

Foster, T. J. (2019). Surface proteins of *Staphylococcus aureus*. Microbiology spectrum, 7(4), 7-4.

Foster, T. J., & Höök, M. (1998). Surface protein adhesins of *Staphylococcus aureus*. Trends in microbiology, 6(12), 484-488.

Foster, T. J., Geoghegan, J. A., Ganesh, V. K., & Höök, M. (2014). Adhesion, invasion and evasion: the many functions of the surface proteins of *Staphylococcus aureus*. *Nature reviews microbiology*, *12*(1), 49-62.

Fowler, V. G., Olsen, M. K., Corey, G. R., Woods, C. W., Cabell, C. H., Reller, L. B. & Oddone, E. Z. (2003). Clinical identifiers of complicated *Staphylococcus aureus* bacteremia. *Archives of internal medicine*, 163(17), 2066-2072.

Frankel, M. B., Hendrickx, A. P., Missiakas, D. M., & Schneewind, O. (2011). LytN, a murein hydrolase in the cross-wall compartment of *Staphylococcus aureus*, is involved in proper bacterial growth and envelope assembly. *Journal of Biological Chemistry*, *286*(37), 32593-32605.

Frankel, M. B., Wojcik, B. M., DeDent, A. C., Missiakas, D. M., & Schneewind, O. (2010). ABI domain-containing proteins contribute to surface protein display and cell division in *Staphylococcus aureus*. *Molecular microbiology*, *78*(1), 238-252.

Gao, J., & Stewart, G. C. (2004). Regulatory elements of the *Staphylococcus aureus* protein A (Spa) promoter. *Journal of bacteriology*, *186*(12), 3738-3748.

Gaudin, C. F., Grigg, J. C., Arrieta, A. L., & Murphy, M. E. (2011). Unique heme-iron coordination by the hemoglobin receptor IsdB of *Staphylococcus aureus*. *Biochemistry*, *50*(24), 5443-5452.

Gautam, S., Kim, T., & Spiegel, D. A. (2015). Chemical probes reveal an extraseptal mode of cross-linking in *Staphylococcus aureus*. *Journal of the American Chemical Society*, *137*(23), 7441-7447.

Geisinger, E., Chen, J., & Novick, R. P. (2012). Allele-dependent differences in quorum-sensing dynamics result in variant expression of virulence genes in Staphylococcus aureus. *Journal of bacteriology*, *194*(11), 2854-2864.

Ghasemian, A., Peerayeh, S. N., Bakhshi, B., & Mirzaee, M. (2015). The microbial surface components recognizing adhesive matrix molecules (MSCRAMMs) genes among clinical isolates of *Staphylococcus aureus* from hospitalized children. *Iranian journal of pathology*, 10(4), 258.

Giannouli, S., Labrou, M., Kyritsis, A., Ikonomidis, A., Pournaras, S., Stathopoulos, C., & Tsakris, A. (2010). Detection of mutations in the FemXAB protein family in oxacillin-susceptible mecA-positive *Staphylococcus aureus* clinical isolates. *Journal of Antimicrobial Chemotherapy*, *65*(4), 626-633.

Gibson, D. (2009). One-step enzymatic assembly of DNA molecules up to several hundred kilobases in size.

Glas, M., McLaughlin, S. H., Roseboom, W., Liu, F., Koningstein, G. M., Fish, A., & Luirink, J. (2015). The soluble periplasmic domains of Escherichia coli cell division proteins FtsQ/FtsB/FtsL form a trimeric complex with submicromolar affinity. *Journal of Biological Chemistry*, *290*(35), 21498-21509.

Goering, R. V., Swartzendruber, E. A., Obradovich, A. E., Tickler, I. A., & Tenover, F. C. (2019). Emergence of oxacillin resistance in stealth methicillin-resistant *Staphylococcus aureus* due to mecA sequence instability. *Antimicrobial agents and chemotherapy*, *63*(8), e00558-19.

Gómez, M. I., Lee, A., Reddy, B., Muir, A., Soong, G., Pitt, A., & Prince, A. (2004). *Staphylococcus aureus* protein A induces airway epithelial inflammatory responses by activating TNFR1. *Nature medicine*, *10*(8), 842-848.

Graille, M., Stura, E. A., Corper, A. L., Sutton, B. J., Taussig, M. J., Charbonnier, J. B., & Silverman, G. J. (2000). Crystal structure of a *Staphylococcus aureus* protein A domain complexed with the Fab fragment of a human IgM antibody: structural basis for recognition of B-cell receptors and superantigen activity. *Proceedings of the National Academy of Sciences*, *97*(10), 5399-5404.

Griesbeck, O., Baird, G. S., Campbell, R. E., Zacharias, D. A., & Tsien, R. Y. (2001). Reducing the environmental sensitivity of yellow fluorescent protein: mechanism and applications. *Journal of biological chemistry*, *276*(31), 29188-29194.

Griffiths, G., & Lucocq, J. M. (2014). Antibodies for immunolabeling by light and electron microscopy: not for the faint hearted. *Histochemistry and cell biology*, *142*(4), 347-360.

Grigg, J. C., Ukpabi, G., Gaudin, C. F., & Murphy, M. E. (2010). Structural biology of heme binding in the *Staphylococcus aureus* Isd system. *Journal of inorganic biochemistry*, 104(3), 341-348.

Gründling, A., & Schneewind, O. (2006). Cross-linked peptidoglycan mediates lysostaphin binding to the cell wall envelope of *Staphylococcus aureus*. Journal of bacteriology, 188(7), 2463-2472.

Gustafson, J. O. H. N., Strässle, A., Hächler, H., Kayser, F. H., & Berger-Bächi, B. (1994). The femC locus of *Staphylococcus aureus* required for methicillin resistance includes the glutamine synthetase operon. *Journal of bacteriology*, *176*(5), 1460-1467.

Hackbarth, C. J., Kocagoz, T., Kocagoz, S., & Chambers, H. F. (1995). Point mutations in *Staphylococcus aureus* PBP 2 gene affect penicillin-binding kinetics and are associated with resistance. *Antimicrobial agents and chemotherapy*, *39*(1), 103-106.

Hallin, M., Friedrich, A. W., & Struelens, M. J. (2009). spa typing for epidemiological surveillance of *Staphylococcus aureus*. *Molecular Epidemiology of Microorganisms: Methods and Protocols*, 189-202.

Hao, Z., Guo, Y., Rao, L., Yu, J., Zhan, Q., Xu, Y., & Yu, F. (2021). Deletion of SarX decreases biofilm formation of *Staphylococcus aureus* in a Polysaccharide Intercellular Adhesin (PIA)-dependent manner by downregulating spa. *Infection and Drug Resistance*, 2241-2250.

Harkins, C. P., Pichon, B., Doumith, M., Parkhill, J., Westh, H., Tomasz, A., & Holden, M. T. (2017). Methicillin-resistant *Staphylococcus aureus* emerged long before the introduction of methicillin into clinical practice. *Genome biology*, *18*(1), 1-11.

Hartleib, J., Köhler, N., Dickinson, R. B., Chhatwal, G. S., Sixma, J. J., Hartford, O. M., & Herrmann, M. (2000). Protein A is the von Willebrand factor binding protein on *Staphylococcus aureus*. *Blood, The Journal of the American Society of Hematology*, *96*(6), 2149-2156.

Hasman, H., Moodley, A., Guardabassi, L., Stegger, M., Skov, R. L., & Aarestrup, F. M. (2010). Spa type distribution in *Staphylococcus aureus* originating from pigs, cattle and poultry. Veterinary microbiology, 141(3-4), 326-331.

Heintzmann, R., & Huser, T. (2017). Super-resolution structured illumination microscopy. *Chemical reviews*, *117*(23), 13890-13908.

Herbert, S., Ziebandt, A. K., Ohlsen, K., Schäfer, T., Hecker, M., Albrecht, D., & Götz, F. (2010). Repair of global regulators in *Staphylococcus aureus* 8325 and comparative analysis with other clinical isolates. *Infection and immunity*, *78*(6), 2877-2889.

Herman-Bausier, P., Labate, C., Towell, A. M., Derclaye, S., Geoghegan, J. A., & Dufrêne, Y. F. (2018). *Staphylococcus aureus* clumping factor A is a force-sensitive molecular switch that activates bacterial adhesion. *Proceedings of the National Academy of Sciences*, *115*(21), 5564-5569.

Herman-Bausier, P., Valotteau, C., Pietrocola, G., Rindi, S., Alsteens, D., Foster, T. J., & Dufrêne, Y. F. (2016). Mechanical strength and inhibition of the *Staphylococcus aureus* collagen-binding protein Cna. *MBio*, *7*(5), e01529-16.

Herman, B. (2020). *Fluorescence microscopy*. Garland Science.

Hesser, A. R., Matano, L. M., Vickery, C. R., Wood, B. M., Santiago, A. G., Morris, H. G., & Walker, S. (2020). The length of lipoteichoic acid polymers controls *Staphylococcus aureus* cell size and envelope integrity. *Journal of bacteriology*, *202*(16), e00149-20.

Hiramatsu, K., Ito, T., Tsubakishita, S., Sasaki, T., Takeuchi, F., Morimoto, Y., Katayama, Y., Matsuo, M., Kuwahara-Arai, K., Hishinuma, T., et al. (2013). Genomic Basis for Methicillin Resistance in *Staphylococcus aureus*. Infect. Chemother. *45*, 117–136.

Ho, M., & Pastan, I. (2009). Mammalian cell display for antibody engineering. In *Therapeutic Antibodies* (pp. 337-352). Humana Press.

Hobby, G. L., Meyer, K., & Chaffee, E. (1942). Observations on the Mechanism of Action of Penicillin. *Proceedings of the Society for Experimental Biology and Medicine*, *50*(2), 281-285.

Hoelzel, C. A., & Zhang, X. (2020). Visualizing and Manipulating Biological Processes by Using HaloTag and SNAP-Tag Technologies. *ChemBioChem*, *21*(14), 1935-1946.

Holland, L. M., Conlon, B., & O'Gara, J. P. (2011). Mutation of tagO reveals an essential role for wall teichoic acids in Staphylococcus epidermidis biofilm development. *Microbiology*, 157(2), 408-418.

Holt, D. C., Holden, M. T., Tong, S. Y., Castillo-Ramirez, S., Clarke, L., Quail, M. A. & Giffard, P. M. (2011). A very early-branching *Staphylococcus aureus* lineage lacking the carotenoid pigment staphyloxanthin. Genome biology and evolution, 3, 881-895.

Honsa, E. S., & Maresso, A. W. (2011). Mechanisms of iron import in anthrax. *Biometals*, 24(3), 533-545.

Honsa, E. S., Maresso, A. W., & Highlander, S. K. (2014). Molecular and evolutionary analysis of NEAr-iron Transporter (NEAT) domains. *PloS one*, 9(8), e104794.

Horsburgh, M. J., Aish, J. L., White, I. J., Shaw, L., Lithgow, J. K., & Foster, S. J. (2002). σB modulates virulence determinant expression and stress resistance: characterization of a functional rsbU strain derived from *Staphylococcus aureus* 8325-4. *Journal of bacteriology*, *184*(19), 5457-5467.

Huang, B., Liu, F. F., Dong, X. Y., & Sun, Y. (2012). Molecular mechanism of the effects of salt and pH on the affinity between protein A and human immunoglobulin G1 revealed by molecular simulations. *The Journal of Physical Chemistry B*, *116*(1), 424-433.

Huang, X., Aulabaugh, A., Ding, W., Kapoor, B., Alksne, L., Tabei, K., & Ellestad, G. (2003). Kinetic mechanism of *Staphylococcus aureus* sortase SrtA. *Biochemistry*, *42*(38), 11307-11315.

Im, K., Mareninov, S., Diaz, M. F. P., & Yong, W. H. (2019). An introduction to performing immunofluorescence staining. *Biobanking: methods and protocols*, 299-311.

Ingavale, S., van Wamel, W., Luong, T. T., Lee, C. Y., & Cheung, A. L. (2005). Rat/MgrA, a regulator of autolysis, is a regulator of virulence genes in *Staphylococcus aureus*. *Infection and immunity*, *73*(3), 1423-1431.

Ito, T., Hiramatsu, K., Oliveira, D., De Lencastre, H., Zhang, K., Westh, H., & Tenover, F. (2009). International Working Group on the Classification of Staphylococcal Cassette Chromosome Elements (IWG-SCC) Classification of staphylococcal cassette chromosome mec (SCCmec): guidelines for reporting novel SCCmec elements. *Antimicrob Agents Chemother*, *53*, 4961-4967.

James, K., Gamba, P., Cockell, S. J., & Zenkin, N. (2017). Misincorporation by RNA polymerase is a major source of transcription pausing in vivo. *Nucleic acids research*, *45*(3), 1105-1113.

Jarick, M., Bertsche, U., Stahl, M., Schultz, D., Methling, K., Lalk, M., & Ohlsen, K. (2018). The serine/threonine kinase Stk and the phosphatase Stp regulate cell wall synthesis in *Staphylococcus aureus*. Scientific reports, 8(1), 13693.

Jensen, C., Li, H., Vestergaard, M., Dalsgaard, A., Frees, D., & Leisner, J. J. (2020). Nisin damages the septal membrane and triggers DNA condensation in methicillin-resistant *Staphylococcus aureus*. *Frontiers in Microbiology*, *11*, 1007.

Jensen, E. C. (2012). Use of fluorescent probes: their effect on cell biology and limitations. *The Anatomical Record: Advances in Integrative Anatomy and Evolutionary Biology*, *295*(12), 2031-2036.

Jenul, C., & Horswill, A. R. (2019). Regulation of *Staphylococcus aureus* virulence. *Microbiology spectrum*, *7*(2), 7-2.

Jevons, M. P., Coe, A. W., & Parker, M. T. (1963). Methicillin resistance in staphylococci. *Lancet*, 904-7.

Jin, J., Hsieh, Y. H., Chaudhary, A. S., Cui, J., Houghton, J. E., Sui, S. F., & Tai, P. C. (2018). SecA inhibitors as potential antimicrobial agents: differential actions on SecA-only and SecA-SecYEG protein-conducting channels. *FEMS microbiology letters*, *365*(15), fny145.

Jin, Y., Zhou, W., Zhan, Q., Zheng, B., Chen, Y., Luo, Q., & Xiao, Y. (2021). Genomic epidemiology and characterization of methicillin-resistant *Staphylococcus aureus* from bloodstream infections in China. *MSystems*, *6*(6), e00837-21.

Johnsson, K. (2008). SNAP-tag Technologies: Novel Tools to Study Protein Function. Available at: https://international.neb.com/tools-and-resources/feature-articles/snap-tag-technologies-novel-tools-to-study-protein-function. Accessed: 09.02.2023.

Jonsson, M., Mazmanian, S. K., Schneewind, O., Bremell, T., & Tarkowski, A. (2003). The role of *Staphylococcus aureus* sortase A and sortase B in murine arthritis. *Microbes and infection*, 5(9), 775-780.

Jonsson, P., Lindberg, M. A. R. T. I. N., Haraldsson, I. N. G. E. R., & Wadström, T. (1985). Virulence of *Staphylococcus aureus* in a mouse mastitis model: studies of alpha hemolysin, coagulase, and protein A as possible virulence determinants with protoplast fusion and gene cloning. *Infection and immunity*, *49*(3), 765-769.

Josefsson, E., O'Connell, D., Foster, T. J., Durussel, I., & Cox, J. A. (1998). The binding of calcium to the B-repeat segment of SdrD, a cell surface protein of *Staphylococcus aureus*. *Journal of Biological Chemistry*, *273*(47), 31145-31152.

Juillerat, A., Gronemeyer, T., Keppler, A., Gendreizig, S., Pick, H., Vogel, H., & Johnsson, K. (2003). Directed evolution of O6-alkylguanine-DNA alkyltransferase for efficient labeling of fusion proteins with small molecules in vivo. *Chemistry & biology*, 10(4), 313-317.

Kajimura, J., Fujiwara, T., Yamada, S., Suzawa, Y., Nishida, T., Oyamada, Y., & Sugai, M. (2005). Identification and molecular characterization of an N-acetylmuramyl-l-alanine amidase Sle1 involved in cell separation of *Staphylococcus aureus*. *Molecular microbiology*, *58*(4), 1087-1101.

Kajimura, J., Fujiwara, T., Yamada, S., Suzawa, Y., Nishida, T., Oyamada, Y., & Sugai, M. (2005). Identification and molecular characterization of an N-acetylmuramyl-l-alanine amidase Sle1 involved in cell separation of *Staphylococcus aureus*. *Molecular microbiology*, *58*(4), 1087-1101.

Kalayu, A. A., Woldetsadik, D. A., Woldeamanuel, Y., Wang, S. H., Gebreyes, W. A., & Teferi, T. (2020). Burden and antimicrobial resistance of S. aureus in dairy farms in Mekelle, Northern Ethiopia. *BMC veterinary research*, *16*, 1-8.

Kameya, H., Kanazaki, M., & Okamoto, S. (2019). Evaluation of the effects of reactive oxygen species on growth of Escherichia coli by electron spin resonance spin trapping. *Food Science and Technology Research*, *25*(3), 443-448.

Katayama, Y., Ito, T., & Hiramatsu, K. (2000). A new class of genetic element, staphylococcus cassette chromosome mec, encodes methicillin resistance in *Staphylococcus aureus*. *Antimicrobial agents and chemotherapy*, *44*(6), 1549-1555.

Khoon, L. Y., & Neela, V. (2010). Secretome of *Staphylococcus aureus*. *Arfican J Microbiol Res*, *4*, 500-508.

Kim, H. K., Cheng, A. G., Kim, H. Y., Missiakas, D. M., & Schneewind, O. (2010). Nontoxigenic protein A vaccine for methicillin-resistant *Staphylococcus aureus* infections in mice. *Journal of Experimental Medicine*, *207*(9), 1863-1870.

Kim, H. K., Thammavongsa, V., Schneewind, O., & Missiakas, D. (2012). Recurrent infections and immune evasion strategies of *Staphylococcus aureus*. *Current opinion in microbiology*, *15*(1), 92-99.

King, N. P., Sakinç, T., Ben Zakour, N. L., Totsika, M., Heras, B., Simerska, P., & Schembri, M. A. (2012). Characterisation of a cell wall-anchored protein of Staphylococcus saprophyticus associated with linoleic acid resistance. *BMC microbiology*, *12*(1), 1-12.

Klar, T. A., Engel, E., & Hell, S. W. (2001). Breaking Abbe's diffraction resolution limit in fluorescence microscopy with stimulated emission depletion beams of various shapes. *Physical Review E*, *64*(6), 066613.

Kobayashi, S. D., & DeLeo, F. R. (2013). *Staphylococcus aureus* protein A promotes immune suppression. *MBio*, *4*(5), e00764-13.

Koenig, R. L., Ray, J. L., Maleki, S. J., Smeltzer, M. S., & Hurlburt, B. K. (2004). *Staphylococcus aureus* AgrA binding to the RNAIII-agr regulatory region. *Journal of bacteriology*, *186*(22), 7549-7555.

Kolberg, K., Puettmann, C., Pardo, A., Fitting, J., & Barth, S. (2013). SNAP-tag technology: a general introduction. *Curr. Pharm. Des*, *19*(30), 5406-5413.

Komatsuzawa, H., Ohta, K., Fujiwara, T., Choi, G. H., Labischinski, H., & Sugai, M. (2001). Cloning and sequencing of the gene, fmtC, which affects oxacillin resistance in methicillin-resistant *Staphylococcus aureus*. *FEMS microbiology letters*, *203*(1), 49-54.

Komatsuzawa, H., Ohta, K., Sugai, M., Fujiwara, T., Glanzmann, P., Berger-Bächi, B., & Suginaka, H. (2000). Tn 551-mediated insertional inactivation of the fmtB gene encoding a cell wall-associated protein abolishes methicillin resistance in *Staphylococcus aureus*. *Journal of Antimicrobial Chemotherapy*, *45*(4), 421-431.

Konetschny-Rapp, S., Jung, G., Meiwes, J., & Zähner, H. (1990). Staphyloferrin A: a structurally new siderophore from staphylococci. *European journal of biochemistry*, *191*(1), 65-74.

Kota, R. K., Reddy, P. N., & Sreerama, K. (2020). Application of IgY antibodies against staphylococcal protein A (SpA) of *Staphylococcus aureus* for detection and prophylactic functions. *Applied Microbiology and Biotechnology*, *104*, 9387-9398.

Kreiswirth, B. N., Löfdahl, S., Betley, M. J., O'reilly, M., Schlievert, P. M., Bergdoll, M. S., & Novick, R. P. (1983). The toxic shock syndrome exotoxin structural gene is not detectably transmitted by a prophage. Nature, 305(5936), 709-712.

Kumar, J. K. (2008). Lysostaphin: an antistaphylococcal agent. *Applied microbiology and biotechnology*, *80*, 555-561.

Kuru, E., Hughes, H. V., Brown, P. J., Hall, E., Tekkam, S., Cava, F., & VanNieuwenhze, M. S. (2012). In situ probing of newly synthesized peptidoglycan in live bacteria with fluorescent D-amino acids. *Angewandte Chemie*, *124*(50), 12687-12691.

Laarman, A. J., Ruyken, M., Malone, C. L., van Strijp, J. A., Horswill, A. R., & Rooijakkers, S. H. (2011). *Staphylococcus aureus* metalloprotease aureolysin cleaves complement C3 to mediate immune evasion. *The Journal of Immunology*, *186*(11), 6445-6453.

Laux, C., Peschel, A., & Krismer, B. (2019). *Staphylococcus aureus* colonization of the human nose and interaction with other microbiome members. *Microbiology Spectrum*, *7*(2), 7-2.

Lee, T. K., & Huang, K. C. (2013). The role of hydrolases in bacterial cell-wall growth. *Current opinion in microbiology*, *16*(6), 760-766.

Leonard, A. C., Goncheva, M. I., Gilbert, S. E., Shareefdeen, H., Petrie, L. E., Thompson, L. K., & Cox, G. (2023). Autolysin-mediated peptidoglycan hydrolysis is required for the surface

display of Staphylococcus aureus cell wall-anchored proteins. *Proceedings of the National Academy of Sciences*, *120*(12), e2301414120.

Li, F., Zhai, D., Wu, Z., Zhao, Y., Qiao, D., & Zhao, X. (2020). Impairment of the cell wall ligase, LytR-CpsA-Psr protein (LcpC), in methicillin resistant *Staphylococcus aureus* reduces its resistance to antibiotics and infection in a mouse model of sepsis. *Frontiers in microbiology*, *11*, 557.

Li, L., Cheung, A., Bayer, A. S., Chen, L., Abdelhady, W., Kreiswirth, B. N., & Xiong, Y. Q. (2016). The global regulon sarA regulates β-lactam antibiotic resistance in methicillin-resistant *Staphylococcus aureus* in vitro and in endovascular infections. *The Journal of infectious diseases*, *214*(9), 1421-1429.

Li, R., Georgiades, P., Cox, H., Phanphak, S., Roberts, I. S., Waigh, T. A., & Lu, J. R. (2018). Quenched stochastic optical reconstruction microscopy (qSTORM) with graphene oxide. *Scientific Reports*, *8*(1), 16928.

Liang, B., Xiong, Z., Liang, Z., Zhang, C., Cai, H., Long, Y., & Zhou, Z. (2022). Genomic Basis of Occurrence of Cryptic Resistance among Oxacillin-and Cefoxitin-Susceptible mecA-Positive *Staphylococcus aureus*. *Microbiology Spectrum*, e00291-22.

Lichtman, J. W., & Conchello, J. A. (2005). Fluorescence microscopy. *Nature methods*, *2*(12), 910-919.

Lim, D., & Strynadka, N. C. (2002). Structural basis for the β lactam resistance of PBP2a from methicillin-resistant *Staphylococcus aureus*. *Nature structural biology*, *9*(11), 870-876.

Lim, D., & Strynadka, N. C. (2002). Structural basis for the β lactam resistance of PBP2a from methicillin-resistant *Staphylococcus aureus*. *Nature structural biology*, *9*(11), 870-876.

Lima, L. M., da Silva, B. N. M., Barbosa, G., & Barreiro, E. J. (2020). β-lactam antibiotics: An overview from a medicinal chemistry perspective. *European journal of medicinal chemistry*, *208*, 112829.

Lindsay, J. A. (2010). Genomic variation and evolution of *Staphylococcus aureus*. *International Journal of Medical Microbiology*, *300*(2-3), 98-103.

Lindsay, J. A., & Holden, M. T. (2006). Understanding the rise of the superbug: investigation of the evolution and genomic variation of Staphylococcus aureus. *Functional & integrative genomics*, *6*, 186-201.

Liu, J., Chen, D., Peters, B. M., Li, L., Li, B., Xu, Z., & Shirliff, M. E. (2016). Staphylococcal chromosomal cassettes mec (SCCmec): A mobile genetic element in methicillin-resistant *Staphylococcus aureus*. *Microbial pathogenesis*, *101*, 56-67.

Liu, Y., Manna, A. C., Pan, C. H., Kriksunov, I. A., Thiel, D. J., Cheung, A. L., & Zhang, G. (2006). Structural and function analyses of the global regulatory protein SarA from *Staphylococcus aureus*. *Proceedings of the National Academy of Sciences*, *103*(7), 2392-2397.

Livermore, D. M. (2003). Linezolid in vitro: mechanism and antibacterial spectrum. *Journal of Antimicrobial Chemotherapy*, *51*(suppl_2), ii9-ii16.

Llarrull, L. I., Fisher, J. F., & Mobashery, S. (2009). Molecular basis and phenotype of methicillin resistance in *Staphylococcus aureus* and insights into new β-lactams that meet the challenge. *Antimicrobial agents and chemotherapy*, *53*(10), 4051-4063.

Lovering, A. L., Safadi, S. S., & Strynadka, N. C. (2012). Structural perspective of peptidoglycan biosynthesis and assembly. *Annual review of biochemistry*, *81*, 451-478.

Lowy, F. D. (1998). *Staphylococcus aureus* infections. *New England journal of medicine*, 339(8), 520-532.

Lowy, F. D. (2003). Antimicrobial resistance: the example of *Staphylococcus aureus*. *The Journal of clinical investigation*, *111*(9), 1265-1273.

Lu, Y., Chen, F., Zhao, Q., Cao, Q., Chen, R., Pan, H., & Lan, L. (2023). Modulation of MRSA virulence gene expression by the wall teichoic acid enzyme TarO. *Nature Communications*, *14*(1), 1594.

Lund, V. A., Gangotra, H., Zhao, Z., Sutton, J. A., Wacnik, K., DeMeester, K., & Foster, S. J. (2022). Coupling Novel Probes with Molecular Localization Microscopy Reveals Cell Wall Homeostatic Mechanisms in *Staphylococcus aureus*. *ACS Chemical Biology*, *17*(12), 3298-3305.

Lund, V. A., Wacnik, K., Turner, R. D., Cotterell, B. E., Walther, C. G., Fenn, S. J., & Foster, S. J. (2018). Molecular coordination of *Staphylococcus aureus* cell division. *Elife*, *7*, e32057.

Mäder, U., Nicolas, P., Depke, M., Pané-Farré, J., Debarbouille, M., van der Kooi-Pol, M. M., & Van Dijl, J. M. (2016). *Staphylococcus aureus* transcriptome architecture: from laboratory to infection-mimicking conditions. *PLoS genetics*, *12*(4), e1005962.

Maggi, S., Massidda, O., Luzi, G., Fadda, D., Paolozzi, L., & Ghelardini, P. (2008). Division protein interaction web: identification of a phylogenetically conserved common interactome between Streptococcus pneumoniae and Escherichia coli. *Microbiology*, *154*(10), 3042-3052.

Mainiero, M., Goerke, C., Geiger, T., Gonser, C., Herbert, S., & Wolz, C. (2010). Differential target gene activation by the *Staphylococcus aureus* two-component system saeRS. *Journal of bacteriology*, *192*(3), 613-623.

Maňásková, S. H., Nazmi, K., van't Hof, W., van Belkum, A., Martin, N. I., Bikker, F. J. & Veerman, E. C. (2016). *Staphylococcus aureus* sortase A-mediated incorporation of peptides: effect of peptide modification on incorporation. *PloS one*, 11(1), e0147401.

Mani, N., Tobin, P., & Jayaswal, R. K. (1993). Isolation and characterization of autolysis-defective mutants of *Staphylococcus aureus* created by Tn917-lacZ mutagenesis. *Journal of Bacteriology*, *175*(5), 1493-1499.

Marbach, A., & Bettenbrock, K. (2012). lac operon induction in Escherichia coli: Systematic comparison of IPTG and TMG induction and influence of the transacetylase LacA. *Journal of biotechnology,* 157(1), 82-88.

Marraffini, L. A., & Schneewind, O. (2007). Sortase C-mediated anchoring of BasI to the cell wall envelope of Bacillus anthracis. *Journal of bacteriology*, *189*(17), 6425-6436.

Marraffini, L. A., DeDent, A. C., & Schneewind, O. (2006). Sortases and the art of anchoring proteins to the envelopes of gram-positive bacteria. *Microbiology and Molecular Biology Reviews*, *70*(1), 192-221.

Masalha, M., Borovok, I., Schreiber, R., Aharonowitz, Y., & Cohen, G. (2001). Analysis of Transcription of the *Staphylococcus aureus* Aerobic Class Ib and Anaerobic Class III

Ribonucleotide Reductase Genes in Response to Oxygen. *Journal of Bacteriology*, 183(24), 7260-7272.

Mateos-Gil, P., Paez, A., Hörger, I., Rivas, G., Vicente, M., Tarazona, P., & Vélez, M. (2012). Depolymerization dynamics of individual filaments of bacterial cytoskeletal protein FtsZ. *Proceedings of the National Academy of Sciences*, *109*(21), 8133-8138.Matias, V. R. F. & Beveridge, T. J., (2006). Native cell wall organization shown by cryo-electron microscopy confirms the existence of a periplasmic space in *Staphylococcus aureus*. J. *Bacteriol*. 183, 1011-1021.

Matsuo, M., Hishinuma, T., Katayama, Y., Cui, L., Kapi, M., & Hiramatsu, K. (2011). Mutation of RNA polymerase β subunit (rpoB) promotes hVISA-to-VISA phenotypic conversion of strain Mu3. *Antimicrobial agents and chemotherapy*, *55*(9), 4188-4195.

Mazmanian, S. K., Liu, G., Jensen, E. R., Lenoy, E., & Schneewind, O. (2000). *Staphylococcus aureus* sortase mutants defective in the display of surface proteins and in the pathogenesis of animal infections. *Proceedings of the National Academy of Sciences*, *97*(10), 5510-5515.

Mazmanian, S. K., Liu, G., Ton-That, H., & Schneewind, O. (1999). *Staphylococcus aureus* sortase, an enzyme that anchors surface proteins to the cell wall. Science, 285(5428), 760-763.

Mazmanian, S. K., Skaar, E. P., Gaspar, A. H., Humayun, M., Gornicki, P., Jelenska, J. & Schneewind, O. (2003). Passage of heme-iron across the envelope of *Staphylococcus aureus*. *Science*, 299(5608), 906-909.

Mazmanian, S. K., Ton-That, H., & Schneewind, O. (2001). Sortase-catalysed anchoring of surface proteins to the cell wall of *Staphylococcus aureus*. *Molecular microbiology*, *40*(5), 1049-1057.

McCallum, N., Meier, P. S., Heusser, R., & Berger-Bachi, B. (2011). Mutational analyses of open reading frames within the vraSR operon and their roles in the cell wall stress response of *Staphylococcus aureus*. *Antimicrobial agents and chemotherapy*, *55*(4), 1391-1402.

Mcdevitt, D., Nanavaty, T., House-Pompeo, K., Bell, E., Turner, N., Mcintire, L., & HöökK, M. (1997). Characterization of the interaction between the *Staphylococcus aureus* clumping factor (ClfA) and fibrinogen. European journal of biochemistry, 247(1), 416-424.

Mcdevitt, D., Nanavaty, T., House-Pompeo, K., Bell, E., Turner, N., Mcintire, L., & HöökK, M. (1997). Characterization of the interaction between the *Staphylococcus aureus* clumping factor (ClfA) and fibrinogen. *European journal of biochemistry*, *247*(1), 416-424.

McGettrick, A. F., & Worrall, D. M. (2004). Extraction of recombinant protein from bacteria. *Protein Purification Protocols*, 29-35.

Meeske, A. J., Riley, E. P., Robins, W. P., Uehara, T., Mekalanos, J. J., Kahne, D., & Rudner, D. Z. (2016). SEDS proteins are a widespread family of bacterial cell wall polymerases. *Nature*, *537*(7622), 634-638.

Merino, N., Toledo-Arana, A., Vergara-Irigaray, M., Valle, J., Solano, C., Calvo, E. & Lasa, I. (2009). Protein A-mediated multicellular behavior in *Staphylococcus aureus*. *Journal of bacteriology*, 191(3), 832-843.

Miller, D. M., & Shakes, D. C. (1995). Immunofluorescence microscopy. *Methods in cell biology*, *48*, 365-394.

Mitrophanov, A. Y., & Groisman, E. A. (2008). Signal integration in bacterial two-component regulatory systems. *Genes & development*, *22*(19), 2601-2611.

Mlynarczyk-Bonikowska, B., Kowalewski, C., Krolak-Ulinska, A., & Marusza, W. (2022). Molecular mechanisms of drug resistance in *Staphylococcus aureus*. *International journal of molecular sciences*, *23*(15), 8088.

Mollwitz, B., Brunk, E., Schmitt, S., Pojer, F., Bannwarth, M., Schiltz, M. & Johnsson, K. (2012). Directed evolution of the suicide protein O 6-alkylguanine-DNA alkyltransferase for increased reactivity results in an alkylated protein with exceptional stability. *Biochemistry*, 51(5), 986-994.

Monk, I. R., Tree, J. J., Howden, B. P., Stinear, T. P., & Foster, T. J. (2015). Complete bypass of restriction systems for major *Staphylococcus aureus* lineages. *MBio*, *6*(3), e00308-15.

Moore, M. J., Qin, P., Keith, D. J., & Boger, D. L. (2023). Improved preparative enzymatic glycosylation of vancomycin aglycon and analogues. *Tetrahedron*, *131*, 133211.

Mootz, J. M., Malone, C. L., Shaw, L. N., & Horswill, A. R. (2013). Staphopains modulate *Staphylococcus aureus* biofilm integrity. *Infection and immunity*, *81*(9), 3227-3238.

Moris, V., Lam, M., Amoureux, L., Magallon, A., Guilloteau, A., Maldiney, T., & Neuwirth, C. (2022). What is the best technic to dislodge Staphylococcus epidermidis biofilm on medical implants?. *BMC microbiology*, *22*(1), 1-14.

MOVITZ, J. (1976). Formation of extracellular protein A by *Staphylococcus aureus*. European Journal of Biochemistry, 68(1), 291-299.

Münch, D., Roemer, T., Lee, S. H., Engeser, M., Sahl, H. G., & Schneider, T. (2012). Identification and in vitro analysis of the GatD/MurT enzyme-complex catalyzing lipid II amidation in *Staphylococcus aureus*. *PLoS pathogens*, *8*(1), e1002509.

Muthukrishnan, G., Quinn, G. A., Lamers, R. P., Diaz, C., Cole, A. L., Chen, S., & Cole, A. M. (2011). Exoproteome of *Staphylococcus aureus* reveals putative determinants of nasal carriage. *Journal of proteome research*, 10(4), 2064-2078.

Myrbråten, I. S., Stamsås, G. A., Chan, H., Morales Angeles, D., Knutsen, T. M., Salehian, Z., & Kjos, M. (2022). SmdA is a novel cell morphology determinant in *Staphylococcus aureus*. *Mbio*, *13*(2), e03404-21.

Nair, D., Memmi, G., Hernandez, D., Bard, J., Beaume, M., Gill, S., & Cheung, A. L. (2011). Whole-genome sequencing of *Staphylococcus aureus* strain RN4220, a key laboratory strain used in virulence research, identifies mutations that affect not only virulence factors but also the fitness of the strain. *Journal of bacteriology*, *193*(9), 2332-2335.

Nega, M., Tribelli, P. M., Hipp, K., Stahl, M., & Götz, F. (2020). New insights in the coordinated amidase and glucosaminidase activity of the major autolysin (Atl) in *Staphylococcus aureus*. *Communications biology*, *3*(1), 695.

Nishiyama, K. I., Suzuki, T., & Tokuda, H. (1996). Inversion of the membrane topology of SecG coupled with SecA-dependent preprotein translocation. *Cell*, *85*(1), 71-81.

Nordengrün, M., Abdurrahman, G., Treffon, J., Wächter, H., Kahl, B. C., & Bröker, B. M. (2021). Allergic reactions to serine protease-like proteins of *Staphylococcus aureus*. *Frontiers in Immunology*, *12*, 651060.

Novick, R. P. (1990). *Molecular biology of the staphylococci*. VCH Publishers.

O'Halloran, D. P., Wynne, K., & Geoghegan, J. A. (2015). Protein A is released into the *Staphylococcus aureus* culture supernatant with an unprocessed sorting signal. *Infection and immunity*, *83*(4), 1598-1609.

O'Neill, A. J. (2010). *Staphylococcus aureus* SH1000 and 8325-4: comparative genome sequences of key laboratory strains in staphylococcal research. *Letters in applied microbiology*, *51*(3), 358-361.

Oku, Y., Kurokawa, K., Matsuo, M., Yamada, S., Lee, B. L., & Sekimizu, K. (2009). Pleiotropic roles of polyglycerolphosphate synthase of lipoteichoic acid in growth of *Staphylococcus aureus* cells. *Journal of bacteriology*, *191*(1), 141-151.

Oriol, C., Cengher, L., Manna, A. C., Mauro, T., Pinel-Marie, M. L., Felden, B., & Rouillon, A. (2021). Expanding the *Staphylococcus aureus* SarA regulon to small RNAs. *Msystems*, *6*(5), e00713-21.

Paharik, A. E., Salgado-Pabon, W., Meyerholz, D. K., White, M. J., Schlievert, P. M., & Horswill, A. R. (2016). The Spl serine proteases modulate *Staphylococcus aureus* protein production and virulence in a rabbit model of pneumonia. *Msphere*, *1*(5), e00208-16.

Pan, T., Guan, J., Li, Y., & Sun, B. (2021). LcpB Is a Pyrophosphatase Responsible for Wall Teichoic Acid Synthesis and Virulence in *Staphylococcus aureus* Clinical Isolate ST59. *Frontiers in microbiology*, 4003.

Pan, Y., Zeng, J., Li, L., Yang, J., Tang, Z., Xiong, W., & Zeng, Z. (2020). Coexistence of antibiotic resistance genes and virulence factors deciphered by large-scale complete genome analysis. *Msystems*, *5*(3), e00821-19.

Panchal, V. V., Griffiths, C., Mosaei, H., Bilyk, B., Sutton, J. A., Carnell, O. T., & Foster, S. J. (2020). Evolving MRSA: High-level β-lactam resistance in *Staphylococcus aureus* is associated

with RNA Polymerase alterations and fine tuning of gene expression. *PLoS pathogens*, *16*(7), e1008672.

Park, E., & Rapoport, T. A. (2012). Mechanisms of Sec61/SecY-mediated protein translocation across membranes. *Annual review of biophysics*, *41*, 21-40.

Pasquina-Lemonche, L., Burns, J., Turner, R. D., Kumar, S., Tank, R., Mullin, N., & Hobbs, J. K. (2020). The architecture of the Gram-positive bacterial cell wall. *Nature*, *582*(7811), 294-297.

Patin, D., Boniface, A., Kovač, A., Hervé, M., Dementin, S., Barreteau, H., & Blanot, D. (2010). Purification and biochemical characterization of Mur ligases from *Staphylococcus aureus*. *Biochimie*, *92*(12), 1793-1800.

Patti, J. M., Allen, B. L., McGavin, M. J., & Höök, M. (1994). MSCRAMM-mediated adherence of microorganisms to host tissues. *Annual Reviews in Microbiology*, 48(1), 585-617.

Paulander, W., Varming, A. N., Bojer, M. S., Friberg, C., Bæk, K., & Ingmer, H. (2018). The agr quorum sensing system in *Staphylococcus aureus* cells mediates death of sub-population. *BMC research notes*, *11*, 1-5.

Paulander, W., Varming, A. N., Bojer, M. S., Friberg, C., Bæk, K., & Ingmer, H. (2018). The agr quorum sensing system in *Staphylococcus aureus* cells mediates death of sub-population. *BMC research notes*, *11*, 1-5.

Peregrín-Alvarez, J. M., Sanford, C., & Parkinson, J. (2009). The conservation and evolutionary modularity of metabolism. *Genome biology*, *10*(6), 1-17.

Pereira, S. F. F., Henriques, A. O., Pinho, M. G., De Lencastre, H., & Tomasz, A. (2007). Role of PBP1 in cell division of *Staphylococcus aureus*. *Journal of bacteriology*, *189*(9), 3525-3531.

Pietrocola, G., Nobile, G., Rindi, S., & Speziale, P. (2017). *Staphylococcus aureus* manipulates innate immunity through own and host-expressed proteases. *Frontiers in cellular and infection microbiology*, *7*, 166.

Pinho, M. G., & Errington, J. (2003). Dispersed mode of *Staphylococcus aureus* cell wall synthesis in the absence of the division machinery. *Molecular microbiology*, *50*(3), 871-881.

Pinho, M. G., Kjos, M., & Veening, J. W. (2013). How to get (a) round: mechanisms controlling growth and division of coccoid bacteria. *Nature reviews microbiology*, *11*(9), 601-614.

Popp, M. W. L., & Ploegh, H. L. (2011). Making and breaking peptide bonds: protein engineering using sortase. *Angewandte Chemie International Edition*, *50*(22), 5024-5032.

Porfírio, S., Carlson, R. W., & Azadi, P. (2019). Elucidating peptidoglycan structure: an analytical toolset. *Trends in microbiology*, *27*(7), 607-622.

Prabudiansyah, I., & Driessen, A. J. (2016). The canonical and accessory Sec system of Gram-positive bacteria. *Protein and Sugar Export and Assembly in Gram-positive Bacteria*, 45-67.

Quiblier, C., Zinkernagel, A. S., Schuepbach, R. A., Berger-Bächi, B., & Senn, M. M. (2011). Contribution of SecDF to *Staphylococcus aureus*resistance and expression of virulence factors. *BMC microbiology*, *11*(1), 1-12.

Quinlivan, E. P., McPartlin, J., Weir, D. G., & Scott, J. (2000). Mechanism of the antimicrobial drug trimethoprim revisited. *The FASEB Journal*, *14*(15), 2519-2524.

Rapoport, T. A. (2007). Protein translocation across the eukaryotic endoplasmic reticulum and bacterial plasma membranes. *Nature*, *450*(7170), 663-669.

Reed, S. B., Wesson, C. A., Liou, L. E., Trumble, W. R., Schlievert, P. M., Bohach, G. A., & Bayles, K. W. (2001). Molecular characterization of a novel *Staphylococcus aureus* serine protease operon. *Infection and immunity*, *69*(3), 1521-1527.

Reniere, M. L., & Skaar, E. P. (2008). *Staphylococcus aureus* haem oxygenases are differentially regulated by iron and haem. *Molecular microbiology*, *69*(5), 1304-1315.

Rieneck, K., Renneberg, J., Diamant, M., Gutschik, E., & Bendtzen, K. (1997). Molecular cloning and expression of a novel *Staphylococcus aureus* antigen. *Biochimica et Biophysica Acta (BBA)-Gene Structure and Expression*, *1350*(2), 128-132.

Rivolta, C. (1986). Airy disk diffraction pattern: comparison of some values of f/No. and obscuration ratio. *Applied optics*, *25*(14), 2404-2408.

Robinson, D. A., Monk, A. B., Cooper, J. E., Feil, E. J., & Enright, M. C. (2005). Evolutionary genetics of the accessory gene regulator (agr) locus in *Staphylococcus aureus*. Journal of bacteriology, 187(24), 8312-8321.

Robson, S. A. (2006). *Studies of the structure and putative complex of the bacterial cell division proteins FtsL, DivIC and DivIB*. University of Connecticut.

Roche, F. M., Massey, R., Peacock, S. J., Day, N. P., Visai, L., Speziale, P., & Foster, T. J. (2003). Characterization of novel LPXTG-containing proteins of *Staphylococcus aureus* identified from genome sequences. *Microbiology*, *149*(3), 643-654.

Ruzin, A., Severin, A., Ritacco, F., Tabei, K., Singh, G., Bradford, P. A., & Shlaes, D. M. (2002). Further evidence that a cell wall precursor [C55-MurNAc-(peptide)-GlcNAc] serves as an acceptor in a sorting reaction. *Journal of bacteriology*, *184*(8), 2141-2147.

Sabath, L. D. (1982). Mechanisms of resistance to beta-lactam antibiotics in strains of *Staphylococcus aureus*. *Annals of internal medicine*, *97*(3), 339-344.

Sabbagh, P., Riahi, S. M., Gamble, H. R., & Rostami, A. (2019). The global and regional prevalence, burden, and risk factors for methicillin-resistant *Staphylococcus aureus* colonization in HIV-infected people: A systematic review and meta-analysis. *American journal of infection control*, *47*(3), 323-333.

Sæderup, K. L., Stødkilde, K., Graversen, J. H., Dickson, C. F., Etzerodt, A., Hansen, S. W. K. & Moestrup, S. K. (2016). The *Staphylococcus aureus* protein IsdH inhibits host hemoglobin scavenging to promote heme acquisition by the pathogen. *Journal of Biological Chemistry*, 291(46), 23989-23998.

Salamaga, B., Kong, L., Pasquina-Lemonche, L., Lafage, L., von und zur Muhlen, M., Gibson, J. F., & Foster, S. J. (2021). Demonstration of the role of cell wall homeostasis in *Staphylococcus aureus* growth and the action of bactericidal antibiotics. *Proceedings of the National Academy of Sciences*, *118*(44), e2106022118.

Sambrook, J., Fritsch, E. F., & Maniatis, T. (1989). *Molecular cloning: a laboratory manual* (No. Ed. 2). Cold spring harbor laboratory press.

Sanchez-Alamo, B., Cases-Corona, C., & Fernandez-Juarez, G. (2023). Facing the challenge of drug-induced acute interstitial nephritis. *Nephron*, *147*(2), 78-90.

Sanderson, M. J., Smith, I., Parker, I., & Bootman, M. D. (2014). Fluorescence microscopy. *Cold Spring Harbor Protocols*, *2014*(10), pdb-top071795.

Saraiva, B. M., Sorg, M., Pereira, A. R., Ferreira, M. J., Caulat, L. C., Reichmann, N. T., & Pinho, M. G. (2020). Reassessment of the distinctive geometry of *Staphylococcus aureus* cell division. *Nature communications*, *11*(1), 4097.

Sasso, E. H., Silverman, G. J., & Mannik, M. J. T. J. O. I. (1991). Human IgA and IgG F (ab') 2 that bind to staphylococcal protein A belong to the VHIII subgroup. *The Journal of Immunology*, *147*(6), 1877-1883.

Savolainen, K., Paulin, L., Westerlund-Wikstrom, B., Foster, T. J., Korhonen, T. K., & Kuusela, P. (2001). Expression of pls, a gene closely associated with the mecA gene of methicillin-resistant *Staphylococcus aureus*, prevents bacterial adhesion in vitro. *Infection and immunity*, *69*(5), 3013-3020.

Scaffidi, S. J., Shebes, M. A., & Yu, W. (2021). Tracking the subcellular localization of surface proteins in *Staphylococcus aureus* by immunofluorescence microscopy. Bio-protocol, 11(10), e4038-e4038.

Schenk, S., & Laddaga, R. A. (1992). Improved method for electroporation of *Staphylococcus aureus*. *FEMS Microbiology Letters*, *94*(1-2), 133-138.

Schermelleh, L., Ferrand, A., Huser, T., Eggeling, C., Sauer, M., Biehlmaier, O., & Drummen, G. P. (2019). Super-resolution microscopy demystified. *Nature cell biology*, *21*(1), 72-84.

Schneewind, O., & Missiakas, D. (2014). Sec-secretion and sortase-mediated anchoring of proteins in Gram-positive bacteria. *Biochimica et Biophysica Acta (BBA)-Molecular Cell Research*, *1843*(8), 1687-1697.

Schneewind, O., & Missiakas, D. (2019). Sortases, surface proteins, and their roles in *Staphylococcus aureus* disease and vaccine development. *Microbiology spectrum*, *7*(1), 7-1.

Schneewind, O., Model, P., & Fischetti, V. A. (1992). Sorting of protein A to the staphylococcal cell wall. *Cell*, *70*(2), 267-281.

Schroeder, K., Jularic, M., Horsburgh, S. M., Hirschhausen, N., Neumann, C., Bertling, A., & Heilmann, C. (2009). Molecular characterization of a novel *Staphylococcus aureus* surface protein (SasC) involved in cell aggregation and biofilm accumulation. *PloS one*, *4*(10), e7567.

Schroeder, M., Brooks, B. D., & Brooks, A. E. (2017). The complex relationship between virulence and antibiotic resistance. *Genes*, *8*(1), 39.

Sharp, J. A., Echague, C. G., Hair, P. S., Ward, M. D., Nyalwidhe, J. O., Geoghegan, J. A., & Cunnion, K. M. (2012). *Staphylococcus aureus* surface protein SdrE binds complement regulator factor H as an immune evasion tactic. *PloS one*, *7*(5), e38407.

Sharp, K. H., Schneider, S., Cockayne, A., & Paoli, M. (2007). Crystal structure of the heme-IsdC complex, the central conduit of the Isd iron/heme uptake system in *Staphylococcus aureus*. *Journal of Biological Chemistry*, 282(14), 10625-10631.

Shinde, K. N., Dhoble, S. J., Swart, H. C., Park, K., Shinde, K. N., Dhoble, S. J., & Park, K. (2012). Basic mechanisms of photoluminescence. *Phosphate Phosphors for Solid-State Lighting*, 41-59.

Sibbald, M. J., Winter, T., van der Kooi-Pol, M. M., Buist, G., Tsompanidou, E., Bosma, T., & van Dijl, J. M. (2010). Synthetic effects of secG and secY2 mutations on exoproteome biogenesis in *Staphylococcus aureus*. *Journal of bacteriology*, *192*(14), 3788-3800.

Siboo, I. R., Chambers, H. F., & Sullam, P. M. (2005). Role of SraP, a serine-rich surface protein of *Staphylococcus aureus*, in binding to human platelets. *Infection and immunity*, *73*(4), 2273-2280.

Silver, L. L. (2003). Novel inhibitors of bacterial cell wall synthesis. *Current opinion in microbiology*, *6*(5), 431-438.

Singh, V., & Phukan, U. J. (2019). Interaction of host and *Staphylococcus aureus* protease-system regulates virulence and pathogenicity. *Medical Microbiology and Immunology*, *208*, 585-607.

Skaar, E. P., & Schneewind, O. (2004). Iron-regulated surface determinants (Isd) of *Staphylococcus aureus*: stealing iron from heme. *Microbes and infection*, *6*(4), 390-397.

Smith, E. J., Visai, L., Kerrigan, S. W., Speziale, P., & Foster, T. J. (2011). The Sbi protein is a multifunctional immune evasion factor of *Staphylococcus aureus*. *Infection and immunity*, *79*(9), 3801-3809.

Solis, N., Parker, B. L., Kwong, S. M., Robinson, G., Firth, N., & Cordwell, S. J. (2014). *Staphylococcus aureus* surface proteins involved in adaptation to oxacillin identified using a novel cell shaving approach. *Journal of proteome research*, *13*(6), 2954-2972.

Sommer, A., Fuchs, S., Layer, F., Schaudinn, C., Weber, R. E., Richard, H., & Strommenger, B. (2021). Mutations in the gdpP gene are a clinically relevant mechanism for β-lactam resistance in methicillin-resistant *Staphylococcus aureus* lacking mec determinants. *Microbial genomics*, *7*(9).

Speziale, P., & Pietrocola, G. (2020). The multivalent role of fibronectin-binding proteins A and B (FnBPA and FnBPB) of *Staphylococcus aureus* in host infections. *Frontiers in microbiology*, *11*, 2054.

Stach, N., Karim, A., Golik, P., Kitel, R., Pustelny, K., Gruba, N., & Dubin, G. (2021). Structural determinants of substrate specificity of SplF protease from *Staphylococcus aureus*. *International Journal of Molecular Sciences*, *22*(4), 2220.

Stagge, F., Mitronova, G. Y., Belov, V. N., Wurm, C. A., & Jakobs, S. (2013). SNAP-, CLIP-and Halo-tag labelling of budding yeast cells. *PloS one*, *8*(10), e78745.

Steele, V. R., Bottomley, A. L., Garcia-Lara, J., Kasturiarachchi, J., & Foster, S. J. (2011). Multiple essential roles for EzrA in cell division of *Staphylococcus aureus*. *Molecular microbiology*, *80*(2), 542-555.

Stelzer, E. H. (2002). Beyond the diffraction limit? *Nature*, *417*(6891), 806-807.

Stewart, P. S., & Costerton, J. W. (2001). Antibiotic resistance of bacteria in biofilms. *The lancet*, *358*(9276), 135-138.

Strommenger, B., Braulke, C., Heuck, D., Schmidt, C., Pasemann, B., Nubel, U., & Witte, W. (2008). SpA typing of *Staphylococcus aureus* as a frontline tool in epidemiological typing. *Journal of clinical microbiology*, *46*(2), 574-581.

Sturme, M. H., Kleerebezem, M., Nakayama, J., Akkermans, A. D., Vaughan, E. E., & De Vos, W. M. (2002). Cell to cell communication by autoinducing peptides in gram-positive bacteria. *Antonie Van Leeuwenhoek*, *81*, 233-243.

Sun, H., Bie, X., Lu, F., Lu, Y., Wu, Y., & Lu, Z. (2009). Enhancement of surfactin production of Bacillus subtilis fmbR by replacement of the native promoter with the Pspac promoter. *Canadian journal of microbiology*, *55*(8), 1003-1006.

Sun, X., Zhang, A., Baker, B., Sun, L., Howard, A., Buswell, J., & Corrêa Jr, I. R. (2011). Development of SNAP-tag fluorogenic probes for wash-free fluorescence imaging. *ChemBioChem*, *12*(14), 2217-2226.

Suree, N., Liew, C. K., Villareal, V. A., Thieu, W., Fadeev, E. A., Clemens, J. J. & Clubb, R. T. (2009). The structure of the *Staphylococcus aureus* sortase-substrate complex reveals how the universally conserved LPXTG sorting signal is recognized. *Journal of Biological Chemistry*, 284(36), 24465-24477.

Sutton, J. A., Carnell, O. T., Lafage, L., Gray, J., Biboy, J., Gibson, J. F., & Foster, S. J. (2021). *Staphylococcus aureus* cell wall structure and dynamics during host-pathogen interaction. *PLoS pathogens*, *17*(3), e1009468.

Suzuki, T. (2011). A new target for *Staphylococcus aureus* associated with keratitis. *Cornea*, *30*, S34-S40.

Suzuki, T., Swoboda, J. G., Campbell, J., Walker, S., & Gilmore, M. S. (2011). In vitro antimicrobial activity of wall teichoic acid biosynthesis inhibitors against *Staphylococcus aureus* isolates. *Antimicrobial agents and chemotherapy*, *55*(2), 767-774.

Taguchi, A., Welsh, M. A., Marmont, L. S., Lee, W., Sjodt, M., Kruse, A. C., & Walker, S. (2019). FtsW is a peptidoglycan polymerase that is functional only in complex with its cognate penicillin-binding protein. *Nature microbiology*, *4*(4), 587-594.

Takahashi, J., Komatsuzawa, H., Yamada, S., Nishida, T., Labischinski, H., Fujiwara, T., & Sugai, M. (2002). Molecular characterization of an atl null mutant of *Staphylococcus aureus*. *Microbiology and immunology*, *46*(9), 601-612.

Tam, K., & Torres, V. J. (2019). *Staphylococcus aureus* secreted toxins and extracellular enzymes. *Microbiology spectrum*, *7*(2), 7-2.

Tan, N. C. W., Tran, H., Roscioli, E., Wormald, P. J., & Vreugde, S. (2012). Prevention of false positive binding during immunofluorescence of *Staphylococcus aureus* infected tissue biopsies. Journal of immunological methods, 384(1-2), 111-117.

Thammavongsa, V., Kern, J. W., Missiakas, D. M., & Schneewind, O. (2009). *Staphylococcus aureus* synthesizes adenosine to escape host immune responses. *Journal of Experimental Medicine*, *206*(11), 2417-2427.

Thomas, P. M., Deming, M. A., & Sarkar, A. (2022). β-Lactamase Suppression as a Strategy to Target Methicillin-Resistant *Staphylococcus aureus*: Proof of Concept. *ACS omega*.

Thompson, T. A., & Brown, P. D. (2021). Small interfering RNAs targeting agrA and sarA attenuate pathogenesis of *Staphylococcus aureus* in Caenorhabditis elegans. *The Journal of Infection in Developing Countries*, *15*(12), 1868-1875.

Timofeyeva, Y., Scully, I. L., & Anderson, A. S. (2014). Immunofluorescence microscopy for the detection of surface antigens in methicillin-resistant *Staphylococcus aureus* (MRSA). In Methicillin-Resistant *Staphylococcus aureus* (MRSA) Protocols (pp. 85-95). Humana Press, Totowa, NJ.

Timofeyeva, Y., Scully, I. L., & Anderson, A. S. (2014). Immunofluorescence microscopy for the detection of surface antigens in methicillin-resistant *Staphylococcus aureus* (MRSA). *Methicillin-Resistant Staphylococcus aureus (MRSA) Protocols*, 85-95.

Tinajero-Trejo, M., Carnell, O., Kabli, A. F., Pasquina-Lemonche, L., Lafage, L., Han, A., & Foster, S. J. (2022). The *Staphylococcus aureus* cell division protein, DivIC, interacts with the cell wall and controls its biosynthesis. *Communications Biology*, *5*(1), 1-13.

Tinajero-Trejo, M., Carnell, O., Kabli, A. F., Pasquina-Lemonche, L., Lafage, L., Han, A., & Foster, S. J. (2022). The *Staphylococcus aureus* cell division protein, DivIC, interacts with the cell wall and controls its biosynthesis. *Communications Biology*, *5*(1), 1-13.

Ton-That, H., Liu, G., Mazmanian, S. K., Faull, K. F., & Schneewind, O. (1999). Purification and characterization of sortase, the transpeptidase that cleaves surface proteins of *Staphylococcus aureus* at the LPXTG motif. *Proceedings of the National Academy of Sciences*, *96*(22), 12424-12429.

Tong, S. Y., Davis, J. S., Eichenberger, E., Holland, T. L., & Fowler, V. G. (2015). *Staphylococcus aureus* infections: epidemiology, pathophysiology, clinical manifestations, and management. *Clinical microbiology reviews*, 28(3), 603-661.

Torres, V. J., Attia, A. S., Mason, W. J., Hood, M. I., Corbin, B. D., Beasley, F. C., & Skaar, E. P. (2010). *Staphylococcus aureus* fur regulates the expression of virulence factors that contribute to the pathogenesis of pneumonia. *Infection and immunity*, *78*(4), 1618-1628.

Torres, V. J., Pishchany, G., Humayun, M., Schneewind, O., & Skaar, E. P. (2006). *Staphylococcus aureus* IsdB is a hemoglobin receptor required for heme iron utilization. Journal of bacteriology, 188(24), 8421-8429.

Tosheva, K. L., Yuan, Y., Pereira, P. M., Culley, S., & Henriques, R. (2020). Between life and death: strategies to reduce phototoxicity in super-resolution microscopy. *Journal of Physics D: Applied Physics*, *53*(16), 163001.

Touhami, A., Jericho, M. H., & Beveridge, T. J. (2004). Atomic force microscopy of cell growth and division in *Staphylococcus aureus*. *Journal of bacteriology*, *186*(11), 3286-3295.

Trad, S., Allignet, J., Frangeul, L., Davi, M., Vergassola, M., Couve, E., & El Solh, N. (2004). DNA macroarray for identification and typing of *Staphylococcus aureus* isolates. *Journal of clinical microbiology*, *42*(5), 2054-2064.

Tsompanidou, E., Denham, E. L., Sibbald, M. J., Yang, X. M., Seinen, J., Friedrich, A. W., & van Dijl, J. M. (2012). The sortase A substrates FnbpA, FnbpB, ClfA and ClfB antagonize colony spreading of *Staphylococcus aureus*.

Turlej, A. G. A. T. A., Hryniewicz, W. A. L. E. R. I. A., & Empel, J. (2011). Staphylococcal cassette chromosome mec (Sccmec) classification and typing methods: an overview. *Pol J Microbiol*, *60*(2), 95-103.

Turner, R. D., Ratcliffe, E. C., Wheeler, R., Golestanian, R., Hobbs, J. K., & Foster, S. J. (2010). Peptidoglycan architecture can specify division planes in *Staphylococcus aureus*. Nature communications, 1(1), 26.

Tzagoloff, H., & Novick, R. (1977). Geometry of cell division in *Staphylococcus aureus*. *Journal of bacteriology*, *129*(1), 343-350.

Urushibara, N., Aung, M. S., Kawaguchiya, M., & Kobayashi, N. (2020). Novel staphylococcal cassette chromosome mec (SCC mec) type XIV (5A) and a truncated SCC mec element in SCC composite islands carrying speG in ST5 MRSA in Japan. *Journal of Antimicrobial Chemotherapy*, *75*(1), 46-50.

Vagner, V., Dervyn, E., & Ehrlich, S. D. (1998). A vector for systematic gene inactivation in Bacillus subtilis. *Microbiology*, *144*(11), 3097-3104.

Valle, J., Toledo-Arana, A., Berasain, C., Ghigo, J. M., Amorena, B., Penadés, J. R., & Lasa, I. (2003). SarA and not σB is essential for biofilm development by *Staphylococcus aureus*. *Molecular microbiology*, *48*(4), 1075-1087.

van Dalen, R., Peschel, A., & van Sorge, N. M. (2020). Wall teichoic acid in *Staphylococcus aureus* host interaction. *Trends in microbiology*, *28*(12), 985-998.

Veggiani, G., & de Marco, A. (2011). Improved quantitative and qualitative production of single-domain intrabodies mediated by the co-expression of Erv1p sulfhydryl oxidase. *Protein expression and purification*, *79*(1), 111-114.

Vollmer, W., & Höltje, J. V. (2004). The architecture of the murein (peptidoglycan) in gram-negative bacteria: vertical scaffold or horizontal layer (s)? *Journal of bacteriology*, 186(18), 5978-5987.

Vollmer, W., Blanot, D., & De Pedro, M. A. (2008). Peptidoglycan structure and architecture. *FEMS microbiology reviews*, 32(2), 149-167.

Vollmer, W., Joris, B., Charlier, P., & Foster, S. (2008). Bacterial peptidoglycan (murein) hydrolases. *FEMS microbiology reviews*, *32*(2), 259-286.

Von Eiff, C., Becker, K., Machka, K., Stammer, H., & Peters, G. (2001). Nasal carriage as a source of *Staphylococcus aureus* bacteremia. *New England Journal of Medicine*, 344(1), 11-16.

Wacnik, K., (2016) "Dissecting cell division in the human pathogen *Staphylococcus aureus*", PhD Thesis, University of Sheffield, Sheffield.

Wacnik, K., Rao, V. A., Chen, X., Lafage, L., Pazos, M., Booth, S., & Foster, S. J. (2022). Penicillin-Binding Protein 1 (PBP1) of *Staphylococcus aureus* Has Multiple Essential Functions in Cell Division. *Mbio*, *13*(4), e00669-22.

Wadenpohl, I., & Bramkamp, M. (2010). DivIC stabilizes FtsL against RasP cleavage. *Journal of bacteriology*, *192*(19), 5260-5263.

Wadsworth, K. D., Rowland, S. L., Harry, E. J., & King, G. F. (2008). The divisomal protein DivIB contains multiple epitopes that mediate its recruitment to incipient division sites. *Molecular microbiology*, *67*(5), 1143-1155.

Waxman, D. J., & Strominger, J. L. (1983). Penicillin-binding proteins and the mechanism of action of beta-lactam antibiotics. *Annual review of biochemistry*, *52*(1), 825-869.

Weidenmaier, C., Kokai-Kun, J. F., Kristian, S. A., Chanturiya, T., Kalbacher, H., Gross, M., & Peschel, A. (2004). Role of teichoic acids in *Staphylococcus aureus* nasal colonization, a major risk factor in nosocomial infections. *Nature medicine*, *10*(3), 243-245.

Weihs, F., (2016) "A supramolecular structure in the membrane of *Staphylococcus aureus*", PhD Thesis, University of Sheffield, Sheffield.

Wheeler, R., Turner, R. D., Bailey, R. G., Salamaga, B., Mesnage, S., Mohamad, S. A., & Foster, S. J. (2015). Bacterial cell enlargement requires control of cell wall stiffness mediated by peptidoglycan hydrolases. *MBio*, *6*(4), e00660-15.

Wiltshire, M. D., & Foster, S. J. (2001). Identification and analysis of *Staphylococcus aureus* components expressed by a model system of growth in serum. *Infection and immunity*, *69*(8), 5198-5202.

Wolz, C., Goerke, C., Landmann, R., Zimmerli, W., & Fluckiger, U. (2002). Transcription of clumping factor A in attached and unattached *Staphylococcus aureus* in vitro and during device-related infection. Infection and immunity, 70(6), 2758-2762.

Wörmann, M. E., Reichmann, N. T., Malone, C. L., Horswill, A. R., & Gründling, A. (2011). *Proteolytic Cleavage Inactivates the Staphylococcus aureus Lipoteichoic Acid Synthase*.

Wu, S. C., Liu, F., Zhu, K., & Shen, J. Z. (2019). Natural products that target virulence factors in antibiotic-resistant *Staphylococcus aureus*. Journal of agricultural and food chemistry, 67(48), 13195-13211.

Wu, S. W., De Lencastre, & Tomasz, A. (1999). The *Staphylococcus aureus* transposon Tn 551: complete nucleotide sequence and transcriptional analysis of the expression of the erythromycin resistance gene. *Microbial Drug Resistance*, *5*(1), 1-7.

Xu, T., Wang, X. Y., Cui, P., Zhang, Y. M., Zhang, W. H., & Zhang, Y. (2017). The Agr quorum sensing system represses persister formation through regulation of phenol soluble modulins in *Staphylococcus aureus*. *Frontiers in microbiology*, *8*, 2189.

Yamada, S., Sugai, M., Komatsuzawa, H., Nakashima, S., Oshida, T., Matsumoto, A., & Suginaka, H. (1996). An autolysin ring associated with cell separation of *Staphylococcus aureus*. *Journal of bacteriology*, *178*(6), 1565-1571.

Yamanaka, M., Smith, N. I., & Fujita, K. (2014). Introduction to super-resolution microscopy. *Microscopy*, *63*(3), 177-192.

Yu, W., Missiakas, D., & Schneewind, O. (2018). Septal secretion of protein A in *Staphylococcus aureus* requires SecA and lipoteichoic acid synthesis. *Elife*, *7*, e34092.

Zapotoczna, M., Jevnikar, Z., Miajlovic, H., Kos, J., & Foster, T. J. (2013). Iron-regulated surface determinant B (IsdB) promotes S taphylococcus aureus adherence to and internalization by non-phagocytic human cells. *Cellular microbiology*, 15(6), 1026-1041.

Zhang, R., Shebes, M. A., Kho, K., Scaffidi, S. J., Meredith, T. C., & Yu, W. (2021). Spatial regulation of protein A in *Staphylococcus aureus*. *Molecular microbiology*, *116*(2), 589-605.

Zhu, Q., Wen, W., Wang, W., & Sun, B. (2019). Transcriptional regulation of virulence factors Spa and ClfB by the SpoVG-Rot cascade in *Staphylococcus aureus*. *International Journal of Medical Microbiology*, *309*(1), 39-53.

Zinchuk, V., Zinchuk, O., & Okada, T. (2007). Quantitative colocalization analysis of multicolor confocal immunofluorescence microscopy images: pushing pixels to explore biological phenomena. *Acta histochemica et cytochemica*, 0707300003-0707300003.

Zong, Y., Bice, T. W., Ton-That, H., Schneewind, O., & Narayana, S. V. (2004). Crystal structures of *Staphylococcus aureus* sortase A and its substrate complex. *Journal of Biological Chemistry*, *279*(30), 31383-31389.

Zong, Y., Xu, Y., Liang, X., Keene, D. R., Höök, A., Gurusiddappa, S., & Narayana, S. V. (2005). A 'Collagen Hug'model for *Staphylococcus aureus* CNA binding to collagen. *The EMBO journal*, *24*(24), 4224-4236.